uOttawa

L'Université canadienne
Canada's university

FACULTÉ DES ÉTUDES SUPÉRIEURES ET POSTOCTORALES

uOttawa

L'Université canadienne
Canada's university

FACULTY OF GRADUATE AND POSDOCTORAL STUDIES

Sarah Labib

AUTEUR DE LA THÈSE / AUTHOR OF THESIS

M.Sc. (Biochemistry)

GRADE / DEGREE

Department of Biochemistry, Microbiology and Immunology

FACULTÉ, ÉCOLE, DÉPARTEMENT / FACULTY, SCHOOL, DEPARTMENT

The Effect of *LMNA* mutations on Lamin A/C and Binding Partner Interactions and Cellular Distribution

TITRE DE LA THÈSE / TITLE OF THESIS

Frédérique Tesson

DIRECTEUR (DIRECTRICE) DE LA THÈSE / THESIS SUPERVISOR

CO-DIRECTEUR (CO-DIRECTRICE) DE LA THÈSE / THESIS CO-SUPERVISOR

Kristi Adamo

Ross Milne

Gary W. Slater

Le Doyen de la Faculte des études supérieures et postdoctorales / Dean of the Faculty of Graduate and Postdoctoral Studies

The effect of *LMNA* mutations on lamin A/C and binding partner interactions and cellular distribution.

Sarah Labib, B.Sc.

Thesis submitted to the Faculty of Graduate and Postdoctoral Studies, in partial fulfillment of the requirements for the M.Sc. degree in Biochemistry

Department of Biochemistry, Microbiology and Immunology

Faculty of Medicine

University of Ottawa

Your file Votre référence
ISBN: 978-0-494-73844-3
Our file Notre référence
ISBN: 978-0-494-73844-3

Abstract

Mutations in the *LMNA* gene, which encodes the nuclear intermediate filament proteins lamin A and lamin C, are associated with over ten tissue-specific diseases, including Dilated Cardiomyopathy (DCM) and lone Atrial Fibrillation (lone AF). There is no clear genotype-phenotype relationship between the location of the mutation and the associated disease phenotype. **The general hypothesis of this thesis is that *LMNA* mutations exert their tissue-specific effects via the perturbation of lamin A and lamin C's specific interacting partners.**

Protein kinase C α, PKCα, is a lamin A/C binding partner implicated in heart failure and cardiac hypertrophy. Furthermore, abnormal PKCα function results in I_{KACh} activity associated with chronic AF. **My first aim is to identify specific phenotypes associated with three laminopathies: lone AF, DCM, and DCM with AF by a) comparing the cellular phenotype induced by *LMNA* mutations associated with lone AF, DCM, and DCM with AF and b) determining the effect of the mutations on the cellular distribution of PKCα.** I found two previously unreported mutant lamin A and C phenotypes – cytoplasmic lamin A/C extrusion and the formation of intranuclear lamin A/C sickle-shaped aggregates associated with one lone AF mutation and one DCM mutation. I show that PKCα is mislocalized to the nucleus in C2C12 cells transfected with the same mutants.

The E2 conjugating enzyme of the Sumo process, Ubc9, is a reported lamin A/C binding partner. Sumo1 is a post-translational modifying protein that is sequestered within mutant lamin A/C aggregates and has increased substrate conjugation in DCM-associated mutant cells. **My second aim is to determine how lamin A and C are involved in the Sumo process by a) investigating Ubc9 cellular distribution and lamin A and C binding in the presence of DCM-associated *LMNA* mutations and b) determining whether lamin A and/or C are**

Sumo1 binding partners. I show that Ubc9 is mislocalized from the inner nuclear membrane to the mutant lamin A/C aggregates. Co-immunoprecipitation did not show lamin A/C sumoylation by Sumo1. Mass spectrometric analysis indicates that heterogeneous ribonucleoprotein U may be a novel lamin A/C binding partner that is sumoylated by Sumo1.

In conclusion, I found that two cellular pathways are perturbed in the presence of *LMNA* mutations and might account for the specific symptoms observed in the tissue-specific laminopathies. Incorrect activation or deactivation of tissue-specific targets may lead to the wide range of tissue-specific diseases associated with *LMNA* mutations.

Acknowledgements

This thesis would not have been possible without the guidance and help of several individuals who in one way or another contributed and extended their valuable assistance in the preparation and completion of this study.

First and foremost I offer my sincerest gratitude to my supervisor, Dr Frédérique Tesson, who has supported me throughout my MSc with her patience and knowledge while allowing me the room to work in my own way. She was always available to discuss ideas and share results and it is this support that made my MSc research possible.

I would also like to thank my co-supervisor, Dr Patrick G Burgon, who provided me with guidance in preparing my experiments and discovering a very exciting new lamin A/C binding partner!

I am grateful for the help of my Thesis Advisory Committee members – Dr Alexander Sorisky and Dr Alexandre Stewart. Dr Sorisky was essential as he provided a non-geneticist point of view to my project. I especially appreciate Dr Stewart's kindness in providing me desk space in his lab at the Heart Institute while my lab was in the process of moving to Roger Guindon. I will never forget his enthusiasm for genetics and molecular biology, as well as for his availability to discuss techniques and interesting articles I came across.

I would also like to express my appreciation to my lab members – Emilie Boudreau, Pallavi Gupta, Pierrette Bolongo, Tracy Jackson, Akil Hamza, and Siham Yasari. Thank you to Pallavi for teaching me about the joys of working with lamin and for her patience in guiding me through techniques I was unfamiliar with before joining the lab. Thank you to Emilie for being a constant support everyday in the lab (even while she was in France), providing me with a

soundboard to run off ideas with. You were the greatest lab partner I could have ever asked for! Thank you to Pierrette for knowing everything in the lab. I don't know how you do it! Thank you to Tracy for being a great friend these past few years. Thank you to Akil for being the best Honor's student we could have asked for. And thank you to Siham for providing guidance in any way she could.

Furthermore, I want to thank all the students and research assistants in the surrounding labs at the Heart Institute – Allen Teng, Melanie Bélanger, Olivia Assogba, Jennifer Prieur, Isabelle Thibodeau, Brian Cheng, Katherine Westcott, and Robert Davies. Your daily presence in the lab made coming in more enjoyable.

Lastly, and most importantly, I would like to thank my family for their continued support. My parents who patiently shared in any frustrations I experienced throughout this process and for accompanying me to the lab on weekends until you were confident I would be safe. Thank you for providing me with support and encouragement all those times when I was discouraged and needed your help. Thank you to my sister, Leah, for putting up with me when I didn't have time to hang out or talk. Thank you to my fiancé Lionel for paying so much attention to me and my project (that sometimes I wonder if he understands it better than I do) and for accepting that my cells dictated how much time I had to spend with him.

Table of Contents

List of Abbreviations

AD-EDMD – Autosomal-Dominant Emery Dreifuss Muscular Dystrophy

AF - Atrial Fibrillation

CFP - Cyan Fluorescent Protein

DCM - Dilated Cardiomyopathy

DMEM - Dulbecco's Modified Eagle's Medium

DNA - Deoxyribonucleic Acid

DTT – Dithiothreitol

ECL - Electrochemilunescence

EMD - Emerin Gene

FBS - Fetal Bovine Syndrome

FLIP - Fluorescence Loss of Intensity after Photobleaching

FPLD - Familial Partial Lipodystrophy

FRAP - Fluorescence Recovery After Photobleaching

GFP - Green Fluorescent Protein

HA - Hemagglutinin

HGPS - Hutchinson-Gilford Progeria Syndrome

hnRNP - Heterogeneous Nuclear Ribonucleoprotein

IDC - Idiopathic Dilated Cardiomyopathy

Ig - Immunoglobulin

IGF-1 - Insulin-Growth Factor 1

LB - Lysogeny Broth

LDL - Low Density Lipoprotein

LGMD-1B - Limb Girdle Muscular Dystrophy Type 1B

LMNA - Lamin A/C gene

MAD - Mandibuloacral Dysplasia

MALDI-TOF - Matrix-Associated Laser Desorption/Ionization Time of Flight Mass Spectrometry

MAPK - Mitogen-Activated Protein Kinase

MAR - Matrix Attachment Region

MEF - Mouse Embryonic Fibroblast

MEM - Modified Eagle's Medium

MLIP - Muscle Lamin Interacting Protein

mRNA - Messenger Ribonucleic Acid

MS – Mass Spectrometry

NDSM - Negatively charged ion Dependent Sumoylation Motif

NEM - N-ethylmaleimide

NLS - Nuclear Localization Signal

NPC - Nuclear Pore Complex

PBS - Phosphate Buffered Saline

PBST - Phosphate Buffered Saline with Tween

PCOS - Polycystic Ovarian Syndrome

PCR - Polymerase Chain Reaction

PDSM - Phosphorylation Dependent Sumoylation Motif

PFA - Paraformaldehyde

PKC - Protein Kinase C

PML - Promyelocytic Leukemia

PPARγ - Peroxisome Proliferator Activated Receptor γ

PPRE - Peroxisome Proliferator Hormone Response Elements

Rce1 - Ras-converting enzyme 1

RNA - Ribonucleic Acid

SDS-PAGE - Sodium Dodecyl Sulfate Polyacrylamide Gel Electrophoresis

SREBP - Sterol Regulatory Element Binding Protein

SUMO - Small Ubiquitin-like Modifier

WB - Western Blot

YFP - Yellow Fluorescent Protein

ZMPSTE24 - Zinc metallopeptidase protein

List of Figures

List of Tables

Chapter 1 - Introduction

1.1 The Structure and Organization of lamin A/C

The nuclear lamina is a distinct meshwork that lines the nucleoplasmic side of the inner nuclear membrane. It is made up of intermediate filament proteins (the lamins) and nuclear membrane associated proteins. The lamins, A-type (lamins A and C) and B-type (lamins B1 and B2), encoded by different genes (LMNA, LMNB1 and LMNB2, respectively) are type V intermediate filament proteins which differ in solubility properties (Gerace and Blobel 1980), expression patterns (Lin and Worman 1997), and localization during mitosis (Gerace and Blobel 1980).

1.1.1 Gene and Expression

The *LMNA* gene, which encodes the A-type lamin proteins, maps to chromosome 1q21.2-q21.3 and is approximately 24 kilobases long and contains 12 exons (Lin and Worman 1993). The first exon codes for the N-terminal head domain and the first part of the rod domain. Exons 2 through 6 code for the rest of the rod and exons 7 though 9 code for the C-terminal tail. Alternative splicing within exon 10 yields two splice variants – lamin A and lamin C. Exons 11 and 12 are lamin A specific (Figure 1.1).

The *LMNA* gene gives rise to four known splice variants: lamin A, lamin C, lamin AΔ10, and lamin C2. Lamin A and lamin C are expressed in all terminally differentiated somatic cells, except in cells of the hematopoietic system (Rober et al 1990). Alternative splicing at the codon for amino acid 566 generates the two most commonly found isoforms - A and C (Lin and Worman 1993). Prelamin A is the transcribed mRNA before post-translational modification to yield mature lamin A. A splice of 743 nucleotides downstream of exon 11 joins the amino acid 566 splice site to yield prelamin A. The lamin C-specific amino acids are translated from

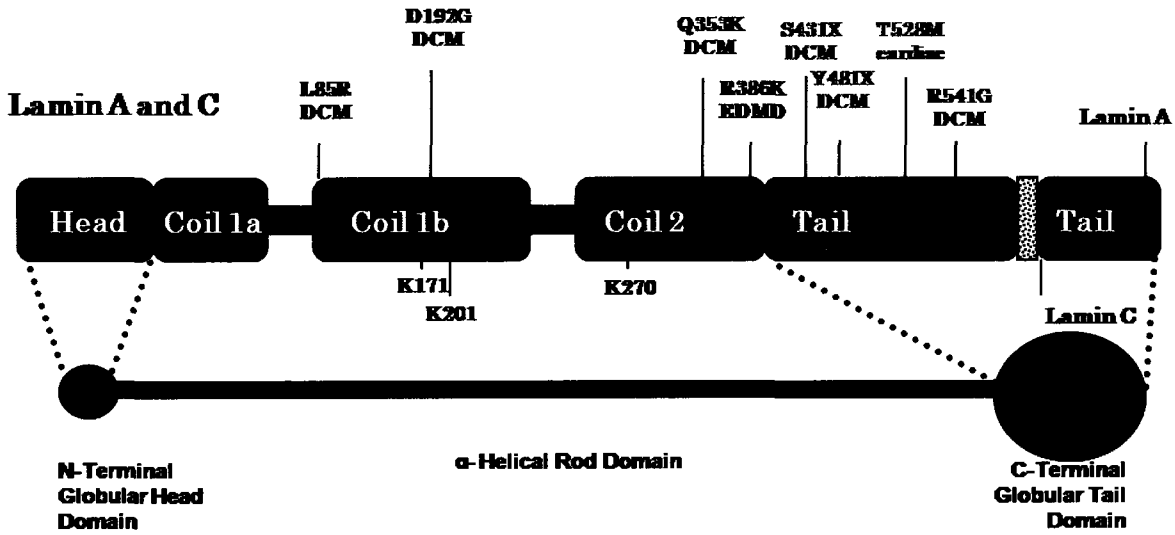

Figure 1.1 Schematic of LMNA gene DNA and lamin A/C protein indicating location of mutations studied above and Sumo consensus sites below. Blue mutations are studied in Chapter 3 and red mutations in Chapter 4. LMNA gene encodes for a small globular head domain, a coiled-coil rod domain and a large, globular tail domain.

contiguous DNA after amino acid 566.

The lamin AΔ10 isoform is identical to lamin A except that it is missing exon 10 (Machiels et al 1996). This isoform is expressed primarily in lung cancer cell lines. Lamin C2 is a germ cell-specific isoform that has an identical sequence to lamin C except the N-terminal segment (with the non-α-helical head and the α-helical 1A domain) is replaced by a short non-α-helical segment (Furukawa et al 1994).

Metazoan cells contain a variety of lamins. Mammalian *LMNA* gene encodes lamin A, C, AΔ10, and C2 while separate genes encode lamin B1 and B2. Drosophila have two lamin genes encoding lamin Dm0 and C, closely associated with B- and A-type lamins, respectively. *C. elegans* have a single lamin gene – lmn-1 which encodes Ce-lamin, which is more closely associated with B-type lamins compared to A-type lamins. In *Xenopus laevis* there are five lamins – LI, LII, and LIII closely related to B-type lamins, lamin A (related to human lamin A), and LIV which has not been characterized.

Prelamin A undergoes specific post-translational modifications for nuclear envelope incorporation involving its C-terminal CAAX motif – CSIM (reviewed in Rusinol and Sinensky 2006) (Figure 1.2). First, a farnesyl group is added to the cysteine of the 74kDa prelamin A CSIM motif by farnesyl transferase. The three C-terminal amino acids are cleaved by either the zinc metallopeptidase ZMPSTE24 or Ras-converting enzyme 1 (Rce1). Carboxymethylation occurs at the cysteine residue by a carboxymethyltransferase. ZMPSTE24 performs a second cleavage 15 amino acids upstream of the farnesylated cysteine to yield the 72kDa mature lamin A.

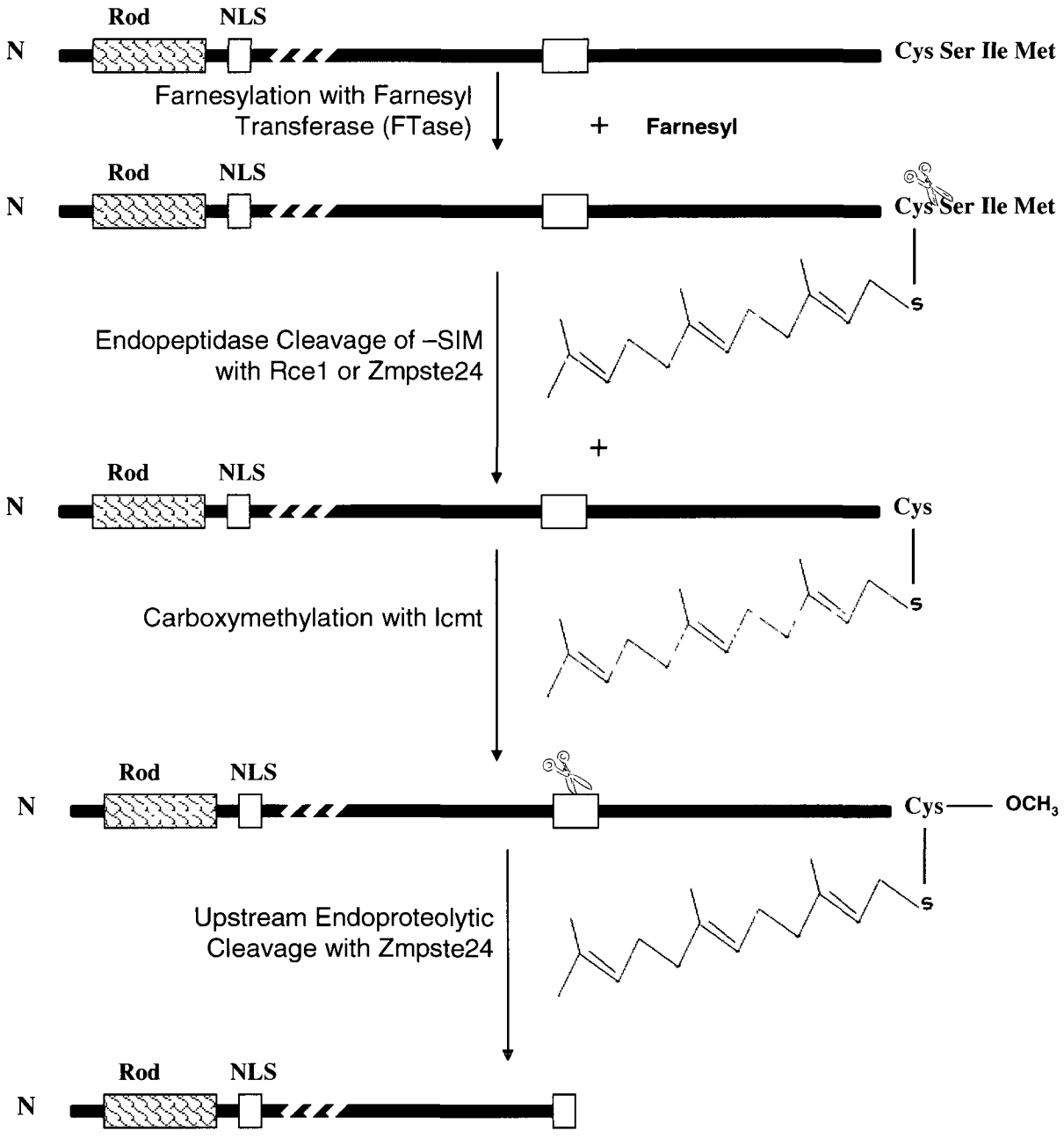

Figure 1.2 Schematic drawing of pre-lamin A post-translational processing into mature lamin A. The CAAX motif in pre-lamin A is CSIM. In the first step, a farnesyl group is attached to the cysteine residue by a farnesyltransferase. Next, The last three residues of proteolitically cleaved by an endopeptidase. The lone cysteine is then carboxymethylated by isoprenyl carboxymethyl transferase (Icmt). Finally, Zmptste24 cleaves an additional 15 amino acids upstream of the CSIM motif to yield mature lamin A.

During mitosis, between prophase and prometaphase, lamin A/C phosphorylation results in the disassembly of the nuclear lamina (Broers et al 1999, Moir et al 2000a). The known phosphorylation sites associated with lamina disassembly are Ser22 and Ser392, flanking the rod domain (Heald and McKeon 1990, Eggert et al 1993). Lamin A/C is a reported substrate for protein kinase C (PKC) (Eggert et al 1993, Haas and Jost 1993, Leukel and Jost 1995), however the particular isoform involved has not been identified. Interestingly, in 2002 (Martelli et al), lamin A/C was identified as an interacting partner of PKCα, a classic PKC, at the C-terminus after residue 499. This interaction is not related to the physiologically relevant PKC phosphorylation sites, Ser403 and Ser404 (Leukel and Jost 1995) and the function of this interaction has yet to be elucidated.

The regulation of the lamin A/C gene expression is not well studied, however there is evidence for the presence of regulatory motifs binding SP1/3, c-Jun, c-Fos, CREBP and p53 (Okumura et al 2000, Muralikrishna and Parnaik 2001, Janaki-Ramaiah and Parnaik 2006, Rahman-Roblick 2007).

Although lamin A/C localization to the inner nuclear lamina is most often mentioned, there is a long line of evidence pointing to nucleoplasmic localization (Goldman et al 1992, Bridger et al 1993, Hozak et al 1995, Broers et al 1999, Moir et al 2000b, Dechat et al 2004). Fluorescence recovery after photobleaching (FRAP) experiments show that nucleoplasmic lamins are relatively stable, indicating they are not just artifacts (Moir et al 2000b, Broers et al 2005).

Lamin A and C proteins are found distributed together in a homogeneous meshwork in a 1:1 ratio, however the independent localization of each isoform is a topic of debate. Wild type lamin A transfected alone is consistently shown to localize to the inner nuclear lamina with some

nucleoplasmic localization. Lamin C, on the other hand, has been shown to localize to the inner nuclear lamina like lamin A (Raharjo et al 2001) as well as in intranuclear aggregates (Pugh et al 1997, Vaughan et al 2001, Sylvius et al 2005, Sylvius et al 2008) (Figure 1.3). In defense of the latter, Pugh et al (1997) studied the incorporation of the respective lamins in Swiss 3T3 cells and found that the incorporation of lamin C into the lamina is made possible by lamin A. The lamin C foci exhibit a close connection with the inner nuclear envelope as determined by electron microscopy (Sylvius et al 2008) and intranuclear lamin C-GFP is more mobile than intranuclear lamin A-GFP, as determined by fluorescence loss of intensity after photobleaching (FLIP) experiments (Broers et al 2005). On the other hand, the lamin C only mouse model expresses lamin C at the inner nuclear lamina as seen in wild type cells (Fong et al 2006), indicating the presence of compensatory mechanisms.

a

Sylvius et al 2008

b

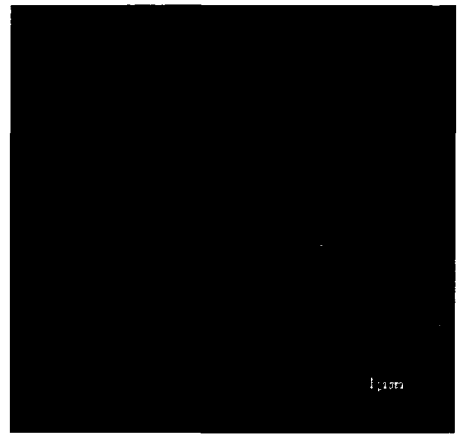

Sylvius et al 2008

Figure 1.3 Nuclear distribution of lamin A and lamin C. (a) Lamin A is found distributed homogeneously at the inner nuclear membrane while (b) lamin C is expressed as small intranuclear aggregates evenly distributed within the nucleus (Sylvius et al 2008). Cos7 cells were transiently transfected with (a) lamin A or (b) lamin C in pECFP and pEYFP fluorescent expression vectors, respectively. Cells were visualized via fluorescent confocal microscopy.

1.1.2 Structure and Assembly

The lamin A/C protein structure is highly conserved among cytoplasmic intermediate filament proteins (Fisher et al 1986, McKeon et al 1986). Notable differences include small N-terminal head and large C-terminal tail domains in lamin A/C.

The formation of a mature lamin molecule is a three step process: (1) Lamin monomers form unstaggered dimers in an α-helical manner with each other. (2) These dimers arrange longitudinally in a polar head-to-tail manner which then (3) associate laterally into intermediate filament-like structures. The formation of the dimers is dependent on the presence of the rod domain (Moir et al 1991, Heitlinger et al 1992). The N-terminal head domain (specifically the last 20 residues) is essential for proper head-to-tail polymer formation (Heitlinger et al 1992, Isobe et al 2007).

The function of the C-terminal tail domain in mature lamin formation is more ambiguous. Deletion of the tail domain allows the dimers to associate in a head-to-tail manner, however they are also able to associate laterally, staggered or antiparallel (Sasse et al 1997). In general, the function of the C-terminal Ig domain is to provide structural support and to mediate intermolecular interactions with other proteins, DNA or phospholipids.

Table 1 Table of lamin A/C interacting proteins including characteristics, domain of interaction and reference

Protein	Characteristics	Reference	Domain of Interaction
Actin	Major constituent of microfilaments and plays an important role in cell shape, movement and structure	Sasseville and Langelier 1998	Carboxy Terminal Domain
Arachidonate 12-lipoxygenase (12R LOX, ALOX12B)	Oxyreductase that converts arachidonic acid to 12R-hydroperoxyeicosatetraenoic acid	Tang et al 2000	Unknown
Barrier-To-Autointegration Factor 1 (BAF)	Plays a role in nuclear reassembly by interacting with both DNA and nuclear membrane proteins to recruit chromatin to the nuclear periphery	Holaska et al 2003	Unknown
C-Fos	Involved in transcriptional and cell cycle control in mammalian cells One component of the dimeric AP-1 transcription factor complex in the regulation of a variety of cellular processes (cell differentiation, cell proliferation, neoplasmic transformation and apoptosis)	Ivorra et al 2006	Unknown
Core histones H2A, H2B, H3, H4	Histones play important roles in the maintenance of chromosome integrity, DNA recombination, and DNA replication Core histones are responsible for creating a protein core around which 146bp of DNA are wrapped in approximately 2 left handed superhelical turns giving rise to the nucleosome core particle	Taniura et al 1995	Unknown
Cyclin D3 (CCND3)	Forms a complex with CDK4 or CDK6 which are involved in the G1/S transition of the cell cycle	Mariappan et al 2007	Residues 383-474
E1B 19K	Inhibitor of apoptosis both during viral infection and transformation	Rao et al 1997	Residues 252-390
Emerin (EMD)	Protein of inner nuclear membrane associated with X-linked Emery Dreifuss muscular dystrophy It mediates membrane anchorage to the cytoskeleton	Clements et al 2000	Residues 384-566
Epidermal Growth Factor (EGF)	Promotes growth and differentiation Has profound effect on differentiation of specific cells in vivo and is a potent mitogenic factor for a variety of cultured cells of both ectodermal and mesodermal origin	Zhong et al 2005	Unknown
hnRNP E1	Involved in several RNA-related biological processes (transcription, pre-mRNA processing, mature mRNA transport to the cytoplasm and translation) Regulates initiation of RNA replication and translation	Zhong et al 2005	Unknown
Lamin B1	Intermediate filament protein Component of the nuclear lamina	Ye and Worman 1995	Unknown
Lamin Companion 1 (Lco1)	Involved in organizing internal lamin network	Vlcek et al Aug 2004	Unknown
Lamina-associated polypeptides 1A and 1B (LAP1A, 1B)	Integral membrane proteins of the nuclear envelope May be involved in the organization of synaptic cell cell contact	Foisner et al 1993	Unknown
Lem domain-containing 3 (LEMD3, MAN1)	Bind directly to BAF Has 2 transmembrane domains	Mansharamani et al 2005	Globular Tail Domain
LEM2	MAN1 related protein Potential function in structural organization of a subset of NE components	Brachner et al 2005	Globular Tail Domain
LUMA	A novel ER protein enriched at the nuclear envelope It is highly conserved with wide tissue distribution	Bengtsson and Otto 2008	Unknown
Mel18	Zinc finger protein localized in the nucleus A sequence-specific DNA-binding protein and is a negative transcriptional regulator	Zhong et al 2005	Unknown

Mesenchymal Lim Interacting Protein (MLIP)	Novel lamin interacting partner Expressed primarily in cardiac muscle, skeletal muscle and brain Essential for muscle differentiation	Personal communication with Patrick G Burgon	Rod 1 Domain
Nuclear Prelamin A Recognition Factor (NARF, IOP2)	Component of the endoprotease complex likely involved in the postranslational maturation of prelamin A to lamin A	Barton et al 1999	Carboxy Terminal Domain of prelamin A
Nuclear Titin (TTN, Connectin)	In non-muscle cells, nuclear isoforms are essential for chromosome condensation and chromosome segragation during mitosis	Zastrow et al 2006	Unknown
PCNA (Proliferating Cell Nuclear Antigen)	Nuclear protein Co-factor for DNA polymerase delta Helps increase processivity of leading strand synthesis during DNA replication	Shumaker et al 2008	Unknown
Protein Kinase C Alpha (PKCA, PRKCA)	Calcium activated and phospholipid-dependent kinase involved in signal transduction and cell communication Normally expressed in cytosol but lots of evidence points to its localization in the nucleus (Buchner 1995 Eur J Biochem) Reports on isolated nuclei say that PKCA can be found constitutively in the nucleus Confocal microscopy experiments show that it is found in cytoplasm and nucleus in resting cells PKCs have been known to phosphorylate nuclear proteins (Buchner 1995 Eur J Biochem)	Martelli et al 2000	Last 166 residues of lamin A
Retinoblastoma 1 (Rb1, Rb)	Regulator of cell proliferation and differentiation Tumor suppression factor	M A Mancini et al 1994, Ozaki et al 1994	Unknown
Sterol Regulatory Element Binding Transcription Factor 1 (SREBF1, SREBP1) a and c	Involved in both cholesterol biosynthesis and adipogenesis, including the expression of genes involved in fatty acid metabolism	Lloyd et al 2002, Capanni et al 2005	Carboxy Terminal Domain
Sterol Regulatory Element Binding Transcription Factor 2 (SREBF2, SREBP2)	Acts mainly to stimulate cholesterol biosynthesis	Lloyd et al 2002, Capanni et al 2005	Carboxy Terminal Domain
SUN1	Role in nuclear positioning by connecting nuclear envelope to cytoplasm NTD positions it at INM and CTD with Nesprin isoforms in NE	Haque et al 2006	Unknown
Synaptic Nuclear Envelope Protein 1 (SYNE1, Nuclear Envelope Spectrin Repeat Protein 1, Nesprin-1, MYNE-1)	Transmembrane protein of the inner nuclear membrane Connects the nucleus to the cytoskeleton by interacting with the nuclear aenvelope and F-actin in the cytoplasm Expressed primarily in cardiac, skeletal and smooth muscle tissue	Mislow et al 2002	Unknown
SYNE-2, Nesprin-2, NUANCE	Localizes more to the outer nuclear membrane than Nesprin-1 and is more abundant in cardiac and skeletal muscle than its cousin	Zhang et al 2005	Unknown
Thymopoietin (TMPO, TP, Lamina-associated polypeptide 2A LAP2)	Non-membrane isoform of LAP family Identified as part of nucleoskeleton and is implicated in nuclear structure organization during cell cycle	Dechat et al 2000	Residues 319-572
Ubiquitin Conjugating Enzyme E21 (Ubc9, UBE1)	E2 conjugating enzyme of SUMO pathway Functions in transfer of ubiquitin or SUMO to an active cystine residue of a substrate protein	Zhong et al 2005	Unknown
Zinc Finger Protein 239 (ZNF239, MOK2)	Transcription factors able to recognize DNA and RNA and nuclear ribonucleoproteins	Dreuillet et al 2002	Residues 243-387

The lamin A/C proteins have over 30 known binding partners, including proteins of the inner nuclear membrane, transcription factors, enzymes and chromatin (Table 1). They can interact with other structural proteins, like actin and emerin, while interacting with transcription factors, like Srebp, and with chromatin. The function of all the interactions is not well understood but some suggest lamin A/C acts as a scaffold for maintaining inner nuclear organization (Heessen and Fornerod 2007). In cells lacking A-type lamin expression or expressing functional mutations in the *LMNA* gene many have reported the mislocalization of binding partners (Rao et al 1997, Bechert et al 2002, Muchir et al 2003, Hubner et al 2006, Ostlund et al 2006, Dreuillet et al 2008).

1.2 Diseases Associated with LMNA Mutations

1.2.1 Laminopathies

Diseases involving mutations in the *LMNA* gene are termed laminopathies and are associated with more than ten distinct phenotypes, affecting striated muscle, nervous tissue, white fat distribution, skin and bone tissue, as well as cause premature aging. There is no clear genotype-phenotype relationship between the location of the mutation and the associated disease phenotype (Figure 1.4).

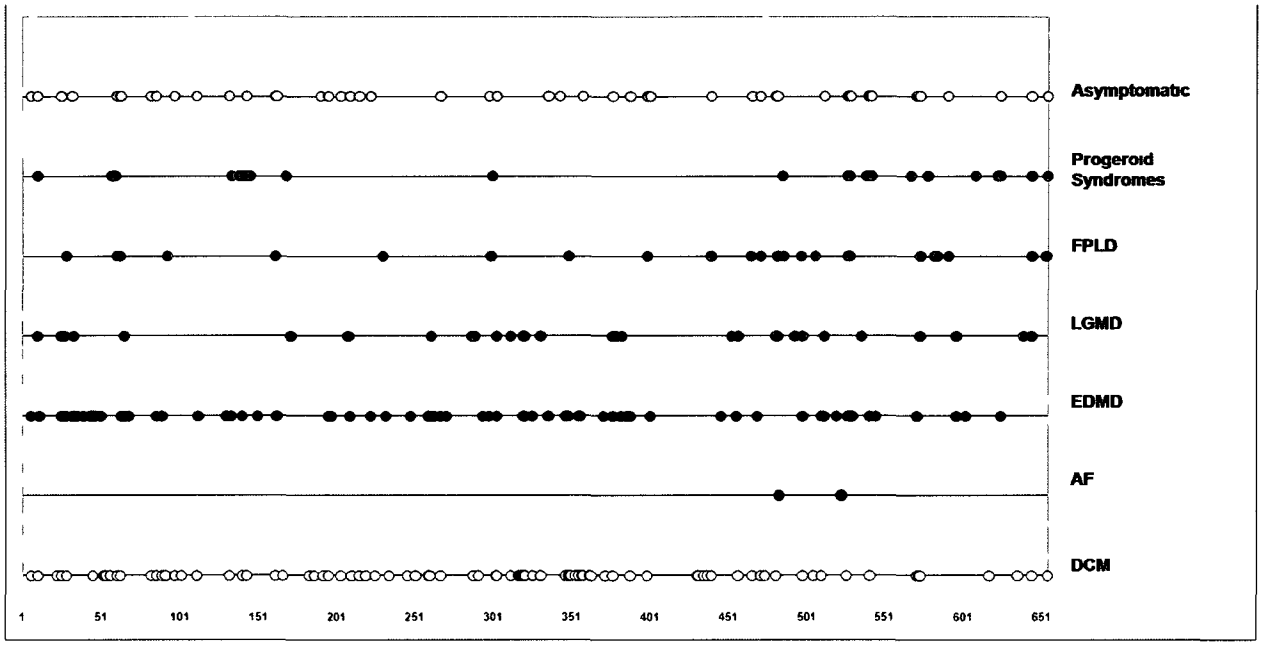

Figure 1.4 Schematic of the LMNA gene with the location of detected mutations and their associated disease. No genotype/phenotype correlation is observed. Mutations were added as part of literature search throughout period of MSc and are added as they are published. Disorders indicated represent the cardiac disorders (Atrial Fibrillation [AF] and Dilated Cardiomyopathy [DCM]), the muscular dystrophies (Emery Dreifuss Muscular Dystrophy [EDMD] and Limb Girdle Muscular Dystrophy [LGMD]), and the lipodystrophies (Familial Partial Lipodystrophy [FPLD]).

1.2.1.1 Cardiac Specific

There are two cardiac-specific diseases associated with mutations in the *LMNA* gene: Dilated Cardiomyopathy (DCM) and lone Atrial Fibrillation (lone AF). Furthermore, the majority of LMNA mutation carriers with various forms of muscular dystrophy develop cardiac complications, such as conduction defects, arrhythmias, and left ventricular dilatation (reviewed in Sylvius and Tesson 2006) indicating a cardiac-specific pathogenicity of LMNA mutations.

Dilated cardiomyopathy

DCM is a primary form of heart muscle disease that is characterized by the dilatation of one or both ventricles and impaired systolic contraction (Richardson et al 1996). DCM hearts weigh 2-3 times normal, sometimes exceeding 1000g, and thin ventricular walls (Luk et al 2009). Diagnosis is based on a low left ventricular ejection fraction (<45%) and increased left ventricular end diastolic diameter (>117%) (Luk et al 2009). Cardiac tissue samples from patients with DCM indicate the presence of myocyte hypertrophy, interstitial fibrosis (Dec et al 1994). DCM is clinically heterogeneous as patients may appear to be symptomless but also have very severe dilatation. In fact, in 75-85% of cases, the initial manifestation of the disease is heart failure (Dec et al 1994). This disease usually manifests in middle age and the majority of deaths occur within three to five years of the onset of symptoms due to progressive heart failure and other complications such as arrhythmias (Dec et al 1994, Luk et al 2009).

DCM is most commonly caused by ischemic injury such as myocardial infarction or coronary artery disease, however it is also a byproduct of severe long-standing hypertension, viral myocarditis, toxin abuse, and radiation. Idiopathic DCM (IDC) has a prevalence of 36 cases per 100,000 population and accounts for approximately 10,000 deaths annually (Dec et al 1994).

IDC has been reported to be associated with viral transmission (Dec et al 1985, Archard et al 1987, Zhang et al 2004), immune abnormalities (Ronnblom et al 1991, Ueno et al 2007) as well as familial transmission. Familial DCM is estimated to account for up to 50% of IDC patients (Malhotra and Mason 2009). Familial DCM is genetically heterogeneous; it is generally inherited following an autosomal dominant pattern (70%), but autosomal recessive (19%), X-linked (10%) and mitochondrial transmission exist (Grunig et al 1998, Mestroni et al 1999). Disease-associated genes include those encoding sarcomere and sarcomere-associated protein genes, cytoskeletal protein genes, nuclear protein genes, and ion channel protein genes or genes regulating calcium metabolism.

Mutations in the *LMNA* gene are one of the most frequently detected mutations in DCM populations, at about 5% (Sylvius and Tesson 2006). This was calculated based on a meta-analysis of the literature of 649 DCM probands genotyped from 1999 to 2006. Most DCM patients with *LMNA* mutations present with a worse prognosis and higher event-rates (Taylor et al 2003, van Berlo et al 2005, Sylvius and Tesson 2006). There are high rates of cardiac dysrhythmias, heart failure, and sudden death (van Berlo et al 2005). A large portion of patients undergo pacemaker implantation, however it does not appear to protect against sudden death in these populations (van Berlo et al 2005).

Lone Atrial Fibrillation

Atrial fibrillation (AF) is characterized by the rapid and random contractions of the atria causing irregular heartbeat. Since some of the impulses from the atria do not pass through the atrioventricular junction, the ventricles cannot contract in response. AF is typically identified by the absence of a P wave on an ECG. AF is found in about 1% of the general population and in 6% of >65 year old population (Feinberg et al 1995).

Usually, AF presents with other cardiac diseases, however it can be present without previous cardiac pathology – lone AF. Lone AF is seen in about 15% of all AF cases. A recent estimate indicates up to 15% of lone AF is of genetic origin (Darbar et al 2003). AF is commonly characterized as an ion channelopathy as mutations have been identified in genes involved in potassium and sodium currents (*KCNQ1* and *SCN5A*). However, non-ion channel genes have also been identified. Recently, *NUP155*, a member of the nuclear pore complexes (NPC), was identified as an AF-associated gene (Zhang et al 2008a). The identified mutation results in the inhibition of heat shock protein 70 (HSP70) mRNA export and import of HSP70 protein.

1.2.1.2 Skeletal Muscle Specific

There are two striated-muscle-specific diseases associated with mutations in the *LMNA* gene: Autosomal Dominant Emery Dreifuss Muscular Dystrophy (AD-EDMD), and Limb Girdle Muscular Dystrophy Type 1B (LGMD1B). The first disease-associated *LMNA* mutation was found in a family of AD-EDMD patients (Bonne et al 1999). Typically these patients present with progressive muscle wasting of the head, upper arms, and lower legs and early contractures of the elbow, Achilles tendons and spinal extensor muscles. These muscular symptoms usually precede cardiac symptoms including cardiomyopathies and atrial conduction defects (Brown et al 2008). Autosomal recessive transmission of this disease is associated with mutations in the gene encoding Emerin, an inner nuclear membrane lamin A/C binding protein. LGMD1B association with *LMNA* mutations was discovered shortly thereafter (Muchir et al 2000) and is associated with muscle wasting of the pelvic and shoulder muscles and presentation of fewer cardiac complications than AD-EDMD.

1.2.1.3 Lipodystrophies

Two main lipodystrophies have been found to be associated with *LMNA* mutations – Dunnigan type familial partial lipodystrophy (FPLD) and Mandibuloacral dysplasia (MAD). FPLD involves a loss of adipose tissue in the trunk and limbs with accumulation of adipose tissue in the neck and face. FPLD often leads to type-II diabetes and increased susceptibility to atherosclerosis. The most common disease associated mutation falls at residue Arg482 (Vigouroux and Capeau 2005), however other associated mutations have also been discovered (Figure 1.4). MAD is an autosomal recessive disorder that involves partial lipodystrophy as well as postnatal growth retardation.

1.2.1.4 Premature Aging Syndromes

The premature aging syndromes tend to fall into a separate category since they are multisystem disorders. In 90% of cases, Hutchinson Gilford Progeria Syndrome (HGPS) is caused by a *denovo* single base substitution that leads to no change in the amino acid sequence (Gly608Gly) but the introduction of a splice site. This leads to the formation of a truncated form of lamin A that is permanently farnesylated – progerin (Eriksson et al 2003).

1.2.2 Complications in Laminopathy Research

Genotype-phenotype relationship

When mutations in the *LMNA* gene were first described, there appeared to be a predictive nature in identifying laminopathies as certain mutations and regions of lamin A/C were associated with particular phenotypes. Over the last 11 years, over 300 mutations have been identified and there does not seem to be any relationship between the location of the mutation

and the associated phenotype (Figure 1.4). Certain laminopathies, however, are associated with hotspots of mutations. Over 90% of HGPS cases are due to a *denovo* single base substitution (Eriksson et al 2003) and FPLD is most commonly associated with mutations at residue Arg482 (Vigouroux and Capeau 2005). However, other mutations have also been found in patients with these disorders (Figure 1.4).

Overlapping phenotypes

Not all laminopathies have clear delineations between phenotypes. AD-EDMD patients often present with cardiomyopathy and cardiac conduction disorders (Brown et al 2008). FPLD patients have been described with skeletal and cardiac muscle involvement (Vantyghem et al 2004) and HGPS patients often develop coronary artery disease.

Overlapping mutations

Furthermore, some mutations are associated with multiple phenotypes in different patients. For example, the Arg644Cys mutation has been found in DCM (Genschel et al 2001, Rankin et al 2008), atypical HGPS (Csoka et al 2004), lipodystrophy (Rankin et al 2008), various skeletal and cardiac muscle complications (Mercuri et al 2005) and in a number of patients with motor neuropathies, scoliosis and contractures (Rankin et al 2008). It has also been reported that one mutation within a family can cause multiple disorders. Brodsky et al (2000) reported a family with a deletion in exon 6 causing a frameshift at codon 320. One member of the family presented with classic DCM, while another presented with mild AD-EDMD and another with mild LGMD1B.

New diseases

In addition to the most commonly described laminopathies mentioned above, *LMNA* mutations are being found in even more disorders with unique phenotypes. Gambineri et al (2008) described the case of two sisters with polycystic ovarian syndrome (PCOS) and partial lipodystrophy with a *LMNA* mutation. Renou et al (2008) described a patient with Heart-Hand Syndrome (also known as Holt-Oram Syndrome) with a *LMNA* mutation. Furthermore, in 2009, we and one other group identified *LMNA* mutations in patients with lone Atrial Fibrillation (AF) (Brauch et al 2009, Saj, Dabrouski, Labib et al manuscript submitted Journal of Translational Research).

1.2.3 Models of Laminopathies

Cardiac Patient histology

There is large variability in the abnormalities observed in tissue biopsies from DCM patients. Some *LMNA* variants (mutations and deletions) exhibit reduced lamin A/C in myocyte nuclei (Arbustini et al 2002, Verga et al 2003, Gupta et al 2010), while others exhibit nuclear membrane damage such as focal disruptions and blebs (Arbustini et al 2002, Verga et al 2003, Gupta et al 2010), the accumulation of mitochondria and other cytoplasmic organelles within the nucleoplasm (Sylvius et al 2005, Bilinska et al 2006, Gupta et al 2010), the accumulation of glycogen in the nucleoplasm (Sylvius et al 2005), chromatin disorganization (Verga et al 2003, Sylvius et al 2005, Gupta et al 2010), and even a complete loss of the nuclear envelope or lamina (Verga et al 2003, Sylvius et al 2005, Bilinska et al 2006, Gupta et al 2010). Patients also exhibit clustering of NPCs at the nuclear membrane (Arbustini et al 2002, Verga et al 2003). However,

not all myocardial samples with *LMNA* mutations present with nuclear abnormalities (Gupta et al 2010).

Skin Fibroblasts

Skin fibroblasts isolated from patients with various laminopathies provide a method to visualize the pathophysiology of disease-associated mutations. These skin fibroblasts most often have abnormalities in nuclear shape, including blebs and herniations (Vigouroux et al 2001, Caux et al 2003, Eriksson et al 2003, Muchir et al 2003, Muchir et al 2004, Verstraeten et al 2009). These areas generally are devoid of B-type lamins, NPCs, lap2β, and chromatin (Vigouroux et al 2001, Caux et al 2003, Muchir et al 2003). Lamin A/C distribution is also affected in these cells, as they are either present in a honeycomb pattern (Vigouroux et al 2001, Novelli et al 2002, Caux et al 2003, Muchir et al 2004) or unevenly distributed along the inner nuclear lamina (Favreau et al 2003). Some fibroblasts had lamin A/C aggregates close to the lamina which did not interact with emerin, DNA or RNA (Capanni et al 2003, Muchir et al 2004).

Animal Models

A number of mouse models of the laminopathies have been developed over the years. Before we begin our discussion of them, it is important to note that the mice with laminopathy symptoms are homozygous for mutations while most human laminopathies are autosomal dominant. Furthermore, the mouse models present some features directly opposite to that observed in humans. For example, fibroblasts from a patient with no *LMNA* expression shows reduced proliferative capacity (Muchir et al 2003), however, fibroblasts from *LMNA* knockout mice show increased proliferative rates (van Berlo et al 2005, Ivorra et al 2006).

The *LMNA* gene knockout mouse model was the first laminopathy mouse model to be developed (Sullivan et al 1999). These mice develop normally until birth but present with postnatal growth retardation starting at 2 weeks. All the mice are dead by 8 weeks due to extensive muscular dystrophy and cardiomyopathy. Embryonic fibroblasts from these mice (referred to as $MEF^{-/-}$ from now on) have irregularly shaped nuclei in >80% of cells and present with herniations devoid of NPCs, lamin B and lap2 as seen in patient skin fibroblasts (Sullivan et al 1999). Mice expressing only one copy of the LMNA gene ($LMNA^{-/+}$) develop normally and at 1 year they develop atrioventricular conduction defects with atrial and ventricular arrhythmias and impaired contractility (Wolf et al 2008).

The DCM mouse model has a point mutation at Asn195Lys originally described in a DCM patient. The homozygous mouse develops cardiac conduction defects and death at three months due to cardiac arrhythmias (Mounkes et al 2005). The $MEF^{N195K/N195K}$ cells have misshapen nuclei, increased nuclear fragility under mechanical strain, and impaired gene transcription.

The EDMD mouse model has a point mutation at His222Pro which was originally identified in an AD-EDMD patient. The homozygous mice do not show any disease phenotypes neonatally or until sexual maturity, however they develop muscular dystrophy and DCM in adulthood similar to humans with AD-EDMD (Arimura et al 2005). All the mice die by 13 months age.

The FPLD mouse model has a point mutation at Arg482Gln driven by the aP2 enhancer/promoter to ensure adipose tissue specific expression. These mice (heterozygous) develop normally until birth but develop FPLD in adulthood (Wojtanik et al 2009).

There are two models of progeria syndromes. The first one developed was a fortunate introduction of a splice site. Mounkes et al (2003) introduced an EDMD mutation (Leu530Pro) which resulted in a splicing defect which left a permanently farnesylated lamin A. The second model produces only progerin and develops classic HGPS symptoms (Yang et al 2005). However, neither of these models develops arterial plaques that are commonly seen in HGPS.

Cell Culture

Since patient tissue samples and skin fibroblasts are not always easily acquired, and since the development of mouse models is a lengthy and expensive process, researchers have turned to the use of established cellular models in an effort to elucidate the mechanisms leading to particular disease phenotypes. In the study of laminopathies, commonly used models are C2C12 cells and Cos7 cells.

C2C12 is a mouse myoblast cell line isolated from C3H mouse leg muscle. These cells express muscle-specific proteins and have the ability to differentiate rapidly, forming contractile myotubes. C2C12 mouse model is used to study striated muscle laminopathies including DCM, as there is no reliable cardiac cell line that expresses cardiac-specific proteins. Cos7 cells are immortalized CV-1 cells (fibroblast) derived from the kidney cells of the African Green Monkey with a version of SV40 monkey virus genome that results in a defect in genomic replication. This is a continuous cell line with very fast *in vitro* growth rates and high transfection rates.

Different point mutations present with variable phenotypes including a honeycomb pattern of lamin A/C protein (Muchir et al 2004, Kandert et al 2007, Kandert et al 2009, Verstraeten et al 2009) and the formation of mutant lamin A/C aggregates (e.g. Raharjo et al 2001, Ostlund et al 2001, Sylvius et al 2005, Sylvius et al 2008), while others appear to have no effect on lamin A/C localization and assembly (Sylvius et al 2008). Furthermore, when the

mutant of each lamin isoform is expressed individually, it presents with a different phenotype compared to the other isoform (Sylvius et al 2008). Since the nuclear lamins play such an important role in nuclear stability (see below), the formation of mutant aggregates indicates the disruption of normal lamina assembly, and thus reduced ability to cope with mechanical stress.

1.3 The Role of lamin A/C in Nuclear Organization and Cellular Function in Laminopathies

A-type lamins display a diverse functional role, exemplified by their various binding partners. Lamin A/C are important for nuclear architecture, as they provide mechanical strength, determine nuclear shape and anchor and space NPCs. They also play an important role in transcription and gene regulation, as well as in cellular signaling.

1.3.1 Nuclear Architecture

The fact that lamins are crucial in the maintenance of nuclear structure is evident in their strong interaction with the inner nuclear membrane, that NPCs are connected by lamins and from the structural abnormalities encountered in laminopathy cells (described above). They provide mechanical strength (Lammerding et al 2004, Broers et al 2004, Pajerowski et al 2007), determine nuclear shape and structure (Sullivan et al 1999, Broers et al 2004, Raharjo et al 2001), and they anchor and space NPCs (Broers et al 2004).

Cells isolated from *LMNA* knockout mice ($MEF^{-/-}$ cells) subjected to mechanical strain were more susceptible to nuclear deformation and cell death compared to normal cells (Lammerding et al 2004, Lammerding et al 2006). $MEF^{-/-}$ cells also showed reduced mechanical

stiffness which necessitates less force required to compress these cells compared to normal (Broers et al 2004). This effect on cellular strength could explain the progression of dystrophic laminopathies due to constant mechanical stress.

Over 80% of $MEF^{-/-}$ nuclei presented with elongated or irregularly shaped nuclei indicating the importance of lamin A/C in nuclear shape. Nuclear lamina structure is based on critical interactions between lamins and inner nuclear membrane proteins and cytoskeletal proteins. When these interactions are impaired, either due to loss of lamin A/C expression or disease-associated *LMNA* mutations, nuclear structure and strength are affected (Raharjo et al 2001, Broers et al 2004).

The NPC is a 125MDa complex of proteins involved in the nucleo-cytoplasmic transport of small proteins (up to 60kDa), mRNA and ions across the nuclear membrane. Lamin A/C plays an essential role in the proper spacing of NPCs (Maeshima et al 2006, Furukawa et al 2009).

1.3.2 Transcription and Gene Regulation

Lamin A/C plays a large role in the regulation of gene transcription. A dominant negative lamin A mutant inhibits RNA polymerase II activity (Spann et al 2002) while overexpression of lamin A/C was shown to downregulate RNA polymerase II transcription (Kumaran et al 2002). Lamin A was also shown to mediate transcriptional repression of promoters with GAL4 binding sites in yeast and in human 293T cells (Lee et al 2009). Furthermore, skin fibroblasts from FPLD patients with *LMNA* mutations showed reduced incorporation of bromouridine indicating that the mutant lamin A/C interferes with RNA transcription (Capanni et al 2003). The mechanism of this impairment is not clear. Possible explanations could be lamin A/C's interactions with chromatin and a variety of transcription factors, as well as through the reported lamin A/C regulation of RNA splicing.

Lamin A/C have been shown to colocalize with RNA splicing factors in Splicing Factor Compartments (SFC) (also known as interchromatin granulated clusters – IGC) (Jagatheesen et al 1999) and overexpression of lamin A and C results in the disruption of these SFCs. SFCs are clusters where splicing factors are concentrated on newly synthesized transcripts prior to assembly. Lamin A/C has also been reported to interact with heterogeneous nuclear riboprotein E1 (hnRNPE1) (Zhong et al 2005), a reported SFC-associated protein (Mintz et al 1999) which has been shown to colocalize with these clusters (Chkheidze and Liebhaber 2003). This particular localization suggests that hnRNPE1 plays a role in pre-mRNA splicing.

Lamins play an important role in chromatin organization. Firstly, A-type lamins interact with chromatin (Burke 1990, Glass and Gerace 1990) via the rod domain (Glass et al 1993) and the tail domain (Taniura et al 1995). They bind particular regions of DNA called Matrix Attachment Regions (MARs) which are responsible for attaching chromatin to the nuclear matrix (Luderus et al 1994). With regards to chromatin organization, $MEF^{-/-}$ cells have a loss of peripheral heterochromatin (Sullivan et al 1999, Nikolova et al 2004). Cells from certain laminopathies also display a loss of peripheral heterochromatin or a general loss of heterochromatin (Vigouroux et al 2001, Sabatelli et al 2001). Epigenetic patterns have been shown to be affected in myoblasts from AD-EDMD patients as well as in C2C12 cells transfected with AD-EDMD mutations (Hakelien et al 2008). It has also been suggested that lamin A relocalizes transcriptional promoters to the heterochromatin-rich nuclear periphery so transcription is not permitted (Lee et al 2009).

The nuclear lamina has been described as a "resting place" for transcription factors (Heessen and Fornerod 2007). In fact, lamin A/C has been reported to interact with seven transcription factors (Table 1): Retinoblastoma protein 1 (Rb1) (Mancini et al 1994, Ozaki et al

1994), MOK2 (Dreuillet et al 2002), Sterol Regulatory Element Binding Proteins 1 and 2 (Lloyd et al 2002, Capanni et al 2005), Mel18 (Zhong et al 2005), Epidermal Growth Factor (Zhong et al 2005), c-Fos (Ivorra et al 2006), and Muscle Lamin Interacting Protein (Mlip) (personal communications with Patrick Burgon). These interactions appear to have a role in transcriptional repression (Dreuillet et al 2002, Ivorra et al 2006) as well as protection from proteasome degradation (Johnson et al 2004).

Srebp1 is a member of the basic helix-loop-helix leucine zipper transcription factor family that binds the sterol regulatory element 1 and is involved in both the regulation of cholesterol biosynthesis (Yokoyama et al 1993) and in adipogenesis (Kim and Spiegelman 1996). In sterol-depleted cells, the 125kDa precursor Srebp1 found in the endoplasmic reticulum membrane is translocated to the Golgi where it is cleaved to generate the 68kDa mature form (Wang et al 1994, DeBose-Boyd et al 1999). The mature Srebp1 translocates to the nucleus where it activates genes involved in cholesterol biosynthesis and adipogenesis such as LDL-receptor, HMG-CoA synthase and peroxisome proliferator-activated receptor-γ (PPARγ). In cells of FPLD patients expressing endogenously high levels of pre-lamin A, Srebp1 is retained at the nuclear rim, thus reducing the amount of DNA-bound Srebp1 (Capanni et al 2005, Maraldi et al 2007). This sequestration results in the down-regulation of PPARγ and therefore reduces adipocyte differentiation.

Muscle lamin interacting protein (Mlip) is a novel lamin A/C binding partner discovered by Patrick G Burgon (University of Ottawa Heart Institute). Mlip was identified in a yeast-2-hybrid screen of a human heart cDNA library with the rod1 domain of lamin A as bait. Bioinformatic analyses of Mlip revealed it to be a novel single copy gene that encodes proteins with no known structural or functional domains. Mlip is localized in the whole cell with diffuse

staining in the cytoplasm and punctate staining in the nucleus, colocalizing with promyelocytic leukemia (PML) nuclear bodies. Preliminary work from Dr. Burgon's lab indicates it is a transcription factor involved in myogenic differentiation.

1.3.3 Signaling

Lamin A/C also plays a role in the regulation of signaling cascades. Muchir et al (2007a,b and 2009b) demonstrated that the mitogen activated protein kinase (MAPK) signaling cascade is activated in His222Pro mouse hearts, specifically identifying activation of ERK pathway in the development of cardiomyopathies caused by LMNA mutations (Muchir et al 2009a). Furthermore, defective Nfκ B signaling was observed in $MEF^{-/-}$ cells (Lammerding et al 2005).

As previously mentioned, PKCα was identified as a lamin A/C binding partner during IGF-1 treatment (Martelli et al 2000). IGF-1 and phorbol-ester treatment have been repeatedly linked to PKCα translocation to the nucleus, specifically to the nuclear rim and interior, excluding the nucleolus (DiVecha et al 1991, Leach et al 1989, Neri et al 1994, Zini et al 1995). Characterization of this interaction indicates that PKCα interacts with lamin A/C at the C-terminal tail, downstream the two PKC phosphorylation sites (Leukel and Jost 1995), thus this binding is not relevant to lamin A/C phosphorylation by PKC (Martelli et al 2002). Lamin A/C acts as a scaffold bringing PKCα to its downstream nuclear substrates such as C23/nucleolin (Martelli et al 2002), PTB-associated splicing factor, p68 RNA helicase, and hnRNP A3 and L (Rosenberger et al 2002).

Ubc9, the E2 conjugating enzyme of the Sumo pathway was identified as a lamin A/C binding partner in a yeast-2-hybrid assay (Zhong et al 2005). Sumoylation, like ubiquitination, is a post-translational modification involving the physical binding of the Sumo protein to its substrates. Sumoylation is associated with several critical cellular processes by regulating the

function and activity of its substrates, many of which are transcription factors. Ubc9 is the only reported conjugating enzyme in the Sumo process and is crucial for its proper substrate targeting. Sumo1 cellular localization is disrupted in C2C12 and Cos7 cells transfected with DCM and EDMD associated *LMNA* mutations (Sylvius et al 2005, Boudreau, Labib et al manuscript in preparation) and substrate conjugation has been shown to be increased (Boudreau, Labib et al manuscript in preparation) (Please see below for more information). Furthermore, Lamin A has been shown to be covalently modified by Sumo 2 and 3 (Zhang and Sarge 2008).

1.3.3.1 Sumo

Post translational modification by a small polypeptide is most often associated with ubiquitylation by ubiquitin. Sumo (small ubiquitin-like modifier) is a highly conserved ubiquitin-like modifier involved in a large variety of critical cellular processes, unlike ubiquitin which is most often associated with the targeting of its substrates for proteasome degradation. Sumo and Ubiquitin share a similar structure, and contain a C-terminal diglycine motif, yet they share less than 20% amino acid sequence identity (Bayer et al 1998).

Prior to protein targeting, the inactive precursor to Sumo undergoes carboxy-terminal cleavage by Sumo-specific isopeptidases (sentrin-specific proteases; SENPs) in order to free the C-terminal diglycine motif for conjugation. There are subsequently three steps in the conjugation of Sumo to its target protein (Figure 1.5). Sumo is activated in an ATP-dependent step by the formation of a thioester link between the C-terminus of Sumo and the Cystein residue of its E1 activation enzyme, Aos1-Uba2. The C-terminal carboxy group of Sumo is then transferred to the Cysteine residue of its E2 conjugating enzyme, Ubc9, in a thioester linkage. Ubc9 transfers Sumo to its substrate protein. An isopeptide bond is formed between the C-terminal Glycine residue of Sumo and the Lysine residue of the target protein, often in the presence of an E3

ligase (Figure 1.6a). Since Sumoylation is a transient and reversible process, the Sumo peptide is cleaved from its target protein with the help of a member of the SENP family of proteases.

The critical step in this process is the interaction with Ubc9, a Sumo-specific member of the E2 family of conjugating enzymes. These enzymes play a central role in the conjugation cascade transporting the ubiquitin or ubiquitin-like protein (Sumo in this case) between the E1 activating enzyme and the substrate. Ubc9 is a single copy gene with ubiquitous expression in all human organs and tissues. It is unique in the E2 family in that it directly interacts with a Sumo consensus sequence - ψKxE where ψ is a large hydrophobic residue (Rodriguez et al 2001, Bernier-Villamor et al 2002). Although Ubc9 is most often associated with Sumoylation, there is increasing evidence of Ubc9 function independent of Sumo as a regulator of nuclear transport and co-regulator of transcription (Kurtzman and Schechter 2001, Kaul et al 2002). Ubc9 expression is upregulated in tumor specimens where it is reported to promote cell invasion and metastasis in a Sumo-independent manner (McDoniels-Silvers et al 2002, Mo and Moschos 2005, Wu et al 2009). Others have shown that single nucleotide polymorphisms (SNP) in Ubc9 in breast tumors are associated with tumor grade (Dunnebier et al 2009) and with Alzheimer's (Ahn et al 2009). Loss of Ubc9 expression results in embryonic lethality in C. elegans (Jones et al 2002) and in mice (Nacerddine et al 2005). Cells from these mice show defects in nuclear organization, chromosome condensation and segregation and failure of RanGAP1 to accumulate at the NPCs (Nacerddine et al 2005).

The classically recognized Sumo consensus sequence is ψKxE where the central Lysine is the site of conjugation. Ubc9 directly recognizes this site and interacts with it and Sumo to catalyze conjugation. Recently, additional sites have been identified in close association to the classic Sumo motif: Phosphorylation-Dependent Sumoylation Motif (PDSM) and Negatively

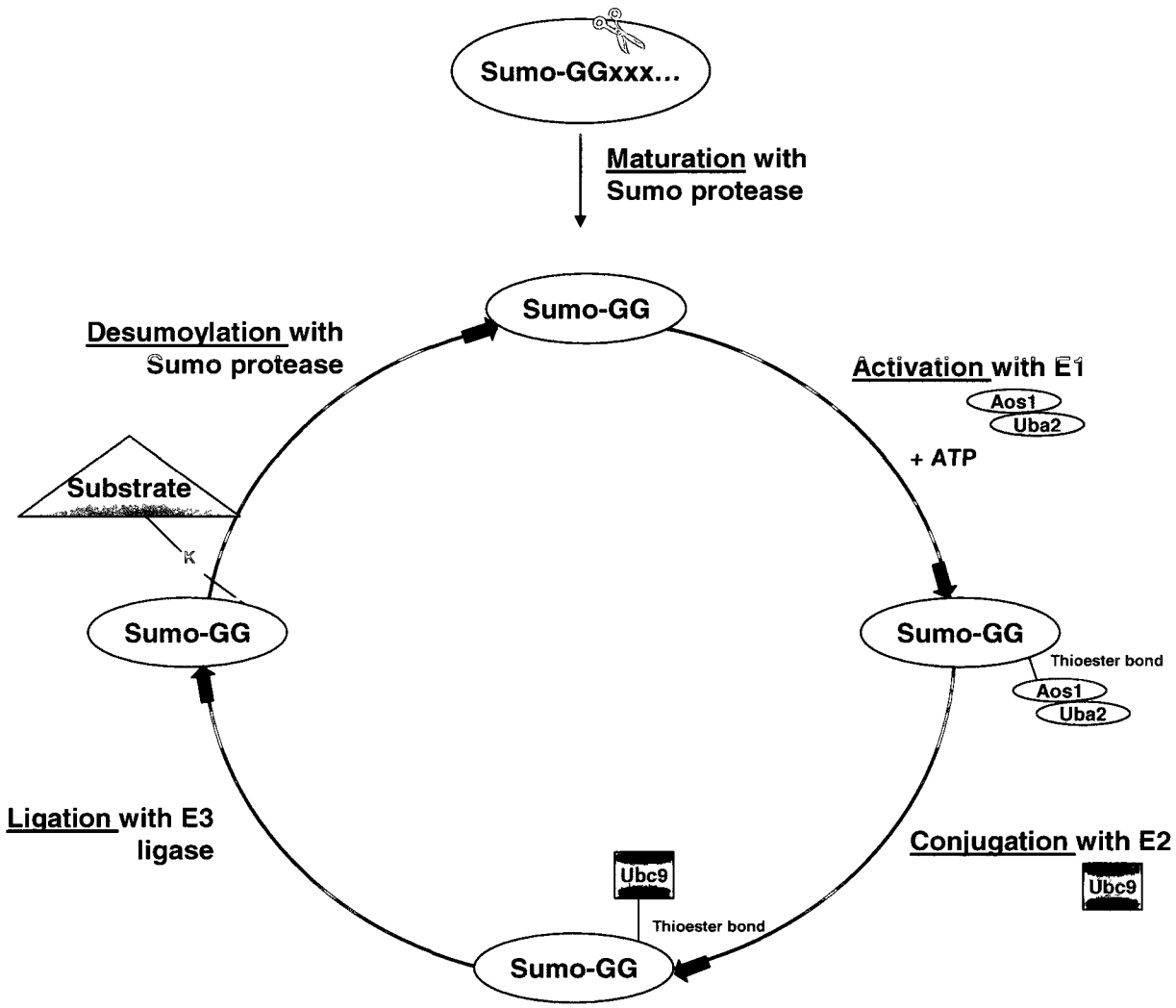

Figure 1.5 Schematic diagram of the Sumo process showing five enzymatic reactions to form an isopeptide bond between the Sumo1 protein and its target protein. The first step in the pathway is a Maturation step where a Sumo protease exposes a carboxy-terminal glycine residue. The Activation step is an ATP-dependent formation of a thioester conjugate between the Sumo C-terminal glycine residue and the cystein of the E1 activating enzyme Aos1-Uba2. The Sumo is then passed from the E1 complex to the E2 conjugating enzyme, Ubc9, forming a thioester intermediate. It is then ligated, with or without the help of an E3 ligating enzyme, to a lysine residue on the target protein. The final step is the deconjugation of Sumo from its target with a Sumo protease.

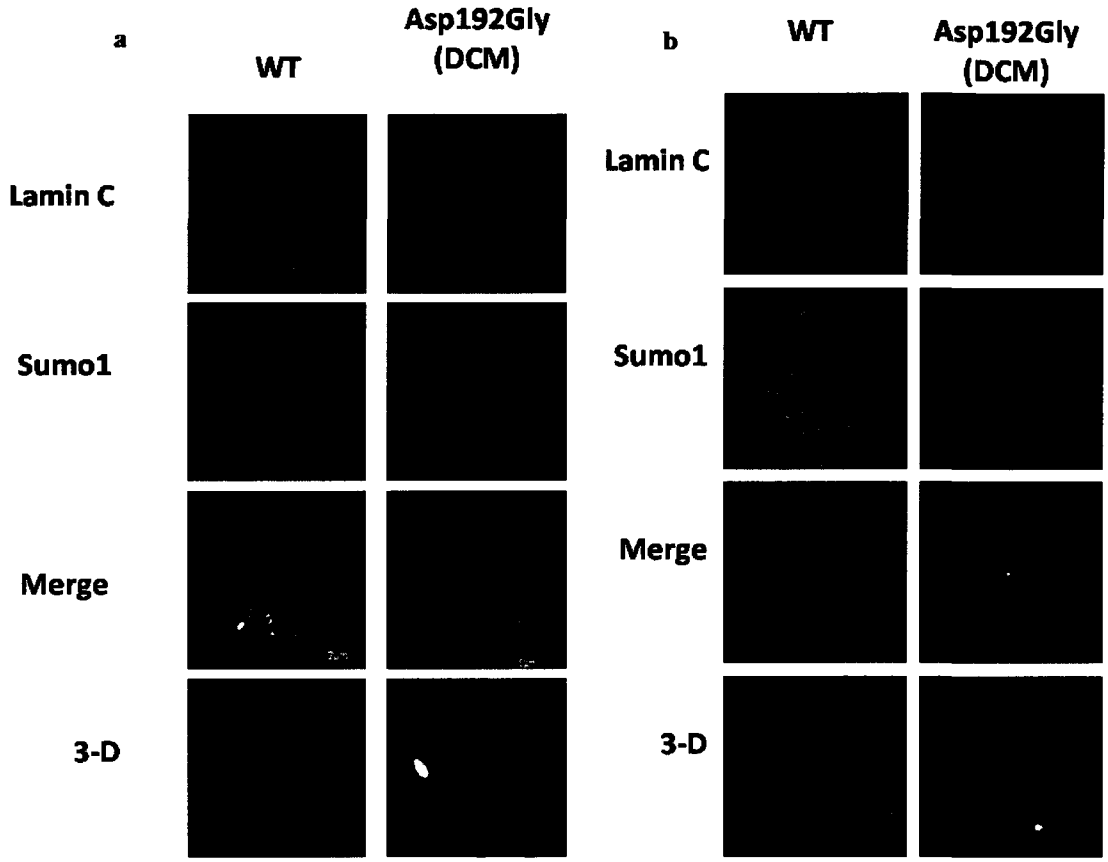

c

```
  1 METPSQRRAT RSGAQASSTP LSPTRITRLQ EKEDLQELND RLAVYIDRVR
 51  SLETENAGLR LRITESEEVV SREVSGIKAA YEAELGDARK TLDSVAKERA
101  RLQLELSKVR EEFKELKARN TKKEGDLIAA QARLKDLEAL LNSKEAALST
151  ALSEKRTLEG ELHDLRGQVA KLEAALGEAK KQLQDEMLRR VDAENRLQTM
201  KEEFLDFQKN IYSEELRETKR RHETRLVEID NGKQREFESR LADALQELRA
251  QHEDQVEQYK KELEKTYSAK LDNARQSAER NSNLVGAAHE ELQQSRIRID
301  SLSAQLSQLQ KQLAAKEAKL RDLEDSLARE RDTSRRLLAE KEREMAEMRA
351  RMQQQLDEYQ ELLDIKLALD MEIHAYRKLL EGEEERLRLS PSPTSQRSRG
401  RASSHSSQTQ GGGSVTKKRK LESTESRSSF SQHARTSGRV AVEEVDEEGK
451  FVRLRNKSNE DQSMGNWQIK RQNGDDPLLT YRFPPKFTLK AGQVVTIWAA
501  GAGATHSPPT DLVWKAQNTW GCGNSLRTAL INSTGEEVAM RKLVRSVTVV
551  EDDEDEDGDD LLHHHHGSHC SSSGDPAEYN LRSRTVLCGT CGQPADKASA
601  SGSGAQVGGP ISSGSSASSV TVTRSYRSVG GSGGGSFGDN LVTRSYLLGN
651  SSPRTQSPQN CSIM
```

Figure 1.6 Sumo1 trapping within mutant lamin C aggregates and location of Sumo consensus sequences in lamin A. (a-b) Sumo1 is normally found homogeneously distributed throughout the nucleus and to a small extent in the cytoplasm. Sumo1 distribution, in the presence of DCM-associated LMNA mutation Asp192Gly is disrupted and found trapped within lamin C aggregates. (a) Cos7 (Nicolas Sylvius) and (b) C2C12 (Sarah Labib) cells were transiently transfected with wild type or mutant lamin C-dsRed and Sumo1-YFP and visualized by fluorescent confocal microscopy. (c) Lamin A amino acid sequence indicating the location of three Sumo1 consensus sequences.

charged amino acid Dependent Sumoylation Motif (NDSM). The PDSM contains a site for phosphorylation three amino acids downstream the classic motif, ψKxExxS/TP (Hietekangas et al 2006) while the NDSM consists of negatively charged amino acids within 10 amino acids downstream (Yang et al 2006 EMBO). Sumo is also capable of interacting with other proteins (Song et al 2004). However, a consensus sequence is not always necessary for Sumo conjugation (see Discussion for more detail).

Vertebrates have three Sumo genes: Sumo1 (also known as PIC1, UBL1, Sentrin, GMP1, and SMT3C), Sumo2 (also known as SMT3A), and Sumo3 (also known as SMT3B). Sumo2 and Sumo3 have 97% sequence identity and are often referred collectively as Sumo2/3, while they only share 50% similarity with Sumo1. Sumo2/3 are able to form chains due to the presence of an internal Sumo consensus sequence within their N-terminal tail (Tatham et al 2001). Sumo1 and Sumo2/3 have distinct target sets (Saitoh and Hinchey 2000, Rosas-Acosta et al 2005, Vertegaal et al 2006) indicating distinct functions.

Of the Sumo paralogues, Sumo1 is the best characterized as it was the first to be discovered and is distinct from Sumo2 and Sumo3. Sumo1 is primarily found conjugated to proteins *in vivo* compared to Sumo2/3 which are mostly found unconjugated (Saitoh and Hinchey 2000) indicating a functional role for Sumo1 at steady state. Sumo1 however appears to be dispensable for normal mammalian development. Initially, a mouse model was developed using the gene trap system which was embryonic lethal (Alkuraya et al 2006). However, in 2008, two groups independently generated Sumo1 knockout mouse models using gene trapping and homologous recombination (Evdokimov et al 2008, Zhang et al 2008b, respectively) showing no

effect on embryonic or postnatal development most likely due to compensatory action by Sumo2/3 on Sumo1 targets (Evdokimov et al 2008).

We have previously shown an effect of certain *LMNA* mutations on Sumo1 function. In wild type cells, Sumo1 is found distributed evenly throughout the nucleoplasm and cytoplasm, however in cells transfected with p.Asp192Gly lamin C, Sumo1 is sequestered within the mutant aggregates (Figure 1.6a). This altered localization has been confirmed in C2C12 cells (Figure 1.6b) and with other mutations, some with Sumo1 sequestration while others have Sumo1 colocalization with the mutant aggregates (Boudreau, Labib et al, manuscript in preparation). In myoblasts isolated from the His222Pro mouse there is aberrant localization of Sumo1 into intranuclear foci and outlining the nuclear envelope (Boudreau, Labib et al, manuscript in preparation). Lamin A/C localization is not affected in these mouse myoblasts (Arimura et al 2005). Sumo1 staining in muscle tissue shows striking nuclear envelope localization in approximately 25% of His222Pro nuclei compared to wild type muscle tissue with homogeneous punctate Sumo1 nuclear and cytoplasmic localization (Boudreau, Labib et al, manuscript in preparation). Correlated with changes in Sumo1 localization, we have also shown that certain *LMNA* mutations increase Sumo1 conjugation profiles in C2C12 cells, as well as the amount of non-conjugated Sumo1 (Boudreau, Labib et al manuscript in preparation). No one has studied Sumo2/3 involvement in laminopathies, however since the 2008 article showing lamin A sumoylation by Sumo2/3 (Zhang and Sarge), we are currently investigating this path.

1.4 Hypotheses and Objectives of Proposed Study

General Hypothesis: *LMNA* mutations exert their tissue-specific effects via the perturbation of lamin A and C's specific interacting partners.

Because of the lack of a clear genotype-phenotype correlation in the laminopathies, I have set out to determine how *LMNA* mutations affect their binding partners with functions and attributes specific to particular tissues and diseases. I will investigate two lamin A and C binding partners, PKCα and Ubc9, signaling molecules involved in several critical cellular processes with the aim of developing personalized therapies for any of the associated disorders.

Aim 1: Identify specific phenotypes associated with three laminopathies: lone AF, DCM, and DCM with AF.

PKCα is a protein kinase implicated in heart failure and cardiac hypertrophy (Braz et al 2004, Vijayan et al 2004). It is a known lamin A/C binding partner that interacts with its carboxy terminal domain. Furthermore, abnormal PKCα function results in irregular I_{Kach} activity associated with chronic AF (Voigt et al 2007). Therefore, I will be investigating the effect of DCM and lone AF associated *LMNA* mutations in the C-terminal tail on PKCα cellular distribution. This will follow an *in vitro* study on whether or not these previously uncharacterized mutations differentially affect the cellular distribution of lamin A/C.

Objectives:

1. To compare the nuclear distribution of lamin A and C induced by *LMNA* mutations associated with lone AF (Thr528Met), DCM (Arg541Gly, Ser431X), and DCM with AF (Tyr481X).

   Methods: Mutagenesis, Cloning, Cellular transfection, Fluorescent confocal microscopy, Indirect Immunofluorescence.

2. To determine the effects of these mutations on lamin A/C binding partner PKCα cellular distribution.

   Methods: Cellular transfection, Fluorescent confocal microscopy, Indirect Immunofluorescence.

Aim 2: Determine how lamin A and C are implicated in the Sumo process.

Lamin A/C is a reported binding partner of Ubc9, Sumo's E2 conjugating enzyme. We have previously shown that the localization and substrate conjugation of Sumo1 is disrupted in the presence of DCM and EDMD associated *LMNA* mutations. Therefore, I will investigate how lamin A/C plays a role in the Sumo1 process by examining Ubc9 cellular distribution, characterizing the interaction between the two proteins, and by looking at lamin A/C sumoylation by Sumo1.

Objectives

1. Is Ubc9 cellular distribution affected by *LMNA* mutations?

   Methods: Cellular transfection, Fluorescent confocal microscopy.

2. Is the interaction between Ubc9 and lamin A/C affected by *LMNA* mutations?

   Methods: Cloning, Cellular transfection, Co-immunoprecipitation, Western blotting.

3. Determine if lamin A/C is sumoylated by Sumo1.

Methods: Cloning, Cellular transfection, Nuclear protein extraction, Co-immunoprecipitation, Western blotting, Confocal microscopy, Mass spectrometry.

Chapter 2 - Experimental Procedures

Cell Culture

C2C12 embryonic mouse myoblast and Cos7 African green monkey kidney cell lines were obtained from ATCC. C2C12 cells are grown and maintained in Dulbecco's Modified Eagle's Medium (DMEM) supplemented with 15% FBS and 1:100 L-glutamine at 37^0C and 5% CO_2. Cells are kept below 80% confluence and in high FBS concentration to discourage cellular differentiation. Cos7 cells are grown and maintained in MEM (Minimum Essential Medium) supplemented with 10% FBS and 1:100 L-glutamine at 37^0C and 5% CO_2.

Cloning and Site-directed Mutagenesis

Site-directed mutagenesis was performed on previously cloned wild type lamin A-CFP and lamin C-YFP to introduce Thr528Met, Arg541Gly, Ser431X, and Ty481X mutations. The mutagenesis reaction was performed using Stratagene's site-directed mutagenesis kit. The following primers were used: a) Thr528Met Forward 5'- GGG AAC AGC CTG CGT ATG GCT CTC ATC AAC TCC-3' and Reverse 5'- GGA GTT GAT GAG AGC CAT ACG CAG GCT GTT CCC-3', b) Arg541Gly Forward 5'- GAA GAA GTG GCC ATG G GCA AGC TGG TGC GC-3' and Reverse 5'- GC GCA CCA GCT TGC C CAT GGC CAC TTC TTC-3', c) Ser431X Forward 5'- GAG AGC CGC AGC AGC TTC TAA CAG CAC GCA CGC ACT AGC-3' and Reverse 5'- GCT AGT GCG TGC GTG CTG TTA GAA GCT GCT GCG GCT CTC-3', d) Tyr481X Forward 5'- GAT GAT CCC TTG CTG ACT TAA CGG TTC CCA CCA AAG TTC AC-3' and Reverse 5'- GT GAA CTT TGG TGG GAA CCG TTA AGT CAG CAA GGG ATC ATC-3'. Briefly, DNA was amplified using High Fidelity PfuUltra Taq Polymerase. PCR products were digested with Dpn1 restriction enzyme for 1 hour at 37^0C to break down the product to facilitate

transformation. DNA was transformed into XL10 Gold E Coli (Stratagene) and grown in LB broth supplemented with Kanamycin. Direct sequencing was performed to confirm presence of mutations. For general upkeep of all clones used, constructs are cloned into DH5α competent cells (Invitrogen). Mini and Maxi preparations of the DNA are performed according to manufacturer protocols (Qiagen and Invitrogen, respectively). All constructs are sequenced prior to use.

Transfection

For protein harvesting, C2C12 cells are transfected with Metafectene Pro (Biontex) and Cos7 cells with Lipofectamine 2000 (Invitrogen). Cells for microscopy are transfected with Lipofectamine 2000 (Invitrogen). Both methods are based on the properties of lipofection which uses liposomes to inject genetic material. Cells are transfected between 70 and 80% confluence and harvested after 18-22 hours. Briefly, plasmic DNA is incubated with lipofection reagent to allow for DNA-liposome complexes to form. These complexes are then incubated with the cells for 4-6 hours to allow for efficient transfer. The following clones are used: WT or mutant lamin A in pECFP (previously cloned, see Sylvius et al 2005), WT or mutant lamin C in pECFP, pEYFP, dsRed2 (see Sylvius et al 2005), Ubc9 in pEGFP (previously cloned) or HA (kind gift from Peter Howley (Yasugi and Howley 1996)), Sumo1 in pEYFP (kind gift from Dr. Heidi E McBride) or HA, and Mlip in pcDNA3 (kind gift from Dr. Patrick G Burgon). All vectors contain CMV promoter for constitutively active expression.

Cell Fixation and Staining

C2C12 cells grown on coverslips are washed with PBS 1X three times and fixed with ice-cold methanol for five minutes at -20^{0}C. Methanol is washed off in three washes with PBS for five minutes each. For cells to be used in mitochondrial, endoplasmic reticulum or PKCα staining, cells are fixed with 4% paraformaldehyde for 20 minutes at room temperature, then washed three times in PBS. Following fixation, cells are blocked and permeabilized with 0.1% TritonX100 in 5% FBS for 20 minutes at room temperature. Cells are hybridized with primary antibody in 1.5% FBS for 1.5 hours at 37^{0}C, washed three times in PBS 1X then incubated with fluorescently labeled secondary antibodies. Cells are washed with PBS 1X three times then coverslips are mounted on glass slides with mounting medium (Dakocytomation #S3023). The following antibodies from Santa Cruz Biotechnology were used: lamin A/C (sc-6215), Ubc9 (sc-10759), Sumo1 (sc-5308), HA (sc-7392), GFP (sc-69779), RanGAP (sc-1862), TOM20 (sc-11415), and PKCα (sc-208), as well as EMD (Novocastra, NCL-EMERIN), Calreticulin (Abcam, ab2907), and Mlip (gift from Patrick G Burgon, University of Ottawa Heart Institute).

Nuclear Protein Extraction

Nuclear protein is extracted using the Active Motif Nuclear Extract kit (AM40010) as described in user manual. Briefly, cells are scraped in PBS with Phosphatase Inhibitors, spun down, resuspended in a hypotonic buffer to lyse cell membranes and spun down. The supernatant is the cytoplasmic fraction. The nuclear pellet is resuspended with lysis buffer supplemented with DTT and protease inhibitors and incubated for 30 minutes. After centrifugation, the supernatant is collected. 20mM N-ethylmaleimide (NEM) is added to the lysis buffer to maintain covalent Sumo linkages prior to use.

Co-Immunoprecipitation

500μg nuclear protein is incubated with 25μl washed Protein G magnetic beads (Dynal – Invitrogen) for 1 hour at 4^0C to reduce nonspecific binding. 2μg primary antibody is added to each sample (anti-GFP sc-9996, anti-HA sc-7392, anti-lamin A/C sc-6215) and incubated rotating at room temperature for three hours. The protein/antibody solution is incubated with 25μl washed Protein G magnetic beads for 1 hour at room temperature. The sample is washed three times in 1X PBS supplemented with 50mM NaCl and 0.1% Tween, boiled with SDS sample buffer with DTT at 95^0C for five minutes, cooled, separated by magnet and loaded onto gel.

Western Blot

Samples are run on 4-20% gradient Tris-Glycine SDS-PAGE gel at constant voltage (180V) for 1.5 hours in a Tris-Glycine Running Buffer (18.8g glycine, 3.3g Tris, 1.0g SDS, 1000ml ddH_2O). The protein is transferred onto nitrocellulose membrane for 2-3 hours at constant current (300mA) in transfer buffer (14.2g glycine, 3.0g Tris, 200ml methanol, 800ml ddH_2O). The membrane is stained with Ponceau Red staining to visualize protein loading and blocked with 5-10% skim milk powder in 1X PBS-Tween (PBST-milk), and incubated overnight with primary antibody. For co-immunoprecipitations, the membrane is blocked for 3 hours at room temperature with Pierce Native IgG Detection Reagent at 1:50 dilution (#21230). The membrane is washed three times in PBST-milk for five minutes each, incubated with secondary antibody at for 1 hour at room temperature, and washed three times with PBST (2 x 10 min, 1 x 5 min). Amersham ECL Western Blotting Detection Reagent is added for 2 minutes (#RPN2109) and the protein is visualized using an electrochemiluminescence detecting machine (AlphaInotech).

Mass Spectrometry

Samples are run on 4-20% gradient Tris-Glycine gel, as described above. The gel is stained in Coomassie Blue for 1 hour at room temperature and destained overnight. Protein bands of interest are cut out and sent to Alphalyse Inc for protein analysis by mass spectrometry. Briefly, the protein samples are reduced and alkylated with iodoacetamide (i.e.. they are carbamidomethylated) and digested with trypsin that cleaves after lysine and arginine residues. The resulting peptides are concentrated and eluted onto an anchorchip for analysis on a Bruker Autoflex III MALDI TOF/TOF instrument. The peptide mixture is analyzed and 5-10 of the peptides are selected for analysis by MS/MS fragmentation for partial peptide sequencing. The combined MS data for each sample is searched against a protein database containing millions of protein sequences. Protein identification is based on a probability-scoring algorithm and the significant best matching protein is reported. The protein score is a measure of how random the match of amino acids is between the predicted sequence and the obtained sequence at a significant level ($p<0.05$). A score of greater than 67 is considered significant. The score is calculated as -10log of the probability of occuring as a random event.

Chapter 3 – The Identification of Specific Phenotypes Associated with Three Laminopathies

The aim of this chapter is to identify specific phenotypes associated with three laminopathies: lone AF, DCM, and DCM with lone AF.

In order to study this, I had two objectives to meet:

3.1 Compare the nuclear distribution of lamin A and C induced by *LMNA* mutations associated with lone AF (Thr528Met), DCM (Arg541Gly, Ser431X), and DCM with AF (Tyr481X).

3.2 Determine the effect of the mutations on lamin A/C binding partner PKCα cellular distribution.

3.1 Mutant Lamin A/C Localization

In order to compare the lamin A/C protein cellular distribution in cell culture, point mutations were introduced into wild type (WT) lamin A and lamin C in fluorescent expression vectors (pECFP and pEYFP) via site-directed mutagenesis. The presence of mutations was confirmed using direct sequencing. Undifferentiated C2C12 mouse myoblast cells were transiently transfected with WT or mutant lamin A and lamin C. The following experiments have been confirmed in over three independent trials. The percentage of cells of a particular phenotype are determined by finding the sum of all the cells in three separate trials.

The following is a description of the point mutations investigated in this chapter. A point mutation, Thr528Met, was found in a 70-year old man with AF and normal left ventricular size and function. A point mutation was found in a proband with DCM, severe heart failure and AF resulting in the formation of a stop codon, Tyr481X. The patient was 36 years old at the onset of symptoms and was given a heart transplant at 40. He has a family history of the disease. A point

mutation, Arg541Gly, was discovered in a family with DCM and sudden death with no AF. A point mutation was found in a patient with DCM and severe heart failure with no AF resulting in the formation of a premature stop codon, Ser431X.

To more closely emulate physiological stoichiometry, lamins A and C were co-transfected. Overexpression of wild type lamin A and C colocalize at the inner nuclear membrane in undifferentiated C2C12 cells, as is observed with endogenous protein staining (Figure 3.1a).

When Thr528Met (lone AF) mutant lamin A and lamin C are transfected into C2C12 cells, aggregates are formed in ~75% of the cells (Figure 3.1d-f). In 45% of these aggregated cells, the aggregates are sickle-shaped as opposed to circular. It appears that the aggregates are forming extensions of lamin protein to other aggregates nearby and it is these extensions that give off the sickle-shape. Furthermore, approximately 10% of cells exhibit leaking of lamin A/C into the cytoplasm.

When the Tyr481X (DCM/AF) mutant lamin A and lamin C are transfected into C2C12 cells, aggregates are found in about 85% of the transfected cells (Figure 3.1c). The aggregates are relatively large and number between 1 and 10 per cell. The majority of cells with aggregates, however, contain between 2 and 4 aggregates per cell.

When Arg541Gly (DCM) mutant lamin A and lamin C are transfected into C2C12 cells, aggregates develop in about 80% of the cells (Figure 3.1g-i). In 60% of these aggregated cells, the aggregates form sickle-shaped aggregates as opposed to the common circular aggregates. They are similar to the sickles seen in the Thr528Met mutants. Furthermore, approximately 10% of the cells exhibit leaking of the lamins into the cytoplasm.

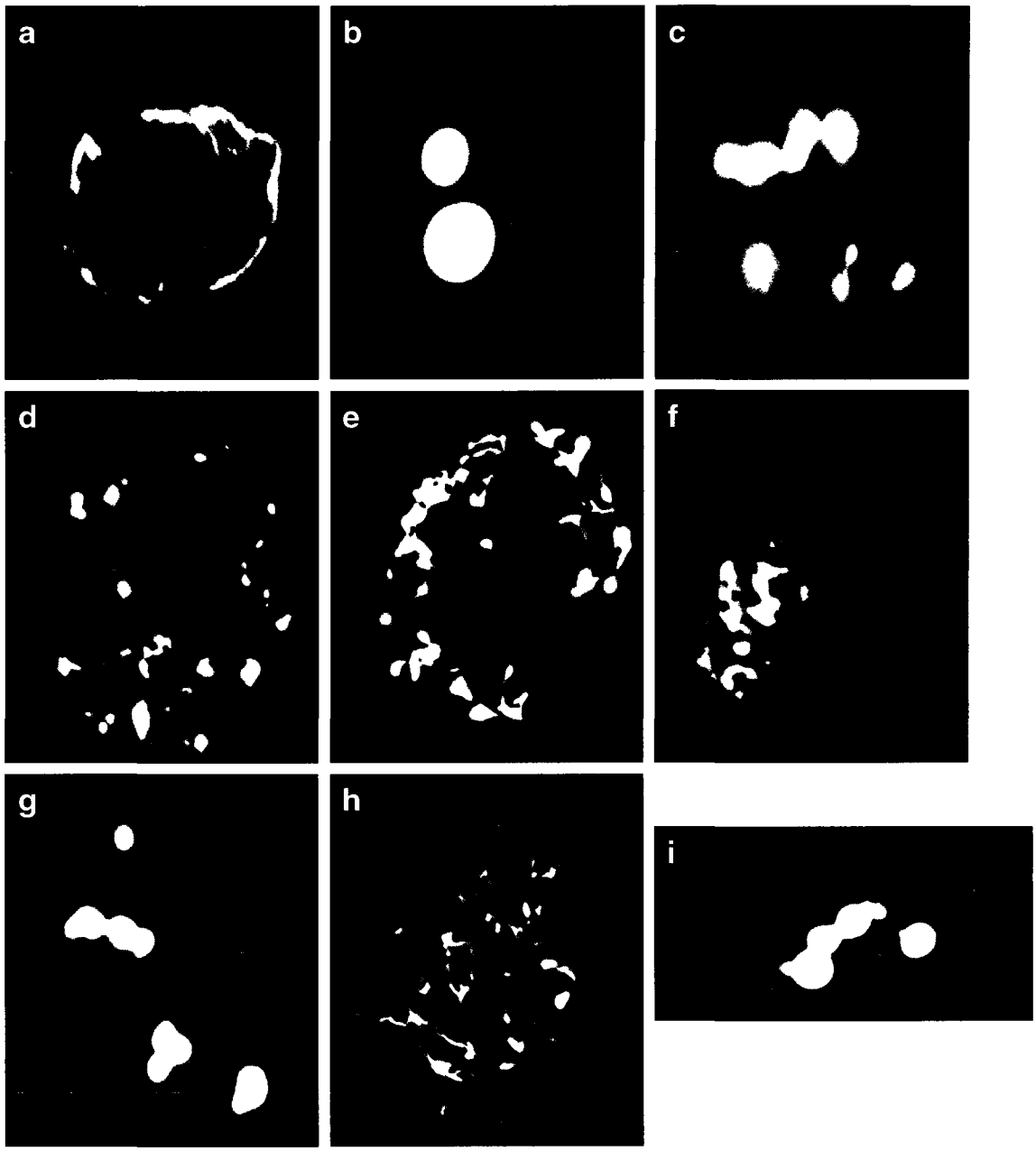

Figure 3.1 AF- and DCM-associated mutant lamin A/C is mislocalized in C2C12 cells. C2C12 cells were transiently transfected with wild type or mutant lamin A and lamin C expressed in fluorescent expression vectors pECFP and pEYFP, respectively. The cells were fixed and visualized by fluorescence microscopy. (a) wild type, (b) Ser431X, (c) Tyr481X, (d-f) Thr528Met representative aggregates, sickles and cytoplasmic leaking, (g-i) Arg541Gly representative aggregates, sickles and cytoplasmic leaking.

When Ser431X (DCM) mutant lamin A and lamin C are transfected into C2C12 cells, about 75% of the cells contain aggregates (Figure 3.1b). These aggregates are relatively large and number between 1 and 10 per cells.

The mutant aggregates are not due to transfection artifacts: cells transfected with wild type and mutant lamins were regulary used in western blotting experiments to control for overexpression between wild type and the different mutants. Figure 3.2 is a representative blot.

3.1.2 Cytoplasmic localization of mutant lamin A/C

Ten percent of cells expressing Thr528Met and Arg541Gly mutant lamin A/C presented with cytoplasmic lamins protruding from the nucleus (Figure 3.1f,i). In order to understand more about the nature of these rogue lamins, we wanted to determine their subcellular localization. Based on the pattern of lamin distribution, we hypothesized that they localized at either the mitochondria or endoplasmic reticulum (ER). We performed indirect immunofluorescence staining with mitochondrial marker TOM20 and ER marker calreticulin. TOM20 is part of a receptor complex on the surface of the mitochondrial outer membrane and calreticulin is a major Ca^{2+} binding protein in the lumen of the ER.

In order to prevent mitochondrial fractionation, cells were exposed to dry air for minimal amounts of time prior to cell fixation. C2C12 cells transfected with the mutants were fixed and stained for TOM20. No colocalization was seen between the lamins and the mitochondria (Figure 3.3).

Calreticulin is seen in the cytoplasm of C2C12 cells. In cells transfected with the mutants, there was partial colocalization between the cytoplasmic lamins and the endoplasmic reticulum (Figure 3.4). Lamin A and C localization is seen in cyan. Cytoplasmic colocalization of lamin

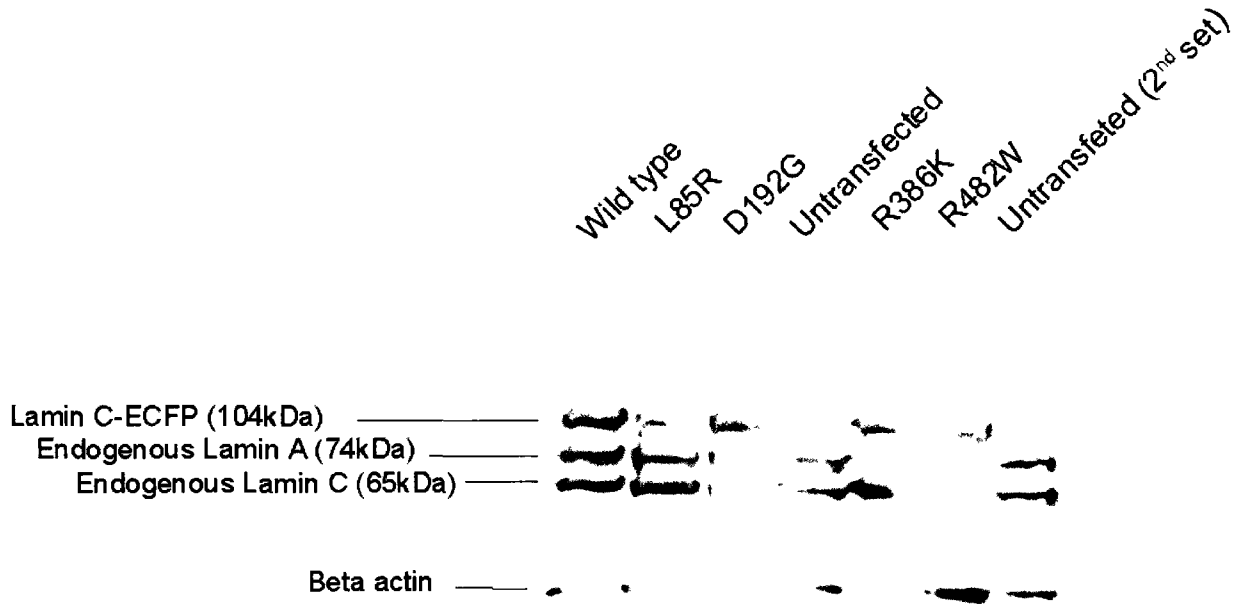

Figure 3.2 Western blot showing equal transfection levels with different lamin C-CFP variants using an anti-lamin A/C antibody. B actin was used as a loading control (Sylvius et al 2008). The mutations used in this blot are those studied in Chapter 4 of this thesis. Western blotting was regularly used as a control of over expression.

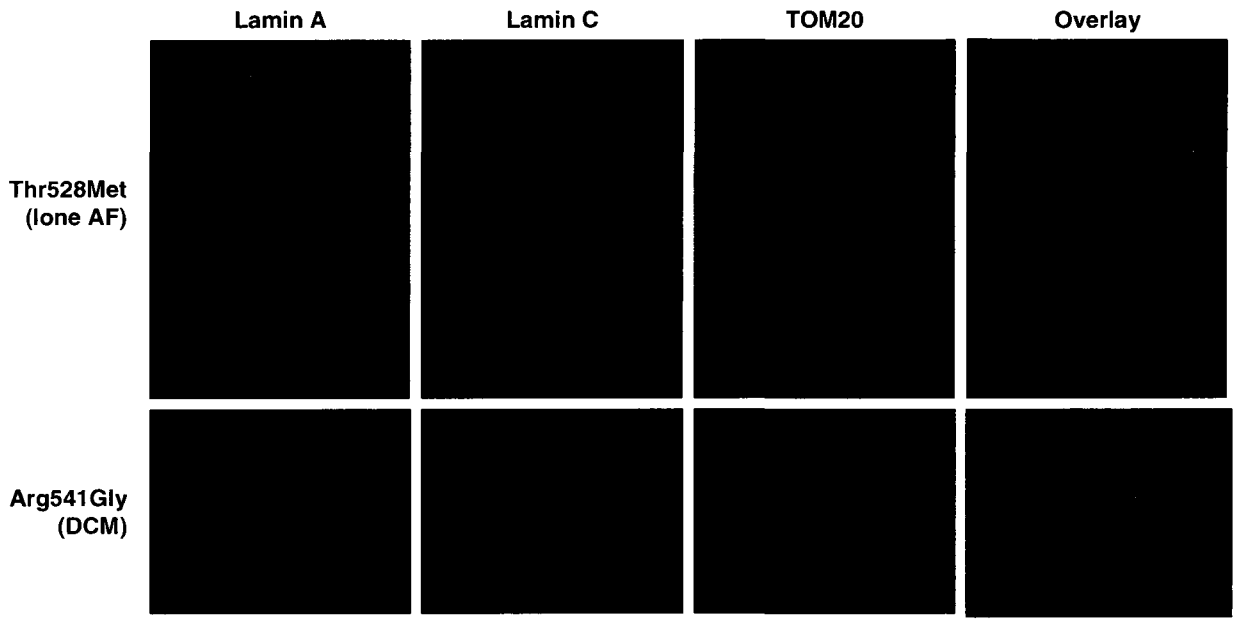

Figure 3.3 Mutant cytoplasmic lamin A/C do not colocalize with mitochondrial marker, TOM20. C2C12 cells were transiently transfected with wild type or mutant lamin A and lamin C in fluorescent expression vectors pECFP and pEYFP, respectively. Cells were fixed with 4% PFA and incubated with primary antibody for TOM20, an outer mitochondrial membrane receptor. Cells were visualized under fluorescent confocal microscopy.

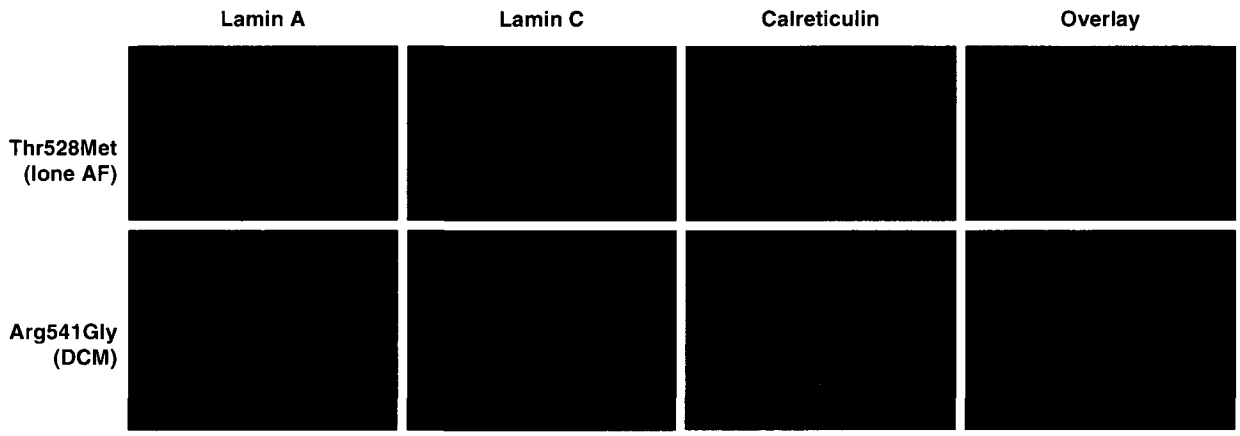

Figure 3.4 Mutant cytoplasmic lamin A/C partially colocalizes with endoplasmic reticulum marker calreticulin. C2C12 cells were transiently transfected with wild type or mutant lamin A and lamin C in fluorescent expression vectors pECFP and pEYFP, respectively. Cells were fixed with ice-cold methanol and incubated with primary antibody for calreticulin. Cells were visualized under fluorescent confocal microscopy.

A/C with calreticulin is seen in purple.

3.2 PKCα cellular distribution

C2C12 cells transfected with WT or mutant lamin A and lamin C were fixed and stained for PKCα. When C2C12 cells were transfected with WT lamin A and lamin C, PKCα was found as expected in the cytoplasm with light staining in the nucleus (Figure 3.5). When Thr528Met (lone AF) mutant lamin A and lamin C are transfected, PKCα presence is increased in the nucleus, while staining is still evident within the cytoplasm. This same phenotype is observed in Arg541Gly (DCM) mutants. However, no change in the cellular distribution of PKCα is observed in cells transfected with Ser431X (DCM) and Tyr481X (DCM/AF) mutants.

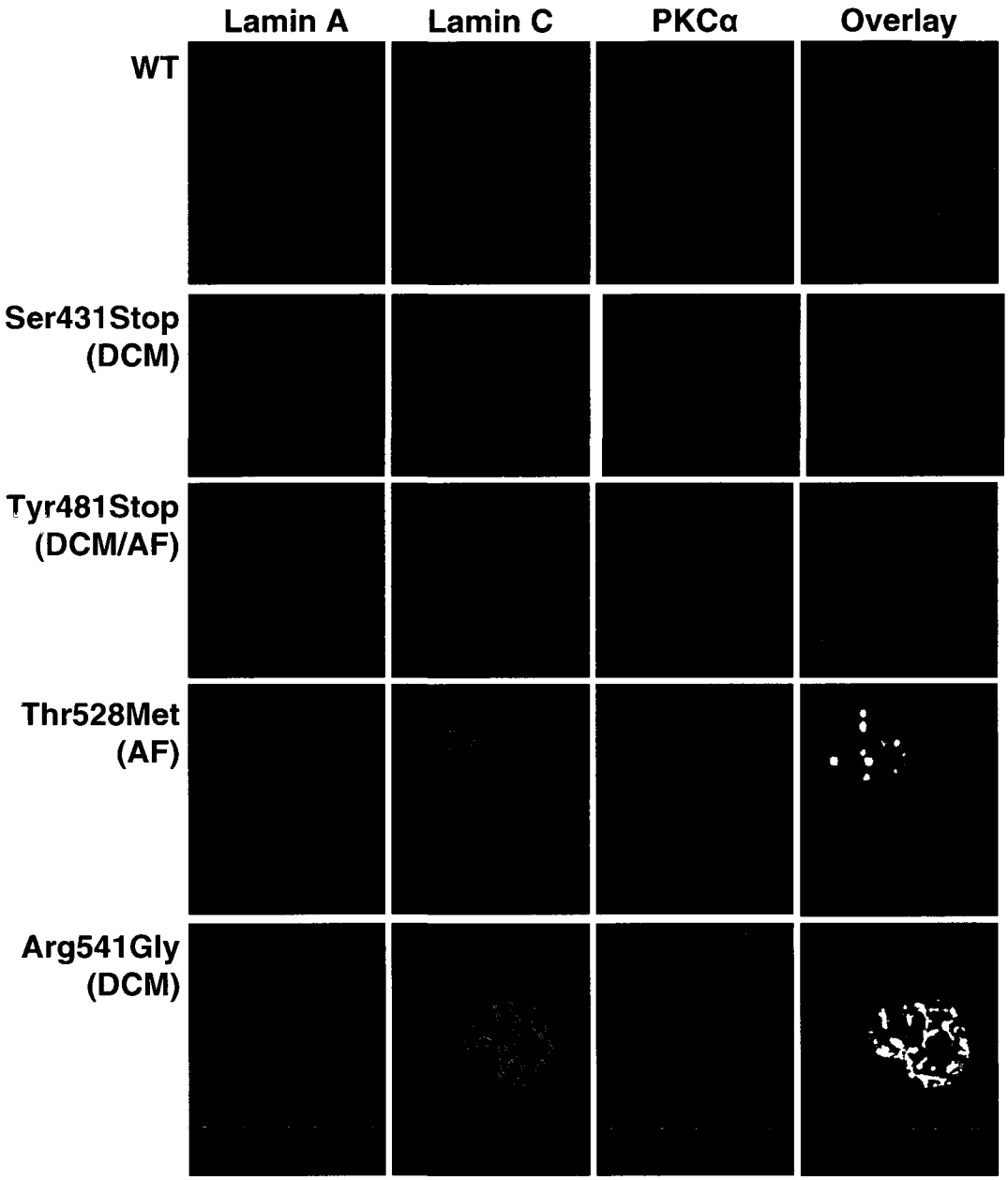

Figure 3.5 PKCα translocates to the nucleus in Thr528Met and Arg541Gly mutant lamin A and C cells. C2C12 cells were transiently transfected with wild type and mutant lamin A and lamin C in fluorescent expression vectors pECFP and pEYFP, respectively. Cells were fixed with 4% PFA and incubated with primary antibody against PKCalpha. Cells were visualized with fluorescent confocal microscopy.

Summary of Chapter 3 Results

The lone AF and DCM-associated mutations result in the perturbation of PKCα cellular distribution, with increased presence in the nucleus compared to wild type cells. This altered localization will affect its overall cellular function as PKCα is involved in many signaling cascades. Interestingly, cellular transfection of fluorescent expression vectors with mutant lamin A and lamin C in C2C12 cells results in the abberrant cellular distribution of lamin A/C. Expression of lone AF-associated p.Thr528Met and the DCM-associated p.Arg541Gly result in the formation of intranuclear aggregates and sickles. The stop mutations, DCM/AF-associated p.Tyr481X and DCM-associated Ser431X, result in the formation of large intranuclear aggregates. Cytoplasmic extrusions of mutant lamin A/C do not colocalize with mitochondrial marker, TOM20, however they appear to partially colocalize with the ER marker calreticulin.

Chapter 4 – Lamin A/C and the Sumo1 Process

In this chapter, I aim to determine how lamin A and C are implicated in the Sumo process. In order to determine the validity of this statement, I have three main objectives to meet:

4.1 Determine the effect of *LMNA* mutations on Ubc9 cellular distribution.

4.2 Determine the effect of *LMNA* mutations on lamin A and C interaction with Ubc9.

4.3 Determine if lamin A/C is sumoylated by Sumo1.

4.1 Ubc9 Cellular Distribution

Since our lab previously showed that lamin A/C mutant aggregates sequestered the Sumo1 protein, we were interested in determining the effect of the mutations on its interaction with reported binding partner Ubc9, the Sumo E2 conjugating enzyme. First we investigated the effect of the mutants on Ubc9 localization. I chose to focus on mutations that are representative of three laminopathies (DCM: Leu85Arg, Asp192Gly, and Gln353Lys; EDMD: Arg386Lys; and FPLD: Arg482Trp) and that were already implicated in altered sumoylation profiles (Boudreau, Labib et al, manuscript submitted).

To more closely emulate physiological stoichiometry, lamins A and C were co-transfected with Ubc9. Overexpressed wild type lamin A and C and Ubc9 colocalize at the inner nuclear membrane in undifferentiated C2C12 cells, as is observed with endogenous protein staining. DCM-associated Leu85Arg and FPLD-associated Arg482Trp lamin A and C-CFP exhibit a phenotype comparable to the wild type (Figure 4.1). DCM-associated Asp192Gly and Gln353Lys lamin A and C-CFP mutants form abnormal aggregates at the periphery of the nucleus. EDMD-associated Arg386Lys lamin A and C-CFP results in large intranuclear aggregates of lamin A/C while still retaining some diffuse intranuclear staining. These results agree with data from our lab and others (Sylvius et al 2005, Raharjo et al 2001, Sylvius et al

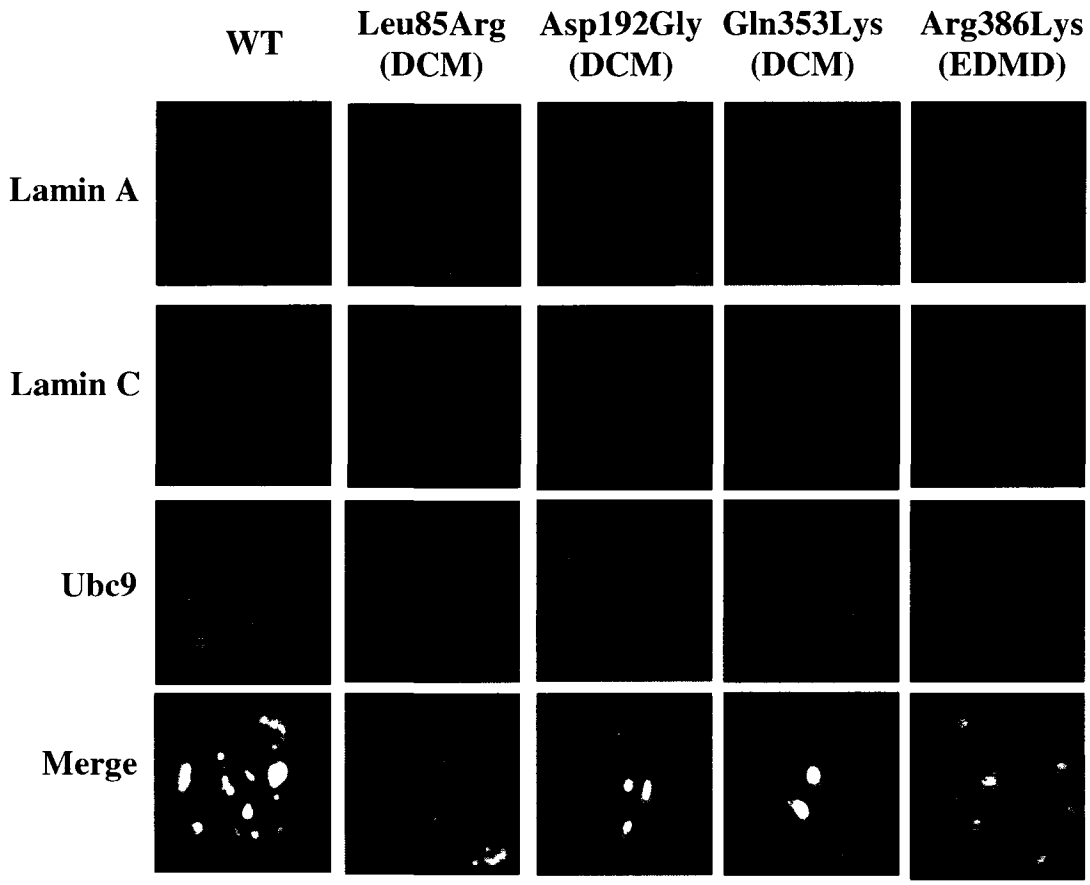

Figure 4.1 Ubc9 is mislocalized in the presence of mutant lamin A and lamin C in C2C12 cells. Cells were transiently transfected with wild type or mutant lamin A-CFP, lamin C-dsRed and Ubc9-GFP and visualized under fluorescent confocal microscopy. Wild type lamin A and C are found homogenously distributed at the inner nuclear envelope. The same phenotype is observed in the DCM-associated Leu85Arg mutation. Here, Ubc9 localizes with the two lamins at the nuclear rim. The DCM-associated Asp192Gly and Gln353Lys and EDMD Arg386Lys mutations result in the expression of lamins A and C in intranuclear aggregates. Ubc9 mislocalizes from the nuclear rim to the location of the mutant aggregates.

2008, Ostlund et al 2001). In the presence of mutant lamin A/C aggregates, Ubc9 is no longer found uniformly expressed at the inner nuclear membrane, rather it appears to co-localize with the mutant lamin A/C speckles. Cells were stained with nuclear pore complex (NPC) protein RanGAP to see if Ubc9 localization with the NPCs is disrupted in the presence of the mutations. As expected, Ubc9 and RanGAP colocalize in wild type cells. However, in Asp192Gly (DCM) and Arg386Lys (AD-EDMD) mutant cells, Ubc9 localization with RanGAP is disrupted, suggesting an effect on NPC distribution (Figure 4.2).

Wild type lamin C alone gives rise to multiple intranuclear aggregates that are evenly distributed throughout the nucleus while wild type lamin A alone is expressed as a homogeneously distributed veil at the inner nuclear envelope (Sylvius et al 2008). C2C12 cells transfected with just lamin A or lamin C (wild type and mutant) yielded similar results to when both A and C are co-transfected, Ubc9 colocalizes with the mutant aggregates (Figure 4.3).

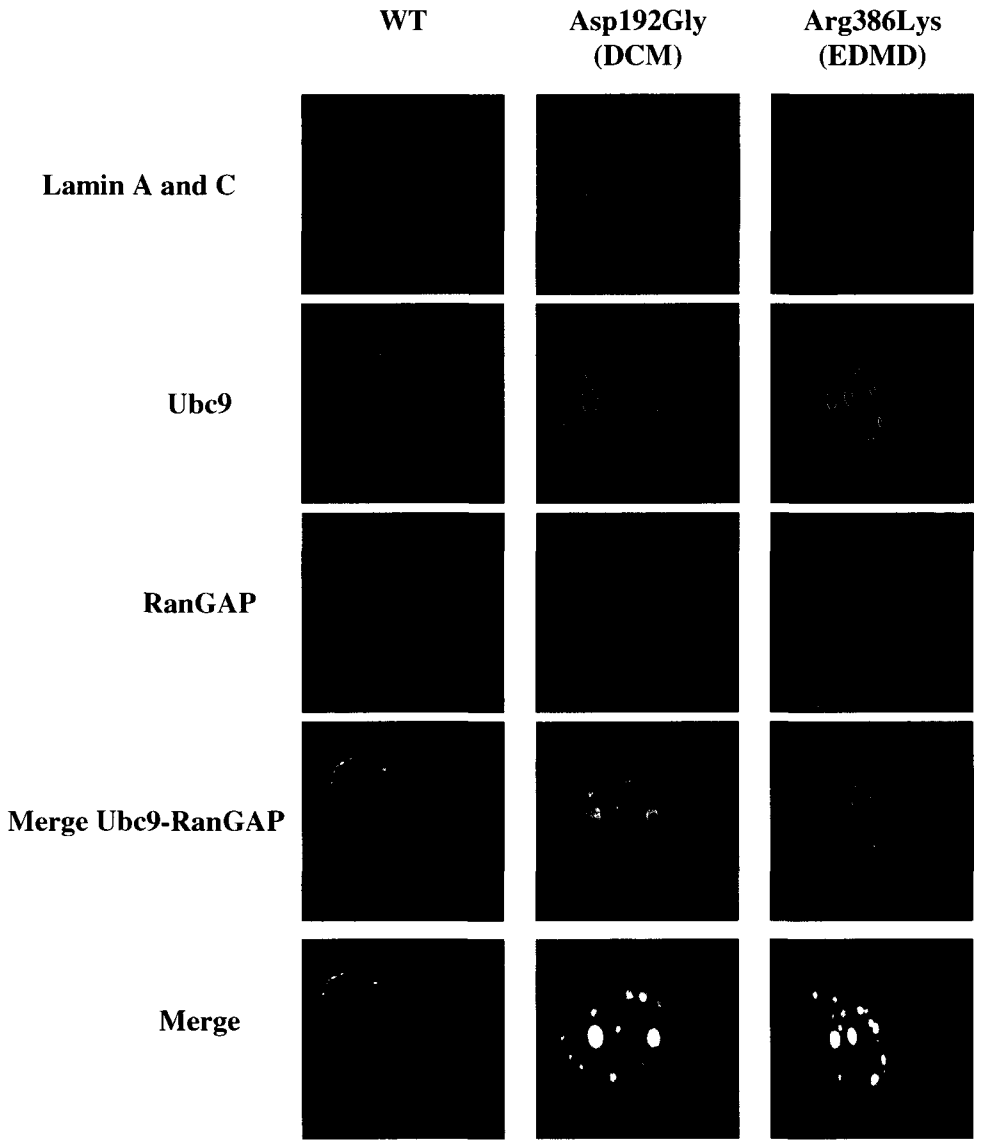

Figure 4.2 Ubc9 is mislocalized with respect to NPC protein RanGAP in mutant lamin A and C expressing cells. C2C12 cells were transiently transfected with wild type and mutant lamin A-CFP and C-CFP and Ubc9-GFP and stained for RanGAP using an anti-RanGAP antibody and fluorescently labeled secondary antibodies. Cells were visualized by fluorescent confocal microscopy. RanGAP is found at the nuclear pore complexes and within the cytoplasm. Ubc9 and WT lamin A/C localize at the nuclear rim with RanGAP. However, in mutant lamin A and C cells, Ubc9 is mislocalized with the mutant aggregates and not with RanGAP.

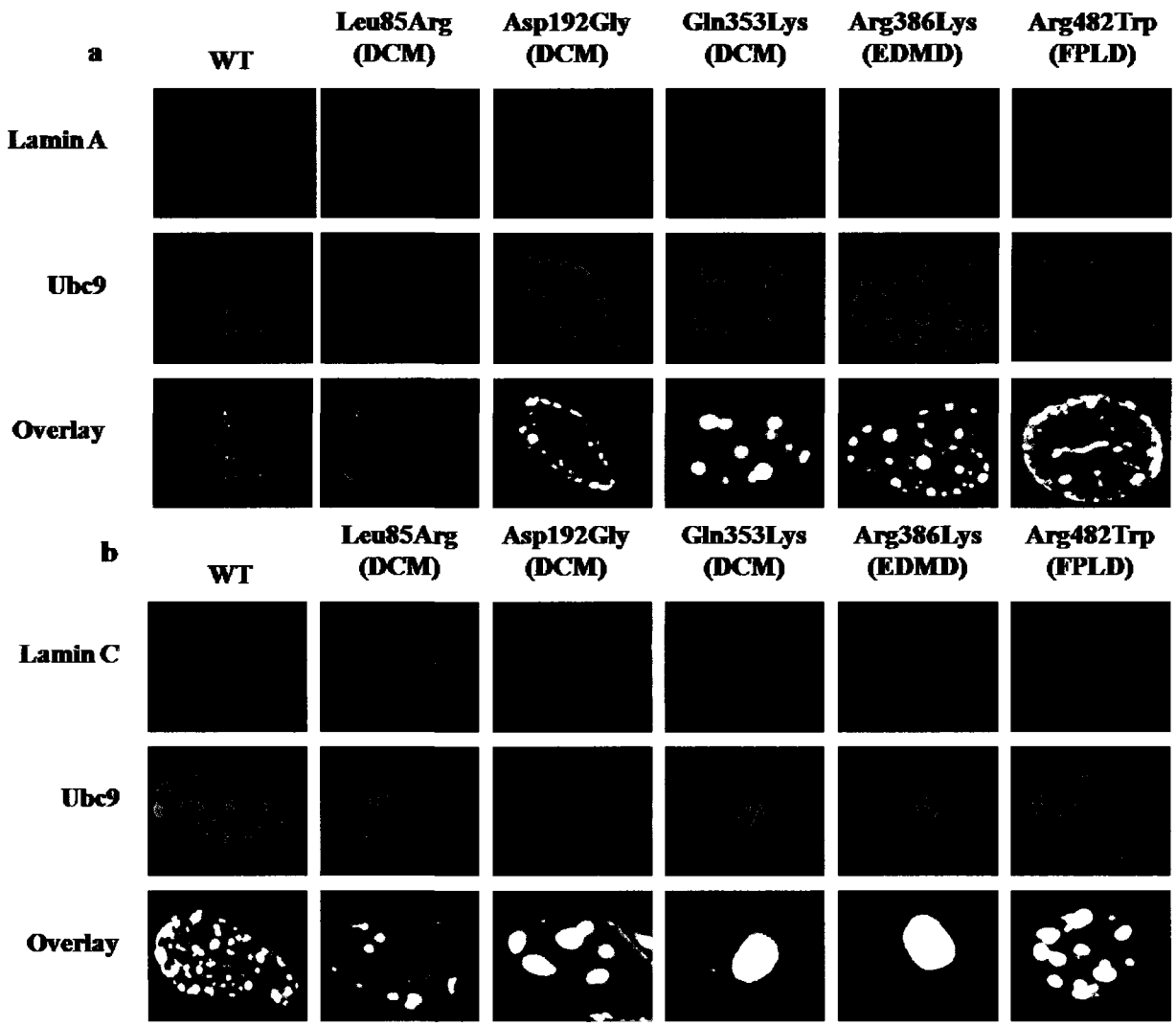

Figure 4.3 Ubc9 cellular distribution is affected in cells transfected with mutant lamin A or lamin C. C2C12 cells were transiently transfected with wild type and mutant (a) lamin A-CFP or (b) lamin C-dsRed and Ubc9-GFP and visualized by fluorescent confocal microscopy. (a) Wild type lamin A is expressed as a homogeneous veil at the inner nuclear membrane. The DCM-associated Leu85Arg and FPLD-associated Arg482Trp mutants do not exhibit any aberrant phenotype compared to the wild type. Ubc9 localizes with these mutant lamin A. The DCM-associated Asp192Gly and Gln353Lys and EDMD-associated Arg386Lys lamin A mutants form intranuclear aggregates that localize close to the nuclear envelope. Ubc9 localizes with the mutant aggregates in these mutant cells and are thus mislocalized from the nuclear membrane. (b) The same phenotype is observed in cells overexpressing WT or mutant lamin C.

4.2 Ubc9 interaction with lamin A/C

Because lamin A/C appears to have an effect on Ubc9 localization, we wanted to see if the mutants have an effect on the physical interaction between the two proteins. In order to do this, mutant lamin A/C immunoprecipitations would be compared to wild type lamin A/C immunoprecipitation. Endogenous immunoprecipitation of wild type lamin A/C failed to co-immunoprecipitate Ubc9 using western blotting analysis (Figure 4.4). Cos7 cells were transfected with Ubc9-HA and endogenous lamin A/C was immunoprecipitated. As a negative control, untransfected lysates were incubated with or without antibody. Emerin, a known lamin A/C binding partner, was used as a positive control of co-immunoprecipitation.

To ensure there is no binding between the proteins in cell models, overexpression of lamins A and C and Ubc9 was performed in order to encourage co-immunoprecipitation. However, this method also failed to co-immunoprecipitate Ubc9 and lamin A/C. Cos7 cells were transfected with wild type lamin A-CFP or lamin C-CFP and Ubc9-HA (Figure 4.5). Lamin A and C were immunoprecipitated using anti-GFP tag antibody and Ubc9 was immunoprecipitated using an anti-HA tag antibody. In the GFP tag immunoprecipitations cells were transfected with empty CFP vectors and Ubc9-HA or just with Ubc9-HA as a negative control. In the HA tag immunoprecipitations, RanGAP, a known Ubc9 binding partner, was used as a positive control of Ubc9 immunoprecipitation. As a negative control, empty CFP vector was transfected with Ubc9-HA or both lamins A and C in CFP vectors with no Ubc9-HA (Figure 4.6). Thus, I was not able to confirm the reported interaction between lamin A/C and Ubc9.

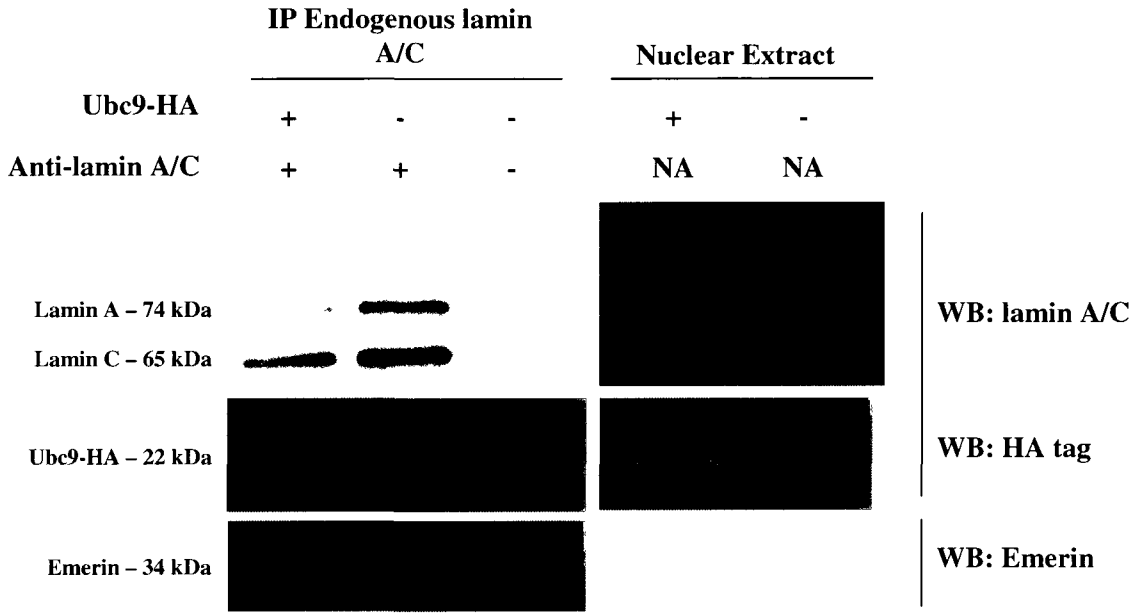

Figure 4.4 Ubc9 does not interact with endogenous lamin A/C. Cos7 cells were transfected with Ubc9-HA or nothing and nuclear lysates were incubated with anti-lamin A/C antibody to immunoprecipitate endogenous lamin A/C. Immunoprecipitates were run on 4-20% SDS-PAGE and transferred to nitrocellulose membrane. Western blotting for HA tag showed no bands at around 22kDa (Ubc9 = 18kDa + HA-tag = 4kDa). Positive control emerin appeared in the IP lanes.

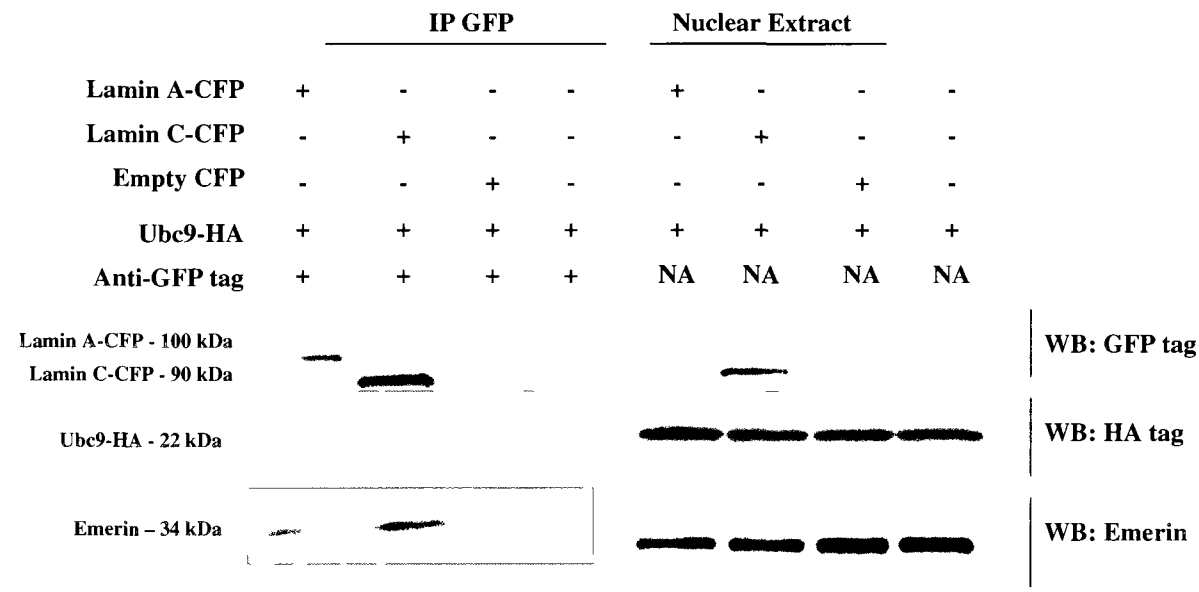

Figure 4.5 Ubc9 does not interact with exogenously expressed lamin A/C. Cos7 cells were transfected with lamin A-CFP, lamin C-CFP or empty CFP vector as well as Ubc9-HA. Nuclear protein was incubated with anti-GFP tag antibody and immunoprecipitates were run on 4-20% SDS-PAGE gel. Western blotting against GFP tag indicates lamin A and lamin C were immunoprecipitated. Western blot for HA tag indicates no Ubc9-HA co-immunoprecipitation. Emerin was used as a positive control.

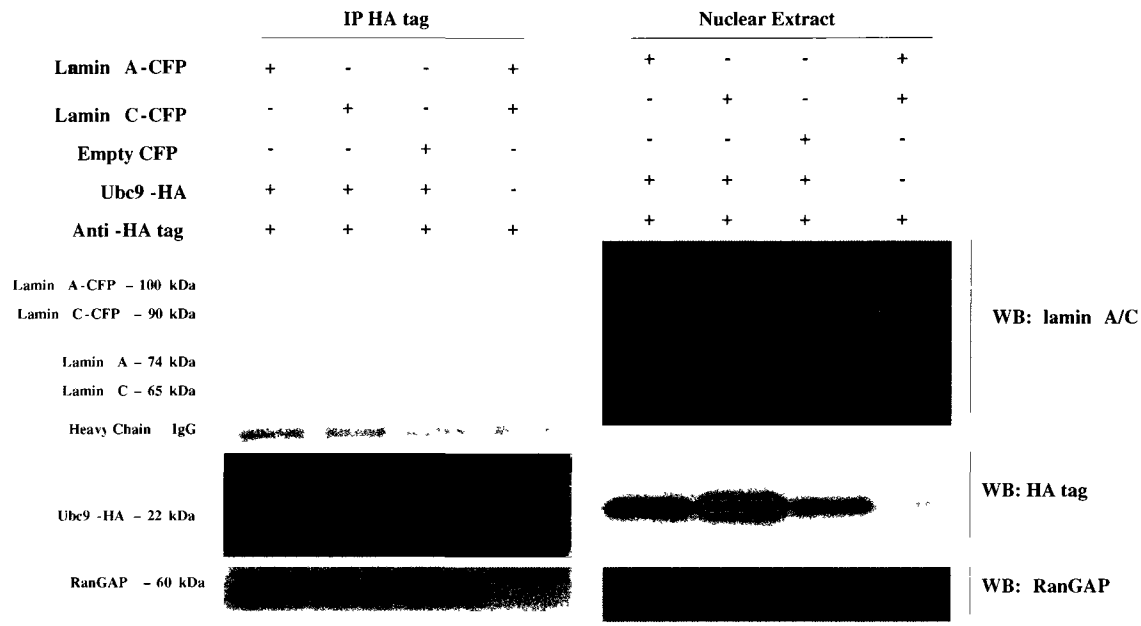

Figure 4.6 HA-Ubc9 immunoprecipitation. Cos7 cells were transfected with lamin A-CFP, lamin C-CFP, empty CFP or both lamin A and C-CFP as well as Ubc9-HA. Nuclear protein was incubated with anti-HA tag antibody and immunoprecipitates were run on 4-20% SDS-PAGE gel. Western blotting against HA tag indicates Ubc9 was immunoprecipitated. Western blot for lamin A/C indicates no lamin A-CFP or lamin C-CFP co-immunoprecipitation. RanGAP was used as a positive control.

4.3 Lamin A/C Sumoylation by Sumo1

Based on our previous findings, we were interested in determining if lamin A/C is sumoylated by Sumo1. We initially looked at endogenous lamin A/C sumoylation. Due to the transient nature of sumoylation and the low steady-state levels of sumoylated proteins, C2C12 cells were transfected with Sumo1-HA (Pichler 2008) and protein was extracted in the presence of NEM to discourage deconjugation. Endogenous lamin A/C was immunoprecipitated using an antibody against both lamins A and C. Western blotting for the HA tag and lamin A/C did not show any bands corresponding to lamin-Sumo1 covalent conjugates (Figure 4.7a). Untransfected cells were used as a negative control while emerin, a known lamin A/C binding partner, was used as a positive control of immunoprecipitation.

These results were confirmed in Cos7 cells transfected with wild type lamin A and lamin C in CFP expression vectors. These cells were used because they have a significantly higher transfection efficiency compared to C2C12 cells (70-80% compared to 30-40%) and because Sumo1 cellular distribution is affected in the presence of *LMNA* mutations in these cells (Sylvius et al 2005). These cells were also transfected with Sumo1-HA. The transfected lamins were immunoprecipiated using an antibody against the CFP tag. Western blotting for the HA tag and GFP tag did not show any bands corresponding to lamin-CFP-Sumo1 conjugates (Figure 4.7b). Empty CFP vector transfection and untransfected cells were used as negative controls.

Western blotting for Sumo1 revealed four bands. These did not correspond to lamin A/C-Sumo1 conjugates, which should come up to 80kDa and 90kDa, respectively. The molecular weight of the observed bands range between 80 and 160kDa and most likely correspond to sumoylated lamin A/C binding partners, whose identity is unknown. Controls were used as described above.

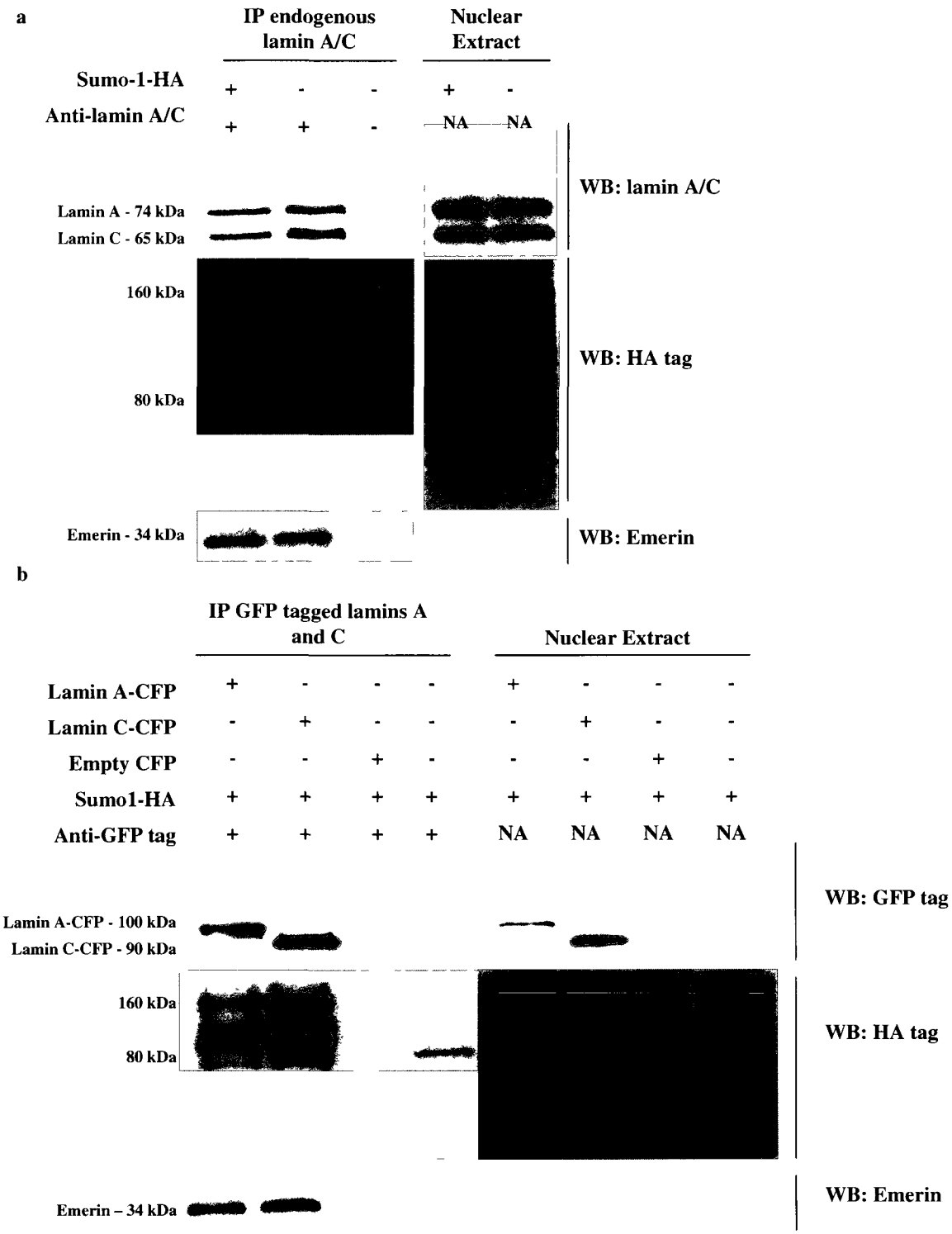

Figure 4.7 Lamin A/C are not sumoylated by Sumo1. Western blots of immunoprecipitation of endogenous and exogenous lamin A and C. (a) C2C12 cells were transiently transfected with Sumo-1-HA and nuclear protein was extracted with NEM. Lysates were incubated with anti-

lamin A/C antibody and immunoprecipitates were run on a 4-20% SDS-PAGE gel. Western blots were probed for lamin A/C and HA tag. Emerin was used as a positive control of lamin A/C immunoprecipitation. (b) Cos7 cells were transfected with lamin A-CFP, lamin C-CFP, or empty CFP vector with Sumo-1-HA. Nuclear protein was extracted with NEM in lysis buffer and lysates were incubated with an antibody against GFP tag. Immunoprecipitates were run on 4-20% SDS-PAGE gel and western blots were probed for GFP tag, HA tag and emerin as a positive control. Lamins A and C did not immunoprecipitate any bands higher than endogenous **(a)** and exogenous **(b)** levels to indicate sumo conjugation. SUMO-1 western blots revealed four bands between 80 and 160 kDa. The identity of these proteins is not known. Untransfected cells were treated with transfection reagents to control for chemical effects.

4.3.1 Determine identity of sumoylated lamin A/C binding partners

In order to identify the proteins that would correspond to the observed bands, we looked to the literature to find known lamin A/C binding partners that are sumoylated and have a molecular weight within the range observed. Of the 30 known lamin A/C binding partners (Table 1), only four are known to be sumoylated. C-Fos and core histones are not compatible with the molecular weights of the immunoprecipitated proteins. Lower bands potentially corresponding to these proteins were detected, however, their location often overlapped with the reduced IgG bands at 50kDa and 25kDa and were therefore not consistently detected.

Sterol-Regulatory Element Binding Protein (Srebp)

The other two binding partners are sterol-regulatory element binding proteins 1 and 2 (Srebp1 and Srebp2) transcription factors involved in adipogenesis and cholesterol biosynthesis. Srebp is mislocalized in cells with LMNA mutations (Lloyd et al 2002). Interestingly, the sumoylated form of Srebp1 and 2 corresponds to the approximate size of one of the four unidentified bands (Nuclear sumoylated Srebp ~80 kDa or cytoplasmic sumoylated Srebp ~135 kDa).

The interaction between lamin A/C and Srebp has been disputed in the literature (Lloyd et al 2002, Capanni et al 2005) so I started by confirming this interaction in my model. Because Srebp expression is extremely low in C2C12 cells and is expressed at high levels in rat liver, nuclear and cytoplasmic protein was extracted from rat liver and Srebp was immunoprecipitated out using an antibody specific to Srebp 1 and 2. In liver, both lamins A and C were co-immunoprecipitated from the nuclear fraction and not from the cytoplasmic fraction, as predicted

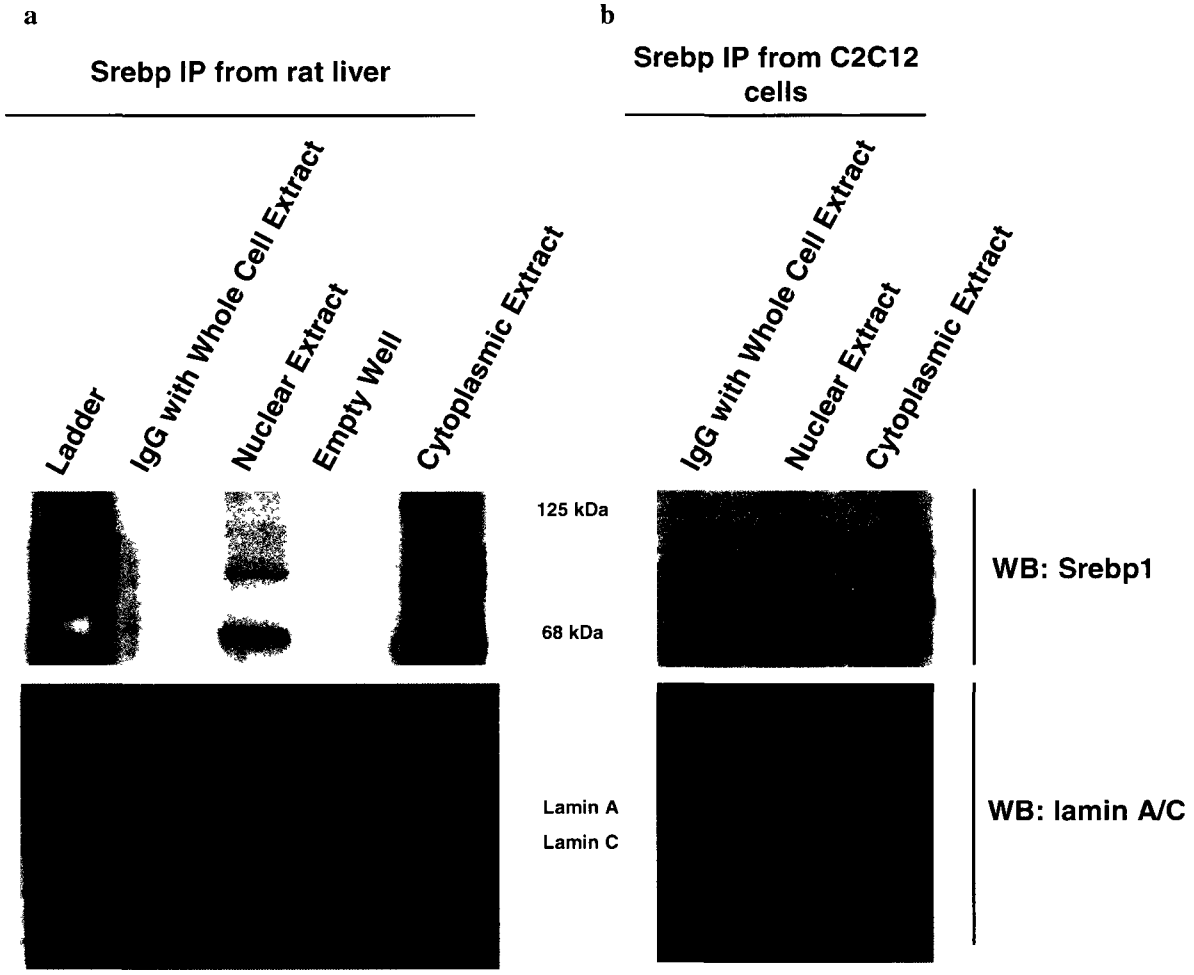

Figure 4.8 SREBP and lamin A/C co-immunoprecipitation. Endogenous SREBP was immunoprecipitated from (a) rat liver and (b) C2C12 whole cell, nuclear, and cytoplasmic protein lysates. Immunoprecipitates were run on 4-20% SDS-PAGE and transferred to nitrocellulose membrane. Western blotting for lamin A/C shows interaction between SREBP and (a) lamin A and lamin C and (b) lamin C.

(Figure 4.8a). However, immunoprecipitation of Srebp from C2C12 cells, from 5mg protein compared to 500ug-1mg, co-immunoprecipitated only lamin C, not lamin A in the nuclear extract (Figure 4.8b). Because the lamin A and C immunoprecipitations co-immunoprecipitated the same proteins, Srebp1 and 2 are not the unidentified proteins.

Mesenchymal Lamin Interacting Partner (MLIP)

Patrick Burgon of the University of Ottawa Heart Institute discovered a novel lamin A/C binding protein, Mlip, mesenchymal lamin interacting protein. Mlip has two Sumo consensus sequences and an 88 kDa isoform corresponds to the 105-110 kDa sumoylated band from the immunoprecipitations.

In order to characterize the interaction between Mlip and lamins A and C, respectively, C2C12 cells were co-transfected with wild type or mutant lamin A or lamin C in fluorescent expression vectors and Mlip. Cells were fluorescently stained for Mlip. Wild type Mlip is uniformly expressed throughout the nucleus and cytoplasm (personal communications with Dr. Burgon). When co-expressed with wild type lamin A, there is no change in the pattern of Mlip expression; additionally, wild type lamin A does not appear to colocalize with Mlip (Figure 4.9a). This same Mlip phenotype is observed in Leu85Arg (DCM), Asp192Gly (DCM), Gln353Lys (DCM), Arg386Lys (AD-EDMD), and Arg482Trp (FPLD) lamin A mutants. However, when WT lamin C and Mlip are co-expressed in C2C12 cells, Mlip appears to be concentrated solely within the nucleus at the WT lamin C aggregates (Figure 4.9b). This same phenotype is observed in the Leu85Arg mutation. In the Asp192Gly (DCM), Gln353Lys (DCM) and Arg386Lys (AD-EDMD) lamin C mutants, Mlip appears concentrated at the mutant speckles but is still expressed in the cytoplasm and nucleoplasm. Furthermore, the lamin A and C

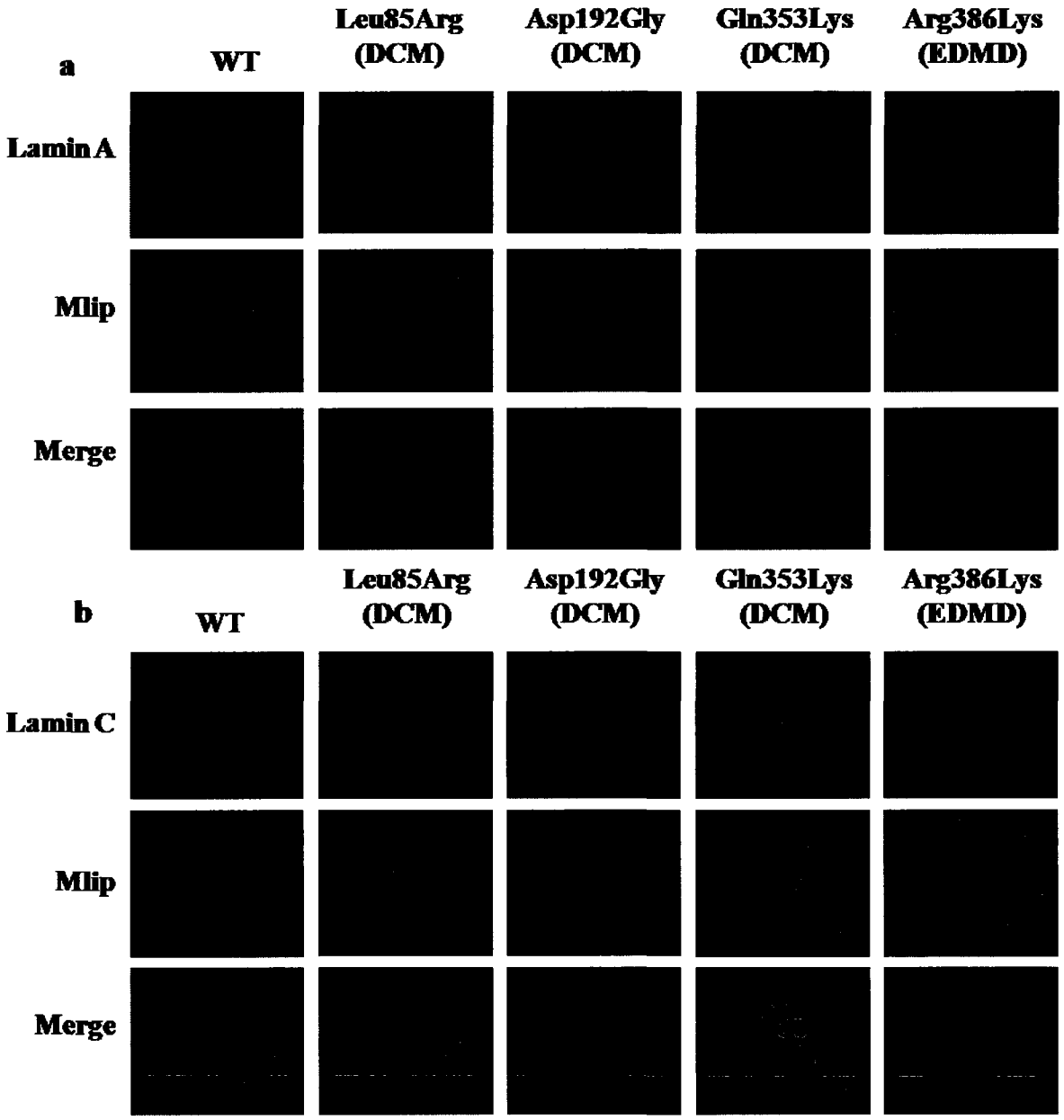

Figure 4.9 Mutations in lamin C affect Mlip cellular distribution. In wild type cells, Mlip is distributed evenly in the nucleus and cytoplasm in C2C12 cells (personal communication with Dr. Burgon). (a) WT lamin A and Mlip do not appear to colocalize at the nuclear rim. The presence of LMNA mutations does not appear to have an effect on Mlip localization within the nucleus. C2C12 cells were transiently transfected with lamin A-CFP and Mlip-pcDNA3 and stained for Mlip with a fluorescently tagged secondary antibody. (b) WT MLIP and lamin C colocalize within the nucleus. Mlip appears to localize with the mutant aggregates in the DCM and EDMD mutant cells. C2C12 cells were transiently transfected with lamin C-dsRed and Mlip-pcDNA and were stained for Mlip with a fluorescent secondary antibody.

immunoprecipitations co-immunoprecipitated the same proteins to the same extent. Mlip appears to have a stronger interaction with lamin C compared to lamin A.

As mentioned earlier, Mlip's amino acid sequence contains two Sumo consensus sequences. In order to determine if Mlip is sumoylated by Sumo1, endogenous Mlip was immunoprecipitated from the C2C12 cells transfected with Sumo1-HA. Western blotting for Sumo1 revealed a band at 55 kDa which may correspond to the sumoylated form of a smaller Mlip isoform (Figure 4.10). Thus, the 88kDa isoform is not the one sumoylated.

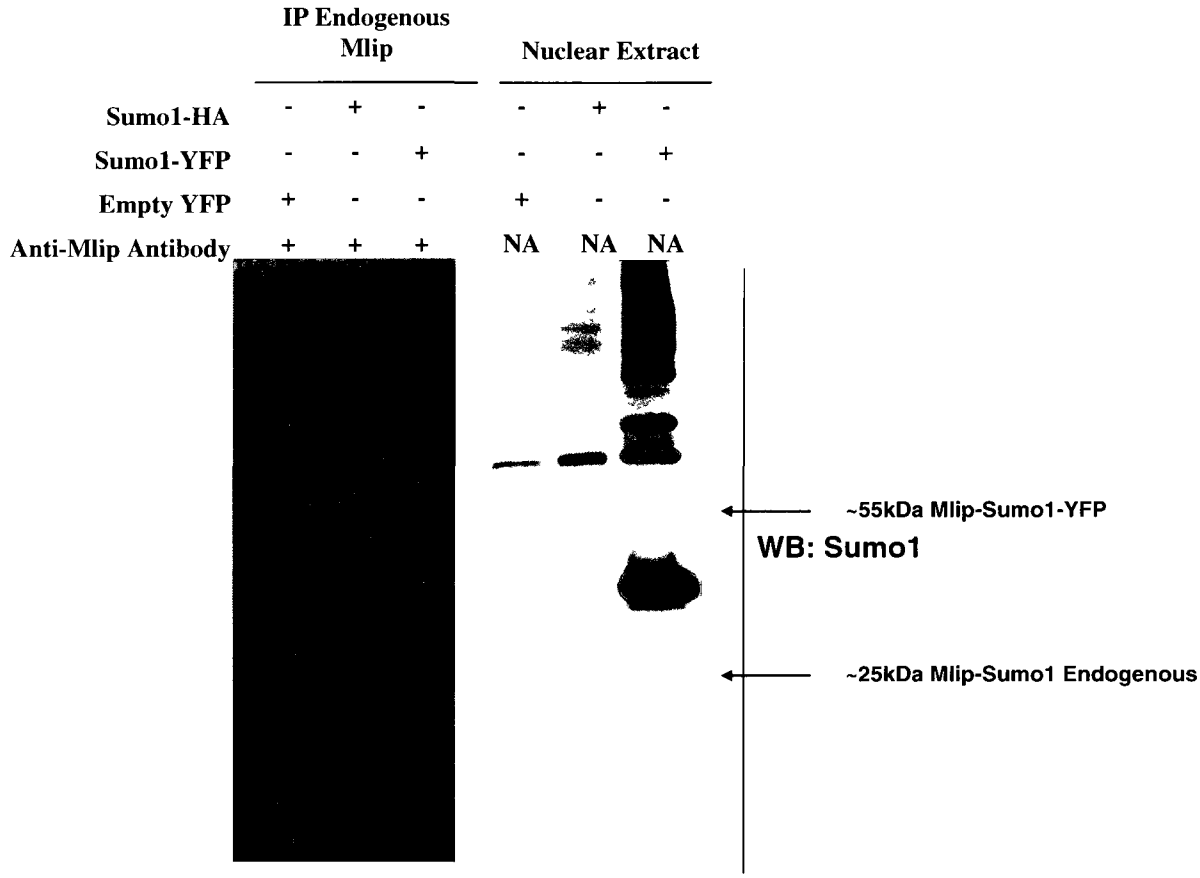

Figure 4.10 Mlip is sumoylated by Sumo1 in C2C12 cells in endogenous Mlip co-immunoprecipitation. Mlip-endogenous Sumo1 conjugate and Mlip-exogenous Sumo1 conjugate indicate small isoform of Mlip, approximately 15kDa in apparent molecular weight, is sumoylated by Sumo1. C2C12 cells were transiently transfected with empty YFP vector, Sumo1-HA, or Sumo1-YFP. Nuclear protein was extracted and lysates were incubated with anti-Mlip antibody. Immunoprecipitates were run on 4-20% SDS-PAGE and western blotting was performed for Sumo1.

Mass Spectrometry

Because Mlip and Srebp are not the co-immunoprecipitated protein bands, samples were sent out for mass spectrometric analysis. In order to differentiate the Sumo1-conjugated lamin A/C binding partner bands compared to just the lamin A/C binding partner bands, two groups of C2C12 cells were used: One with Sumo1 transfected and the other untransfected. Endogenous lamin A/C was immunoprecipitated using an antibody against lamin A/C. 75% of the immunoprecipitates were reduced and run on a 4-20% SDS-PAGE gel. Coomassie staining was performed and three bands present only in the lane with Sumo1 transfection were cut out and sent out for mass spectrometric analysis (Figure 4.11).

One protein was identified with reported molecular weight approximately less than the observed molecular weight on the SDS-PAGE gel: heterogeneous nuclear ribonucleoprotein U (hnRNPU) with a significant protein score of 95. Coomassie blue staining indicated this protein to be approximately 120 kDa. The estimated molecular weight reported for hnRNPU is 88 kDa (Figure 4.12). One other band, appearing around 65 kDa was identified as albumin with a significant protein score of 72 (Figure 4.13). However, albumin presence in C2C12 cells cannot be explained so I discarded this identification as a non-informative result. The last band, appearing at about 110 kDa was not identified by mass spectrometry (Figure 4.14) possibly due to insufficient protein.

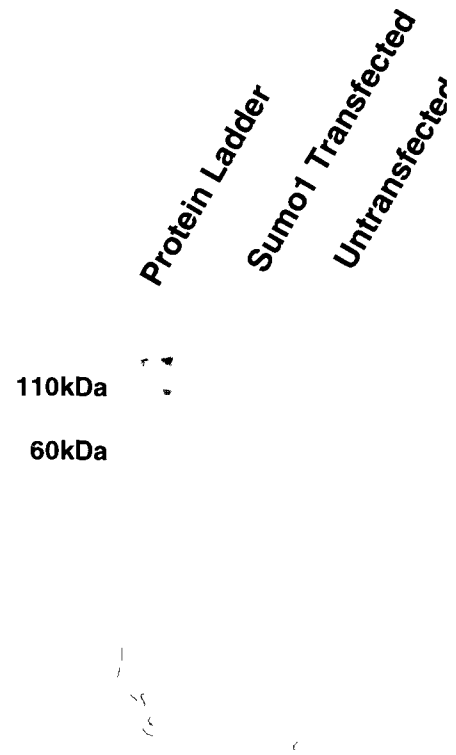

Figure 4.11 Coomassie blue staining of lamin A/C co-immunoprecipitates sent out for mass spectrometric analysis. C2C12 cells were transfected with or without Sumo1. Lamin A and lamin C were immunoprecipitated by incubation with an antibody against lamin A/C. Immunoprecipitates were eluted and run on 4-20% SDS-PAGE for protein separation and stained with Coomassie blue dye to visualize proteins. Bands of interest were cut out and sent for MS analysis with Alphalyse Inc.

Sample name: endo110b

Protein Information

Protein name:	**heterogeneous nuclear ribonucleoprotein U [Rattus norvegicus]**
Alphalyse number	ALPHA15593
GI number	gi|148747541
MW	87673
pI	5.92
Mascot score	95
Sequence coverage	15%
Bioinformatic tools	[illegible]

Analysis Information

- MS analysis method: MALDI-TOF peptide mass fingerprint and MALDI-TOF/TOF peptide sequencing
- Enzyme: Trypsin
- Variable modifications: Carbamidomethyl (C), Oxidation (M)
- Database search program: Mascot ver. on 2.2.07
- Peptide Tolerance: 50 ppm
- Allowed up to 1 miscleavage
- Database: NRDB1 (9983056 protein sequences)

Protein sequence

Matched peptides shown in bold underline

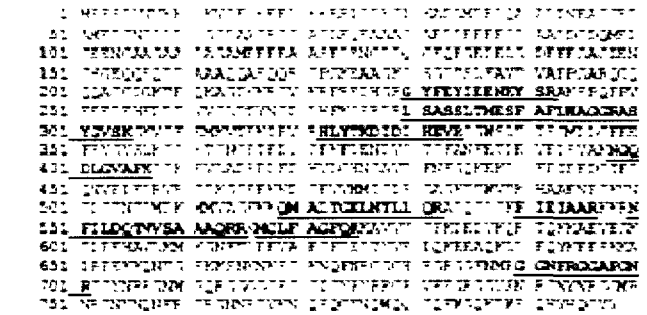

Peptides used for identification

Peptides shown in bold have been analysed by MS/MS sequencing

Start - End	Observed	Mr(expt)	Mr(calc)	Delta	Miss	Sequence
232 - 242	1697.79	1696.78	1696.77	0.00	1	R.GYEYIEENKYSR.A (Ions score 241)
[illegible]						
[illegible]						

Figure 4.12 MS data identifying hnRNPU as one of the four unidentified sumoylated lamin A/C binding partners. The band was cut out of the SDS-PAGE from figure 4.11 was seen at approximately 120kDa. The sample was called endo110b because it was from an endogenous lamin A/C immunoprecipitation and the band was located slightly above the 110 kDa marker. The protein analysis report indicates that the estimated molecular weight of hnRNPU is 88kDa. The Mascot score is calculated by -10Log(P) where P is the probability that the observed match is random (www.matrixscience.com). A score greater than 67 is considered significant ($p<0.05$).

Sample name: endo65

Protein Information

Protein name:	albumin
Alphalyse number:	ALPHA15591
GI-number	gi|229552
MW:	66088
pI:	5.76
Mascot score:	72
Sequence coverage:	21%
Bioinformatic tools:	1: NCBI Entrez 2: Blast (Blastp) NCBI 3: Conserved Domains in NCBI

Analysis Information

- MS analysis method: MALDI-TOF peptide mass fingerprint and MALDI-TOF-TOF peptide sequencing
- Enzyme: Trypsin
- Variable modifications: Carbamidomethyl (C),Oxidation (M)
- Database search program: Mascot version 2.2.03
- Peptide Tolerance: 60 ppm
- Allowed up to 1 miscleavage
- Database: NRDB1 9983056 protein sequences

Protein sequence

Matched peptides shown in bold underline

```
   1 MKWVTFISLL FLFSSAYSRG VFRRDAHKSE VAHRFKDLGE ENFKALVLIA
  51 FAQYLQQCPF EDHVKLVNEV TEFAKTCVAD ESAENCDKSL HTLFGDKLCT
 101 VATLRETYGE MADCCAKQEP ERNECFLQHK DDNPNLPRLV RPEVDVMCTA
 151 FHDNEETFLK KYLYEIARRH PYFYAPELLF FAKRYKAAFT ECCQAADKAA
 201 CLLPKLDELR DEGKASSAKQ RLKCASLQKF GERAFKAWAV ARLSQRFPKA
 251 EFAEVSKLVT DLTKVHTECC HGDLLECADD RADLAKYICE NQDSISSKLK
 301 ECCEKPLLEK SHCIAEVENDE MPADLPSLAA DFVESKDVCK NYAEAKDVFL
 351 GMFLYEYARR HPDYSVVLLL RLAKTYETTL EKCCAAADPH ECYAKVFDEF
 401 KPLVEEPQNL IKQNCELFEQ LGEYKFQNAL LVRYTKKVPQ VSTPTLVEVS
 451 RNLGKVGSKC CKHPEAKRMP CAEDYLSVVL NQLCVLHEKT PVSDRVTKCC
 501 TESLVNRRPC FSALEVDETY VPKEFNAETF TFHADICTLS EKERQIKKQT
 551 ALVELVKHKP KATKEQLKAV MDDFAAFVEK CCKADDKETC FAEEGKKLVA
```

Peptides used for identification

Peptides shown in bold have been analysed by MS/MS sequencing

Start - End	Observed	Mr(expt)	Mr(calc)	Delta	Miss	Sequence
65 - 76	1419.69	1418.68	1418.69	-0.01	1	F.SLHTLFGDKLCT.V Carbamidomethyl C
137 - 143	927.50	926.49	926.49	0.00	0	K.YLYEIAR.R (Ions score 111
137 - 144	1056.59	1055.58	1055.58	-0.01	1	K.YLYEIARR.H
205 - 216	1331.66	1330.65	1330.65	-0.01	1	R.ALKAWSVAR.L
241 - 261	2249.06	2247.05	2246.04	0.01	1	K.LCVLHEKTPVSDRVTKCCTESLVNR.R Carbamidomethyl C

Figure 4.13 MS data identifying albumin as a protein co-immunoprecipitated with endogenous lamin A/C. The band was cut out of the SDS-PAGE from figure 4.11 was seen at approximately 65kDa. The sample was called endo65 because it was from an endogenous lamin A/C immunoprecipitation and the band was located in between the 60 and 70 kDa protein markers. The protein analysis report indicates that the estimated molecular weight of albumin is 66kDa. The Mascot score is calculated by -10Log(P) where P is the probability that the observed match is random (www.matrixscience.com). A score greater than 67 is considered significant ($p<0.05$).

Sample name: endo110a

Protein Information

Protein name:	No identification
Alphalyse number:	ALPHA15592
GI-number:	
MW:	
pI:	
Mascot score:	
Sequence coverage:	

Figure 4.14 MS unable to identify a protein. The band was cut out of the SDS-PAGE from figure 4.11 was seen at approximately 110kDa. The sample was called endo110 because it was from an endogenous lamin A/C immunoprecipitation and the band was located at the 110kDa protein marker. No protein was identified.

Summary of Chapter 4 Results

Ubc9 interaction with lamin A/C has previously been reported (Zhong et al 2005), therefore I investigated how *LMNA* mutations disrupt its cellular distribution. Although I show an effect on its cellular distribution, I was not able to confirm the interaction between the two proteins. I have shown that lamin A/C is not sumoylated by Sumo1 and identified a novel potentially sumoylated lamin A/C binding partner, hnRNPU. Immunoprecipitation of Srebp1 from C2C12 cells shown that Srebp1 interacts with lamin C more than with lamin A and that Mlip localization is affected by the overexpression of lamin C more than by lamin A.

Chapter 5 – Discussion

One of the greatest challenges researchers in the laminopathy field face is in discovering the tissue-specific effects of individual mutations. As previously mentioned, there is no direct genotype-phenotype relationship in laminopathies. In this thesis, I set out to determine how *LMNA* mutations exert their tissue-specific effects by investigating perturbations in lamin A/C interaction with its binding partners, focusing on PKCα signaling and Sumo1 post-translational modification.

5.1 Mutation in LMNA gene is associated with novel phenotype: lone Atrial Fibrillation

The identification of two novel mutations in the *LMNA* gene associated with AF in one year is very interesting. This discovery has raised more questions in the laminopathy research field as we are now faced with one more associated disorder to differentiate.

5.1.1 AF- and DCM-associated LMNA mutations can cause abnormal intranuclear lamin A/C localization

I compared the nuclear distribution of lone AF-mutant lamin A and C with AF/DCM-mutants and DCM-mutants. All four mutations are located in the C-terminal globular tail region of the lamin A/C protein. Several *in vitro* studies conclude it is the N-terminal head domain, and not the tail domain, that is mainly responsible for head-to-tail associations (Gieffers and Krohne 1991, Moir et al 1991, Heitlinger et al 1992, Isobe et al 2007), however none of them can conclusively state the C-terminal tail domain's exact biological function (Dhe-Phagnon et al 2002). The non-helical tail domain is composed entirely of Beta sheets (Dhe Phagnon et al 2002)

and is the location of a phosphorylation site necessary for lamin disassembly during mitosis (Heald and McKeon 1990).

The location of the Thr528 and Arg541 residues are of special importance to the C-terminal tail of lamin A/C. They are among 32 amino acids that form the densely packed hydrophobic core of the tail (Dhe-Phagnon et al 2002). The Thr528 and Arg541 are highly conserved among intermediate filament proteins (Krimm et al 2002) and among lamins of other species (Dhe Phagnon et al 2002). The mutations we analyzed at these sites, Thr528Met and Arg541Gly, present a phenotype with multiple aggregates of the mutant proteins, and often the formation of sickles connecting these aggregates. Residue 528, Threonine, is a polar neutral residue that points towards the core of the β-sandwich. The alcohol group of its side chain forms hydrogen bonds with the backbone and other side chain oxygens in order to stabilize the configuration of the lamin Ig-domain β-sheets (Krimm et al 2002). Methionine has a non-polar neutral side chain which would weaken the interactions and has a low potential for Hydrogen bonding. It is also a START codon that signals the initiation of protein translation from mRNA. The Arginine at residue 541 contains a buried polar positive side chain that stabilizes the β-sandwich via hydrogen bonding and contacts with the core of the Ig-domain (Krimm et al 2002). Glycine's nonpolar neutral side chain, like Methionine, will interfere with these interactions. The altered polarity caused by the mutations appear to be affecting the higher order assembly of lamin A/C tails by forming aggregates and sickles. The formation of the sickles, compared to the aggregates, indicates a particular level of proper filament formation as it appears the proteins are still weakly associating with one another. This may also affect its interaction with its binding partners, thus affecting their specific functions.

The formation of these "sickles" has not been reported in any other studies of *LMNA* mutations. However, others have identified similarly shaped lamins *in vitro*. Broers et al (1999) identified similar shapes in cells transfected with lamin A with exon 10 deleted. They called these shapes "intra- and trans-nuclear tubule-like structures". No studies have investigated the effect of the aggregating lamins on nuclear strength, however we and others have shown increased mobility of mutant lamins as well as a reduced ability to form contacts with the inner nuclear membrane (Broers et al 2005, Sylvius et al 2008). From these studies we can infer that the aggregates and sickles are reducing the lamina stability.

The presence of cytoplasmic lamins in 10% of cells expressing Thr528Met and Arg541Gly mutations has never been reported with any other *LMNA* mutations. A tail-deletion model of lamin, truncated at residue 407 before the NLS, results in the formation of tubular lamins solely in the cytoplasm similar to what I observed (Loewinger and McKeon 1988, Holtz et al 1989). These lamins were localized around the nucleus at the ER based on ER colocalization studies (Holtz et al 1989). Although lamins have not been found in the cytoplasm in laminopathy mutations, its binding partners Emerin and Nesprin 1α have been found localized to the ER in skin fibroblasts of LGMD patients with a *LMNA* mutation (Muchir et al 2003), in $MEF^{-/-}$ cells (Sullivan et al 1999) and in RNAi treated HeLa cells (Harborth et al 2001).

Indirect immunofluorescent staining of transfected C2C12 cells for the endoplasmic reticulum protein, calreticulin, indicates a partial colocalization with the cytoplasmic mutant lamin A/C. The nuclear shape of the C2C12 cells is still in tact which means that the nuclear contents will not leak out into the cytoplasm. However, it is likely that due to the reduced integrity of the nuclear envelope due to the *LMNA* mutations, the mutant lamin A/C proteins were able to approach the endoplasmic reticulum membranes by the outer nuclear membrane

continuity with the NPC. In the aforementioned articles regarding Emerin and Nesprin mislocalization, they attribute this to the function of lamin A/C as a scaffold that anchors the proteins at the nuclear envelope.

The discovery of a lone Thr528Met point mutation is the first time this mutation has been found without another mutation. It has been described twice in clinical cases in the presence of another mutation. Savage et al (2004) found point mutations Thr528Met and Ser583Leu together in a family with FPLD and Verstraeten et al (2006) found Thr528Met and Met540Thr in an HGPS patient. The HGPS patient's skin fibroblasts showed a honeycomb pattern of lamins A and C. This honeycomb pattern was previously seen in an EDMD patient (Arg545Cys; Kandert et al 2009), an FPLD patient (Arg439; Verstraeten et al 2009, Ser143Phe; Kandert et al 2007), and in multiple other laminopathies (Muchir et al 2004). Another mutation at residue Thr528 has been described in a family with AD-EDMD (Bonne et al 2000), Thr528Lys. Expression of this mutation in C2C12 cells has no effect on lamin distribution (Ostlund et al 2001). I hypothesize that this substitution probably does not affect lamin assembly since Threonine and Lysine both have polar side chains and thus can still face into the centre of the β-sandwich (Krimm et al 2002).

We are the first group to identify and characterize the point mutation Arg541Gly (Malek, Labib et al Manuscript submitted, Clinical Genetics). Our group previously characterized another point mutation found at this site, Arg541Ser, which converted Arginine to Serine, which has a polar neutral side chain in a family with DCM (Sylvius et al 2005). Here, lamin C Arg541Ser was transfected into Cos7 cells. The cells developed a phenotype with multiple, spherical aggregates, however no work was done with co-transfection of mutant lamin A and lamin C. Three other groups also found a mutation at this site, Arg541Cys, in a patient with apical left

ventricular aneurism (Forissier et al 2003), DCM (Saj et al 2009), and cardiac arrest and left ventricular fibrosis (Hookana et al 2008). None of these groups performed experiments on cellular models. Skin fibroblasts from a DCM patient with Arg541Cys mutation had blebs in the nuclear envelope (Muchir et al 2004). We are currently investigating the expression of lamin A/C with p.Arg541Cys. This residue can be considered a hotspot for DCM, however, a family with EDMD has also been reported with a mutation at this site, Arg541His (Vytopil et al 2003).

The formation of a stop codon at Ser431 and Tyr481 results in the truncation of the lamin A/C protein at the beginning of the C-terminal tail. The location of the two mutations are past the site of phosphorylation (Ser392) necessary for lamin disassembly during mitosis (Heald and McKeon 1990) thus allowing for proper lamin assembly and function during the cell cycle. However, the Tyr481 locus is the base of the C-terminal tail's larger groove, which is reported to serve as a site for intermolecular interactions (Dhe-Phagnon et al 2002). Thus, termination of lamin A/C before this groove will affect the formation of Beta sheets. Deletion of the C-terminal tail downstream of the NLS eliminates the 3' CAAX motif, responsible for membrane localization, which explains the presence of the lamin A/C aggregates within the nucleus and not at the inner nuclear membrane. Furthermore, the Ig-fold domain's function is to mediate interactions with other proteins (Dhe-Phagnon et al 2002), including inner nuclear membrane protein Emerin (Clements et al 2000). Our results indicate that the loss of the C-terminal tail affects the secondary assembly of lamin A/C into filaments. Two groups have reported a mutation at the Tyr481 locus in patients with LGMD (Kitaguchi et al 2001, Spuler et al 2005). No publications have reported a mutation in *LMNA* at the Ser431 site.

5.1.2 AF- and DCM-associated *LMNA* mutations affect PKCα cellular distribution

The functional consequence of the nuclear translocation of PKCα with respect to laminopathies is unknown. Under normal circumstances, PKCα is found throughout the cytoplasm and at perinuclear regions, and to a very small extent within the nucleus (Leach et al 1989, Neri et al 1994). However, upon stimulation by phorbol-12-myristate-13-acetate (PMA) and insulin-like growth factor 1 (IGF-I), PKCα translocates to the nucleus (Leach et al 1989, Divecha et al 1991, Neri et al 1994, Zini et al 1995, Neri et al 1998). The mode and the function of nuclear translocation are not well understood. Zini et al (1995) found that 50% of nuclear PKCα are associated with the nuclear matrix compared to only a small percentage with cytoplasmic filaments, perhaps implicating them in nuclear structure. Furthermore, PKCα translocation to the nucleus appears to be dependent on cytoplasmic integrity (Schmalz et al 1996). When the cytoskeleton is disrupted, PKCα nuclear translocation cannot be induced.

This appears to be in opposition to my theory that the disrupted lamina integrity by the Thr528Met and Arg541Gly mutations cause a disturbance of the cytoskeletal network, as seen in $MEF^{-/-}$ cells where mechanical compression results in a disorganized cytoskeleton (Broers et al 2004). Thus, it is possible that non-PMA- and non-IGF-induced PKCα nuclear transport is associated with nucleo-cytoskeletal interactions. PKCα nuclear translocation is not associated with classical methods of nuclear transport such as the use of NLS and NPC (Schmalz et al 1996, 1998). It is also possible that the nuclear disruption due to the *LMNA* mutations prevents the nuclear export of PKCα, however there is no work in the literature that supports this theory.

Interestingly, PKCα has been shown to induce MAPK activation (Braz et al 2002) via ERK1/2 phosphorylation in cells induced for PKCα nuclear translocation. His222Pro mouse

hearts also show an increase in MAPK activation (Muchir et al 2009a). My work appears to link these two studies, suggesting that the destabilization of the nuclear lamina induces PKCα nuclear translocation which then activates the MAPK signaling cascade, thus leading to the development of the cardiac phenotype in laminopathies.

PKCα is strongly implicated in cardiac hypertrophy in addition to the MAPK activation. Braz et al (2002) and Vijayan et al (2004) also showed that PKCα, and not other PKC isozymes, was able to induce hypertrophy via enhanced sarcomeric organization, increased ANF expression, increased cell surface area, and increased H^3-leucine incorporation. Furthermore, inhibition of PKCα expression via dominant-negative adenoviral infection suppressed the induced hypertrophy.

Although myocyte hypertrophy is associated with DCM according to patient histology, the cells do not express all the markers of classic hypertrophy (Ahmad et al 2005). Furthermore, lone AF by nature does not present with other cardiac abnormalities. At this time, we cannot make a further causative link between PKCα and DCM or AF. We are currently determining the effect of the *LMNA* mutations on PKCα cytoplasmic and nuclear activity. In this vein, we are using two common methods of determining PKCα activation: PKCα phosphorylation and Histone H1 activation. PKCα is phosphorylated upon activation and measurement of its phosphorylation has become a marker of its activation (Ng et al 1999). We are performing western blotting for phosphorylated PKCα in nuclear and cytoplasmic cell fractions to determine how the mutations are affecting PKCα function. If we see an effect by this method, we will confirm by performing a kinase assay on histone H1, a known PKCα substrate.

5.2 Lamin A/C plays an integral role in the Sumo1 process

Sumoylation is a post-translational modification which commonly targets proteins involved in transcriptional regulation, most often repression. Certain *LMNA* mutations disrupt the Sumo1 sumoylation process via the impaired nuclear distribution of its major components, Sumo1 and Ubc9 (Sylvius et al 2005, Boudreau, Labib et al manuscript in preparation). This has the potential to affect the post-translational regulation of tissue-specific sumoylated proteins, which can lead to the tissue-specific symptoms observed in patients with various laminopathies.

Although lamin A/C contains three Sumo consensus sequences and Sumo1 colocalizes with mutant lamin A/C, I did not identify any interaction between the two proteins. In 2008, Zhang and Sarge found that lamin A/C is preferentially modified by Sumo2/3 over Sumo1, at Lys201 within a Sumo consensus sequence. DCM-associated *LMNA* mutations within the Sumo consensus motif, Glu203Gly and Glu203Lys, decreased sumoylation of lamin A. They state that the function of lamin A sumoylation is in correctly localizing the lamin A protein since mutations at Lys201 and Glu203 resulted in the formation of intranuclear foci (Zhang and Sarge 2008). However, this presentation is not unique to these mutations and may not be directly associated with altered lamin A sumoylation (see Introduction Models of Laminopathies section). The functional significance of Sumo2/3 conjugation compared to Sumo1 were not discussed, however since Sumo2/3 is involved in acute and reversible stress response (Saitoh and Hinchey 2000), altered sumoylation of lamin A by Sumo2/3 may result in a defective stress response mechanism. This agrees with the data from Zhang and Sarge (2008) which showed increased cell death in mutant cells.

Given that WT lamin A/C is not sumoylated by Sumo1, we hypothesized that the disruption of components of this process in our mutants could be occurring due to the introduction of novel sites of sumoylation, causing lamin A/C to be sumoylated. The mutations we have investigated (Asp192Gly, Gln353Lys, Arg386Lys) do not introduce new consensus sequences, however Gln353Lys and Arg386Lys do introduce new lysine residues that may be sumoylated by Sumo1. Since Asp192Gly is one of the two mutations with the most significant effects on Sumo1 conjugation (Boudreau, Labib et al manuscript in preparation), we discarded this hypothesis as a potential mechanism of action.

The presence of Sumo consensus sites however does not necessarily imply a target will be sumoylated. There are many examples where this is the case, such as the ubiquitin E3 ligase Mdm2 (Miyauchi et al 2002), the Epstein-Barr virus immediate-early gene BZLF1 (Adamson and Kenney 2001), the transcription repressor and death-domain-associated-protein Daxx (Jang et al 2002), the transcription factor cAMP-response element-binding protein (CREB) (Comerford et al 2003), and the intracellular effector protein Smad4 which is sumoylated at 2 lysines – one in a consensus motif and the other not (Lin et al 2003). The protein's conformational state has been proposed as the determining factor for sumoylation as seen with the ubiquitin E2 enzyme E2-25K (Pichler et al 2002). The Sumo attachment site is a lysine residue not in a consensus sequence whereas neighbouring Sumo consensus lysine residues are not modified. Furthermore, certain target proteins depend on other post-translational modifications to be recognized by Sumo's E2 conjugating enzyme, Ubc9, such as phosphorylation (see Introduction). No PDSM is present in the lamin A/C amino acid sequence, nor is there a NDSM.

5.2.1 An apparent paradox - lamin A/C is sumoylated by Sumo2/3 but doesn't interact with Ubc9?

Interestingly, although I show an effect of *LMNA* mutations on the cellular distribution of Ubc9, I could not replicate the interaction between lamin A/C and Ubc9 as seen in Zhong et al (2005). Which begs the question, if lamin A/C are sumoylated by Sumo2/3 (Zhang and Sarge 2008) why do we not see an interaction between lamin A/C and Ubc9? There are two possible explanations for this apparent paradox – (i) Tissue-specific sumoylation and (ii) Ubc9-independent sumoylation.

Zhang and Sarge (2008) showed lamin A/C sumoylation by Sumo2/3 in HeLa cells, human skin fibroblasts, and in mouse heart extracts. They performed endogenous and exogenous co-immunoprecipitations in these cell models. The lamin A/C-Ubc9 interaction was confirmed in human skin fibroblast cells (Zhong et al 2005). I attempted to replicate the lamin A/C-Ubc9 interaction in C2C12 mouse myoblast cells and in Cos7 kidney cells. I theorize that there are cellular factors inherent to skin fibroblast cells that promote lamin A/C sumoylation and Ubc9 interaction, thus implying tissue-specific sumoylation.

The tissue distribution of sumoylated proteins has not been well documented. It is widely accepted that Sumo1, Sumo2, and Sumo3 are ubiquitously expressed in all tissue types, however the determination of their relative abundance has been neglected. Xu and Au (2005) delineated the tissue distribution of Sumo1, Sumo2 and Sumo3 indicating subtle differences in expression. Sumo1 appears mostly evenly expressed with marginally higher expression in the pancreas, liver and testes, while Sumo2 and Sumo3 have a more varied expression pattern with low expression in muscle, kidney and lung cells and high expression in spleen, liver, ovaries, and heart. This may explain why my co-immunoprecipitations did not identify endogenously sumoylated lamin

A/C by Sumo1 in muscle and kidney cell lines. Interestingly, in plants, sumoylation was recently shown to occur in a tissue-specific manner as well (Reed et al 2010).

Regardless, this tissue-specificity concerning individual proteins has been neglected. Hemelaar et al (2004) performed gel electrophoresis on cell lysates incubated with radioactively labeled Sumo1. They identified four bands that were expressed in a tissue-specific manner with expression in mouse thymus or spleen or in a mouse lymphoma cell line, EL-4 (Hemelaar et al 2004) however they did not discover the identity of the proteins.

In support of this tissue-specific hypothesis, Kagey et al (2003) proposed that a target's specific E3 ligase must be present to promote sumoylation. In this study they identified carboxy-terminus binding protein 2 (CtBP2) as a Sumo conjugate *in vitro* but not *in vivo*. *In vitro*, they were able to enhance conjugation with a particular E3 ligase, Pc2 (Kagey et al 2003). Perhaps the cellular models I used, Cos7 and C2C12, do not endogenously express the E3 ligase inherent to fibroblast cells that facilitate lamin A/C sumoylation and Ubc9 interaction.

My second explanation for the discrepancies in my data is that lamin A/C is sumoylated by Sumo2/3 in a Ubc9-independent manner. It is commonly accepted that Ubc9 is necessary for substrate recognition and subsequent ligand binding. However, the assumption that all sumoylated proteins interact with Ubc9 has yet to be tested. For example, the study that determined CREB sumoylation by Sumo1 did not determine if Ubc9 interacts with the protein (Comerford et al 2003). Interestingly, CREB sumoylation occurs at non consensus motifs. Ubc9 is reported to undergo substrate recognition at the consensus motifs (Rodriguez et al 2001, Bernier-Villamor et al 2002).

Thus, perhaps the interaction between lamin A/C and Ubc9 reported in 2005 (Zhong et al) was not real. There were a number of inconsistencies which beg us to ask if the interaction

reported was an artifact. The purpose of the study was to find novel and specific interacting partners to progerin, the truncated form of lamin A seen in HGPS patients. To do this, they performed a yeast-2-hybrid with progerin as bait, screening a generic Matchmaker library. Of the 22 clones that were sequenced, two of them matched Ubc9. This interaction between progerin and Ubc9 was confirmed using endogenous co-immunoprecipitation from human fibroblast cells. No results for this were shown. This interaction was confirmed using an *in vitro* pull down for Ubc9, as well as for the three other novel binding partners they identified. Results were only shown for one of the partners, hnRNPE1. This was followed by endogenous co-immunoprecipitation of lamin A/C and Ubc9 from patient fibroblasts. No positive or negative controls were employed.

Furthermore, the antibody used to immunoprecipitate Ubc9 is a monoclonal anti-E2 antibody (ProteinTech Group) which recognizes not only Ubc9, but potentially all E2 conjugating enzymes involved in the conjugation of Ubiquitin and Ubiquitin-like proteins. Following dozens of failed attempts on my part to co-immunoprecipitate wild type lamin A/C and Ubc9, using various extraction protocols, immunoprecipitation buffers, beads and cell types, we purchased the antibody used in this paper and tested its specificity. Figure 5.1 represents the non-specific nature of the anti-E2 antibody used in this paper compared to the anti-Ubc9 antibody used in my experiments. Based on these findings, it is possible that one of the proteins that this antibody recognizes interacts with lamin A/C.

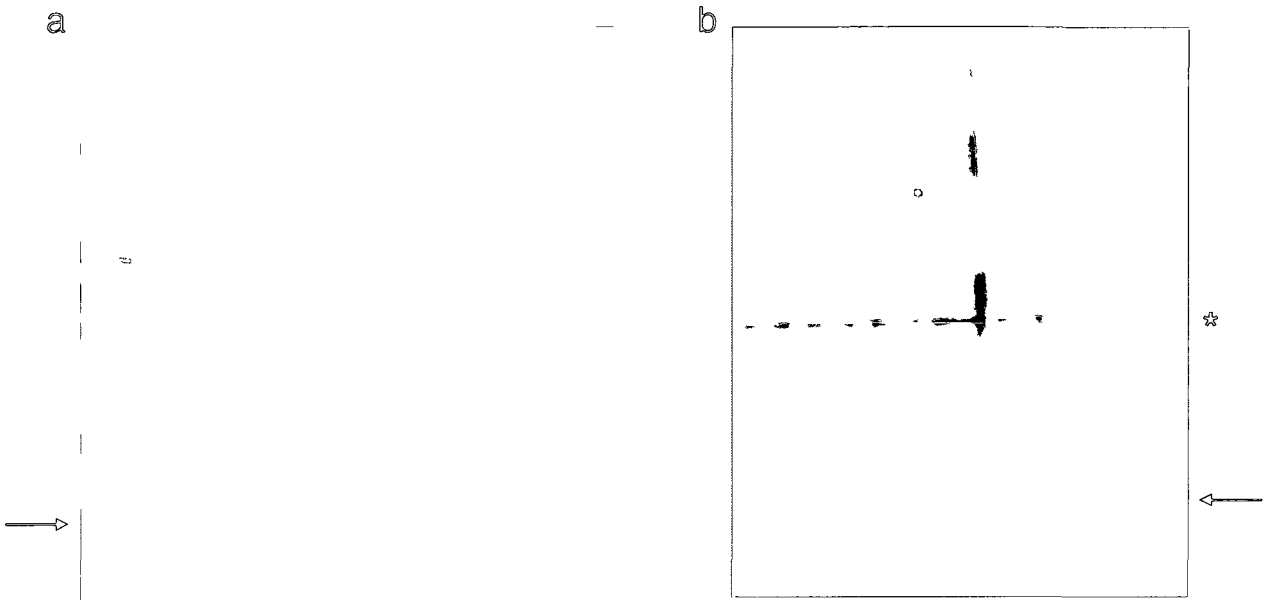

Figure 5.1 Western blots of Ubc9 indicating specificity of various antibodies. (a) monoclonal anti-E2 (Protein Tech Group, IL) and (b) polyclonal anti-Ubc9 (H-81 Santa Cruz Biotech). Both blots were stripped to be reprobed. * in (b) represents unstripped protein from anti-lamin A/C western blot. Arrow points to endogenous Ubc9 level.

5.2.2 Significance of Ubc9 mislocalization

I show that regardless of lamin A/C localization, Ubc9 faithfully colocalizes with it. Lamin A/C is proposed to act as a scaffold where different proteins rest (Heessen and Fornerod 2007). This could explain Ubc9 mislocalization to mutant aggregates, however I could not identify any discernable interaction between the two proteins, endogenously or exogenously. I then hypothesized that this "shadowing" of Ubc9 with lamin A/C is due to the mislocalization of the NPCs, since lamin A/C anchors and spaces them and since Ubc9 is known to localize there. I show that RanGAP is mildly mislocalized to the nucleus and not at the nuclear rim in the presence of certain lamin A/C mutants. This indicates that Ubc9 may interact with an intermediate protein that binds lamin A/C and that when lamin A/C are found in mutant aggregates this protein moves Ubc9 and potentially other components of the NPC within the nucleus. We are currently investigating this theory by determining the effect of the LMNA mutations on the localization of Nup153, a NPC protein known to interact with lamin A/C and components of the sumoylation pathway (Zhang et al 2002).

5.2.3 The identity of the four unknown sumoylated lamin A/C binding partners

During my attempts to determine if lamin A/C are sumoylated by Sumo1, I noticed bands in my immunoprecipitation western blots that could correspond to sumoylated lamin A/C binding proteins. We were interested in identifying the binding partners in an attempt to identify known lamin A/C binding partners that are sumoylated in our cellular system, mouse myoblasts, as they relate to muscular dystrophy's sometimes present in DCM patients with LMNA mutations.

The four bands there were consistently shown were between 80 and 160 kDa, therefore the identified proteins would be ~15 kDa smaller (since Sumo1 is ~11 kDa and the HA tag adds about 4 kDa). Of the over 30 known lamin A/C binding partners (Table 1), only four are known to be sumoylated by Sumo1 in mammalian cells – c-Fos, core histones and Srebp1 and Srebp2. C-Fos and core histones are ubiquitously expressed and are not compatible with the molecular weights of the identified proteins. Lower bands were detected that may correspond to these proteins, however, their location often overlapped with the reduced IgG bands at 50 kDa and 25 kDa and where therefore not consistently detected. Srebp therefore became the prime candidate as the unknown binding partners – its nuclear and cytoplasmic forms being 68 and 125 kDa, respectively.

SREBP

Although Srebp1 is not one of the four unknown sumoylated lamin A/C binding partners, it is an interesting candidate for determining the tissue-specific effects of LMNA mutations, especially with respect to lipodystrophies. As I mentioned in the introduction, Srebp1 is retained at the nuclear rim in FPLD skin fibroblasts. Under normal circumstances when cellular demand for sterol rises, Srebp1 which is anchored in the membranes of the ER travels to the Golgi where it is cleaved from its inactive form (125 kDa) to its active form (68 kDa). This transcriptionally active Srebp1 translocates to the nucleus and activates the expression of PPARγ by binding to its sterol response element promoter sequence. PPARγ targets the peroxisome proliferator response element (PPRE) to regulate the expression of genes involved n adipogenesis and insulin sensitivity. Maraldi et al (2007) proposed a model for Srebp1 in adipocytes and pre-adipocytes in FPLD cells where Srebp1 is retained at the nuclear rim. Here, Srebp1 will have lost its DNA-binding ability thus impairing PPARγ-dependent adipogenesis and reducing insulin sensitivity.

Srebp sumoylation by Sumo1 represses its transcriptional activity (Hirano et al 2003). Overexpression of constitutively active Sumo1 reduced the amounts of Srebp effectors HMG-CoA synthase and LDL receptor mRNA. Furthermore, luciferase reporter assays determined that Srebps mutated at Sumo binding sites were transcriptionally inactive. The authors did not comment on whether the repression is due to Sumo blocking Srebp's interaction site with co-factors or if the modification affects Srebp's DNA-binding affinity.

I propose that in FPLD cells with *LMNA* mutations, Srebp1 is retained at the nuclear rim because of over-sumoylation by Sumo1 (Figure 5.2). We have shown an increased nuclear retention of Sumo1 in lamin A/C mutant cells and in the His222Pro mutant EDMD mouse model (Boudreau, Labib et al manuscript in preparation). This nuclear Sumo1 may be constitutively modifying Srebp1 at the nuclear rim, thus preventing it from binding DNA. Srebp trapping at the nuclear rim is also preventing it from proteasomal degradation by ubiquitin (Hirano et al 2001).

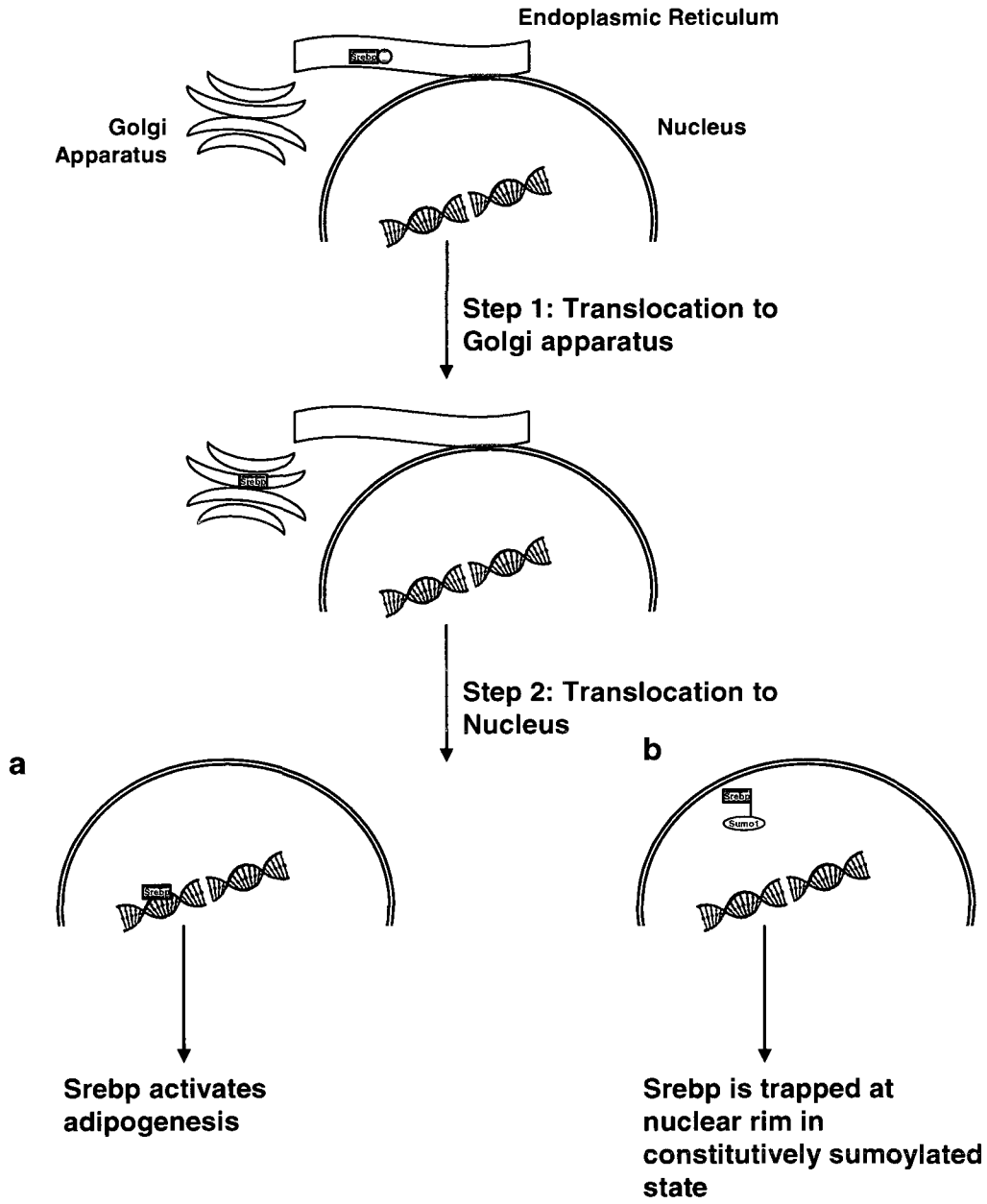

Figure 5.2 Schematic diagram of Srebp function in pre-adipocyte/adipocytes in normal and diseased states. Upon detection of increases in sterol levels, the Srebp precursor moves from the endoplasmic reticulum to the Golgi apparatus where it is cleaved into its active form. The active Srebp translocates to the nucleus where under normal conditions it activates adipogenesis. However, in FPLD patients, Srebp is trapped at the nuclear rim. I hypothesize that these trapped Srebp are sumoylated by Sumo1 which has been shown to inhibit its transactivation ability. Squares represent Srebp. Ovals represent Sumo1.

MLIP

Identifying Mlip as a potentially sumoylated protein has great implications on Mlip's function as a myogenic transcription factor, since many of Sumo1's target proteins are transcription factors. C2C12 cells not expressing Mlip display reduced myotube formation and a decreased expression of myogenin, myoD and myosin heavy chain (MHC). Inhibition of myogenesis due to transcriptional repression induced by sumoylation may play a role in the development of striated muscle laminopathies, especially of the muscular dystrophies. Our lab has shown that in the presence of laminopathic mutations there is an increase in the conjugation of Sumo1 to its nuclear targets (Boudreau, Labib et al Manuscript in preparation). Thus if Mlip is not being de-sumoylated in striated muscle this can lead to the inhibition of muscle differentiation seen in muscular dystrophies associated with LMNA mutations (Figure 5.3).

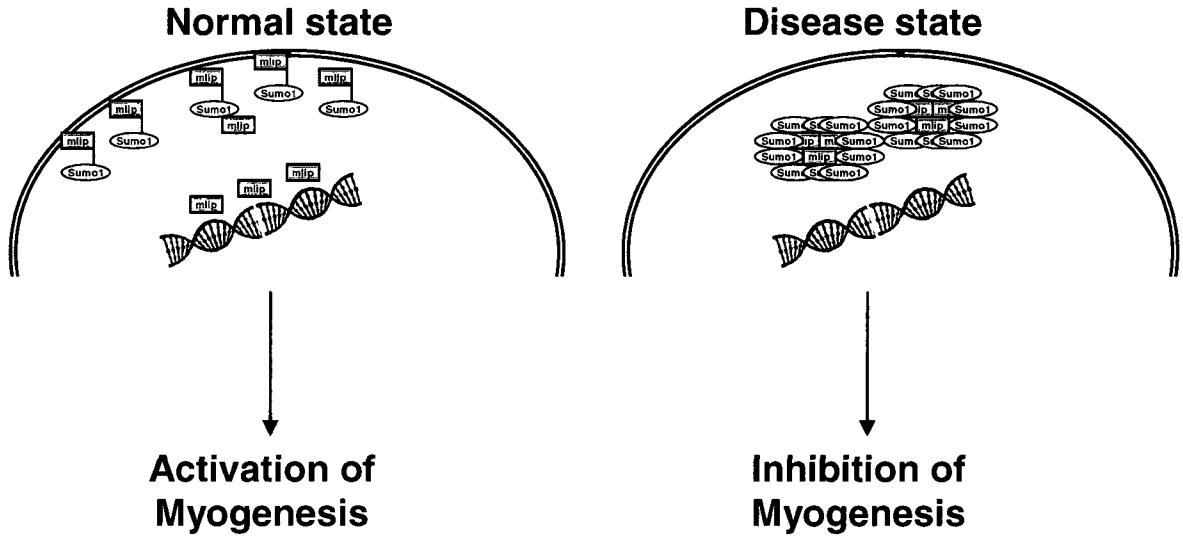

Figure 5.3 Schematic diagram of myocyte nucleus showing effect of Mlip sumoylation in normal and diseased states. I hypothesize that under normal circumstances, non-sumoylated Mlip is capable of binding DNA and activating myogenesis. Steady-state sumoylation is also present. In cells of patients with LMNA mutations, Mlip may be constitutively sumoylated thus inhibiting myogenesis and leading to dystrophic conditions seen in laminopathies. Squares represent Mlip. Ovals represent Sumo1.

HNRNPU

The samples sent out for mass spectrometric analysis yielded one protein that is a reported lamin A/C binding partner – hnRNPU. The hnRNPs are a family of over 30 RNA binding proteins, termed hnRNP A1 through U. They play a major role in the regulation of pre-mRNA splicing, pre-mRNA 3' end processing and polyadenylation, and mRNA nuclear transport. HnRNPs translocate mRNA to the cytoplasm via nuclear pore complexes. HnRNPU has an estimate molecular weight of 88kDa, the largest of the hnRNP family, however western blotting shows them to be ~120 kDa likely due to their multiple phosphorylation sites (Kiledjian and Dreyfuss 1992). In 2004, Vassileva and Matunis identified two hnRNPs as Sumo modified proteins. As part of their work, they performed an immunoprecipitation of ^{35}S-Methionine labeled hnRNP complexes and ran them on 2D gels. The gels were incubated with Sumo enzymes in the presence or absence of ATP. Here they identified strong spots representing hnRNP C-Sumo and M-Sumo. On the same gels, there is a faint spot slightly above hnRNPU in the presence of ATP, indicating it may be post-translationally modified by Sumo. The writers of this paper did not further investigate this. Incidentally, hnRNPU has multiple potential sumoylation sites (Figure 5.4). HnRNPE1 was shown to interact with lamin A/C in the same paper that identified the interaction with Ubc9 (Zhong et al 2005). This was the protein that all the results were shown for.

Since the band identified migrated to 120 kDa, this does not correspond to a Sumo1-shifted hnRNPU. However, it was present only in the lane of the Sumo1 transfected cells. This may imply that the increase in Sumo1 expression resulted in an upregulation of this protein and/or may have stimulated the interaction between lamin A/C and hnRNPU. The function of this effect warrants further investigation.

- mssspvnvkk lkvse**lkee**l kkrrlsdkg**l** **kad**lmdrlqa aldneaggrp amepgngsld lggdaagrsg agleqeaaag aeddeeeegi aaldgdqmel geengaagaa dagameeeea asedengddq gfqegedelg deeegagden ghgeqqsqpp aaaaqqqpsq qrgagkeaag kssgptslfa vtvappgarq gqqqaggdgk teqkggdkkr gvkrpredhg rgyfeyieen kysrakspqp pveeedehfd dtvvcldtyn cdlhfkisrd rlsassltme sfaflwaggr asygvskgkv cfemkvteki pvrhlytkdi dihevrigws lttsgmllge eefsygyslk giktcncete dygekfdend vitcfanfet develsyakn gqdlgvafki skevladrpl fphvlchnca vefnfgqkek pyfpipedct fiqnvpledr vrgpkgpeek kdcevvmmig lpgagkttwv tkhaaenpgk ynilgtntim dkmmvagfkk qmadtgklnt llqrapqclg kfieiaarkk rnfildqtnv saaaqrrkmc lfagfqrkav vvc**pkde**dyk qrtq**kkae**ve gkdlpehavl kmkgnftlpe vaecfdeity velqkeeaqk lleq**ykee**sk kalppekkqn tgskksnknk sgknqfnrgg ghrgrggfnm rggnfrggap gnrggynrrg nmpqrggggg sggigypypr gpvfpgrggy snrgnynrgg mpnrgnynqn frgrgnnrgy knqsqgynqw qqgqfwgqkp wsqhyhqgyy

Figure 5.4 hnRNPU amino acid sequence indicating the location of the Sumo1 consensus sequences.

I was not able to determine the identity of the four proteins seen on the western blot. This could be because the Coomassie blue staining of the weaker bands were washed off during the process. On the other hand, not seeing any difference between the immunoprecipitation of lamin A/C with and without Sumo1 transfection implies that the bands I saw on my western blot did not belong to sumoylated lamin A/C binding partners. We will continue attempting to identify these partners.

5.3 Differential function of lamin A and lamin C

As I mentioned in the Introduction to my thesis, there is conflicting data on the nuclear distribution of lamin A/C. Nuclear staining of cells indicate lamin A/C localization at the inner nuclear membrane, however Hozak et al (1995) hypothesized that there are nucleoplasmic lamins but antibodies could not penetrate to the core because of densely packed chromatin. They used restriction enzymes to cut through the chromatin fibers and found lamins within the nuclear regions. This initiated a series of studies using GFP fused lamins which allows for the visualization of the lamins in living cells and without the issue of poor antibody penetration (Broers et al 1999, Moir et al 2000b). In my studies, I also used lamins fused to GFP or GFP mutants (CFP, YFP). In cells expressing lamin A and lamin C, the lamins can be seen at the nuclear rim but also within the nucleoplasm, consistent with previous findings. The function of the nucleoplasmic lamins are varying. They have been implicated in cell proliferation and inhibition of DNA replication (Kennedy et al 2000, Moir et al 2000a), transcription (Spann et al 2002) and chromatin organization (Shimi et al 2008, Vaughan et al 2000).

The cellular distribution of lamin C is another topic of debate. Cellular studies have shown that overexpression of lamin C leads to localization in the nucleus as aggregates (Pugh et al 1997, Vaughan et al 2001, Sylvius et al 2005, Sylvius et al 2008). However, other studies show lamin C localization to be identical to lamin A localization (Gerace et al 1984, Raharjo et al 2001, Fong et al 2006). These studies employed different methods in order to reach their conclusions. Gerace et al (1984) found that although lamin A and lamin C incorporated in the nuclear envelope, their relative rates of incorporation differed – lamin A incorporates itself significantly faster than does lamin C. Pugh et al (1997) microinjected fluorescently labeled lamin A and lamin C in quiescent 3T3 cells and saw that lamin A and lamin C follow separate assembly pathways but that lamin C depends on lamin A levels for nuclear envelope incorporation. Thus, in my studies, I worked with either lamin A and lamin C separately or together in 1:1 ratios to restore stoichiometry in order to study both pathways. Consistent with Pugh et al (1997) and Gerace et al (1984), I see that lamin C overexpression results in the formation of intranuclear lamin aggregates, however, once stoichiometry is restored, lamin C localization is at the inner nuclear membrane. In support of this hypothesis, Vaughan et al (2001) studied lamin A and lamin C organization in SW13 cells, which express lamin A at minimal levels, and they found that here, lamin C is detected as aggregates within the nucleoplasm, perhaps within the nucleolus. This indicates that there is some dependence on lamin A for nuclear rim localization.

We and others have also shown that the individual isoforms behave differently when mutated (Raharjo et al 2001, Sylvius et al 2008). If the same mutation can affect the individual isoforms in different ways, this could implicate each of them in alternate mechanisms that lead to laminopathies. In support of this, I have shown that lamins A and C display different affinities

for their binding partners. In C2C12 cells, Srebp1 appears to interact exclusively with lamin C while Mlip appears to colocalize more strongly with lamin C than with lamin A. Furthermore, Sumo1 is seen sequestered within lamin C aggregates to a greater degree than when lamin A and C are co-expressed (Sylvius et al 2005, Boudreau, Labib et al manuscript in preparation). In order to account for these apparent discrepancies, we must study the individual isoforms separately and together.

5.4 A possible explanation for the lack of genotype-phenotype relationship

I would like to address the biggest issue facing the laminopathy research field – the lack of genotype-phenotype relationship, specifically among diseases affecting the striated muscle (Figure 1.4). I propose that the *LMNA* mutations are pathological only in that they cause the lamina to be more susceptible to viral infection.

The nuclear lamina plays an important role as a barrier to most viruses. Upon infection, the viral genome is transported to the nucleus via the NPC (Greber et al 2003). The viral DNA undergoes replication and packaging within the host's nucleus but the ~120nm nucleocapsid cannot be released through the NPC that can accommodate a maximum of 38nm. Viral protein kinases have been shown to phosphorylate lamin A/C resulting in the dissolution of the nuclear lamina, simulating lamin A/C phosphorylation during mitosis, allowing the viral capsid to exit the nucleus (Mou et al 2007, Lee et al 2008).

For years, researchers have theorized that a proportion of idiopathic DCM is due to a previous exposure to a virus (Martino et al 1993), however, it can be very difficult to recognize

evidence of a viral infection as time progresses (Dec et al 1985). I hypothesize that the *LMNA* mutations are pathogenic simply because they cause the lamina to be more susceptible to successful viral infection. Furthermore, lamin A/C expression was found to be down-regulated in cardiac tissue biopsies from patients with DCM (Asakura and Kitakaze 2009), indicating that even in the absence of *LMNA* mutations, muscle weakness is associated with lamin A/C expression.

This theory has not been studied with respect to *LMNA* mutations and DCM, however, a link has been made between DCM associated with the dystrophin gene and virally mediated DCM (Badorff et al 1999, Xiong et al 2002) where they found that Coxsackieviral protease 2A cleaves dystrophin and that viral replication and release is more efficient in dystrophin deficient mice, respectively. As I mentioned in the Introduction, the penetrance of *LMNA* mutations with a disease is not 100% (see Figure 1.4 asymptomatic patients), therefore, an environmental explanation for the wide variety of disorders associated with the mutations is an interesting path to take in the study of laminopathies.

5.5 Conclusions

In my thesis, I have presented evidence for my main hypothesis, that *LMNA* mutations exert their tissue-specific effects via the perturbation of lamin A and C's specific interacting partners.

With the intention of detecting the specific cellular phenotypes associated with three cardiac-specific disorders with *LMNA* mutations, I have shown that a lone AF-associated mutation and a DCM-associated mutation result in PKCα misloclaization to the nucleus. The deregulation of PKCα signaling may have serious downstream consequences that can attribute to

the symptoms observed in cardiac-specific disorders. Although no discernable differences in the cellular distribution of lamin A and C were observed, I did identify two previously unreported lamin A/C characteristics that may help us in understanding the function of the protein in the cell and in the development of cardiac-specific laminopathies: cytoplasmic lamin A/C extrusion and sickle-shaped lamin A/C aggregates. Both phenotypes point to the formation of a weakened lamina which will make the affected cells more susceptible to damage under constant mechanical stress in contractile tissues, such as cardiac and skeletal muscles.

On the other hand, I have also implicated Sumo1 post-translational modification in the development of laminopathies by identifying a mislocalization of Ubc9, the Sumo E2 conjugating enzyme, in the presence of *LMNA* mutations. I have also identified a potentially novel sumoylated lamin A/C binding partner, hnRNPU. The indirect disturbance of the Sumo1 process because of *LMNA* mutations will affect the function of its tissue-specific substrate proteins. Identifying these substrates will help determine how *LMNA* mutations exert their tissue-specific effects.

Furthermore, I have furthered our current knowledge about the different functions of lamin A and lamin C with respect to their differential interactions with Srebp1 and Mlip, adipocyte- and muscle-specific binding partners, respectively. Lamin A and C both interact with Srebp1 in rat liver lysates, however only lamin C interacts with Srebp1 in myoblast cells. Similary, Mlip localization appears to be affected by lamin C more so than by lamin A. I have also provided novel hypothetical mechanisms of how *LMNA* mutations result in their altered activity via disabled Sumoylation which will either trap these transcription factors at the mutant aggregates or at the inner nuclear membrane.

References

Adamson AI, Kenney S. Epstein-Barr virus immediate-early protein BZLF1 is Sumo1 modified and disrupts promyelocytic leukemia bodies. Journal of Virology. 75: 2388-2399. 2001.

Ahmad F, Seidman JG, Seidman CE. The genetic basis for cardiac remodeling. Annual Review of Genomics and Human Genetics. 6: 185-216. 2005.

Ahn K, Song JH, Kim DK, Park MH, Jo SA, Koh YH. Ubc9 gene polymorphisms and late-onset Alzheimer's disease in the Korean population: A genetic association study. Neuroscience Letters. 465: 272-275. 2009.

Alkurya FS, Saadi I, Lund JJ, Turbe-Doan A, Morton CC, Maas RL. Sumo1 happloinsufficiency leads to cleft lip and palate. Science. 313: 1751. 2006.

Arbustini E, Pilotto A, Repetto A, Grasso M, Negri A, Diegoli M, Campana C, Scelsi L, Baldini E, Gavazzi A, Tavazzi L. Autosomal dominant dilated cardiomyopathy with atrioventricular block: a lamin A/C defect-related disease. Journal of the American College of Cardiology. 39: 981-990. 2002.

Archard LC, Richardson PJ, Olsen EG, Dubowitz V, Sewry C, Bowles NE. The role of Coxsackie B viruses in the pathogenesis of myocarditis, dilated cardiomyopathy and inflammatory muscle disease. Biochemical Society symposium. 53:51-62. 1987.

Arimura T, Helbling-Leclerc A, Massart C, Varnous S, Niel F, Lacene E, Fromes Y, Toussaint M, Mura A-M, Keller DI, Amthor H, Isnard R, Malissen M, Schwartz K, Bonne G. Mouse model carrying H222P-LMNA mutation develops muscular dystrophy and dilated cardiomyopathy similar to human striated muscle laminopathies. Human Molecular Genetics. 14: 155-169. 2005.

Asakura M and Kitakaze M. Global gene expression profiling in the failing myocardium. Circulation Journal. 73: 1568-1576. 2009.

Badorff C, Lee G-H, Lamphear BJ, Martone ME, Campbell KP, Rhoads RE, Knowlton KU. Enteroviral protease 2A cleaves dystrophin: evidence of cytoskeletal disruption in an acquired cardiomyopathy. Nature Medicine. 5: 320-326. 1999.

Barton RM, Worman HJ. Prenylated prelamin A interacts with Narf, a novel nuclear protein. Journal of Biological Chemistry. 274: 30008-30018. 1999.

Bayer P, Arndt A, Metzger S, Mahajan R, Melchior F, Jaenicke R, Becker J. Structure determination of the small ubiquitin-related modifier Sumo1. Journal of Molecular Biology. 280: 275-286. 1998.

Bechert K, Lagos-Quintana M, Harborth J, Weber K, Osborn M. Effects of expressing lamin A mutant protein causing Emery-Dreifuss muscular dystrophy and familial partial lipodystrophy in HeLa cells. Experimental Cell Research. 286: 75-86. 2002.

Bengtsson L, Otto H. LUMA interacts with emerin and influences its distribution at the inner nuclear membrane. Journal of Cell Science. 121: 536-548. 2008.

Bernier-Villamor V, Sampson DA, Matunis MJ, Lima CD. Structural basis for E2-mediated Sumo conjugation revealed by a complex between ubiquin-conjugating enzyme Ubc9 and RanGAP1. Cell. 108: 345-356. 2002.

Bilinska ZT, Sylvius N, Grzybowski J, Fidzianska A, Machalak E, Walczak E, Walski M, Bieganowska K, Szymaniak E, Kusmierczyk-Droszcz B, Lubiszewska B, Wagner T, Tesson F, Ruzyllo W. Dilated cardiomyopathy caused by LMNA mutations. Clinical and morphological studies. Kardiologia Polska. 64: 812-819. 2006.

Bonne G, Di Barletta MR, Varnous S, Becane HM, Hammouda EH, Merlini L, Muntoni F, Greenberg CR, Gary F, Uritzberea JA, Duboc D, Fardeau M, Toniolo D, Schwartz K. Mutations in the gene encoding lamin A/C cause autosomal dominant Emery-Dreifuss muscular dystrophy. Nature Genetics. 21: 285-288. 1999.

Bonne G, Mercuri E, Muchir A, Uritzberea A, Becane HM, Recan D, Merlini L, Wehnert M, Boor R, Reuner U, Vorgerd M, Wicklein EM, Eymard B, Duboc D, Penisson-Besnier I, Cuisset JM, Ferrer X, Desguerre I, Lacombe D, Bushby K, Pollitt C, Toniolo D, Fardeau M, Schwartz K, Muntoni F. Clinical and molecular genetic spectrum of autosomal dominant emery-dreifuss muscular dystrophy due to mutations of the lamin A/C gene. Annals of Neurology. 48: 170-180. 2000.

Brachner A, Reipert S, Foisner R, Gotzmann J. LEM2 is a novel MAN1-related inner nuclear membrane protein associated with A-type lamins. Journal of Cell Science. 118: 5797-5810. 2005.

Brauch KM, Chen LY, Olson TM. Comprehensive mutation scanning of LMNA in 268 patients with lone atrial fibrillation. American Journal of Cardiology. 103: 1426-1428. 2009.

Braz JC, Bueno OF, De Windt LJ, Molkentin JD. PKCalpha regulates the hypertrophic growth of cardiomyocytes through extracellular signal-regulated kinase1/2 (ERK1/2). The Journal of Cell Biology. 156: 905-919. 2002.

Braz JC, Gregory K, Pathak A, Zhao W, Sahin B, Klevitsky R, Kimbali TF, Lorenz JN, Nairn AC, Liggett SB, Bodi I, Wang S, Schwartz A, Lakatta EG, DePaoli-Roach AA, Robbins J, Hewett TE, Bibb JA, Westfall MV, Kranias EG Molkentin JD. PKC-alpha regulates cardiac contractility and propensity toward heart failure. Nature Medicine. 10: 248-254. 2004.

Bridger JM, Kill IR, O'Farrell M, Hutchison CJ. Internal lamin structures within G1 nuclei of human dermal fibroblasts. Journal of Cell Science. 104: 297-306. 1993.

Brodsky GL, Muntoni F, Miocic S, Sinagra G, Sewry C, Mestroni L. Lamin A/C gene mutation associated with dilated cardiomyopathy with variable skeletal muscle involvement. Circulation. 101: 473-476. 2000.

Broers JLV, Machiels BM, van Eys GJJM, Kuijpers HJH, Manders EMM, van Driel R, Ramaekers FCS. Dynamics of the nuclear lamina as monitored by GFP-tagged A-type lamins. Journal of Cell Science. 112: 3463-3475. 1999.

Broers JLV, Peeters EAG, Kuijpers HJH, Endert J, Bouten CVC, Oomens CWJ, Baaijens FPT, Ramaekers FCS. Decreased mechanical stiffness in LMNA-/- cells is caused by defective nucleo-cytoskeletal integrity:. mplications for the development of laminopathies. Human Molecular Genetics. 13: 2567-2580. 2004.

Broers JLV, Kuijpers HJH, Ostlund C, Worman HJ, Endert J, Ramaekers FCS. Both lamin A and lamin C mutations cause lamina instability as well as loss of internal nuclear lamin organization. Experimental Cell Research. 304: 582-592. 2005.

Brown SC, Piercy RJ, Muntoni F, Sewry CA. Investigating the pathology of Emery-Dreifuss muscular dystrophy. Biochemical Society Transactions. 36: 1335-1338. 2008.

Burke B. On the cell-free association of lamins A and C with metaphase chromosomes. Experimental Cell Research. 186: 169-176. 1990.

Capanni C, Cenni V, Mattioli E, Sabatelli P, Ognibene A, Columbaro M, Parnaik VK, Wehnert M, Maraldi NM, Squarzoni S, Lattanzi G. Failure of lamin A/C to functionally assemble in R482L mutated familial partial lipodystrophy fibroblasts: altered intermolecular interaction with emerin and implications for gene transcription. Experimental Cell Research. 291: 122-134. 2003.

Capanni C, Mattioli E, Columbaro M, Lucarelli E, Parnaik VK, Novelli G, Wehnert M, Cenni V, Maraldi NM, Squarzoni S, Lattanzi G. Altered pre-lamin A processing is a common mechanism leading to lipodystrophy. Human Molecular Genetics. 14: 1489-1502. 2005.

Caux F, Dubosclard E, Lascols O, Buendia B, Chazouillères O, Cohen A, Courvalin JC, Laroche L, Capeau J, Vigouroux C, Christin-Maitre S. A new clinical condition linked to a novel mutation in lamins A and C with generalized lipoatrophy, insulin-resistant diabetes, disseminated leukomelanodermic papules, liver steatosis, and cardiomyopathy. The Journal of Clinical Endocrinology & Metabolism. 88: 1006-1013. 2003.

Chkheidze AN and Liebhaber SA. A novel set of nuclear localization signals determine distributions of the alphaCP RNA-binding proteins. Molecular and Cellular Biology. 23: 8405-8415. 2003.

Clements L, Manilal S, Love DR, Morris GE. Direct interaction between emerin and lamin A. Biochemical and Biophysical Research Communications. 267: 709-714. 2000.

Comerford KM, Leonard MO, Karhausen J, Carey R, Colgan SP, Taylor CT. Small ubiquitin-related modifier-1 modification mediates resolution of CREB-dependent responses to hypoxia. Proceedings of the National Academy of Science. 100: 986-991. 2003.

Csoka AB, Cao H, Sammak PJ, Constantinescu D, Schatten GP, Hegele RA. Novel lamin A/C gene (LMNA) mutations in atypical progeroid syndromes. Journal of Medical Genetics. 41: 304-308. 2004.

Darbar D, Herron KJ, Ballew JD, Jahangir A, Gersh BJ, Shen WK, Hammill SC, Packer DL, Olson TM. Familial atrial fibrillation is a genetically heterogeneous disorder. Journal of the American College of Cardiology. 41: 2185-2192. 2003.

DeBose-Boyd RA, Brown MS, Li WP, Nohturfft A, Goldstein JL, Espenshade PJ. Transport-dependent proteolysis of Srebp: relocation of site-1 protease from Golgi to ER obviates the need for Srebp transport to Golgi. Cell. 99: 703-712. 1999.

Dec GW Jr, Palacios IF, Fallon JT, Aretz HT, Mills J, Lee DC, Johnson RA. Active myocarditis in the spectrum of acute dilated cardiomyopathies. Clinical features, histological correlates, and clinical outcome. New England Journal of Medicine. 312:885-890. 1985.

Dec GW, Fuster V. Idiopathic Dilated cardiomyopathy. New England Journal of Medicine. 331:1564-1575. 1994.

Dechat T, Korbei B, Vaughan OA, Vlcek S, Hutchinson CJ, Foisner R. Lamina-associated polypeptide 2alpha binds intranuclear A-type lamins. Journal of Cell Science. 113: 3473-3484. 2000.

Dechat T, Gajewski A, Korbei B, Gerlich D, Daigle N, Haraguchi T, Furukawa K, Ellenberg J, Foisner R. Lap2alpha and BAF transiently localize to telomeres and specific regions on chromatin during nuclear assembly. Journal of Cell Science. 117: 6117-6128. 2004.

Dhe Phagnon S, Werner ED, Chi YI, Shoelson SE. Structure of the globular tail of nuclear lamin. The Journal of Biological Chemistry. 277: 17381-17384. 2002.

Divecha N, Banfic H, Irvine RF. The polyphosphoinositide cycle exists in the nuclei of Swiss 3T3 cells under the control of a receptor (for IGF-I) in the plasma membrane, and stimulation of the cycle increases nuclear diacylglycerol and apparently induces translocation of protein kinase C to the nucleus. The EMBO Journal. 10: 3207-3214. 1991.

Dreuillet C, Tillit J, Kress M, Ernoult-Lange M. In vivo and in vitro interaction between human transcription factor MOK2 and nuclear lamin A/C. Nucleic Acids Research. 30: 4634-4642. 2002.

Dreuillet C, Harper Maryannick, Tillit J, Kress M, Ernoult-Lange M. Mislocalization of human transcription factor MOK2 in the presence of pathogenic mutations of lamin A/C. Biology of the Cell. 100: 51-61. 2008.

Dunnebier T, Bermejo JL, Haas S, Fischer HP, Pierl CB, Justenhoven C, Brauch H, Baisch C, Gilbert M, Harth V, Spickenheuer A, Rabstein S, Pesch B, Bruning T, Ko YD, Hamann U. Common variants in the Ubc9 gene encoding the Sumo-conjugating enzyme are associated with breast tumor grade. International Journal of Cancer. 125: 596-602. 2009.

Eggert M, Radomski N, Linder D, TripierD, Traub P, Jost E. Identification of novel phosphorylation sites in murine A-type lamins. European Journal of Biochemistry. 213: 659-671. 1993.

Eriksson M, Brown WT, Gordon LB, Glynn MW, Singer J, Scott L, Erdos MR, Robbins CM, Moses TY, Berglund P, Dutra A, Pak E, Durkin S, Csoka AB, Boehnke M, Glover TW, Collins FS. Nature. 423: 293-298. 2003.

Evdokimov E, Sharma P, Lockett SJ, Lualdi M, Kuehn MR. Loss of Sumo1 in mice affects RanGAP1 localization and formation of PML nuclear bodies, but is not lethal as it can be compensated by Sumo2 or Sumo3. Journal of Cell Science. 121: 4106-4113. 2008.

Favreau C, Dubosclard E, Ostlund C, Vigouroux C, Capeau J, Wehnert M, Higuet D, Worman HJ, Courvalin JC, Buendia B. Experimental Cell Research. 282: 14-23. 2003.

Feinberg WM, Blackshear JL, Laupacis A, Kronmal R, Hart RG. Prevalence, age distribution, and gender of patients with atrial fibrillation. Analysis and Implications. Archives of Internal Medicine. 13: 469-473. 1995.

Fisher DZ, Chaudhary N, Blobel G. cDNA sequencing of nuclear lamins A and C reveals primary and secondary structural homology to intermediate filament proteins. Proceedings of the National Academy of Science USA. 83: 6450-6454. 1986.

Foisner R, Gerace L. Integral membrane proteins of the nuclear envelope interact with lamins and chromosomes, and binding is modulated by mitotic phosphorylation. Cell. 73: 1267-1279. 1993.

Fong LG, Ng JK, Lammerding J, Vickers TA, Meta M, Cote N, Gavino B, Qiao X, Chang SY, Young SR, Yang SH, Stewart CL, Lee RT, Bennett CF, Bergo MO, Young SG. Prelamin A and lamin A appear to be dispensable in the nuclear lamina. The Journal of Clinical Investigation. 116: 743-752. 2006.

Forissier JF, Bonne G, Bouchier C, Duboscq-Bidot L, Richard P, Wisnewski C, Briault S, Moraine C, Dubourg O, Schwartz K, Komajda M. Apical left ventricular aneurysm without atrio-ventricular block due to a lamin A/C gene mutation. European Journal of Heart Failure. 5: 821-825. 2003.

Furukawa K, Inagaki H, Hotta Y. Identification and cloning of an mRNA coding for a germ-cell specific A-type lamin in mice. Experimental Cell Research. 212: 426-430. 1994.

Furukawa K, Ishida K, Tsunoyama T, Toda S, Osoda S, Horigome T, Fisher PA, Sugiyama S. A-type and B-type lamins initiate layer assembly at distinct areas of the nuclear envelope in living cells. Experimental Cell Research. 315: 1181-1189. 2009.

Gambineri A, Semple RK, Forlani G, Genghini S, Grassi I, Hyden CSS, Pagotto U, O'Rahilly S, Pasquali R. Monogenic polycystic ovary syndrome due to a mutation in the lamin A/C gene is sensitive to thiazolidinediones but not to metformin. European Journal of Endocrinology. 159: 347-353. 2008.

Genschel J, Bochow B, Kuepferling S, Ewert R, Hetzer R, Lochs H, Schmidt HHJ. A R644C mutation within lamin A extends the mutations causing dilated cardiomyopathy. Human Mutation Mutation and Polymorphism Report #201. 2001.

Gerace L, Blobel G. The nuclear envelope lamina is reversibly depolymerized during mitosis. Cell. 19: 277-287. 1980.

Gerace L, Comeau C, Benson M. Organization and modulation of nuclear lamina structure. Journal of Cell Science. 1: 137-160. 1984.

Gieffers C and Krohne G. In vitro reconstitution of recombinant lamin A and a lamin A mutant lacking the carboxy-terminal tail. European Journal of Cell Biology. 55: 191-199. 1991.

Glass JR and Gerace L. Lamins A and C bind assemble at the surface of mitotic chromosomes. Journal of Cell Biology. 111: 1047-1057. 1990.

Glass CA, Glass JR, Taniura H, Hasel KW, Blevitt JM, Gerace L. The alpha-helical rod domain of human lamins A and C contains a chromatin binding site. The EMBO Journal. 12: 4413-4424. 1993.

Goldman AE, Moir RD, Montag-Lowy M, Stewart M, Goldman RD. Pathway of incorporation of microinjected lamin A into the nuclear envelope. The Journal of Cell Biology. 119: 725-735. 1992.

Greber UF and Fassati A. Nuclear import of viral DNA genomics. Traffic. 4: 136-143. 2003.

Grunig E, Tasman JA, Kucherer H, Franz W, Kubler W, Katus HA. Frequency and phenoytpe of familial dilated cardiomyopathy. Journal of the American college of cardiology. 31:186-194. 1998.

Gupta P, Bilinska ZT, Sylvius N, Boudreau E, Veinot JP, Labib S, Bolongo PM, Hamza A, Jackson T, Ploski R, Walski M, Grzybowski J, Walczak W, Religa G, Fidzianska A, Tesson F. Genetic and ultrastructural studies in dilated cardiomyopathy patients: a large deletion in the

lamin A/C gene is associated with cardiomyocyte nuclear envelope disruption. Basic Research in Cardiology. 105: 365-377. 2010.

Haas M, Jost E. Functional analysis of phosphorylation sites in human lamin A controlling lamin disassembly, nuclear transport and assembly. European Journal of Cell Biology. 62: 237-247. 1993.

Hakelien AM, Delbarre E, Gaustad KG, Buendia B, Collas P. Expression of the myodystrophic R453W mutation of lamin A in C2C12 myoblasts causes promoter-specific and global epigenetic defects. Experimental Cell Research. 314: 1869-1880. 2008.

Haque F, Lloyd DJ, Smallwood DT, Dent CL, Shanahan CM, Fry AM, Trembath RC, Shackleton S. SUN1 interacts with nuclear lamin A and cytoplasmic nesprins to provide a physical connection between the nuclear lamina and the cytoskeleton. Molecular and Cellular Biology. 26: 3738-3751. 2006.

Harborth J, Elbashir SM, Bechert K, Tuschl T, Weber K. Identification of essential genes in cultured mammalian cells using small interfering RNAs. Journal of Cell Science. 114: 4557-4565. 2001.

Heald R, McKeon F. Mutations of phosohorylation sites in lamin A that prevent nuclear lamina disassembly in mitosis. Cell. 61: 579-589. 1990.

Heessen S and Fornerod M. The inner nuclear envelope as a transcription factor resting place. European Molecular Biology Organization. 8: 914-919. 2007.

Heitlinger E, Peter M, Lustig A, Villiger W, Nigg EA, Aebi U. The role of the head and tail domain in lamin structure and assembly: analysis of bacterially expressed chicken lamin A and truncated B2 lamins. Journal of Structural Biology. 108: 74-91. 1992.

Hemelaar J, Borodovsky A, Kessler BM, Reverter D, Cook J, Kolli N, Gan-Erdene T, Wilkinson KD, Gill G, Lima CD, Ploegh HL, Ovaa H. Specific and covalent targeting of conjugating and deconjugating enzymes of ubiquitin-like proteins. Molecular and cellular biology. 24: 84-95. 2004.

Hietakangas V, Anckar J, Blomster HA, Fujimoto M, Palvimo JJ, Nakai A, Sistonen L. PDSM, a motif for phosphorylation-dependent Sumo modification. Proceedings of the National Academy of Science. 103: 45-50. 2006.

Hirano Y, Yoshida M, Shimizu M, Sato R. Direct demonstration of rapid degradation of nuclear sterol regulatory element-binding proteins by the ubiquitin-proteasome pathway. The Journal of Biological Chemistry. 276: 36431-36437. 2001.

Hirano Y, Murata S, Tanaka K, Shimizu M, Sato R. Sterol regulatory element-binding proteins are negatively regulated through Sumo1 modification independent of the ubiquitin/26 S proteasome pathway. The Journal of Biological Chemistry. 278: 16809-16819. 2003.

Holaska JM, Lee KK, Kowalski AK, Wilson KL. Transciptional repressor germ cell-less (GCL) and barrier to autointegration factor (BAF) compete for binding to emerin in vitro. Journal of Biological Chemistry. 278: 6969-6975. 2003.

Holtz D, Tanaka RA, Hartwig J, McKeon F. The CaaX motif of lamini A functions in conjunction with the nuclear localization signal to target assembly to the nuclear envelope. Cell. 59: 969-977. 1989.

Hookana E, Junttila MJ, Sarkioja T, Sormunen R, Niemela M, Raatikainen MJ, Uusimaa P, Lizotte E, Peuhkurinen K, Brugada K, Huikuri HV. Cardiac arrest and left ventricular fibrosis in a Finnish family with the lamin A/C mutation. Journal of Cardiovascular Electrophysiology. 19: 743-747. 2008.

Hozak P, Sasseville AMJ, Raymond Y, Cook PR. Lamin proteins form an internal nucleoskeleton as well as a peripheral lamina in human cells. Journal of Cell Science. 108: 635-644. 1995.

Hubner S, Eam JE, hubner A, Jans DA. Laminopathy-inducing lamin A mutants can induce redistribution of lamin binding proteins into nuclear aggregates. Experimental Cell Research. 312: 171-183. 2006.

Isobe K, Gohara R, Ueda T, Takasaki Y, Ando S. The last twenty residues in the head domain of mouse lamin A contain important structural elements for formation of head-to-tail polymers in vitro. Bioscience Biotechnology and Biochemistry. 71: 1252-1259. 2007.

Ivorra C, Kubicek M, Gonzalez JM, Sanz-Gonzalez SM, Alvarez-Barrientos A, O'Connor JE, Burke B, Andres V. A mechanism of AP1 suppression through interaction of c-Fos with lamin A/C. Genes and Development. 20: 307-320. 2006.

Jagatheesan G, Thanumalayan S, Muralikrishna Bh, Rangaraj N, Karande AA, Parnaik VK. Colocalization of intranuclear lamin foci with RNA splicing factors. Journal of Cell Science. 112: 4651-4661. 1999.

Janaki-Ramaiah M and Parnaik VK. An essential GT motif in the lamin A promoter mediates activation by CREB-binding protein. Biochemical and Biophysical Research Communications. 348: 1132-1137. 2006.

Jang MS, Ryu SW, Kim E. Modification of Daxx by small ubiquitin-related modifier-1. Biochemical and Biophysical Research Communications. 295: 495-500. 2002.

Johnson BR, Nitta RT, Frock RL, Mounkes L, Barbie DA, Stewart CL, Harlow E, Kennedy BK. A-type lamins regulate retinoblastoma protein function by promoting subnuclear localization and preventing proteasomal degradation. Proceedings of the National Academy of Science. 101: 9677-9682. 2004.

Jones D, Crowe E, Stevens TA, Candido EP. Functional and phylogenetic analysis of the ubiquitylation system in Caenorhabditis elegans: ubiquitin-conjugating enzymes, ubiquitin-activating enzymes, and ubiquitin-like proteins. Genome Biology. 3: research00002.1-00002.15. 2002.

Kagey MH, Melhuish TA, Wotton D. The polycomb protein Pc2 is a Sumo E3. Cell. 113: 127-137. 2003.

Kandert S, Luke Y, Kleinhenz T, Neumann S, Lu W, Jaeger VM, Munck M, Wehnert M, Muller CR, Zhou Z, Noegel AA, Dabauvalle MC, Karakesisoglou I. Nesprin-2 giant safeguards nuclear envelope architecture in LMNA S143F progeria cells. Human Molecular Genetics. 16: 2944-2959. 2007.

Kandert S, Wehnert M, Muller CR, Buendia B, Dabauvalle MC. Impaired nuclear functions lead to increased senescence and inefficient differentiation in human myoblasts with a dominant p.R545C mutation in the LMNA gene. European Journal of Cell Biology. 88: 593-608. 2009.

Kaul S, Blackford JA Jr, Cho S, Simons SS Jr. Ubc9 is a novel modulator of the induction properties of glucocorticoid receptors. Journal of Biological Chemistry. 277:12541-12549. 2002.

Kennedy BK, Barbie DA, Classoc M, Dyson N, Harlow E. Nuclear organization of DNA replication in primary mammalian cells. Genes and Development. 14: 2855-2868. 2000.

Kiledjian M and Dreyfuss GG. Primary structure and binding activity of the hnRNP U protein: binding RNA through RGG box. The EMBO Journal. 11: 2655-2664. 1992.

Kim JB and BM Spiegelman. ADD1/SREBP1 promotes adipocyte differentiation and gene expression linked to fatty acid metabolism. Genes and Development. 10: 1096-1107. 1996.

Kitaguchi T, Matsubara S, Sato M, Miyamoto K, Hirai S, Schwartz K, Bonne G. A missense mutation in the exon 8 of lamin A/C gene in a Japanese case of autosomal dominant limb-girdle muscular dystrophy and cardiac conduction block. Neuromuscular Disorder. 11: 542-546. 2001.

Krimm I, Ostlund C, Gilquin B, Couprie J, Hossenlopp P, Mornon JP, Bonne G, Courvalin JC, Worman HJ, Zinn-Justin S. The Ig-like structure of the C-terminal domain of lamin AC, mutated in muscular dystrophies, cardiomyopathies, and partial lipodystrophy. Structure. 10: 811-823. 2002.

Kumaran RI, Muralikrishna B, Parnaik VK. Lamin A/C speckles mediate spatial organization of splicing factor compartments and RNA polymerase II transcription. Journal of Cell Biology. 159: 783-793. 2002.

Kurtzman AL and Schechter N. Ubc9 interacts with a nuclear localization signal and mediates nuclear localization of the paired-like homeobox protein Vsx-1 independent of Sumo1 modification. Proceedings of the National Academy of Science. 98: 5602-5607. 2001.

Lammerding J, Schulze PC, Takahashi T, Kozlov S, Sullivan T, Kamm RD, Stewart CL, Lee RT. Lamin A/C deficiency causes defective nuclear mechanics and mechanotransduction. Journal of Clinical Investigation. 113: 370-378. 2004.

Lammerding J, Hsiao J, Schulze PC, Kozlov S, Stewart CL, Lee RT. Abnormal nuclear shape and impaired mechanotransduction in emerin-deficient cells. The Journal of Cell Biology. 170: 781-791. 2005.

Lammerding J, Fong LG, Ji JY, Reue K, Stewart CL, Young SG, Lee RT. Lamins A and C but not lamin B1 regulate nuclear mechanics. The Journal of Biological Chemistry. 281: 25768-25780. 2006.

Leach KL, Powers EA, Ruff VA, Kaufman S. Type 3 protein kinase C localization to the nuclear envelope of phorbol ester-treated NIH 3T3 cells. The Journal of Cell Biology. 109: 685-695. 1989.

Lee C-P, Huang Y-H, Lin S-F, Chang Y, Chang Y-H, Takada K, Chem M-R. Epstein-Barr virus BGLF4 kinase induces disassembly of the nuclear lamina to facilitate virion production. Journal of Virology. 82: 11913-11926. 2008.

Lee DC, Welton KL, Smith ED, Kennedy BK. A-type nuclear lamins act as transcriptional repressors when targeted to promoters. Experimental Cell Research. 315: 996-1007. 2009.

Leukel M, Jost E. Two conserved serines in the nuclear localization signal flanking region are involved in the nuclear targeting of human lamin A. European Journal of Cell Biology. 68: 133-142. 1995.

Lin F, Worman HJ. Structural organization of the human gene encoding nuclear lamin A and nuclear lamin C. The Journal of Biological Chemistry. 268: 16321-16326. 1993.

Lin F, Worman HJ. Expression of nuclear lamins in human tissues and cancer cell lines and trancription from the promoters of the lamin A/C and B1 genes. Experimental Cell Research. 236: 378-384. 1997.

Lin X, Liang M, Liang YY, Brunicardi FC, Melchior F, Feng XH. Activation of transforming growth factor Beta signaling by Sumo1 modification of tumor suppressor Smad4/DPC4. The Journal of Biological Chemistry. 278: 18714-18719. 2003.

Lloyd DJ, Trembath RC, Shackleton S. A novel interaction between lamin A and Srebp1: implications for partial lipodysstrophy and other laminopathies. Human Molecular Genetics. 11: 769-777. 2002.

Loewinger L, McKeon F. Mutations in the nuclear lamin proteins resulting in their abberrant assembly in the cytoplasm. The EMBO Journal. 7: 2301-2309. 1988.

Luderus MEE, den Blaauwen JL, de Smit OJB, Compton DA, van Driel R. Binding of matrix attachment regions to lamin polymers involves single-stranded regions and the minor groove. Molecular and Cellular Biology. 14: 6297-6305. 1994.

Luk A, Ahn E, Soor GS, Butany J. Dilated cardiomyopathy: a review. Journal of Clinical Pathology. 62: 219-225. 2009.

Machiels BM, Zorenc AHG, Endert JM, Kuijpers HJH, van Eys GJJM, Ramaekers FCS, Broers JLV. An alternative splicing product of the lamin A/C gene lacks exon 10. The Journal of Biological Chemistry. 271: 9249-9253. 1996.

Maeshima K, Yahata K, Sasaki Y, Nakatomi R, Tachibana T, Hashikawa T, Imamoto F, Imamoto N. Cell-cycle-dependent dynamics of nuclear pores: pore-free islands and lamins. Journal of Cell Science. 119: 4442-4451. 2006.

Malhotra R, Mason PK. Lamin A/C deficiency as a cause of familial dilated cardiomyopathy. Current Opinions in Cardiology. 24: 203-208. 2009.

Mancini MA, Shan B, Nickerson JA, Penman S, Lee WH. The retinoblastoma gene product is a cell cycle-dependent, nuclear matrix-associated protein. Proceedings of the National Academy of Science USA. 91: 418-422. 1994.

Mansharamani M, Wilson KL. Direct binding of nuclear membrane protein MAN1 to emerin in vitro and two modes of binding to barrier-to-autointegration factor. Journal of Biological Chemistry. 280: 13863-13870. 2005.

Maraldi NM, Capanni C, Lattanzi G, Camozzi D, Facchini A, Manzoli FA. Srebp1 interaction with prelamin A forms: A pathogenic mechanism for lipodystrophic laminopathies. Advanced Enzyme Regulation. 48: 209-223. 2007.

Mariappan I, Gurung R, Thanumalayan S, Parnaik VK. Identification of cyclin D3 as a new interaction partner of lamin A/C. Biochemical and Biophysical Research Communications. 355: 981-985. 2007.

Martelli AM, Tabellini G, Bortul R, Manzoli L, Bareggi R, Baldini G, Grill V, Zweyer M, Narducci P, Cocco L. Enhanced nuclear diacylglycerol kinase activity in response to a mitogenic stimulation of quiescent swiss 3T3 cells with insulin-like growth factor I. Cancer Research. 60: 815-821. 2000.

Martelli AM, Bortul R, Tabellini G, Faenza I, Cappellini A, Bareggi R, Manzoli L, Cocco L. Molecular characterization of protein kinase C alpha binding to lamin A. Journal of Cellular Biochemistry. 86: 320-330. 2002.

Martino TA, Liu P, Sole MJ. Viral infection and the pathogenesis of dilated cardiomyopathy. Circulation Research. 74: 182-188. 1993.

McDoniels-Silvers AL, Nimri CF, Stoner GD, Lubet RA, You M. Differential gene expression in human lung adenocarcinomas and squamous cell carcinomas. Clinical Cancer Research. 8: 1127-1138. 2002.

McKeon FD, Kirschner MW, Caput D. Homologies in both primary and secondary structure between nuclear envelope and intermediate filament proteins. Nature. 319: 463-468. 1986.

Mercuri E, Brown SC, Nihoyannopoulos P, Poulton J, Kinali M, Richard P, Piercy RJ, Messina S, Sewry C, Burke MM, McKenna W, Bonne G, Muntoni F. Extreme variability of skeletal and cardiac muscle involvement in patients with mutations in exon 11 of the lamin A/C gene. Muscle Nerve. 31: 602-609. 2005.

Mestroni L, Rocco C, Gregori D, Sinagra G, Di Lenarda A, Miocic S, Vatta M, Pinamonti B, Muntoni F, Caforio ALP, McKenna WJ, Falaschi A, Giacca M, Camerini F, the Heart Muscle Disease Study Group. Familail dilated cardiomyopathy: evidence for genetic and phenotyic heterogenity. Journal of the American College of Cardiology. 34: 181-190. 1999.

Mintz PJ, Patterson SD, Neuwald AF, Spahr CS, Spector DL. Purification and biochemical characterization of interchromatin granule clusters. The EMBO Journal. 18: 4308-4320. 1999.

Mislow JM, Kim MS, Davis DB, McNally EM. Myne-1, a spectrin repeat transmembrane protein of the myocyte inner nuclear membrane, interacts with lamin A/C. Journal of Cell Science. 115: 61-70. 2002.

Miyauchi Y, Yogosawa S, Honda R, Nishida T, Yasuda H. Sumoylation of Mdm2 by protein inhibitor of activated STAT (PIAS) and RanBP2 enzymes. The Journal of Biological Chemistry. 277: 50131-50136. 2002.

Mo YY, Moschos SJ. Targeting Ubc9 for cancer therapy. Expert Opinion on Therapeutic Targets. 9: 1203-1216. 2005.

Moir RD, Donaldson AD, Stewart M. Expression in Escherichia coli of human lamins A and C: influence of head and tail domains on assembly properties and paracrystal formation. Journal of Cell Science. 99: 363-372. 1991.

Moir RD, Spann TP, Herrmann H, Goldman RD. Disruption of nuclear lamin organization blocks the elongation phase of DNA replication. The Journal of Cell Biology. 149: 1179-1191. 2000a

Moir RD, Yoon M, Khuon S, Goldman RD. Nuclear lamins A and B1: Different pathways of assembly during envelope formation in living cells. The Journal of Cell Biology. 151: 1155-1168. 2000b

Mou F, Forest T, Baines JD. Us3 of herpes simplex virus type 1 encodes a promiscuous protein kinase that phosphorylates and alters localization of lamin A/C in infected cells. Journal of Virology. 81: 6459-6470. 2007.

Mounkes LC, Kozlov SV, Hernandez L, Sullivan T, Stewart CL. A progeroid syndrome in mice is caused by defects in A-type lamins. Nature. 423: 298-301. 2003.

Mounkes LC, Kozlov SV, Rottman JN, Stewart CL. Expression of an LMNA-N195K variant of A-type lamins results in cardiac conduction defects and death in mice. Human Molecular Genetics. 14: 2167-2180. 2005.

Muchir A, Bonne G, van der Kooi AJ, van Meegen M, Baas F, Bolhuis PA, de Visser M, Schwartz K. Identification of mutations in the gene encoding lamins A/C in autosomal dominant limb girdle muscular dystrophy with atrioventricular conduction disturbances (LGMD1B). Human Molecular Genetics. 22: 1453-1459. 2000.

Muchir A, van Engelen BG, Lammens M, Mislow JM, McNally E, Schwartz K, Bonne G. Nuclear envelope alterations in fibroblasts from LGMD1B patients carrying nonsense Y259X heterozygous or homozygous mutation in lamin A/C gene. Experimenta Cell Research. 291: 352-362. 2003.

Muchir A, Medioni J, Laluc M, Massart C, Arimura T, van der Kooi AJ, Desguerre I, Mayer M, Ferrer X, Briault S, Hirano M, Worman HM, Mallet A, Wehnert M, Schwartz K, Bonne G. Nuclear envelope alterations in fibroblasts from patients with muscular dystrophy, cardiomyopathy, and partial lipodystrophy carring lamin A/C gene mutations. Muscle & Nerve. 30: 444-450. 2004.

Muchir A, Pavlidis P, Bonne G, Hayashi YK, Worman HJ. Activation of MAPK in hearts of EMD null mice: similarities between mouse models of X-linked and autosomal dominant Emery-Dreifuss muscular dystrophy. Human Molecular Genetics. 16: 1884-1895. 2007a.

Muchir A, Pavlidis P, Decostre V, Herron AJ, Arimura T, Bonne G, Worman HJ. Activation of MAPK pathways link LMNA mutations to cardiomyopathy in Emery-Dreifuss muscular dystrophy. The Journal of Clinical Investigation. 117: 1282-1293. 2007b.

Muchir A, Shan J, Bonne G, Lehnart SE, Worman HJ. Inhibition of extracellular signal-regulated kinase signaling to prevent cardiomyopathy caused by mutation in the gene encoding A-type lamins. Human Molecular Genetics. 18: 241-247. 2009a.

Muchir A, Wu W, Worman HJ. Reduced expression of A-type lamins and emerin activates extracellular signal-regulated kinase in cultured cells. Biochimica et Biophysica Acta. 1792: 75-81. 2009b.

Muralikrishna Bh, Parnaik VK. Sp3 and AP-1 mediate transcriptional activation of the lamin A proximal promoter. European Journal of Biochemistry. 268: 3736-3743. 2001.

Nacerddine K, Lehembre F, Bhaumik M, Artus J, Cohen-Tannoudji M, Babinet C, Pandolfi PP, Dejean A. The Sumo pathway is essential for nuclear integrity and chromosome segregation in mice. Developmental Cell. 9: 769-779. 2005.

Neri LM, Billi AM, Manzoli L, Rubbini S, Gilmour RS, Cocco L, Martelli AM. Federation of European Biochemical Societies. 347: 63-68. 1994.

Neri LM, Borgatti P, Capitani S, Martelli AM. Nuclear diacylglycerol produced by phosphoinositide-specific phospholipase C is responsible for nuclear translocation of protein kinase C-alpha. The Journal of Biological Chemistry. 273: 29738-29744. 1998.

Ng T, Squire A, Hansra G, Bornancin F, Prevostel C, Hanby A, Harris W, Barnes D, Schmidt S, Mellor H, Bastiaens PIH, Parker PJ. Imaging protein kinase C alpha activation in cells. Science. 283: 2085-2089. 1999.

Nikolova V, Leimena C, McMahon AC, Tan JC, Chandar S, Jogia D, Kesteven S, Michalicek J, Otway R, Verheyen F, Rainer S, Stewart CL, Martin D, Feneley MP, Fatkin D. Defects in nuclear structure and function promote dilated cardiomyopathy in lamin A/C-deficient mice. The Journal of Clinical Investigation. 113: 357-369. 2004.

Novelli G, Muchir A, Sangiuolo F, Helbling-Leclerc A, D'Apice MR, Massart C, Capon F, Sbraccia P, Federici M, Lauro R, Tudisco C, Pallotta R, Scarano G, Dallapiccola B, Merlini L, Bonne G. Mandibuloacral dysplasia is caused by a mutation in LMNA-encoding lamin A/C. American Journal of Human Genetics. 71: 426-431. 2002.

Okumura K, Nakamachi K, Hosoe Y, Nakajima N. Identification of a novel retinoic-acid responsive element within the lamin A/C promoter. Biochemical Biophysical Research Communications. 269: 197-202. 2000.

Ostlund C, Bonne G, Schwartz K, Worman HJ. Properties of lamin A mutants found in Emery-Dreifuss muscular dystrophy, cardiomyopathy and Dunnigan-type partial lipodystrophy. Journal of Cell Science. 114: 4435-4445. 2001.

Ostlund C, Sullivan T, Stewart CL, Worman HJ. Dependence of diffusional mobility of integral inner nuclear membrane proteins on A-type lamins. Biochemistry. 45: 1374-1382. 2006.

Ozaki T, Saijo M, Murakami K, Enomoto H, Taya Y, Sakiyama S. Complex formation between lamin A and the retinoblastoma gene product: identification of the domain on lamin A required for its interaction. Oncogene. 9: 2649-2653. 1994.

Pajerowski JD, Dahl KN, Zhong FL, Sammak PJ, Discher DE. Physical plasticity of the nucleus in stem cell differentiation. Proceedings of the National Academy of Science. 104: 15619-15624. 2007.

Pichler A, Gast A, Seeler JS, Dejean A, Melchior F. The nucleoporin RanBP2 has Sumo1 E3 ligase activity. Cell. 108: 109-120. 2002.

Pichler, A. Analysis of sumoylation. Methods Mol Biol. 446:131-138. 2008.

Pugh GE, Coates PJ, EB, Raymond Y, Quinlan RA. Distinct nuclear assembly pathways for lamins A and C lead to their increase during quiescence in Swiss 3T3 cells. Journal of Cell Science. 110: 2483-2493. 1997.

Raharjo WH, Enarson P, Sullivan T, Stewart CL, Burke B. Nuclear envelope defects associated with LMNA mutations cause dilated cardiomyopathy and Emery-Dreifuss muscular dystrophy. Journal of Cell Science. 114: 4447-4457. 2001.

Rahman-Roblick R, Roblick UJ, Hellman U, Conrotto P, Liu T, Becker S, Hirschberg D, Jornvall H, Auer G, Wiman KG. p53 targets identified by protein expression profiling. Proceedings of the National Academy of Science USA. 104: 5401-5406. 2007.

Rankin J, Auer-Grumbach M, Bagg W, Colclough K, Duong NT, Fenton-May J, Hattersley A, Hudson J, Jardiner P, Josifova D, Longman C, McWilliam R, Owen K, Walker M, Wehnert M, Ellard S. Extreme phenotypic diversity and nonpenetrance in families with the LMNA gene mutation R644C. American Journal of Medical Genetics. 146A: 1530-1542. 2008.

Rao L, Modha D, White E. The E1B 19K protein associates with lamins in vivo and its proper localization is required for inhibition of apoptosis. Oncogene. 15: 1587-1597. 1997.

Reed JM, Dervinis C, Morse AM, Davis JM. The Sumo conjugation pathway in Populus: genomic analysis, tissue-specific and inducible Sumoylation and in vitro de-Sumoylation. Planta. 232: 51-59. 2010.

Renou L, Stora S, Yaou RB, Volk M, Sinkovec M, Demay L, Richard P, Peterlin B, Bonne G. Heart-hand syndrome of Slovenian type: a new kind of laminopathy. Journal of Medical Genetics. 45: 666-671. 2008.

Richardson P, McKenna W, Bristow M, Maisch B, Mautner B, O'Connell J, Olsen E, Thiene G, Goodwin J, Gryarfas I, Martin I, Nordet P. Report of the 1995 World Health Organization/Intern Society and Federation of Cardiology Task Force on the Definition and Classification of Cardiomyopathies. Circulation. 93:841-842. 1996.

Rober RA, Sauter H, Weber K, Osborn M. Cells of the cellular immune and hemopoietic system of the mouse lack lamins A/C: distinction versus other somatic cells. Journal of Cell Science. 95: 587-598. 1990.

Rodriguez MS, Dargemont C, Hay RT. Sumo-1 conjugation in vivo requires both a consensus modification motif and nuclear targeting. The Journal of Biological Chemistry. 276: 12654-12659. 2001.

Ronnblom LE, Forsberg H, Evrin PE. Increased level of HLA-DR-expressing T lymphocytes in peripheral blood from patients with idiopathic dilated cardiomyopathy. Cardiology. 78:161-167. 1991.

Rosas-Acosta G, Russel WK, Deyrieux A, Russel DH, Wilson VG. A universal strategy for proteomic studies of Sumo and other ubiquitin-like modifiers. Molecular and Cellular Proteomics. 4: 56-72. 2005.

Rosenberger U, Lehmann I, Weise C, Franke P, Hucho F, Buchner K. Identification of PSF as a protein kinase Calpha-binding protein in the cell nucleus. Journal of Cellular Biochemistry. 86: 394-402. 2002.

Rusinol AE, Sinensky MS. Farnesylated lamins, progeroid syndromes and farnesyl transferase inhibitors. Journal of Cell Science. 119: 3265-3272. 2006.

Sabatelli P, Lattanzi G, Ognibene A, Columbaro M, Capanni C, Merlini L, Maraldi NR, Squarzoni S. Nuclear alterations in autosomal-dominant emery-dreifuss muscular dystrophy. Muscle & Nerve. 24: 826-829. 2001.

Saitoh H and Hinchey J. Functional heterogeneity of small ubiquitin-related protein modifiers Sumo1 versus Sumo2/3. The Journal of Biological Chemistry. 275: 6252-6258. 2000.

Saj M, Jankowska A, Lewandowski M, Szwed H, Szperl M, Ploski R, Bilinska ZT. Dilated cardiomyopathy with profound segmental wall motion abnormalities and ventricular arrhythmia caused by the R541C mutation in the LMNA gene. International Journal of Cardiology. Epub ahead of print. Jan 21. 2009.

Sasse B, Lustig A, Aebi U, Stuurman N. In vitro assembly of Drosophila lamin Dm0. European Journal of Biochemsitry. 250: 30-38. 1997.

Sasseville AM, Langelier Y. In vitro interaction of the carboxy-terminal domain of lamin A with actin. FEBS Letters. 425: 485-489. 1998.

Savage DB, Soos MA, Powlson A, O'Rahilly S, McFarlane I, Halsall DJ, Barroso I, Thomas EL, Bell JD, Scobie I, Belchetz PE, Kelly WF, Schafer AJ. Familial partial lipodystrophy associated with compound heterozygosity for novel mutations in the LMNA gene. Diabetologia. 47: 753-756. 2004.

Schmalz D, Kalkbrenner F, Hucho F, Buchner K. Transport of protein kinase C alpha into the nucleus requires intact cytoskeleton while the transport of a protein containing a canonical nuclear localization signal does not. Journal of Cell Science. 109: 2401-2406. 1996.

Schmalz D, Hucho F, Buchner K. Nuclear import of protein kinase C occurs by a mechanism distinct from the mechanism used by proteins with a classical nuclear localization signal. Journal of Cell Science. 111: 1823-1830. 1998.

Shimi T, Pfleghaar K, Kojima S, Pack CG, Solovei I, Goldman AE, Adam SA, Shumaker DK, Kinjo M, Cremer T, Goldman RD. The A- and B-type nuclear lamin networks: microdomains involved in chromatin organization and transport. Genes and Development. 22: 3409-3421. 2008.

Shumaker DK, Solimando L, Sengupta K, Shimi T, Adam SA, Grunwald A, Strelkov SV, Aebi U, Cardoso MC, Goldman RD. The highly conserved nuclear lamin Ig-fold binds to PCNA: its role in DNA replication. The Journal of Cell Biology. 181: 269-280. 2008.

Song J, Durrin LK, Wilkinson TA, Krontiris TG, Chen Y. Identification of a Sumo-binding motif that recognizes Sumo-modified proteins. Proceedings of the National Academy of Science USA. 101: 14373-14378. 2004.

Spann TP, Goldman AE, Wang C, Huang S, Goldman RD. Alteration of nuclear lamin organization inhibits RNA polymerase II-dependent transcription. The Journal of Cell Biology. 156: 603-608. 2002.

Spuler S, Geier C, Osterziel KJ, Gutberlet M, Genschel J, Lehmann TN, Zinn-Justin S, Gilquin B, Schmidt H. A new LMNA mutation causing limb girdle muscular dystrophy 1B. Journal of Neurology. 252: 621-623. 2005.

Sullivan T, Escalante-Alcalde D, Bhatt H, Anver M, Bhat N, Nagashima K, Stewart CL, Burke B. Loss of A-type lamin expression compromises nuclear envelope integrity leading to muscular dystrophy. The Journal of Cell Biology. 147: 913-919. 1999.

Sylvius N, Bilinska ZT, Veinot JP, Fidzianska A, Bolongo PM, Poon S, McKeown P, Davies RA, Chan K-L, Tang ASL, Dyack S, Grzybowski J, Ruzyllo W, McBride H, Tesson F. In vivo and in vitro examination of the functional significances of novel lamin gene mutations in heart failure patients. Journal of Medical Genetics. 42: 639-647. 2005.

Sylvius N, Tesson F. Lamin A/C and cardiac diseases. Current Opinions in Cardiology. 21:159-165. 2006.

Sylvius N, Hathaway A, Boudreau E, Gupta P, Labib S, Bolongo PM, Rippstein P, McBride H, Bilinska ZT, Tesson F. Specific contribution of lamin A and lamin C in the development of laminopathies. Experimental Cell Research. 314: 2362-2375. 2008.

Tang K, Finley RL Jr, Nie D, Honn KV. Identification of 12-lipoxygenase interaction with cellular proteins by yeast two-hybrid screening. Biochemistry. 39: 3185-3191. 2000.

Taniura H, Glass C, Gerace L. A chromatin binding site in the tail domain of nuclear lamins that interacts with core histones. The Journal of Cell Biology. 131: 33-44. 1995.

Tatham MH, Jaffray E, Vaughan OA, Desterro JM, Botting CH, Naismith JH, Hay RT. Polymeric chains of Sumo2 and Sumo3 are conugated to protein substrates by SAE1/SAE2 and Ubc9. Journal of Biological Chemistry. 276: 35368-35374. 2001.

Taylor MRG, Fain PR, Sinagra G, Robinson ML, Robertson AD, Carniel E, Lenarda AD, Bohlmeyer TJ, Ferguson DA, Brodsky GL, Boucek MM, Lascor J, Moss AC, Li WLP, Stetler

GL, Muntoni F, Bristow MR, Mestroni L. Natural history of dilated cardiomyopathy due to lamin A/C gene mutations. Journal of the American College of Cardiology. 41:771. 2003.

Ueno A, Murasaki K, Hagiwara N, Kasanuki H. Increases in circulating T lymphocytes expressing HLA-DR and CD40 ligand in patients with dilated cardiomyopathy. Heart Vessels. 22:316-321. 2007.

Van Berlo JH, de Voogt WG, van der Kooi AJ, van Tintelen JP, Bonne G, Ben Yaou RB, Duboc D, Rossenbacker T, Heidbuchel H, de Visser M, Crigjns HJGM, Pinto YM. Meta-analysis of clinical characteristics of 299 carriers of LMNA gene mutations: do lamin A/C mutations portend a high risk of sudden death? Journal of Molecular Medicine. 83:79-83. 2005.

Vantyghem MC, Pigny P, Maurage CA, Rouaix-Emery N, Stojkovic T, Cuisset JM, Millaire A, Lascols O, Vermersch P, Wemeau JL, Capeau J, Vigoroux C. Patients with familial partial lipodystrophy of the Dunnigan type due to a LMNA R482W mutation show muscular and cardiac abnormalities. The Journal of Clinical Endocrinology and Metabolism. 89: 5337-5346. 2004.

Vassileva MT and Matunis MJ. Sumo modification of heterogeneous nuclear ribonucleoproteins. Molecular and Cellular Biology. 24: 3623-3632. 2004.

Vaughan OA, Alvarez-Reyes M, Bridger JM, Broers JLV, Ramaekers FCS, Wehnert M, Morris GE, Whitfield WGF, Hutchison CJ. Both emerin and lamin C depend on lamin A for localization at the nuclear envelope. Journal of Cell Science. 114: 2577-2590. 2001.

Verga L, Concardi M, Pilotto A, Bellini O, Pasotti M, Repetto A, Tavazzi L, Arbustini E. Loss of lamin A/C expression revealed by immuno-electron microscopy in dilated cardiomyopathy with atrioventricular block caused by LMNA gene defects. Virchows Archiv: an international journal of pathology. 443: 664-671. 2003.

Verstraeten VL, Broers JL, van Steensel MA, Zinn-Justin S, Ramaekers FC, Steijlen PM, Kamps M, Kuijpers HJ, Merckx D, Smeets HJ, Hennekam RC, Marcelis CL, van den Wijngaard A. Compound heterozygosity for mutations in LMNA causes a progeria syndrome without prelamin A accumulation. Human Molecular Genetics. 15: 2509-2522. 2006.

Verstraeten VLRM, Caputo S, van Steensel MAM, Duband-Goulet I, Zinn-Justin S, Kamps M, Kuijpers HJH, Ostlund C, Worman HJ, Briede JJ, Le Dour C, Marcelis CLM, van Geel M, Steijlen PM, van den Wijngaard A, Ramaekers FCS, Broers JLV. The R439C mutation in LMNA causes lamin oligomerization and susceptibility to oxidative stress. Journal of Cell and Molecular Medicine. 13: 959-971. 2009.

Vertegaal ACO, Anderson JS, Ogg SC, Hay RT, Mann M, Lamond AI. Distinct and overlapping sets of Sumo1 and Sumo2 target proteins revealed by quantitative proteomics. Molecular and Cellular Proteomics. 5: 2298-2310. 2006.

Vigouroux C, Auclair M, Dubosclard E, Pouchelet M, Capeau J, Courvalin JC, Buendia B. Nuclear envelope disorganization in fibroblasts from lipodystrophic patients with heterozygous R482Q/W mutations in the lamin A/C gene. Journal of Cell Science. 114: 4459-4468. 2001.

Vigouroux C, Capeau J. A-type lamin-linked lipodystrophies. Novartis Foundation Symposium. 264: 166-182, 227-230. 2005.

Vijayan K, Szotek EL, Martin JL, Samarel AM. Protein kinase C-alpha-induced hypertrophy of neonatal rat ventricular myocytes. The American Journal of Physiology Heart Circulation Physiology. 287: H2777-H2789. 2004.

Vlcek S, Foisner R, Wilson KL. Lco1 is a novel widely expressed lamin-binding protein in the nuclear interior. Experimental Cell Research. 298: 499-511. 2004.

Voigt N, Friedrich A, Bock M, Wettwer E, Christ T, Knaut M, Strasser RH, Ravens U, Dobrev D. Differential phosphorylation-dependent regulation of constitutively active and muscarinic receptor-activated IK,Ach channels in patients with chronic atrial fibrillation. 74: 426-437. 2007.

Vytopil M, Beneditti S, Ricci E, Galluzzi G, Dello Russo A, Merlini L, Boriani G, Gallina M, Morandi L, Politano L, Moggio M, Chiveri L, Hausmanova-Petrusewicz I, Ricotti R, Vohanka S, Toman J, Toniolo D. Mutation analysis of the lamin A/C gene (LMNA) among patients with different cardiomuscular phenotypes. Journal of Medical Genetics. 40: e132. 2003.

Wang X, Sato R, Brown MS, Hua X, Goldstein JL. Srebp1, a membrane-bound transcription factor released by sterol-regulated proteolysis. Cell. 77: 53-62. 1994.

Wojtanik KM, Edgemon K, Viswanadha S, Lindsey B, Haluzik M, Chen W, Poy G, Reitman M, Londos C. The role of LMNA in adipose: a novel mouse model of lipodystrophy based on the Dunnigan-type familial partial lipodystrophy mutation. Journal of Lipid Research. 50: 1068-1079. 2009.

Wolf CM, Wang L, Alcalai R, Pizard A, Burgon PG, Ahmad F, Sherwood M, Branco DM, Wakimoto H, Fishman GI, See V, See V, Stewart CL, Conner DA, Berul CI, Seidman CE, Seidman JG. Lamin A/C haploinsufficiency causes dilated cardiomyopathy and apoptosis-triggered cardiac conduction system disease. Journal of Molecular and Cellular Cardiology. 44: 293-303. 2008.

Wu F, Zhu S, Ding Y, Beck WT, Mo YY. MicroRNA-mediated regulation of Ubc9 expression in cancer cells. Clinical Cancer Research. 15: 1550-1557. 2009.

Xiong D, Lee G-H, Badorff C, Dorner A, Lee S, Wolf P, Knowlton KU. Dystrophin deficiency markedly increases enterovirus-induced cardiomyopathy: a genetic predisposition to viral heart disease. Nature Medicine. 8: 872-877. 2002.

Xu Z, Au SWN. Mapping residues of Sumo precursors essential in differential maturation by Sumo-specific protease, SENP1. The Biochemical Journal. 386: 325-330. 2005.

Yang SH, Bergo MO, Toth JI, Qiao X, Hu Y, Sandoval S, Meta M, Bendale P, Gelb MH, Young SG, Fong LG. Blocking protein farnesyltransferase improves nuclear blebbing in mouse fibroblasts with a targeted Hutchinson-Gilford progeria syndrome mutation. Proceedings of the National Academy of Science. 102: 10291-10296. 2005.

Yang SH, Galanis A, Witty J, Sharrocks AD. An extended consensus motif enhances the specificity of substrate modification by Sumo. The European Molecular Biology Organization Journal. 25: 5083-5093. 2006.

Yasugi T, Howley PM. Identification of the structural and functional human homolog of the yeast ubiquitin conjugating enzyme Ubc9. Nucleic Acids Research. 24: 2005-2010. 1996.

Ye Q, Worman HJ. Protein-protein interactions between human nuclear lamins expressed in yeast. Experimental Cell Research. 219: 292-298. 1995.

Yokoyama C, Wang X, Briggs MR, Admon A, Wu J, Hua X, Goldstein JL, Brown MS. Srebp-1, a basic-helix-loop-helix-leucine zippler protein that controls transcription of the low density lipoprotein receptor gene. Cell. 75: 187-197. 1993.

Zastrow MS, Flaherty DB, Benian GM, Wilson KL. Nuclear titin interacts with A- and B-type lamins in vitro and in vivo. Journal of Cell Science. 119: 239-249. 2006.

Zhang Y-Q, Sarge KD. Sumoylation regulates lamin A function and is lost in lamin A mutants associated with familial cardiomyopathies. Journal of Cell Biology. 182: 35-39. 2008.

Zhang H, Saitoh H, Matunis MJ. Enzymes of the Sumo modification pathway localize to filaments of the nuclear pore complex. Molecular and Cellular Biology. 22: 6498-6508. 2002.

Zhang H, Li Y, McClean DR, Richardson PJ, Florio R, Sheppard M, Morrison K, Latif N, Dunn MJ, Archard LC. Detection of enterovirus capsid protein VP1 in myocardium from cases of myocarditis or dilated cardiomyopathy by immunohistochemistry: further evidence of enterovirus persistence in myocytes. Medical microbiology and immunology. 193:109-114. 2004.

Zhang Q, Ragnauth CD, Skepper JN, Worth NF, Warren DT, Roberts RG, Weissberg PL, Ellis JA, Shanahan CM. Nesprin-2 is a multi-isomeric protein that binds lamin and emerin at the nuclear envelope and forms a subcellular network in skeletal muscle. Journal of Cell Science. 118: 673-687. 2005.

Zhang X, Chen S, Yoo S, Chakrabarti S, Zhang T, Ke T, Oberti C, Yong SL, Fang F, Li L, de la Fuente R, Wang L, Chen Q, Wang QK. Mutation in nuclear pore component NUP155 leads to atrial fibrillation and early sudden cardiac death. Cell. 135: 1017-1027. 2008a.

Zhang FP, Mikkonen L, Jorma Toppari, Palvimo JJ, Thesleff I, Janne OA. Sumo1 function is dispensable in normal mouse development. Molecular and Cellular Biology. 28: 5381-5390. 2008b.

Zhong N, Radu G, Ju W, Brown WT. Novel progerin-interactive partner proteins hnRNP E1, EGF, Mel 18, and Ubc9 interact with lamin A/C. Biochemical and Biophysical Research Communications. 338: 855-861. 2005.

Zini N, Martelli AM, Neri LM, Bavelloni A, Sabatelli P, Santi S, Maraldi NM. Immunocytochemical evaluation of protein kinase C translocation to the inner nuclear matrix in 3T3 mouse fibroblasts after IGF-I treatment. Histochemistry. 103: 447-457. 1995.

APPENDIX I

Basic Res Cardiol
DOI 10.1007/s00395-010-0085-4

ORIGINAL CONTRIBUTION

Genetic and ultrastructural studies in dilated cardiomyopathy patients: a large deletion in the lamin A/C gene is associated with cardiomyocyte nuclear envelope disruption

Pallavi Gupta · Zofia T. Bilinska · Nicolas Sylvius · Emilie Boudreau · John P. Veinot · Sarah Labib · Pierrette M. Bolongo · Akil Hamza · Tracy Jackson · Rafal Ploski · Michal Walski · Jacek Grzybowski · Ewa Walczak · Grzegorz Religa · Anna Fidzianska · Frederique Tesson

Received: 28 October 2009 / Revised: 12 January 2010 / Accepted: 13 January 2010
© Springer-Verlag 2010

Abstract *Major nuclear envelope abnormalities such as disruption and/or presence of intranuclear organelles have rarely been described in cardiomyocytes from dilated cardiomyopathy (DCM) patients. In this study, we screened a series of 25 unrelated DCM patient samples for: (a) cardiomyocyte nuclear abnormalities and (b) mutations in LMNA and TMPO as these are two DCM-causing genes that encode proteins involved in maintaining nuclear envelope architecture. Among the 25 heart samples investigated, we identified major cardiomyocyte nuclear abnormalities in 8 patients. Direct sequencing allowed the detection of three heterozygous LMNA mutations (p.D192G, p.Q354K and p.R541S) in three patients. By multiplex ligation-dependant probe amplification (MLPA/quantitative real-time PCR), we found a heterozygous deletion encompassing exons 9–11 of the LMNA gene in one patient. Immunostaining demonstrated that this deletion led to a decrease in lamin A/C expression in cardiomyocytes from this patient. This LMNA deletion as well as the p.D192G mutation was found in patients displaying major cardiomyocyte nuclear envelope abnormalities, while the p.Q354K and p.R541S mutations were found in patients without specific nuclear envelope abnormalities. None of the DCM patients included in the study carried a mutation in the TMPO gene. Taken together, we found no evidence of a genotype–phenotype relationship between the onset and the severity of DCM, the presence of nuclear abnormalities and the presence or absence of LMNA mutations. We demonstrated*

P. Gupta · N. Sylvius · E. Boudreau · S. Labib · P. M. Bolongo · A. Hamza · T. Jackson · F. Tesson
Faculty of Health Sciences, University of Ottawa,
451 Smyth, Ottawa, ON K1H 8M5, Canada
e-mail: ftesson@uottawa.ca

Z. T. Bilinska · J. Grzybowski
1st Department of Coronary Artery Disease,
Institute of Cardiology, Alejska 42, 04-628 Warsaw, Poland

Present Address:
N. Sylvius
Department of Biochemistry, University of Leicester,
Leicester LE1 4HN, UK

J. P. Veinot
Department of Pathology and Laboratory Medicine,
University of Ottawa Anatomical Pathology,
Ottawa Hospital, Ottawa, ON K1Y 4E9, Canada

R. Ploski
Department of Medical Genetics, Warsaw Medical University,
Pawinskiego Street 3c, 02-106 Warsaw, Poland

M. Walski
Department of Cell Ultrastructure,
M. Mossakowski Medical Research Centre,
Polish Academy of Science, Pawinskiego Street 5,
02-106 Warsaw, Poland

E. Walczak
Department of Pathology, Institute of Rheumatology,
Spartanska 1, 02-637 Warsaw, Poland

G. Religa
2nd Department of Cardiac Surgery, Institute of Cardiology,
Alejska 42, 04-628 Warsaw, Poland

A. Fidzianska
Neuromuscular Unit, Medical Research Centre,
Polish Academy of Science and Pawinskiego 5,
02-106 Warsaw, Poland

Published online: 03 February 2010

that a large deletion in *LMNA* associated with reduced levels of the protein in the nuclear envelope suggesting a haploinsufficiency mechanism can lead to cardiomyocyte nuclear envelope disruption and thus underlie the pathogenesis of DCM.

Keywords Lamin A/C · Thymopoietin · Mutation · Dilated cardiomyopathy · Cardiomyocyte · Nucleus ultrastructure

Introduction

Dilated cardiomyopathy (DCM) is characterized by dilatation of cardiac chambers and impaired contraction. Severity of symptoms and age of onset are highly variable. To date, mutations in 28 genes have been associated with autosomal dominant DCM [3, 9–11, 18, 20, MIM#115200]. *LMNA*, which encodes lamin A/C, is one of the most commonly implicated genes in DCM. Mutations in *LMNA* are associated with a high risk of dysrhythmia, sudden death and heart failure [1, 11]. Furthermore, symptomatic DCM patients carrying *LMNA* mutations display a worse prognosis than DCM patients carrying a mutation in another DCM-associated gene [2, 11, 20, 25, 41, 45, 48].

The A-type lamins A and C, alternatively spliced products from *LMNA*, are type V intermediate filament proteins expressed in terminally differentiated somatic cells. They are components of a thin filamentous meshwork—the nuclear lamina—underlying the nucleoplasmic side of the inner nuclear membrane, and are also present in the nucleoplasm [5, 24, 25, 31]. Lamins have traditionally been considered key components in providing structural support to the nucleus and anchoring chromatin and nuclear pore complexes to the nuclear envelope [24, 41, 82]. Intranuclear lamins have proposed functions in DNA replication [20, 25, 28, 29], transcription [42] and chromatin organization [38, 81]. In order to carry out their functions, lamins interact with a number of nuclear envelope proteins, chromatin and transcription factors. Among the genes encoding the lamin A/C interacting proteins, *TMPO*, the gene encoding nucleoplasmic thymopoietin alpha [also called lamina-associated polypeptide 2 (LAP2) alpha] has been shown to harbour a mutation in DCM patients [47]. The identified mutation occurred in the C-terminal domain of thymopoietin alpha, a region known to interact with lamin A/C (residues 319–566) [9]. Three thymopoietin isoforms, alpha, beta and gamma are encoded by *TMPO* [6]. The three isoforms share an identical amino terminal sequence but have divergent carboxy terminal sequences [9]. Thymopoietin is thought to play an important role in maintaining nuclear architecture through its binding with lamins and other proteins.

Cardiomyocytes from DCM patients with *LMNA* mutations exhibit the following characteristics: (a) reduced lamin A/C expression in myocyte nuclei on immunofluorescence/immunohistochemistry studies and (b) two types of ultrastructural changes, minor nuclear envelope damage, such as focal disruptions, blebs and nuclear pore clustering, and major morphologic alterations, including a complete loss of the nuclear envelope and accumulation of mitochondria, glycogen and/or lipofuscin in the nucleoplasm [2, 7, 13, 44, 81]. To date, these major nuclear envelope defects were only found in a DCM patient carrying the p.D192G *LMNA* mutation [7, 13, 44]. However, in non-genotyped DCM patients as well as in heart failure patients, minor nuclear defects such as irregular nuclear envelope, enlarged and bizarre shaped nuclei, indentations, giant and multiple nucleoli and irregularly distributed chromatin are commonly found [1, 4, 34, 37]. There is considerable heterogeneity in the abnormalities observed from one cardiac sample to the next as well as within one particular sample [7, 44].

The aim of the present study was to ascertain whether: (1) major nuclear envelope abnormalities are a common feature in patients with DCM and (2) *LMNA* and/or *TMPO* mutations are associated with nuclear envelope defects in cardiomyocytes from a series of 25 unrelated DCM patients.

Materials and methods

Patient recruitment

Written informed consent was obtained from all patients in accordance with study protocols approved by the hospital ethics committees. Diagnosis of DCM was established based on WHO/ISFC criteria modified by Mestroni and colleagues [21] that included severe LV systolic dysfunction (LV dilatation exceeding 117% of normal value corrected for age and body surface area) and LV ejection fraction (LVEF) ≤ 45% measured in angiography, without significant coronary artery disease (≥50% lumen diameter reduction of one of the main coronary arteries). Exclusion criteria included hypertension, or acquired or congenital heart disease. All patients underwent clinical examination, evaluation of functional status according to NYHA classification, ECG study, two-dimensional echocardiography with Doppler and/or coronary angiography to exclude coronary artery disease. Left ventricular enlargement was calculated according to the method of Henry. A total of 25 index cases recruited in Canada and Poland were enrolled in the study.

Cardiac tissue collection, electron microscopy and immunostaining

Cardiac tissue samples were collected from endomyocardial biopsies performed on clinical indication or from explanted heart tissue. Samples were immediately processed in 1.6–3% gluteraldehyde. Fixed heart tissues were processed into thick and thin sections according to the standard methods. Tissue sections were examined with a Hitachi 7100 or JEM 1200EX electron microscope.

For indirect immunofluorescence examinations, 8 µm cryostat sections were stained with two monoclonal antisera against lamin A/C (NCL-LAM-A/C) (Novocastra Laboratories, Newcastle, UK) and A4, kindly provided by Dr. Hutchison (Department of Biological Science, University of Dundee, UK). A4 antibody detects only lamin A as its recognition site lies after amino acid 572. NCL-LAM-A/C recognizes both lamin A and lamin C. In brief, antibodies diluted 1:10 were applied to tissue sections for 60 min. Sections were rinsed with PBS and incubated for another 60 min with the appropriate Rodamine Red X conjugated goat anti-rabbit IgG secondary antibody diluted 1:50 with PBS. After being washed with PBS, the sections were mounted in gelmount and viewed with an Upton Zeiss standard LAB16 microscope with epifluorescence optics.

Screening of *LMNA* and *EMPO* coding sequences

Genomic DNA was isolated from white blood cells (Qiagen Flexigene kit). To screen for somatic mutations, DNA was extracted from cardiac tissues using a Qiamp Mini DNA extraction kit (Qiagen).

Intronic oligonucleotide primers flanking each of the exons were designed based on published sequences (Genbank accession number: L12389, L12400 and L12401 for *LMNA* and UCSC genome bioinformatics database for *EMPO*). All DNA samples were subjected to PCR and direct sequencing (ABI Prism Big Dye, ABI PRISM 3100 genetic analyzer). If there was any suspicion of genomic variation in a given patient, another sample of DNA collected independently was systematically double-strand sequenced (Table 1). Sequences were compared to two control samples from individuals without known cardiovascular disease. Each sample's electropherogram was analyzed by two independent investigators.

Multiplex-ligation dependant probe amplification (MLPA) analysis was performed to screen for deletions and duplications in the *LMNA* gene coding sequence according to the manufacturer's instructions (SALSA MLPA KIT P45 LMNA, MRC Holland). The probe mix contained probes for 10 of the 12 coding exons of *LMNA*, but not

Table 1 Primer pairs and annealing temperatures used to amplify *LMNA* and *EMPO* coding regions

		Primer sequences (5′ to 3′)		PCR annealing temperature (°C)
LMNA	Exon	Forward	Reverse	
	1A	TCTGTCCTTCGACCCGAG	GTAGACCCGCCAAGCGATC	51
	2A	CGCAGGACCTGCAGGAGCT	GCCCTCTCACTCCTTCC	56
	3	CCTTCAAGTTCTTGTGTTCTGTGAC	CCTAGCCCAGCCCAAGTCTGTC	58
	4	CGCCTCCCAGGAACTAATTCTG	CTCCCTGCCACCATCTGC	63
	5	GCTGTAGCAGTGATGCCCAAC	CCAAAGCCCTGAGAAGTGAAG	62
	6	ATCCTGGAGAGAGTAGCCAG	TCTAGTCAAGGCCAGTTGCC	60
	7	CCCCACTTGGTCTCCCTCTCC	CCCTGATGCAGCTGTATCCCC	60
	8	GAGGCCTCAATTGCAGGCAGGC	GAAAAGGACACTTACCCCAGC	62
	9	CGTAGCGCTGGGGTAAGTGTC	CTCGTCCAGCAAGCAGCCAG	60
	10	GTAAGCAGCAGGCCCGACAAAG	GATGCCATGGAATATTCCTGTG	58
	11A	CGTCAGTCCCAGACTCGC	ACCAGATTGTCCCCGAAG	55
	11B	GTCACTCGCAGCTACCGC	CCACCTCGTCCTACCCCT	52
	12	CTTGTCTGACCCCAGACTGGAG	AGGGAAAAGGAAGCGACGAGAAAT	65
EMPO	1	GTCTAAGGGGAAGGGTGGAG	CAGACCCACACGTCAAAGAAC	60
	2	CCAATTTGGTAGTGAGTTTCCA	TAATTTGGGGTCCTCTTCA	60
	3	TGACTCTCATCCTAAATGAAAC	TGAGCTCTCATCCTAAATGAAAC	57
	4	CCTTTGTCTACCAGGGCAAATC	GGCAGCCATCTTCACTCATC	60
	5	AAACCAGGGTTCCCGATTA	TGGATTAGTGTTGTCAGGACGTT	60
	6	CCAGTATGGCCCTTATTAAAGTA	CTCCCTCCCACTCCAAAAA	60
	7	AAGAGACACCTTGGAACCATGTG	ACCATTGTACCTGGCTCCAAA	60
	8	TCAGGGAATGTCCTTGGAAT	GCAGTTTTTATTCACCAGAGAA	60

for exons 5 and 9 because of the close proximity of exons 4 and 5, and exons 8 and 9. The probe mix also contained 15 probes for other human genes. Two of these probes recognize genes localized on chromosome 1. One of these probes was located 94 kb upstream of *LMNA* exon 1 and another 100 kb downstream of *LMNA* exon 12. MLPA amplification products were analyzed on an ABI model 3130XL Genetic Analyzer (Applied Biosystems) with the GeneMapper software V3.7, using Genescan 500LIZ internal size standard (Applied Biosystems). Each patient's electropherogram was compared to three controls. We used the Coffalyzer MLPA DAT (MRC-Holland) software to analyze MLPA data. Resulting normalized ratios were ~1.0 for every wild-type peak, 0.5 for heterozygous deletions and 1.5 for heterozygous duplications.

Quantitative real-time PCR was used to confirm the deletion found in *LMNA* (Roche LightCycler 2.0) [15]. Primers were designed for *LMNA* exon 9 (forward, 5′-cgaccctcgggtaatgtc-3′, reverse, 5′-ctcgtccagcaagca gccag-3′). PCR was set up in capillaries in a total volume of 20 µl; each PCR mixture contained 2.5 mM $MgCl_2$, 2 µl of color stream mix, 0.5 µM of mixture of forward and reverse primers and 2 µl of DNA. Standard curves for both the housekeeping gene (β2-microglobulin) and target gene were generated. Two different types of sample DNA (i.e., one sample from the DCM patient carrying the deletion and one sample from a DCM patient without the deletion) were utilized to ensure that the gene dosage ratio of the target to the housekeeping gene was disrupted only when a deletion was present. Using the slope and y-intercept of the standard curve, the LightCycler system calculated the concentrations (M) of sample and control DNA for both the reference gene (β2 microglobulin) and the target gene (Lamin A/C). These concentrations were then used to calculate the gene dosage ratio using the following equation:

$$R = \frac{M_{\text{target}}(\text{patient})/M_{\text{deletion}}(\text{patient})}{M_{\text{target}}(\text{control})/M_{\text{deletion}}(\text{control})}$$

where $R = 0.5$ (0.4–0.7) indicates deletion, $R = 1$ (0.8–1.2) indicates normal copy number and $R = 1.5$ (1.3–1.7) indicates duplication.

Statistical analysis

LVEF and LVEDD in percentage values were compared between patients with major cardiomyocyte nuclear abnormality and patients with non-specific cardiomyocyte nuclear abnormality using a two-tailed Student's *t* test (level of significance 5%).

Results

Ultrastructural characteristics of endomyocardial samples

Ultrastructural analysis of endomyocardial samples enabled us to distinguish two groups of DCM patients. One group consisted of eight individuals exhibiting major nuclear envelope abnormalities on electron micrographs (Fig. 1) and the second consisted of 17 patients with minor and non-DCM specific abnormalities.

Among the patients with nuclear envelope defects, the proportion of defective cells ranged from a small percentage to as much as 80% (patients 2 and 6). The most obvious abnormality, occurring in four of eight patients, was infusion and accumulation of mitochondria and other cytoplasmic organelles into the nuclear matrix (patients 1, 2, 5 and 6) (Fig. 1a, d). The membranes of these organelles appeared discontinuous from the nuclear envelope (Fig. 1a, d). The nuclear envelope was usually irregular (Fig. 1a–c) and partially disrupted or totally missing in six of eight patients (patients 1, 2, 4, 5, 6 and 8) (Fig. 1a, c, d). Chromatin disorganization was also observed (patients 2 and 6). In contrast, samples from the 17 patients in the second group displayed modest and non-specific nuclear membrane alterations, such as nuclear irregularity, that are commonly found in DCM patients regardless of the presence of *LMNA* mutations (Fig. 2e, f).

Clinical characteristics of the patient cohort

Clinical characteristics of the 25 DCM patients (19 males and 6 females) included in our study are shown in Table 2. There was considerable heterogeneity in terms of the clinical characteristics and severity of DCM across the cohort of 25 patients.

In the group of eight patients who exhibited nuclear envelope abnormalities, age at disease onset ranged from 14 to 63 years, four patients had a family history of DCM (Table 2, Fig. 2, [14]), while none had a suspicion of muscular dystrophy. Disease severity ranged from mild DCM to progressive heart failure and LVEF values ranged from <10 to 50%. Various arrhythmias were present in all eight patients; two patients required ICD (patients 1 and 7) and one required pacemaker (patient 5). Three patients had received a heart transplant (patients 4, 5 and 6) and two patients had died of heart failure (patients 2 and 3). In addition, patient 5 presented with hypothyroidism and patient 7 with mild mental retardation. No other phenotypic abnormality was identified within this population.

A similar degree of heterogeneity was also observed among the 17 patients with no major nuclear envelope

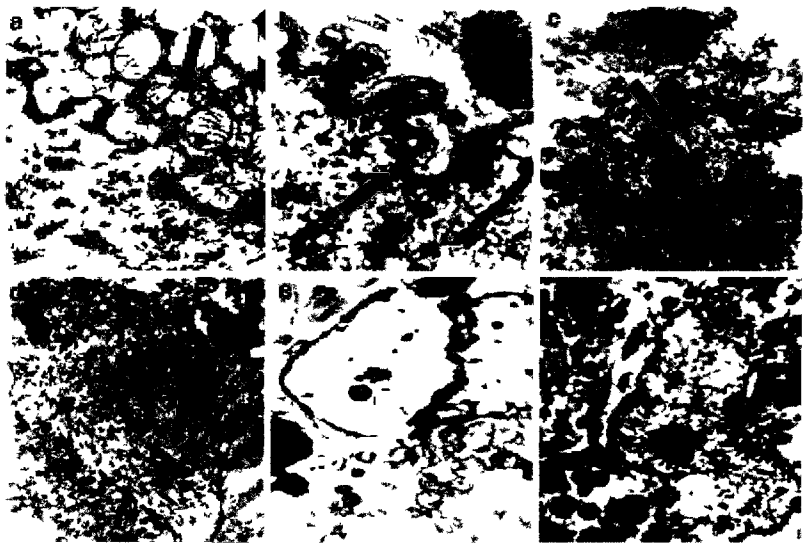

abnormalities are at disease onset ranged from 12 to 61 years. 11 patients had a family history of DCM (Table 1, Fig. 1 [11]). 1 patient had documented skeletal myopathy (patient 10 and 1 had elevated CPK values (up to 6,811 U/l, patient 18). LVEF values ranged from 11 to 38%. Conduction defects were present in all but two patients (data were not available for four patients); four patients required ICD and two had pacemakers. Twelve patients had received heart transplants and two patients had died of heart failure (patients 13 and 21).

We compared mean LVEF and LVEDD in percentage values between patients exhibiting major nuclear envelope abnormalities and patients with minor and non-DCM specific abnormalities. No significant correlation between the severity of the phenotype and the presence of nuclear envelope defect was detected ($p > 0.05$).

Screening of *LMNA* and *TMPO* coding sequences

We screened the complete coding sequence as well as the intron–exon boundaries of *LMNA* (12 exons) and *TMPO* (18 exons) for mutations using direct sequencing of DNA extracted from white blood cells of all 25 patients. We identified three patients with *LMNA* mutations, one in the group with major nuclear envelope defects (patient 2, p.D192G) and two in the group with non-specific nuclear envelope abnormalities (patient 1, p.R541S and patient 10, p.Q354K). Patient 2 and 1 and their *LMNA* mutations have been described previously [11]. All these mutations were absent in DNA from more than 100 controls. No mutation was found in *TMPO*. Previously reported polymorphisms in both *LMNA* (synonymous polymorphisms rs538089, rs505358, rs4641) and *TMPO* (non-synonymous polymorphism rs1459334) were detected. We also found a c.C1341A synonymous polymorphism in *LMNA* exon 8, which has not been previously reported, in two control individuals. Mutations in the corresponding codon have been previously reported in patients with limb-girdle muscular dystrophy 1B (p.R377H [1], p.R377L [2]).

Sequencing analysis cannot detect large heterozygous deletions or duplications. In an attempt to ascertain whether the defects resulted from deletions or duplications in *LMNA*, we performed multiplex ligation-dependant probe amplification (MLPA) on the *LMNA* coding sequence in all 25 DCM patients. One DCM patient (Table 2, patient 1) with major nuclear abnormality displayed a MLPA normalized ratio peak area of ~ 0.5 for exons 8–12 (Fig. 3). This indicated the presence of a heterozygous deletion encompassing exons 8 to 12 (~ 4.4 kbp). The remaining probes, including those for exons 1 and 2, displayed a normalized ratio of ~ 1.0 indicating normal copy number (Fig. 3). We confirmed the presence of the deletion using

Table 2 Patients' clinical characteristics at the time of the heart surgery, *LMNA* mutation status and nuclear envelope defect [...]

Patient	*LMNA* mutation	Family history	Nuclear envelope defect	Age at surgery (years)	NYHA class	Echocardiography	Ventricular arrhythmia or LVEF/LVEDD (%)	Dysrhythmias	Clinical status
Major nuclear envelope defects and *LMNA* mutation									
1	Deletion exons 9–12	Yes	Irregular and broken nuclear envelope, accumulation of mitochondria within and around the nuclei	F 39	II	LVEDD 52 mm LVEF 50%	97 bpm 120/80	nsVT, couplets, frequent VE, ICD	Mild progressive HF No MD
2*	p.D192G (c.575A > G)	Yes	Complete loss of nuclear envelope, accumulation of mitochondria, glycogen and/or lipid vacuoles in the nucleoplasm, chromatin disorganization	M 26	IV	LVEDD 69 mm LVEF 20%	67 175 127/72	LAVB, LAFB	Died at 27 while awaiting for a heart transplant No MD
Major nuclear envelope defects and not *LMNA* mutation									
3	No	Yes	Blebbing of nuclear envelope, separation of inner and outer nuclear membrane	M 63	III	LVEDD 64 mm LVEF 36%	71 160 136/85	SVT, VT	Died of progressive HF 4 years after diagnosis No MD
4	No	Yes	Extrusion of nucleoplasm from the cardiomyocyte nucleus into the cytoplasm	M 21	III	LVEDD 75 mm LVEF 25%	80/1 6 153/7	nsVT	HFx at 24 No MD
5	No	No	Irregular nuclear border, lack of nuclear membrane, presence of mitochondria within nuclear matrix	M 29	III	LVEDD 94 mm LVEF 30%	84 1 6 120/8	RBBB, LPFB in VT Pacemaker at 32	Progressive HF, HFx at 40 No MD
6	No	No	Focal disruption of nuclear envelope, chromatin disorganization	F 34	IV	LVEDD 64 mm LVEF < 10%	88 152 144/7	Recurrent VT/VF	HFx at 34 No MD
7	No	No	Mechanism unclear, focal disruption of nuclear envelope, penetration of mitochondria into nucleus	M 34	III	LVEDD 71 mm LVEF 20%	97 168 155/6	nsVT, couplets, frequent VE, ICD at 20	Progressive HF No MD
8	No	No	Irregular shape of nuclei	M 36	III	LVEDD 66 mm LVEF 30%	87 160 156/0	LBBB, nsVT	Progressive HF No MD
Non-specific nuclear envelope defects and *LMNA* mutation									
9*	p.R541S (c.1621C > A)	Yes	No	M 17	IV	LVEDD 64 mm LVEF 25%	93 152 147/3	NA	HFx at 13 No MD
10	p.Q353K (c.1057C > A)	Yes	No	M 48	IV	LVEDD 67 mm LVEF 27%	94 160 138/1	ICD	HFx at 38 Skeletal myopathy

Table 2 continued

Patient	*LMNA* mutation	Family history	Nuclear envelope defect	Sex/age at onset (years)	NYHA class	Echocardiography	Weight (kg)/height (cm)/LVEDD (%)	Dysrhythmias	Clinical status
Non specific nuclear envelope defects and no *LMNA* mutation									
11	No	Yes	No	M/27	II	LVEDD 60 mm, LVEF 38%	100/186/117.2	Permanent AF, single VE	Improved after AF ablation, LVEF 45% No MD
12	No	Yes	No	M/26	III	LVEDD 75 mm, LVEF 20%	73/183/154.8	Single VE	Stable HF No MD
13	No	Yes	No	M/40	NA	LVEDD 77 mm, LVEF 19%	73/168/164.3	ICD, pacemaker	Died at 59, poor candidate denied for HTx No MD
14	No	Yes	No	F/14	IV	LVEDD 58 mm, LVEF 14%	37/155/139.4	No	HTx at 14 No MD
15	No	Yes	No	M/36	II	LVEDD 78 mm, LVEF 25%	48/185/154.9	Single VEs	Stable HF No MD
16	No	Yes	No	M/27	III	LVEDD 78 mm, LVEF 10%	72/186/160.7	Sinus tachycardia	HTx within several months No MD
17	No	Yes	No	M/34	IV	LVEDD 78 mm, LVEF 20%	73/178/163.1	I degree AVB	Fulminant HF leading to HTx within several months No MD
18	No	Yes	No	M/35	III	LVEDD 58 mm, LVEF 15%	80/170/121.1	Frequent sVT	Atrial septal aneurysm, HTx at 39 No MD CPK value up to 600 U/l
19	No	No	No	F/13	NA	LVEDD 69 mm, LVEF 10%	41/164/160.3	NA	HTx at 13 No MD
20	No	No	No	F/61	NA	LVEDD 69 mm, LVEF 12%	88/165/145.3	ICD	Pericarditis, HTx at 62 No MD
21	No	No	No	M/54	III	LVEDD 88 mm, LVEF 20%	109/178/175.1	Pacemaker	Died at 60, waiting for HTx No MD

Table 2 continued

Patient	*LMNA* mutation	Family history	Nuclear envelope defect	Sex/age at onset (years)	NYHA class	Echocardiography	Weight/height (LVEDD)	Dysrhythmias	Clinical status
22	No	No	No	M/48	III–IV	LVEDD 86 mm LVEF 33%	[illegible]	No	HTx at 62 No MD
23	No	No	No	M/23	NA	LVEDD 80 mm LVEF 15%	[illegible]	ICD	HTx at 57 No MD
24	No	No	No	F/12	NA	LVEF 15%	[illegible]/NA	NA	HTx at 12 No MD
25	No	No	No	M/20	NA	LVEF 15%	[illegible]/NA	NA	HTx at 22 No MD

Clinical characteristics and mutation where previously described for patients 2 and 4 [illegible]

AF atrial fibrillation, *AVB* atrioventricular block, *HF* heart failure, *HTx* heart transplantation, *ICD* implantable cardioverter defibrillator, *LAFB* left anterior fascicular block, *LPFB* left posterior fascicular block, *LVEDD* left ventricle end diastolic diameter, *LVEF* left ventricle ejection fraction, *MD* muscular disease, *NA* not available, *RBBB* right bundle branch block, *VEx* ventricular extrasystole, *VE* ventricular ectopy, *VT* ventricular tachycardia, *nsVT* nonsustained ventricular tachycardia, *SVT* supraventricular tachycardia, *VT/VF* ventricular tachycardia/ventricular fibrillation

qPCR (*R* value of 0.5 for the patient with the deletion and 1 for the patient without the deletion) (Fig. 4).

Lastly, to assess whether the nuclear envelope defects in the remaining patients could result from somatic mutations, we screened for *LMNA* and *TMPO* mutations in the heart from sporadic cases with nuclear envelope defect for which cardiac tissue was available (patients 5, 6) as well as in heart from patients without defective nuclear envelope (patients 19, 20, 21, 22, 23, 24 and 25). This analysis did not reveal any somatic mutations.

In summary, a large degree of clinical heterogeneity was evident in the cohort of DCM patients studied regardless of the presence of nuclear envelope abnormalities, *LMNA* mutation or family history of DCM.

Immunostaining result

To gain further insight into the functional significance of the heterozygous deletion of exons 3–12 of *LMNA* observed in patient 1, we performed indirect immunofluorescence analysis of endomyocardial samples from this patient as well as a control patient with no *LMNA* mutation, using antibodies directed against both lamin A and C. All cardiomyocyte nuclei were immunostained with antibodies directed against lamin A and C epitopes (Fig. 5). The immunostaining was reduced in patient 1 as compared to the control patient indicating significant attenuation of lamin expression (Fig. 5).

Discussion

Among heart samples from 25 unrelated DCM patients, we identified major cardiomyocyte nuclear abnormalities in 8 individuals and non-specific nuclear abnormalities in the remaining patients. The presence of nuclear abnormalities, along with the fact that all patients presented with dysrhythmias and/or severe heart failure leading to cardiac transplantation, prompted us to analyze the sequence of *LMNA* and *TMPO*, two DCM-causing genes involved in maintaining nuclear envelope architecture.

Direct sequencing allowed the identification of three heterozygous *LMNA* genomic variations (p.D192G, p.R541S and p.Q353K) in three patients. Since sequencing analysis cannot detect large heterozygous deletions or duplications, we performed multiplex ligation-dependant probe amplification (MLPA) on the *LMNA* coding sequence in all 25 DCM patients. We found a heterozygous deletion encompassing exons 3–12 of the *LMNA* gene. This deletion was confirmed using quantitative real-time PCR. All variations were absent in DNA from more than 100 controls. The occurrence of *LMNA* mutation in our population is high probably due to fact that the studied

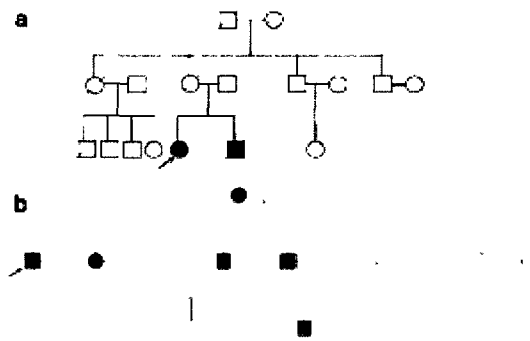

Fig. 2 Pedigree of the families with *LMNA* mutations. *Arrow* indicates proband, *black filled symbol* dilated cardiomyopathy patient, *open symbol* asymptomatic individual. **a** Deletion of exons 9–12. **b** p.Q353K

population presented with cardiac condition requiring undergoing endomyocardial biopsies or cardiac transplantation. Moreover, various arrhythmias were present in all but two patients. Since mutations in *LMNA* are usually associated with a worse prognosis than any other DCM-associated gene mutation [2, 17, 18, 25, 41, 46, 48] as well as with dysrhythmia [41, 45], our population was probably biased toward *LMNA* mutations carriers. None of the patients carried a mutation in the *EMPO* gene.

While rare findings of small deletions in the lamin A/C gene in patients with laminopathies have been reported previously, to our knowledge, this study is the first to document a large deletion encompassing most exons of the lamin A/C gene in a DCM patient. Walter et al. [53] found a 15 amino acid deletion (−5 to 12 nucleotides) in the 5′ end of the *LMNA* gene in a patient with Emery–Dreifuss muscular dystrophy (EDMD) that resulted in loss of the

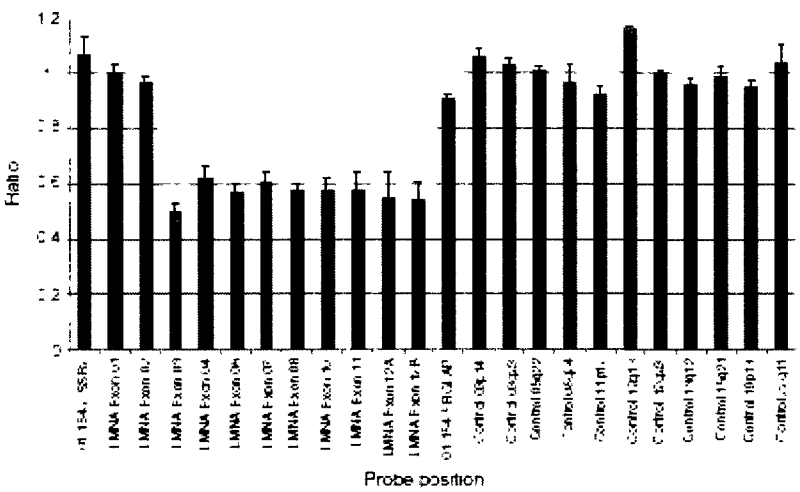

Fig. 3 MLPA analysis graph showing the heterozygous *LMNA* deletion of exons 9–12 in patient 1. Exons 9–12 display a normalized ratio (0.5), indicating a loss of genetic material. Exons 1–2 and the remaining control probes display a normalized ratio (0.9–1.0), indicating normal copy number. The control probes are targeted within the same chromosome and to different chromosomes as indicated by their locus

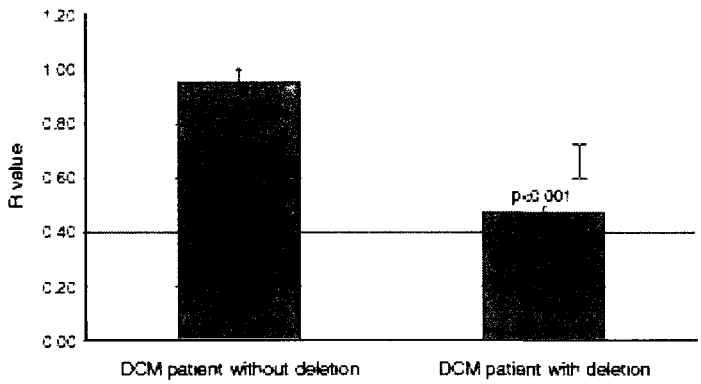

Fig. 4 Confirmation of the deletion of exons 9–12 in *LMNA* in patient 1 using qPCR. *R* values were calculated as described in the "Materials and methods". Patient 14 without the deletion had a *R* value of 0.955, which indicates a normal copy number of the exon. The *R* value for patient 1 is 0.476, which indicates the presence of only one copy of the exon ($n = 3$)

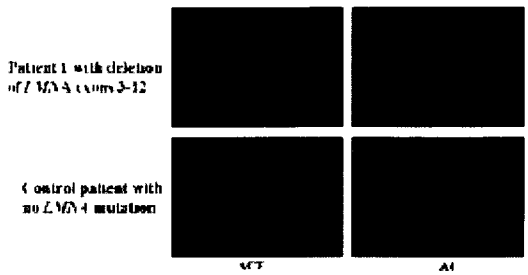

Fig. 5 Indirect immunofluorescence analysis of endomyocardial biopsy from patient 1 carrying the *LMNA* heterozygous exon 3–12 deletion and from a control patient with no *LMNA* mutation. Endomyocardial biopsy was taken from the right ventricle. Immunostaining was performed using anti-lamin A/C monoclonal antibody WF and antibody 9A which detects lamin A only (see [5] for details). Nuclei were counterstained with DAPI and the primary antibodies were detected with secondary antibody conjugated with FITC

translation initiator codon. van Tintelen et al. [10] reported a 674 bp deletion encompassing exon 1 and the adjacent non-coding exon in a patient with myocardial fibrosis. The presence of the exon 1 p.Q6StopX *LMNA* mutation resulting in reduced levels of lamin A/C proteins has also been reported in a family with EDMD [5].

Most *LMNA* mutations that cause DCM are heterozygous point mutations, only some of which have been associated with cardiomyocyte nuclear envelope defects [2, 3, 11, 15]. It has been suggested that mutations causing such abnormalities have a dominant-negative effect on the function of normal lamin protein. Impaired lamin integration into the nuclear lamina due to the dominant-negative effects of a mutation may cause disruption of the lamina and ultimately compromise nuclear envelope integrity. Our results suggest that, apart from the dominant-negative effects of mutant lamin A/C protein, lamin haploinsufficiency can also cause nuclear envelope defects and underlie the pathogenesis of DCM. Since the deletion encompasses *LMNA* exon 3 to 12, it is likely that the observed nuclear abnormalities are not due to the expression of a putative truncated protein composed of exons 1–2 only. It was shown that the potential truncated protein resulting from the Y259X nonsense mutation (exon 4) was not detectable in patient fibroblasts [15]. Similarly, in the mouse model with the *LMNA* exon 8–11 deletion, the 54-kDa truncated protein resulting from this deletion was not detected [14]. Furthermore, immunostaining revealed reduced lamin A/C in the patient's cardiomyocyte nuclei. That lamin haploinsufficiency can cause such defects is further corroborated by the fact that a heterozygous *LMNA* mouse model in which cardiac lamin A/C levels were diminished by 50% compared to wild-type, demonstrated early-onset conduction system disease and late-onset DCM [54]. Furthermore, misshapen cardiomyocyte nuclei and heterochromatin clumping were also observed [54].

The *LMNA* deletion of exons 3–12 was observed in a patient presenting with major nuclear envelope abnormalities—notably broken nuclear envelope and accumulation of mitochondria within and around the nuclei. This suggests that haplo-insufficiency is the mechanism underlying the observed nuclear abnormalities. Among their many functions, lamins play an integral role in maintaining the mechanical stability of the nucleus; hence we can speculate that the nuclear envelope defects observed in the patient carrying this *LMNA* deletion results from the reduced levels of lamin A/C protein.

Apart from the observed deletion, one of our patients with nuclear envelope defects carried a p.D192G point mutation in the *LMNA* gene. When expressed in COS-cells, this mutation resulted in a discontinuous nuclear lamina due to the formation of multiple lamin aggregates [11, 15]. These results therefore corroborated the pathological findings from the patient with the mutation.

In our study, not all *LMNA* mutations were found to cause nuclear envelope abnormalities in patients' cardiomyocytes; indeed, two patients with *LMNA* point mutations demonstrated no specific nuclear envelope abnormalities in the samples taken from explanted heart tissue: one patient carried a p.Q354K mutation, while the second carried the p.R541S mutation. It is possible that the number of abnormal nuclei was so low in these two patients that it resulted in a false-negative finding. Patient age at the time of tissue collection and the protein domain affected by the mutation were considered as possible explanations for the observed discrepancies in nuclear envelope phenotype. Age at the time of tissue collection was 48 and 12 years for the patients carrying mutations p.Q354K and p.R541S, respectively, both of which were associated with normal nuclear envelope ultrastructure. The patients with *LMNA* deletion and p.D192G mutation, both of whom demonstrated nuclear envelope abnormalities, were 49 and 26 years of age, respectively. Hence, there was no apparent relationship between age and observed nuclear envelope phenotype. It was also considered possible that the presence of nuclear envelope abnormalities may depend upon the protein domain affected by each mutation [11, 15]. The p.D192G mutation, which was associated with major nuclear envelope abnormalities, is located in the central α-helical rod domain at the distal end of coil 1B. This highly conserved region of the lamin A/C protein is critical for the formation of the α-helical coiled-coil dimer, the basic building block for the construction of lamin filaments. In contrast, the p.Q354K mutation in exon 6 affected a highly conserved residue localized in the central rod domain coil 2B fragment. Based on the coil 2B fragment crystal

structure, mutations in this domain are unlikely to alter the dimer structure but may interfere with essential molecular interactions occurring in later stages of filament assembly, lamina formation and/or chromatin interaction [12]. Similarly, the p.R541S mutation is located in highly conserved residues in a region of gene shared by lamin A and C isoforms within the carboxyl-terminal end. The buried side chain of R541 participates in the stabilization of the carboxy-terminal β-sandwich through hydrophobic contacts with the core of the domain [22]. Mutations in this domain could therefore destabilize the three-dimensional structure of the C-terminal domain of lamin A/C. This domain also carries sites for many lamin A/C interacting proteins. Therefore, both p.Q353K and p.R541S mutations could theoretically disrupt multiple functions of lamin A and C, including the maintenance of nuclear architecture. Unexpectedly, the ultrastructural phenotype associated with these mutations was indistinguishable from controls. Hence, our results do not support the presence of a relationship between the position of the mutation and the resulting ultrastructural phenotype.

The six patients demonstrating nuclear ultrastructural defects without *LMNA* or *TMPO* mutations showed that germ-line mutations in these genes are not a prerequisite for nuclear envelope defects. However, we could not discount the possibility that some of these individuals possessed somatic *LMNA* or *TMPO* mutations restricted to diseased cardiac tissue. The fact that only a percentage of observed cardiomyocytes from these patients displayed an abnormal nucleus lends support to this hypothesis. Indeed, somatic mutation occurring in a selective subpopulation of progenitor cell lineage is one of the molecular mechanisms leading to such tissue mosaicism. Furthermore, in other cardiovascular diseases such as idiopathic ventricular tachycardia or idiopathic atrial fibrillation, both germ-line and somatic missense mutations have been linked to the disease [11, 21]. We therefore screened for the presence of *LMNA* and *TMPO* mutations in DNA extracted from heart tissues of patients who did not have familial DCM, but were unable to identify any somatic mutations. Another possibility is that mutation in genes encoding lamin A/C-binding proteins are responsible for the major cardiomyocyte nuclear abnormalities observed in these patients [15, 16, 30, 55–57].

We showed here that there is no clear correlation between the presence or position of the *LMNA* mutation and either clinical phenotype with respect to DCM onset or severity or cardiomyocyte ultrastructural phenotype. We also found no apparent correlation between genotype and either severity of the ultrastructural aberration (i.e., the degree of nuclear envelope disruption) or the proportion of observed cells displaying abnormal nuclei. Furthermore, there was no significant correlation between the severity of the disease and the presence of ultra-structural nuclear envelope defects. Although a quantitative analysis was not possible due to the small sample size, overall, we found no evidence of a relationship between the onset and the severity of DCM, the presence of nuclear abnormalities and the presence or absence of *LMNA* mutations.

Taken together, our results suggest that lamin A/C haplo-insufficiency, documented by reduced protein level in the patient's cardiomyocyte nuclear envelope caused by a large deletion in the *LMNA* gene, can lead to nuclear envelope disruption and underlie the pathogenesis of DCM. However, the finding that two patients without cardiomyocyte nuclear abnormalities had *LMNA* mutations indicates that *LMNA* mutations may not necessarily lead to major cardiomyocyte nuclear envelope defects. Furthermore, patients with major nuclear envelope abnormalities may not have *LMNA* or *TMPO* mutation. This demonstrates that patients with a clinical suspicion of laminopathy and marked abnormality of cardiomyocyte nuclei can be free of both *LMNA* and *TMPO* mutations and may carry a mutation in another gene encoding a protein involved in the maintenance of the nuclear architecture.

Acknowledgments This work was supported by Canadian Institutes for Health Research (operating grants MOP-84152 and 77685) and by Heart and Stroke Foundation (Grants-NA 5101 and 6628 awarded to P. Tesson) and by an internal grant from the Institute of Cardiology, Warsaw, Poland (no 2.5/VIII/03). At the time the study was conducted, N. Sylvius was the recipient of the fellowships awarded by the Heart and Stroke Foundation of Ontario Program Grant 5275 and Astra Zeneca/Canadian Society of Hypertension/CIHR and Pallavi Gupta was the recipient of Ontario Graduate Scholarship in Science and Technology (OGSST). We acknowledge the important contribution of the Canadian Cardiovascular Genetics Centre (Ottawa, Canada).

Conflict of interest statement The authors declare that they have no conflict of interest.

References

1. Arbustini E, Gavazzi A, Pozzi R, Grasso M, Pucci A, Campana C, Graziani G, Martinetti M, Ciccia M, Salvaneschi L, Martinelli L, Montemartini C, Vigano M (1989) The morphologic spectrum of dilated cardiomyopathy and its relation to immune response genes. Am J Cardiol 64:981–985
2. Arbustini E, Pilotto A, Repetto A, Grasso M, Negri A, Diegoli M, Campana C, Scelsa L, Baldini E, Gavazzi A, Tavazzi L (2002) Autosomal dominant dilated cardiomyopathy with atrioventricular block: a lamin A/C defect-related disease. J Am Coll Cardiol 39:981–990
3. Arimura T, Hayashi T, Matsumoto Y, Shibata H, Hiroe S, Nakamura T, Inagaki N, Hinohara K, Takahashi M, Matsuzu S, Sawaoka T, Izumi T, Bonne G, Schwartz K, Kimura A (2007) Structural analysis of four and half LIM protein 2 in dilated cardiomyopathy. Biochem Biophys Res Commun 357:162–167
4. Baandrup U, Florio RA, Roters F, Olsen EG (1981) Electron microscopic investigation of endomyocardial biopsy samples in

hypertrophy and cardiomyopathy. A semiquantitative study in 48 patients. Circulation 63:1289–1298

5. Bécane HM, Bonne G, Varnous S, Muchir A, Ortega V, Hammouda EH, Urtizberea JA, Lavergne T, Fardeau M, Eymard B, Weber S, Schwartz K, Duboc D (2000) High incidence of sudden death with conduction system and myocardial disease due to lamins A and C gene mutation. J Pac Clin Electrophysiol 23:1661–1666

6. Berger R, Theodor L, Shoham J, Gokkel E, Brok-Simoni F, Avraham KB, Copeland NG, Jenkins NA, Rechavi G, Simon AJ (1996) The characterization and localization of the mouse thymopoietin/lamina-associated polypeptide 2 gene and its alternatively spliced products. Genome Res 6:361–370

7. Bilinska ZT, Sylvius N, Grzybowski J, Fidzianska A, Michalak E, Walczak E, Walski M, Bieganowska K, Szymaniak E, Kusmierczyk-Droszcz B, Lubiszewska B, Wagner T, Tesson F, Ruzyllo W (2006) Dilated cardiomyopathy caused by *LMNA* mutations. Clinical and morphological studies. Polish Heart J 64:812–818

Bridger JM, Kill IR, O'Farrell M, Hutchison CJ (1993) Internal lamin structures within G1 nuclei of human dermal fibroblasts. J Cell Sci 104:297–306

9. Dacinkow S, Erdmann J, Knueppel T, Gille C, Froemmel C, Hummel M, Hetzer R, Regitz-Zagrosek V (2002) Novel mutations in sarcomeric protein genes in dilated cardiomyopathy. Biochem Biophys Res Commun 298:116–120

10. Dechat T, Korbei B, Vaughan OA, Vlcek S, Hutchison CJ, Foisner R (2000) Lamina-associated polypeptide 2 alpha binds intranuclear A-type lamins. J Cell Sci 113:3473–3484

11. Duboscq-Bidot L, Xu P, Charron P, Neyroud N, Dilanian G, Millaire A, Bors V, Komajda M, Villard E (2008) Mutations in the Z-band protein myopalladin gene and idiopathic dilated cardiomyopathy. Cardiovasc Res 77:118–125

12. Favreau C, Dubosclard E, Östlund C, Vigouroux C, Capeau J, Wehnert M, Higuet D, Worman HJ, Courvalin JC, Buendia B (2003) Expression of lamin A mutated in the carboxyl-terminal tail generates an aberrant nuclear phenotype similar to that observed in cells from patients with Dunnigan-type partial lipodystrophy and Emery-Dreifuss muscular dystrophy. Exp Cell Res 282:14–23

13. Fidzianska A, Bilinska ZT, Tesson F, Wagner T, Walski M, Grzybowski J, Ruzyllo W, Hausmanowa-Petrusewicz I (2008) Obliteration of cardiomyocyte nuclear architecture in a patient with *LMNA* gene mutation. J Neurol Sci 271:91–96

14. Gollob MH, Jones DL, Krahn AD, Danis L, Gong XQ, Shao Q, Liu X, Veinot JP, Tang AS, Stewart AF, Tesson F, Klein GJ, Yee R, Skanes AC, Guiraudon GM, Ebihara L, Bai D (2006) Somatic mutations in the connexin 40 gene (GJA5) in atrial fibrillation. N Engl J Med 354:2677–2688

15. Gruenbaum Y, Margalit A, Goldman RD, Shumaker DK, Wilson KL (2005) The nuclear lamina comes of age. Nature Rev Mol Cell Biol 6:21–31

16. Haque F, Lloyd DJ, Smallwood DT, Dent CL, Shanahan CM, Fry AM, Trembath RC, Shackleton S (2006) SUN1 interacts with nuclear lamin A and cytoplasmic nesprins to provide a physical connection between the nuclear lamina and the cytoskeleton. Mol Cell Biol 26:3738–3751

17. Hermida-Prieto M, Monserrat L, Castro-Beiras A, Laredo R, Soler R, Peteiro J, Rodriguez E, Bouzas B, Alvarez N, Muniz J, Crespo-Leiro M (2004) Familial dilated cardiomyopathy and isolated left ventricular noncompaction associated with lamin A/C gene mutations. Am J Cardiol 94:50–54

18. Inagaki N, Hayashi T, Arimura T, Koga Y, Takahashi M, Shibata H, Teraoka K, Chikamori T, Yamashina A, Kimura A (2006) αB-crystallin mutation in dilated cardiomyopathy. Biochem Biophys Res Commun 342:379–386

19. Karkkainen S, Peuhkurinen K (2007) Genetics of dilated cardiomyopathy. Ann Med 39:91–107

20. Kennedy BK, Barbie DA, Classon M, Dyson N, Harlow E (2000) Nuclear organization of DNA replication in primary mammalian cells. Genes Dev 14:2855–2868

21. Ki CS, Hong JS, Jeong GY, Ahn KJ, Choi KM, Kim DK, Kim JW (2002) Identification of lamin A/C (*LMNA*) gene mutations in Korean patients with autosomal dominant Emery-Dreifuss muscular dystrophy and limb-girdle muscular dystrophy 1B. J Hum Genet 47:225–228

22. Krimm I, Östlund C, Gilquin B, Couprie J, Hossenlopp P, Mornon JP, Bonne G, Courvalin JC, Worman HJ, Zinn-Justin S (2002) The Ig-like structure of the C-terminal domain of lamin A/C, mutated in muscular dystrophies, cardiomyopathy, and partial lipodystrophy. Structure 10:811–823

23. Lerman BB, Dong B, Stein KM, Markowitz SM, Linden J, Catanzaro DF (1998) Right ventricular outflow tract tachycardia due to a somatic cell mutation in G protein subunit alpha i2. J Clin Invest 101:2862–2868

24. Liu J, Ben-Shahar TR, Riemer D, Treinin M, Spann P, Weber K, Fire A, Gruenbaum Y (2000) Essential roles for *Caenorhabditis elegans* lamin gene in nuclear organization, cell cycle progression, and spatial organization of nuclear pore complexes. Mol Biol Cell 11:3937–3947

25. Meier J, Campbell KH, Ford CC, Stick R, Hutchison CJ (1991) The role of lamin LIII in nuclear assembly and DNA replication, in cell-free extracts of *Xenopus* eggs. J Cell Sci 98:271–279

26. Mercuri E, Brown SC, Nihoyannopoulos P, Poulton J, Kinali M, Richard P, Piercy RJ, Messina S, Sewry C, Burke MM, McKenna W, Bonne G, Muntoni F (2005) Extreme variability of skeletal and cardiac muscle involvement in patients with mutations in exon 11 of the lamin A/C gene. Muscle Nerve 31:602–609

27. Mestroni L, Maisch B, McKenna WJ, Schwartz K, Charron P, Rocco C, Tesson F, Richter A, Wilke A, Komajda M (1999) Guidelines for the study of familial dilated cardiomyopathies. Collaborative research group of the European Human and Capital Mobility Project on familial dilated cardiomyopathy. Eur Heart J 20:93–102

28. Moir RD, Montag-Lowy M, Goldman RD (1994) Dynamic properties of nuclear lamins: lamin B is associated with sites of DNA replication. J Cell Biol 125:1201–1212

29. Moir RD, Spann TP, Herrmann H, Goldman RD (2000) Disruption of nuclear lamin organization blocks the elongation phase of DNA replication. J Cell Biol 149:1179–1192

30. Moir RD, Yoon M, Khuon S, Goldman RD (2000) Nuclear lamins A and B1: different pathways of assembly during nuclear envelope formation in living cells. J Cell Biol 15:1155–1168

31. Muchir A, Bonne G, van der Kooi AJ, van Meegen M, Baas F, Bolhuis PA, de Visser M, Schwartz K (2000) Identification of mutations in the gene encoding lamins A/C in autosomal dominant limb girdle muscular dystrophy with atrioventricular conduction disturbances (LGMD1B). Hum Mol Genet 9:1453–1459

32. Muchir A, Medioni J, Laluc M, Massart C, Arimura T, van der Kooi AJ, Desguerre I, Mayer M, Ferrer X, Briault S, Hirano M, Worman HJ, Mallet A, Wehnert M, Schwartz K, Bonne G (2004) Nuclear envelope alterations in fibroblasts from patients with muscular dystrophy, cardiomyopathy, and partial lipodystrophy carrying lamin A/C gene mutations. Muscle Nerve 30:444–450

33. Muchir A, van Engelen BG, Lammens M, Mislow JM, McNally E, Schwartz K, Bonne G (2003) Nuclear envelope alterations in fibroblasts from LGMD1B patients carrying nonsense Y259X heterozygous or homozygous mutation in lamin A/C gene. Exp Cell Res 291:352–362

34. Rowan RA, Masek MA, Billingham ME (1988) Ultrastructural morphometric analysis of endomyocardial biopsies. Idiopathic dilated cardiomyopathy, anthracycline cardiotoxicity, and normal myocardium. Am J Cardiovasc Pathol 2:137–144

35. Perrot A, Hussein S, Ruppert V, Schmidt HH, Wehnert MS, Duong NT, Posch MG, Panek A, Dietz R, Kindermann I, Böhm M, Michalewska-Wludarczyk A, Richter A, Maisch B, Pankuweit S, Özcelik C (2009) Identification of mutational hot spots in LMNA encoding lamin A/C in patients with familial dilated cardiomyopathy. Basic Res Cardiol 104:90–99
36. Schneider M, Franzoska J, Sanz J, Kanel TV, Gallati S (2006) Detection of exon deletions (CFTR) by relative quantification on the lightcycler. Clin Chem. 52:2005–2012
37. Scholz D, Diener W, Schaper J (1994) Altered nucleus/cytoplasm relationship and degenerative structural changes in human dilated cardiomyopathy. Cardioscience 5:127–138
38. Shimi T, Pfleghaar K, Kojima S, Pack CG, Solovei I, Goldman AE, Adam SA, Shumaker DK, Kinjo M, Cremer T, Goldman RD (2008) The A- and B-type nuclear lamin networks: microdomains involved in chromatin organization and transcription. Genes Dev 22:3409–3421
39. Shumaker DK, Kuczmarski ER, Goldman RD (2003) The nucleoskeleton: lamins and actin are major players in essential nuclear functions. Curr Opin Cell Biol 15:358–366
40. Smythe C, Jenkins HE, Hutchison CJ (2000) Incorporation of the nuclear pore basket protein nup153 into nuclear pore structures is dependent upon lamina assembly: evidence from cell-free extracts of Xenopus eggs. EMBO J 19:3918–3931
41. Spann TP, Goldman AE, Wang C, Huang S, Goldman RD (2002) Alteration of nuclear lamin organization inhibits RNA polymerase II-dependent transcription. J Cell Biol 156:603–608
42. Strelkov SV, Schumacher J, Burkhard P, Aebi U, Herrmann H (2004) Crystal structure of the human lamin A coil 2B dimer: implications for the head-to-tail association of nuclear lamins. J Mol Biol 343:1067–1080
43. Sullivan T, Escalante-Alcalde D, Bhatt H, Anver M, Bhat N, Nagashima K, Stewart CL, Burke B (1999) Loss of A-type lamin expression compromises nuclear envelope integrity leading to muscular dystrophy. J Cell Biol 147:913–920
44. Sylvius N, Bilinska ZT, Veinot JP, Fidzianska A, Bolongo PM, Poon S, McKeown P, Davies RA, Chan KL, Tang AS, Dyack S, Grzybowski J, Ruzyllo W, McBride H, Tesson F (2005) In vivo and in vitro examination of the functional significances of novel lamin gene mutations in heart failure patients. J Med Genet 42:639–647
45. Sylvius N, Hathaway A, Boudreau E, Gupta P, Labib S, Bolongo P, Rippstein P, McBride H, Bilinska ZT, Tesson F (2008) Specific contributions of lamin A and lamin C in the development of laminopathies. Exp Cell Res 314:2362–2375
46. Taylor MR, Fain PR, Sinagra G, Robinson ML, Robertson AD, Carniel E, Di Lenarda A, Bohlmeyer TJ, Ferguson DA, Brodsky GL, Boucek MM, Lascor J, Moss AC, Li WL, Stetler GL, Muntoni F, Bristow MR, Mestroni L (2003) Natural history of dilated cardiomyopathy due to lamin A/C gene mutations. J Am Coll Cardiol 41:771–780
47. Taylor MR, Slavov D, Gajewski A, Vlcek S, Ku L, Fain PR, Carniel E, Di Lenarda A, Sinagra G, Boucek MM, Cavanaugh J, Graw SL, Ruegg P, Feiger J, Zhu X, Ferguson DA, Bristow MR, Gotzmann J, Foisner R, Mestroni L (2005) Thymopoietin (lamina-associated polypeptide 2) gene mutation associated with dilated cardiomyopathy. Hum Mutat 26:566–574
48. van Berlo JH, de Voogt WG, van der Kooi AJ, van Tintelen JP, Bonne G, Yaou RB, Duboc D, Rossenbacker T, Heidbuchel H, de Visser M, Crijns HJ, Pinto YM (2005) Meta-analysis of clinical characteristics of 299 carriers of *LMNA* gene mutations: do lamin A/C mutations portend a high risk of sudden death? J Mol Med 83:79–83
49. van Tintelen JP, Tio RA, Kerstjens-Frederikse WS, van Berlo JH, Boven LG, Suurmeijer AJH, White SJ, den Dunnen JTD, te Meerman GJ, Vos YJ, van der Hout AH, Osinga J, van den Berg MP, van Veldhuisen DJ, Buys CHC, Hofstra RMW, Pinto YM (2007) Severe myocardial fibrosis caused by a deletion of the 5' end of the lamin A/C gene. J Am Coll Cardiol 49:2430–2439
50. Vaughan OA, Whitfield WGF, Hutchison CJ (2000) Functions of nuclear lamins. Protoplasma 211:1–7
51. Verga L, Concardi M, Pilotto A, Bellini O, Pasotti M, Repetto A, Tavazzi L, Arbustini E (2003) Loss of lamin A/C expression revealed by immuno-electron microscopy in dilated cardiomyopathy with atrioventricular block caused by *LMNA* gene defects. Virchows Arch 443:664–671
52. Vlcek S, Dechat T, Foisner R (2001) Nuclear envelope and nuclear matrix: interactions and dynamics. Cell Mol Life Sci 58:1758–1765
53. Walter MC, Witt TN, Weigel BS, Reilich P, Richard P, Pongratz D, Bonne G, Wehnert MS, Lochmüller H (2005) Deletion of the *LMNA* initiator codon leading to a neurogenic variant of autosomal dominant Emery-Dreifuss muscular dystrophy. Neuromuscular Disord 15:40–44
54. Wolf CM, Wang L, Alcalai R (2008) Lamin A/C haploinsufficiency causes dilated cardiomyopathy and apoptosis-triggered cardiac conduction system disease. J Mol Cell Cardiol 44:293–303
55. Zastrow MS, Flaherty DB, Benian GM, Wilson KL (2006) Nuclear titin interacts with A- and B-type lamins in vitro and in vivo. J Cell Sci 119:239–249
56. Zastrow MS, Vlcek S, Wilson KL (2004) Proteins that bind A-type lamins: integrating isolated clues. J Cell Sci 117:979–987
57. Zhong N, Radu G, Ju W, Brown WT (2005) Novel progerin-interactive partner proteins hnRNP E1, EGF, Mel 18, and UBC9 interact with lamin A/C. Biochem Biophys Res Commun 338:855–861

APPENDIX II

available at www.sciencedirect.com

ScienceDirect

www.elsevier.com/locate/yexcr

Specific contribution of lamin A and lamin C in the development of laminopathies

Nicolas Sylvius[a,*,1], *Andrea Hathaway*[a], *Emilie Boudreau*[a], *Pallavi Gupta*[a], *Sarah Labib*[a], *Pierrette M. Bolongo*[a], *Peter Rippstein*[b], *Heidi McBride*[b], *Zofia T. Bilinska*[c], *Frederique Tesson*[a]

[a] Laboratory of [illegible], University of Ottawa Heart Institute, [illegible] Ruskin Street, Ottawa, [illegible]
[b] [illegible] Ottawa Heart Institute, [illegible] Ruskin Street, Ottawa, Canada [illegible]
[c] [illegible] Institute of Cardiology, [illegible] Poland

ARTICLE INFORMATION

Article Chronology:
Received [illegible] January [illegible]
Revised version received
28 April 200[illegible]
Accepted 28 April 200[illegible]
Available online [illegible] May [illegible]

Keywords:
[illegible]
Lamin A/C
Laminopathy
Nuclear envelope
[illegible]
Electron microscopy

ABSTRACT

[illegible]

Introduction

The lamin A/C gene (LMNA) has been implicated in numerous diseases referred to as laminopathies that affect the heart, skeletal muscle, adipose tissue, bone, peripheral nerves, skin or cause premature aging [1].

Lamins A and C are type V intermediate filament proteins expressed in terminally differentiated somatic cells and synthesized by alternative splicing of LMNA. Both proteins share the same first 566 amino acids but differ in their carboxyl terminus. Lamin A and C have 646 and [illegible] amino acids respectively and are known for their structural role in supporting the nuclear architecture and anchoring chromatin and the nuclear pore complexes to the nuclear membrane. Indeed, along with B type lamins, they are the main component of the lamina, a filamentous meshwork underlying the inner nuclear

* Corresponding author. [illegible] Evry Cedex, France.
E-mail address: [illegible] (N. Sylvius).
[1] Current address: [illegible] Evry Cedex, France.

0014-4827/$ – see front matter © 200[illegible] Elsevier Inc. All rights reserved.
[illegible]

membrane. However, they are also present within the nucleus [illegible]. In addition to participating in nuclear architecture, there is a growing body of evidence showing that lamin A/C plays a key role in gene transcription regulation, DNA repair and replication [illegible] and cell differentiation regulation [illegible]. The list of lamins A and C partners is regularly growing [illegible], which confirms that these proteins are involved in multiple functions, some of which are still being unravelled. For instance, it has recently been shown that lamin A and C are tightly connected to the cytoskeleton, thus revealing a nuclear–cytoskeletal continuity [illegible]. Also, some LMNA mutations have been reported to affect the posttranslational machinery of the cell. It has been shown that the nuclear localization of SUMO1 (ubiquitin related modifier 1) is totally disrupted in the presence of the DCM associated D192G lamin C mutant [11].

Whether or not lamin A is required for lamin C to be localized into the nuclear envelope remains debated. The early death of lmna knockout mice (lmna[illegible]) [illegible] or the dramatic lamina defect observed when silencing lamin A/C in human endometrial stromal cells [illegible] clearly demonstrate that at least one of the two proteins is required for survival. However, a recent study in fibroblasts from mice expressing only lamin C have shown that lamin C is normally targeted to the nuclear envelope [illegible] as well as nuclear shape [illegible] these fibroblasts [illegible] altered and the mice [illegible] [illegible] times [illegible]. Furthermore, lamin C has also been shown to be sufficient for proper localization of both emerin [illegible] and nesprin [illegible] at the nuclear envelope. These studies therefore suggest that lamin C can substitute for lamin A on its own and provide functional support to the nuclear envelope. However, these results strikingly contradict several other studies which showed that lamin A targets both lamin C and emerin to the nuclear envelope [illegible].

Furthermore, nuclear envelope alterations associated with LMNA mutations have long been reported [illegible]. Mice expressing M371K lamin A exhibit cardiomyocytes with convoluted nuclear envelopes, intranuclear inclusions and chromatin clumps in nuclei [illegible]. Several LMNA mutations are known to result in the aggregation of lamin A or C [illegible]. In a previous report, we found DCM causing LMNA mutations leading to the aggregation of nuclear lamin C as well [illegible]. However, the physiological consequences of these aggregates as well as the impact of these mutations on lamin C specifically or on the complex lamin A/lamin C have only been partially investigated. It is unclear whether or not these lamin A and lamin C aggregates retain the capability to incorporate themselves into the nuclear envelope either in combination or independently.

In humans, most reported LMNA mutations are found in Emery–Dreifuss muscular dystrophy and dilated cardiomyopathy (DCM) but the spectrum of phenotypes is constantly extending [illegible]. Nuclear fragility and/or abnormalities in the tissue cell specific gene expression are the main two hypotheses proposed to explain how mutations in this gene cause such a large spectrum of diseases [1]. However, the exact pathophysiological mechanisms remain puzzling. In this study, we propose to further examine wild type and mutated lamin A and C behaviour separately and then in combination. In an attempt to better clarify the lamin A and lamin C respective functions and shed light on the properties of lamin A/C affected in laminopathies, we compared various LMNA mutations previously reported in DCM (L85R, D192G, N195K) [illegible], autosomal dominant Emery–Dreifuss muscular dystrophy (R386K) [illegible] or lipodystrophy (R482W) [illegible].

Methods

Expression plasmid and mutagenesis

Our cloning procedures of wild type and mutated full length human lamin A and C as C-terminal fusions to either the enhanced cyan, yellow or red fluorescent protein sequence of respectively pECFP-C1, pEYFP-C1 and pDsRed-C1 fluorescent expression vectors have previously been described [illegible]. L85R, D192G, N195K, R386K and R482W point mutations were introduced in the lamin A and lamin C cDNAs by site-directed mutagenesis using primers previously published [illegible]. All clones were systematically sequenced.

Fluorescent microscopy

Images were captured on an Olympus [illegible] inverted microscope and processed using [illegible] software [illegible] Olympus Fluoview FV [illegible] confocal microscope with a [illegible] [illegible] [illegible] using the Olympus FV [illegible] software version [illegible] [illegible].

Fluorescence recovery after photobleaching experiments (FRAP)

FRAP experiments were performed on living transfected Cos7 cells at [illegible]. Only the transfected cells displaying a phenotype characteristic of the mutation investigated were considered for FRAP experiments. To minimize cell physiology disturbance, we chose to photobleach selected areas for 1[illegible] iterations at [illegible] power of the argon laser. After photobleaching, 4[illegible] images were captured every 5 s for 21[illegible] at 1.5% power of the argon laser. FRAP was performed during such a short period of time to limit bias due to nuclear rotation and cell movement. Average fluorescence intensity in each region of interest was normalized to total cellular fluorescence loss during bleach and imaging phase as $I_{rel} = T_0 I_t / T_t I_0$ as described by Phair et al. [illegible] (T_0: total cellular intensity during prebleach, T_t: total cellular intensity at time t, I_0: average intensity in the region of interest during pre-bleach, I_t: average intensity in the region of interest at time t). Fluorescence of surrounding cells was taken into account in cases of cells exhibiting a single speckle (mutation D192G and R386K). A non linear regression was used to create a best fit curve. Difference in the t[illegible] between L85R, D192G, R386K and wild type lamin C aggregates was assessed by a T test.

Immunocytochemistry

Transfected cells were fixed on coverslips with 4% paraformaldehyde in phosphate buffered saline (PBS) and permeabilized with 1[illegible]% Triton-1[illegible] for 5 min. Cells were incubated with the primary antibody (RanGap1 (N-19) polyclonal antibody, Santa Cruz) in 1% fetal bovine serum [illegible], and with Alexa Fluor 594 labeled Rabbit Anti-Goat antibody (Molecular Probes) for 30 min. The coverslips were mounted on a glass slide with mowiol

Immunoblotting

Western blot analysis was performed as previously described by Sylvius et al. [1]. The primary antibody used was goat anti-lamin A/C (N-18) poly clonal antibody and mouse anti beta actin (Ab1 monoclonal antibody (Santa Cruz) and the secondary antibodies were peroxidase-linked anti-goat and anti-rabbit antibodies (Santa Cruz).

Cell preparation for EM

Cells were fixed in 1.5% glutaraldehyde in 0.1 M sodium cacodylate buffer pH 7.2. They were then resuspended in 1% bovine serum albumin infiltrated for 30 min and pelleted by centrifugation. The supernatant was removed and the cell pellets were resuspended with 1% glutaraldehyde in 0.1 M sodium cacodylate buffer pH 7.2. The resultant fine pellets were cut into 1 mm pieces post fixed in 1% osmium tetroxide dehydrated in ascending alcohols and embedded in spurr epoxy resin. Thin sections were stained with uranyl acetate and lead citrate and examined with a Jeol 100 TEM equipped with AMT software.

Results

We transiently expressed the full-length human wild type and the various mutant lamin A and C DNAs fused to the 5′-terminus of variants of the Aequorea victoria green fluorescent protein (GFP) (lamin-FP) in fibroblast COS7 and rat cardiomyoblast H9C2 cells. To assess the consequences of mutations on

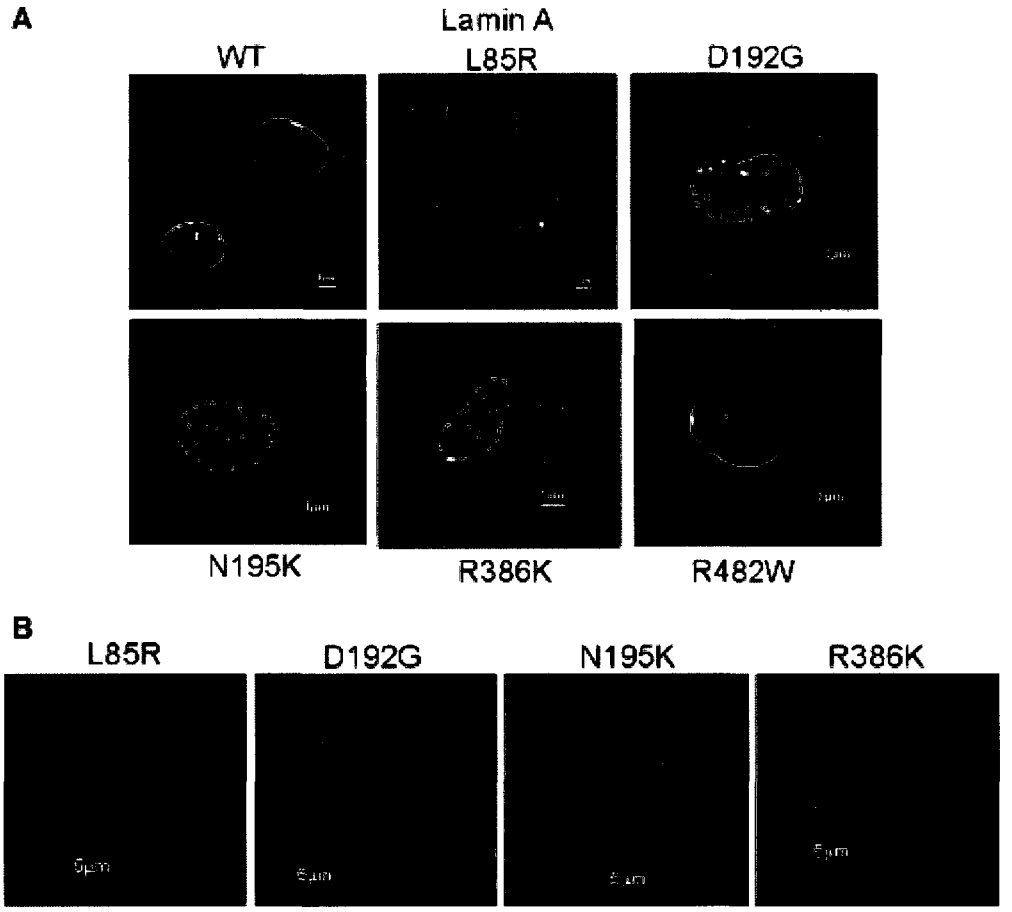

Fig. 1 – A. Nuclei expressing wild type or the various lamin A mutant constructs transiently expressed as ECFP fusion protein in COS7 cells. Cells were visualized by wide-field fluorescence microscopy with an excitation wavelength of 433 nm. Wild type lamin A, as well as L85R and R482W lamin A mutants homogeneously organize throughout the nucleus. In contrast, D192G, N195K and R386K lamin A mutants accumulate in abnormal aggregates. The nuclear membrane appears granular and discontinued. B. The abnormal lamin A aggregation previously found in COS7 cells expressing D192G, N195K and R386K lamin A, was confirmed in nuclei of rat cardiomyoblast H9C2 cells as opposed to cells expressing wild type or L85R lamin A (not shown).

Fig 2 – Confocal microscopy picture of H9C2 cell nuclei transiently expressing D192G lamin A as ECFP fusion protein. Mutated lamin A organizes as aberrant aggregates. However, the spherical organization of these aggregates reveal that they are likely embedded in the nuclear envelope

lamin A and C properties. Specifically, we used confocal immunofluorescence microscopy to examine the cells expressing lamin A [illegible] and C [illegible] separately and then together.

Lamin A mutants aggregate

The wild type phenotype was characterized by a [illegible] [illegible] of the protein [illegible] at the nuclear [illegible] and [illegible] lamin A [illegible] [illegible] aberrant phenotype compared to the wild type [illegible] A and B [illegible] noted that the [illegible] expressing L85R lamin A were carefully analyzed [illegible] this mutant was previously reported as slightly different from the wild type [illegible]. In contrast, D192G, N195K and R386K lamin A [illegible] accumulated in abnormal giant aggregates (Fig. 2A and B), which is consistent with results already described in [illegible] cells [illegible]. Several immunofluorescence microscopy [illegible] performed in cell lines transfected with

lamin A [illegible] have reported the aggregation of lamin A as intranuclear foci or nuclear aggregates inside the nucleoplasm [illegible]. To confirm this statement in our analyses, we used confocal immunofluorescence microscopy and 3D reconstruction of the cell (Fig. [illegible]). Although we could not exclude the presence of nucleoplasmic aggregates, it was obvious that the aggregates were massively present at the periphery of the nucleus and led to a punctate aspect of the nucleus [illegible] shown [illegible]. [illegible] punctate aspect [illegible] that lamin A [illegible] mutants retain the ability [illegible] at the nuclear envelope [illegible].

Abnormal lamin C aggregation is a common feature of several LMNA mutations

We then examined the effect of these mutations on lamin [illegible] A [illegible] previously [illegible] wild type lamin [illegible] [illegible] multiple small intranuclear aggregates [illegible]

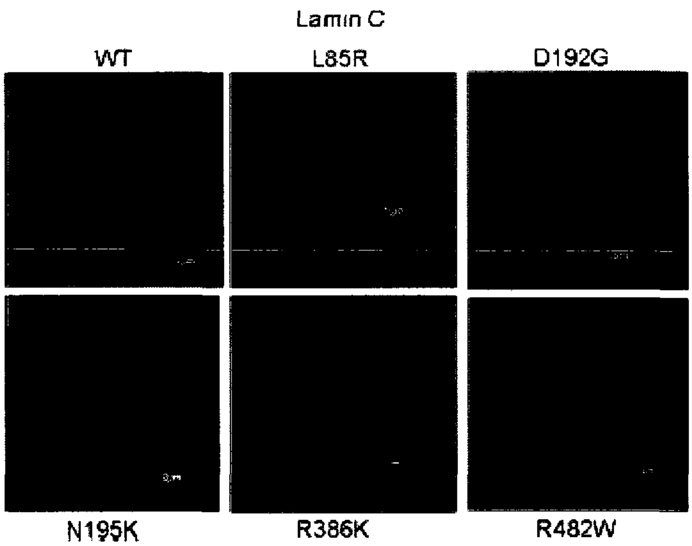

Fig 3 – Nuclei expressing wild type or the various mutated lamin C constructs transiently expressed as ECFP fusion protein in COS7 cells. Prior to visualization by wide-field fluorescence microscopy, Hoechst 33258 dye was used to locate the nuclei (in blue). Excitation wavelengths were 433 nm for lamin C-ECFP and 365 nm for Hoechst 33258. Note that the aberrant aggregation of the lamin C (in red) within the nucleus visualized by Hoechst 33258 dye is common to several LMNA mutations. Only R482W lamin C mutants responsible for lipodystrophy gave rise to a phenotype similar to the wild type

that are evenly distributed throughout the nucleus [11]. R482W lamin C-FP showed a phenotype similar to the wild type whereas D192G lamin C-FP accumulated in one or two intranuclear giant speckles [11], which agrees with previously published studies performed on COS7 or HeLa cells [11,12]. Interestingly, L85R, D192G, N195K, and R386K lamin C-FP mutants also showed a dramatic aggregation in the vast majority of transfected cells (Fig. 3). In COS7 cells, the respective mean speckle diameters were 4.4 (+/- 2 um) (n = 3) for L85R lamin C-FP, 5.2 (+/- 1 um) (n = 11) for D192G lamin C-FP, 5.3 (+/- 2.5 um) (n = 3) for N195K lamin C-FP, 7.1 (+/- 4 um) (n = 12) for R386K lamin C-FP, and 2.3 (+/- 1.5 um) (n = 11) for wild type lamin C-FP. The mean nuclear diameter was 15 um (+/- 1.5 um) for all transfected COS7 cells. Intriguingly, L85R lamin C-FP exhibited an aberrant phenotype compared to wild type lamin C-FP, as opposed to its counterpart lamin A-FP which behaved similarly

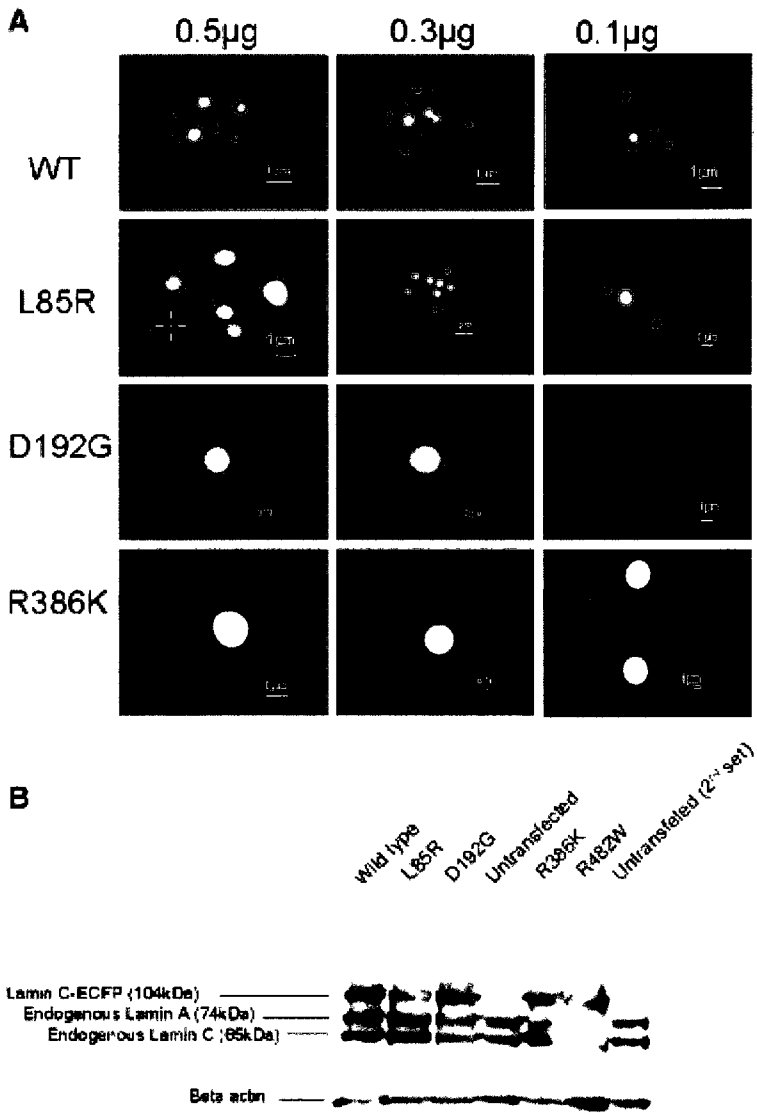

Fig. 4 – A. Transient transfections of COS7 cells with varying quantity of either wild type or mutated lamin C-FP constructs. Cells were visualized by wide-field fluorescence microscopy with an excitation wavelength of 433 nm. The phenotype observed with mutated lamin C-FP is not due to a too elevated quantity of vectors used to transfect the cells. B. Representative Western blot analysis of COS7 cells transfected with the different lamin C-FP variants and using anti lamin A/C antibody. Results show equal over-expression for all construct.

to the wild type lamin A-FP. This suggests that both proteins were differentially affected by the mutation. Aberrant aggregation of nuclear lamin C-FP was observed in less than 20% of COS7 cells expressing wild type lamin C-FP. This proportion was similar to that we previously reported [11].

To ensure that this abnormal lamin C aggregation was not an artifact due to the over-expression of the protein we transfected COS7 cells using lower concentrations of constructs (1.3 μg and 1 μg). Lamin C-FP mutants formed giant aggregates at each tested concentration indicating that the formation of large

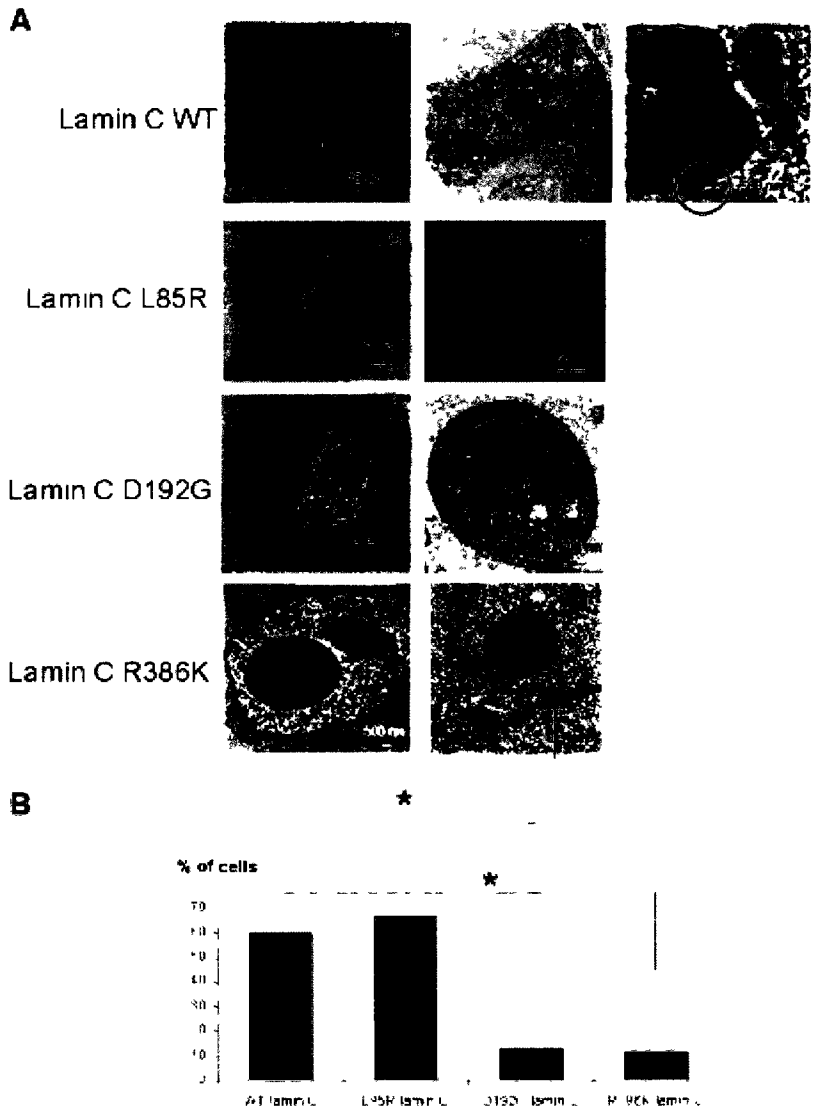

Fig. 5 – A. Electron micrographs of COS7 cells transiently transfected with lamin C-FP constructs. In 60% of cells, wild type lamin C nuclear aggregates were localized in close contact with the nuclear envelope (a–c). Notably, wild type aggregates were able to establish close contact with the nuclear envelope (circle) (c). Similarly, L85R lamin C aggregates organized in contact with the nuclear envelope (d–e). Conversely, in 88% and 87.5% of cells respectively, D192G and R386K lamin C aggregates were found within the nucleoplasm without any contact with the nuclear envelope (f–i). In 30% of cells expressing R386K lamin C, nuclei presented with lamin C aggregates localized outside the nuclear envelope (j–k). B. Percentage of transfected cells displaying lamin C nuclear aggregates in direct contact with the nuclear envelope. χ^2 test showed that the number of cells displaying lamin C aggregates in close contact with the nuclear envelope is significantly different in transfected cells expressing D192G or R386K lamin C mutants compared to the wild type ($p < 0.01$).

aggregates was not an artifact due to an exaggerated dose of DNA (Fig. 4A). Furthermore, Western blotting quantification of lamin mutant GFP revealed no differences in the transfection efficiency compared to the wild type, confirming that these mutant aggregates did not result from transfection artifact (Fig. 4B).

Mutated lamin C loses its ability to incorporate into the nuclear envelope

We further assessed whether lamin C aggregates retain their ability to join the nuclear envelope. As a means to better see envelope shape and potential misshapen nuclei, we chose to

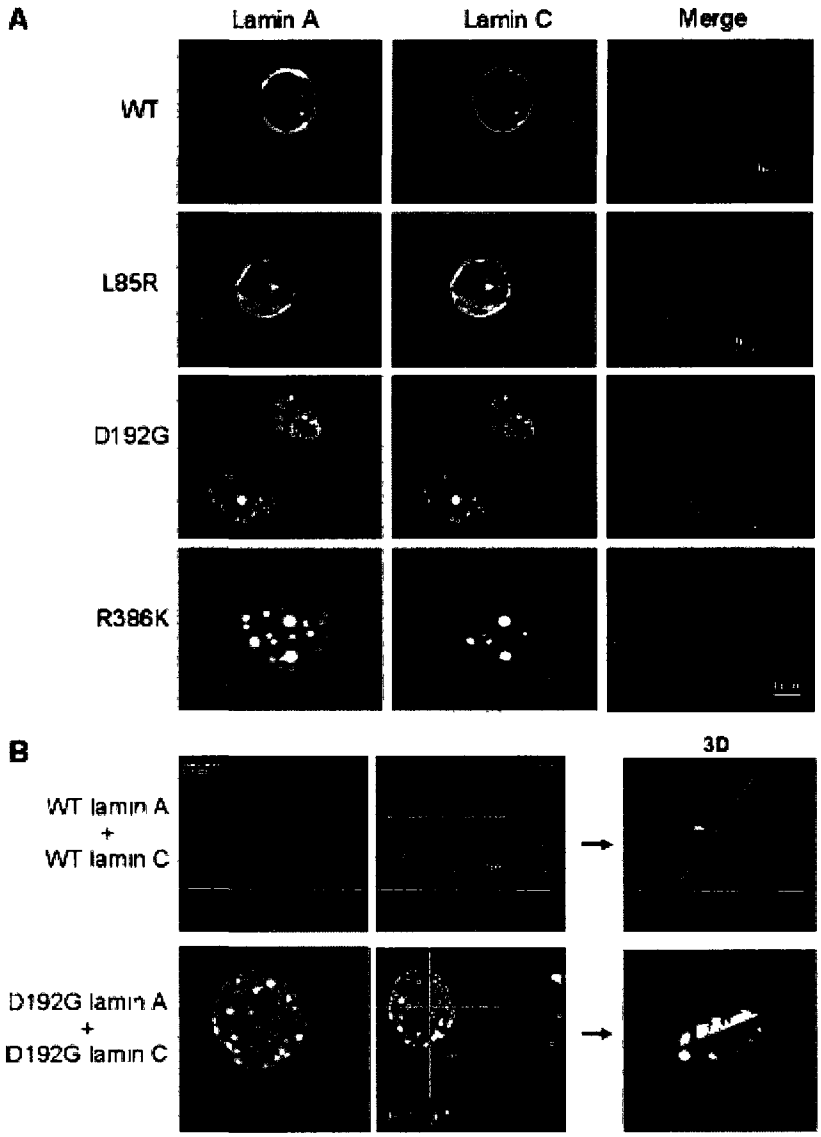

Fig. 6 – A. COS7 cell nuclei transiently co-expressing wild type or mutated lamin A and lamin C constructs. Lamins A and C were inserted into pECFP-C1 and pDsRed2-C1 fluorescent expression vectors respectively. Cells were visualized by wide-field fluorescence microscopy with excitation wavelengths of 433 nm for lamin A-FP and 558 nm for DsRed2-lamin C. Compared to the wild type, the complex lamin A/C forms aggregates and the membrane appears granular and discontinued.
B. Laser-scanning confocal microscopy of COS7 cells nuclei transiently co-transfected with either wild type or mutated lamin A and lamin C. Lamin A (in red) and lamin C (in green) were inserted into pECFP-C1 and pEYFP-C1 fluorescent expression vectors; respectively. Excitation wavelengths were 433 nm for lamin A-FP and 558 nm for DsRed2-lamin C.

perform electron microscopy on COS7 cells expressing the wild type or the various lamin C-FP mutants. We restricted the analysis to wild-type lamin C and L85R, D192G and R386K lamin C mutants since each of these mutants are representative of a single phenotype. No nuclear deformation was observed in any of the transfected cells. However, in most cells expressing wild type lamin C-FP (60%), lamin C aggregates were in close contact with the nuclear envelope (Fig. 5Aa–b). Clearly, close connection between wild type lamin C aggregates and the nuclear envelope are possible (Fig. 5Ac). Conversely, the number of cells exhibiting such a proximity between aggregates and the nuclear envelope was dramatically reduced in the case of D192G and R386K lamin C-FP (12% and 12.5% respectively, wild type n = 47, D192G n = 38, $p < 0.01$; R386K n = 17, $p < 0.01$) (Fig. 5Af–i and 5B). In most of these cells, speckles were found within the nucleoplasm and did not exhibit any close connection with the nuclear envelope as opposed to cells expressing wild type lamin C-FP. In the case of L85R lamin C-FP, the percentage of cells exhibiting lamin C aggregates in contact with the nuclear envelope was similar to the wild type (L85R, n = 24, $p < 0.1$) (Fig. 5B). This finding implies that wild type lamin C is able to establish connections with the nuclear envelope in the absence of lamin A. It also implies that mutations D192G and R386K cause the inhibition of the lamin C/nuclear envelope interaction. The L85R mutation has no effect on this interaction. Again, this supports the hypothesis that each LMNA mutation has specific consequences in regard to lamin A/C properties. It is noteworthy to mention that a significant proportion of cells (30%, n = 17, $p < 0.05$) expressing R386K lamin C exhibited aggregates abnormally localized outside the nuclear membrane (Arrows in Fig. 5Ae). This is rarely observed in nuclei of cells expressing wild type (<8%, n = 47), or the other lamin C mutants (<15% for D192G, n = 38, $p < 0.05$; <12% for L85R, n = 24, $p < 0.05$). However, electron microscopy analysis of the nuclear envelope of cells expressing R386K lamin C did not reveal any obvious abnormality.

Nuclear localization of lamin A/C mutant complexes in COS7 cells

To find out whether lamin A/C complexes localized in the nuclear envelope, we then co-expressed the wild type and each mutated lamin A-FP with its corresponding lamin C, except for [illegible] lamin A since these mutants are similar to D192G and wild type respectively. To circumvent bleed-through issues due to confluent spectral profile exhibited by CFP and YFP fluorophores, the wild type and the various lamin A-FP mutants were expressed concomitantly with their counterpart lamin C cloned in pDsRed [illegible] expression vector. When co-expressed, wild type lamin A-FP and wild type lamin C were homogeneously distributed throughout the nuclear envelope, outlining the nucleus with a rim-like appearance (Fig. 6A). In contrast, D192G and R386K mutants resulted in abnormal aggregation of the complex lamin A/C which [illegible]

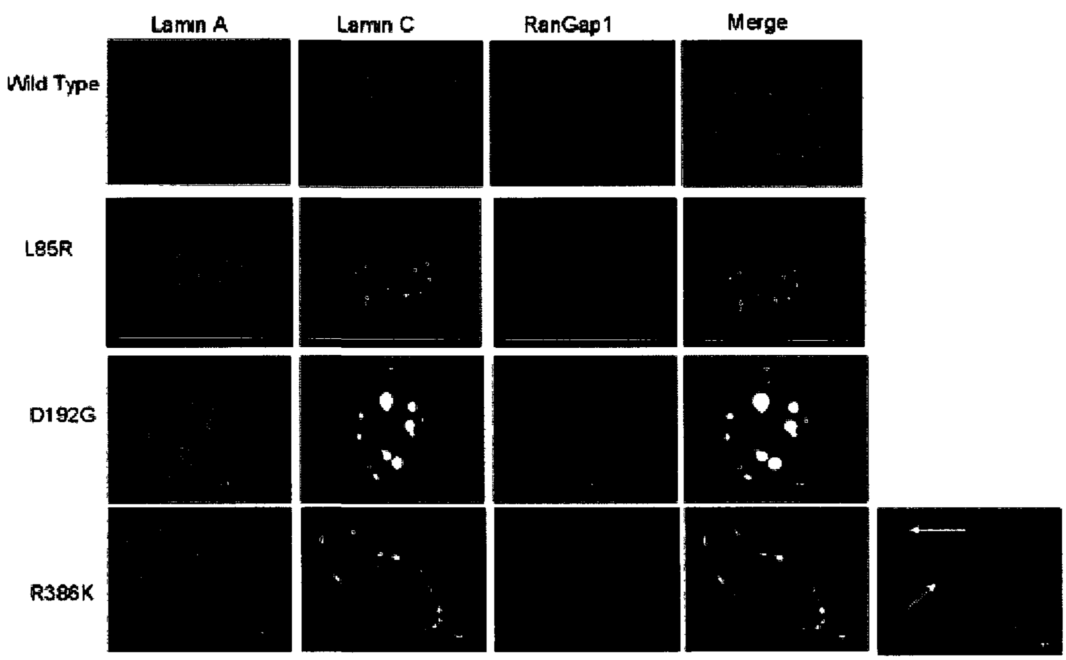

Fig. 7 – Confocal immunofluorescence microscopy pictures of COS7 cells nuclei transiently co-expressing wild type or mutated lamin A-FP and lamin C-FP and immunostained with the anti RanGaP1 polyclonal antibody (N-19). RanGap appears normally distributed in the nuclear envelope. Arrows indicate nuclei with R386K lamin C aggregates localized outside the nuclear envelope.

consistent with previous results [11,18]. Cells expressing L85R lamin A-FP and L85R DsRed2-lamin C exhibited a phenotype similar to the wild type, which suggests that co-expression of both lamins rescues the wild type phenotype. Although L85R DsRed2-lamin C formed speckles within the nucleus (Figs. 3 and 4), we showed that these speckles retained the capacity to make contact with the nuclear envelope (Fig. 5A). Most importantly, even when mutated, lamins A and lamin C always co-localized and were situated in close contact with the nuclear envelope as made evident by confocal microscopy (Fig. 5B). However, in some cells expressing R386K lamins A and C, we observed aberrant localizations of lamin A/C aggregates outside of the nuclear envelope visualized by anti RanGap1 (Arrows in Fig. 7), similarly to cells expressing R386K lamin C-FP only (Fig. 5A). Furthermore, the expression of lamin A mutants did not disturb the distribution of endogenous RanGap1 as revealed by immunostaining with an anti RanGap1 (N-19) polyclonal antibody (Fig. 7). Notably, RanGap1 was not enriched in lamin A/C aggregates (Fig. 7). Since RanGAP1 is a Ran GTPase-activating protein present on the cytoplasmic side of nuclear pore complex during interphase, this result suggests that the nuclear pore complexes were correctly localized in the nuclear rim of transfected cells.

Mutated lamin C molecules present in giant aggregates exhibit increased mobility

It has been shown that some LMNA mutations are associated with an increased mobility of lamin A within the nuclear envelope [19] which indicates that some LMNA mutations affect the mobility of lamin A/C molecules. We hypothesized that the inability of lamin C mutants to properly incorporate into the nuclear envelope would reflect a different rigidity of the molecular structure of lamin C aggregates compared to the wild type. This would lead to defective connection with the nuclear envelope. To assess the mobility of the lamin C molecules inside the aggregates, we performed Fluorescence Recovery After Photobleaching (FRAP) on living COS7 cells expressing L85R, D192G, R386K or wild type lamin C-FP. A defined area of selected aggregates was bleached by a series of high-powered spot laser pulses (Fig. 8A). The recovery of fluorescence in this area was then monitored as a mean to assess the mobility of lamin C

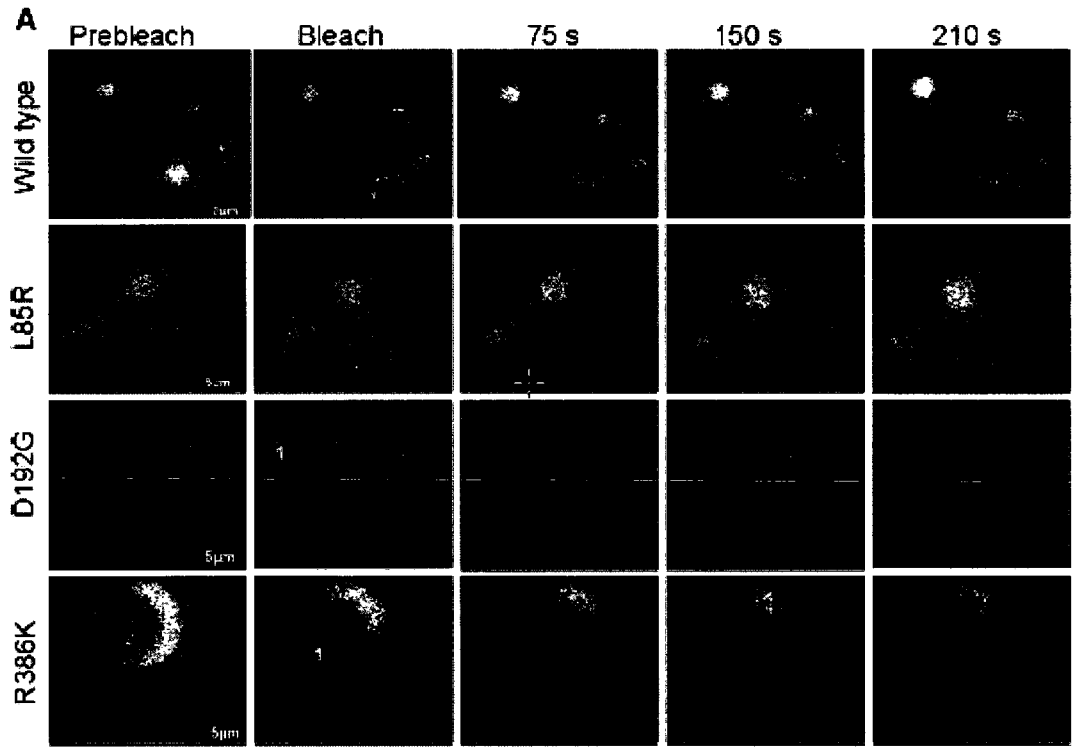

Fig. 8 – A. FRAP experiments on wild type and L85R, D192G and/or R386K lamin C nuclear aggregates of COS7 cells. The boxed regions were bleached and the fluorescence recovery was monitored over a 210 s period. B. Quantitative experiments showing normalized fluorescence recovery after photobleaching of a targeted region of the lamin C nuclear aggregates in COS7 cells. (a) The fluorescence intensity in the bleached area is expressed as a relative recovery. Error bars indicates SEM, $n = 7$. 1 is the level of fluorescence before bleaching. (b) We assessed the time after photobleaching required for fluorescence to recover the median value between the prebleach and just after the bleach ($t_{1/2}$) as a mean to reflect the dynamics of molecule.

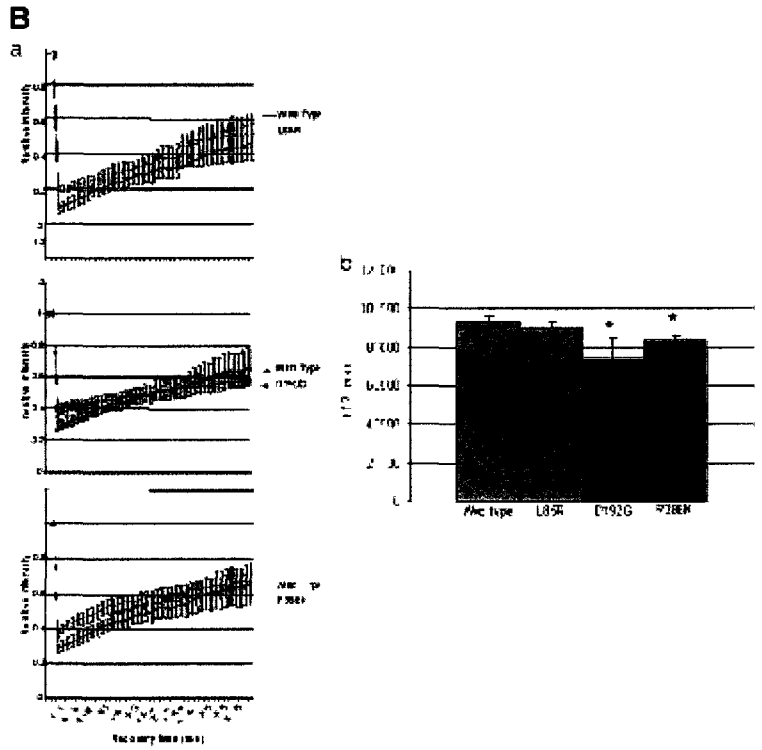

Fig. 8 (continued).

mobile within aggregates. To test whether the time after bleaching required to observe 50% of the plateau (half time) was significantly decreased in D192G, R388H or P482L lamin C IF aberrant speckles compared to wild type lamin C IF speckles, we revealed that the dynamics of mutated lamin C molecules is significantly higher within D192G and R388H lamin C aggregates than within wild type aggregates. In contrast, in L85F lamin C aggregates, the difference is not significant. These data, in agreement with the wild type, the D192G and R388H lamin C intranucleoplasmic aggregates molecules appeared to be more mobile which is indicative of a less stable structure of the mutants. This finding was corroborated by three minute film showing that R388H lamin C IF speckles were more prone to move and fuse to each other (data not shown). No difference was observed with L85F (Fig. 7A and B) and P482A (data not shown) aggregates compared to the wild type.

Discussion

In order to better differentiate and define lamin A and lamin C functions, we used a cell model to express the lamins inducibly and then together. In view of the conflicting results in previous cellular reports on the effect of LMNA mutations, we duplicated some of the experiments in COS7 cell and HeLa cells and compared. Results are summarized in Table

Mutated lamins A organize as nuclear envelope aggregates

Our results showed that some mutated lamin A (D192G, N195K, R388H) form abnormal aggregates when expressed alone which is in contrast with previous studies [ ]. However, in contrast to previous cellular reports, lamin A aggregates observed in mutants bear [ ]. We found that lamin A aggregates mainly localized at the nuclear periphery of the nucleus [ ], suggesting that although unable to properly organize in the nuclear lamina and form the lamina, lamin A mutants keep the capability of association with the nuclear envelope. Alternatively, other mutants (L85F, P482A) behave in a way that was undistinguishable from the wild type.

Lamin C mutants form aberrant intranucleoplasmic aggregates and lose their ability to join the nuclear envelope

We also expressed lamin C alone and found that aberrant lamin C aggregation within the nucleoplasm is a defect common to several LMNA mutations (L85F, D192G, N195K, R388H) unlike functionally only the mutations responsible for skeletal and cardiac diseases were found to result in the atypical aggregation whereas mutation P482A involved in human lipodystrophy did not result in noticeable abnormalities in the localization or distribution of either lamin A or lamin C. This finding suggests that the pathophysiological mechanism of laminopathies with

Table 1 – Summary of the phenotypes observed for the LMNA mutations selected in the study

Variants	Diseases	Phenotypes		
		Lamin A alone	Lamin C alone	Lamin A+C
Wild type		Homogenous distribution throughout the nuclear envelope	Numerous small intranuclear aggregates mainly in close contact with the nuclear envelope	Homogenous distribution throughout the nuclear envelope
L85R	DCM	Homogenous distribution throughout the nuclear envelope similarly to the wild type	Rare intranuclear giant aggregates which may make contact with the nuclear envelope	Homogenous distribution similarly to the wild type
D192G	DCM	Aggregates located at the periphery of the nucleus	Rare intranuclear giant aggregation without contact with the nuclear envelope. Lamin C molecules display increased mobility	Aberrant aggregation of lamin A/C complexes connected to the nuclear envelope
N195K	DCM	Aggregates located at the periphery of the nucleus	Rare intranuclear giant aggregates	
R386K	AD-EDMD	Aggregates located at the periphery of the nucleus	Rare intranuclear giant aggregates without contact with the nuclear envelope. Significant proportion of these aggregates localize outside the nuclear membrane. Lamin C molecules display increased mobility	Aberrant aggregation of lamin A/C complexes connected to the nuclear envelope
R482W	FPLD	Homogenous distribution throughout the nucleus similarly to the wild type	Phenotype indistinguishable from the wild type	

AD-EDMD: Autosomal dominant muscular dystrophy; DCM: Dilated cardiomyopathy; and FPLD: Dunnigan type familial partial lipodystrophy.

cardiac involvement distinct from lipodystrophy and engage lamin C but not lamin A is in turn evident by the absence of abnormal phenotype in cells expressing lamin A with the dilated cardiomyopathy mutation L85R. Other mutations responsible for cardiomyopathy or muscular dystrophy have also been reported to result in aberrant lamin A or C aggregation such as mutation [illegible] [illegible]. However, all mutations should be tested to corroborate this conclusion and determine if the lamin C aggregation in the nucleoplasm could be regarded as a potential hallmark of laminopathies with cardiac or muscular involvement. So far, more than two hundred mutations have been reported of which most are listed in the database http://www.umd.be/LMNA/ [illegible].

Compared to some previous reports [illegible], we sometimes obtained divergent phenotypes of cells expressing the lamin mutants. For example, Raharjo et al. showed that L85R lamin A exhibits a punctate distribution across the nuclear surface slightly different from the wild type, which opposes our results and other studies [illegible]. Also, N195K and R386K lamin A mutants have been shown to relocalize to the nucleoplasm [illegible]. These discrepancies may be explained by protocol differences such as (i) the antibody used which can be directed against lamin A, lamin C, or both lamins, (ii) the expression vectors used for the transfection which requires either direct or indirect immunofluorescence analysis, (iii) the cell lines used (C2C12, HeLa, COS-7, SW13, H9C2) as each cell type expresses different levels of endogenous A-type lamin and differently handles the expression of exogenous lamin A/C.

It is interesting to note that aberrant lamin C aggregation may also be present in a small proportion of nuclei expressing wild type lamin C. This suggests that the presence of these aggregates corresponds to a transient stage of the cell cycle. We can hypothesize that cells expressing these mutants would be longer fixed in this stage. Recently, it has been shown that the mutant lamin A involved in Hutchinson-Gilford Progeria Syndrome and harboring a 50 amino acids deletion alters the cell cycle progression [illegible].

Furthermore, several studies have suggested that lamin A plays a key role in targeting lamin C and Emerin to the nuclear envelope [illegible]. However, recent work in embryonic fibroblasts from mice expressing lamin C only [illegible] showed that lamin C and emerin are normally localized into the nuclear envelope even in the absence of lamin A [illegible]. Furthermore, Lmna [illegible] fibroblasts from these mice display nuclear envelope with only very minimal alterations. The extrapolation of these results to humans is hazardous since mouse models often exhibit differences compared to human laminopathies [illegible]. For example, two mutated H222P alleles are necessary to develop muscular dystrophy in mice whereas the patients are heterozygous [illegible]. Similarly, the clinical phenotype of Lmna L530P/L530P mice, harboring an Emery–Dreifuss mutation, is consistent with human progeria syndrome [illegible]. In this study, we used a cell model expressing lamin C only, and brought evidence that wild type lamin C has the capacity to establish close connections with the nuclear envelope on its own (Fig. [illegible]A and B). This strongly suggests that lamin C can behave independently and that lamin A is not necessary for lamin C to be present in the nuclear envelope. This finding also argues in favor of a potential substitution of lamin A by lamin C in the nuclear envelope which is consistent with the study by Fong et al. However, it is important to note that our finding does not contradict the fact that lamin C is intranuclear when expressed alone and is re-incorporated into the nuclear lamina when expressed with lamin A, as previously reported [illegible]–15]. This likely reflects that the presence of lamin C in the nuclear lamina requires a precise lamin C/lamin A stoichiometry to be respected. This may also explain why the incorporation of lamin C into the nuclear lamina proceeds via intranuclear foci [illegible].

Furthermore, our results showed that the lamin C mutants tested here were seldom part of the nuclear lamina (Fig. 5A). As a consequence, an altered ability of lamin C to establish connections with the nuclear envelope due to mutations in *LMNA* gene should also be considered to explain the major alterations of the nuclear membrane observed in cardiomyocytes from patients [11,12,14]. To further analyze the pathophysiology of laminopathies and propose a potential explanation as for why the mutant lamin C interactions with the nuclear envelope is altered, we performed FRAP experiments on the nuclear aggregates formed by lamin C mutants. Our result revealed that lamin C molecules were significantly more mobile within D192G and R386K lamin C-FP intranuclear aggregates compared to the wild type, thereby indicating that these aberrant lamin C aggregates were significantly less stable. Interestingly, the increased lamin C velocity was observed only with the mutants that exhibited an altered ability to interact with nuclear envelope and that led to an abnormal aggregation in the nucleoplasm (D192G, R386K). In view of these results, we can postulate that the lamin C molecules involved in these aggregates preferably interact with each other to the detriment of the nuclear envelope. However, it would be interesting to investigate other mutants to corroborate a potential correlation between the size of intranuclear aggregates, the velocity of nuclear lamin C and its capacity to associate with the nuclear envelope. Altogether, these results provide novel insight into the pathophysiological mechanism of laminopathies.

LMNA mutations alter lamin A and C interactions with their partners but not RanGap 1 distribution

We showed that L85R lamin C aggregates exhibited neither altered stability nor altered capacity to be connected to the nuclear membrane, as opposed to D192G, N195K, and R386K mutants. These findings likely indicate that the maintenance of these properties is not correlated to the size of nuclear aggregates. However, we cannot exclude that the formation of such aberrant intranuclear accumulations did not affect other lamin A/C properties, such as the interactions with lamin A/C partners. Nuclear lamina is known to participate in the organization of nuclear pores within the nuclear membrane [42]. Since we did not find any mislocalization of RanGap1 with any of the mutants tested, we can hypothesize that the localization of nuclear pore complex within the nuclear envelope is not affected. Therefore, in our cell model, the nuclear-cytoplasm trafficking of macromolecules through the nuclear envelope is most likely unaffected by the presence of mutated lamin A/C (Fig. 7). However, further experiments have to be performed to confirm this hypothesis. Indeed, it has been shown that embryonic fibroblasts from mice lacking A-type lamin exhibited a loss of the nuclear pore protein Nup153 from one pole of the nuclei indicating exclusion of nuclear pore complex from this area [92]. Similarly, Muchir et al. found that Nup153 was absent in pole of fibroblasts from patients with type 1B limb-girdle muscular dystrophy and carrying the nonsense Y259X mutation [21]. Recently, the prelamin A Y646F mutant has been found to co-localize with nuclear pore complex in embryonic kidney (HEK-293) cells [41]. Our divergent results may be explained by the fact that the mutations we investigated are not responsible for either 1B limb-girdle muscular dystrophy or progeria and that the cell type used in our model has endogenous lamin A/C which is likely sufficient to anchor nuclear pore complexes in the nuclear envelope.

Lastly, in a previous report, we showed that lamin C nuclear aggregation results in the aberrant trapping of SUMO1, a post translational modifier of numerous proteins [11]. Among these proteins, there are several transcription factors including the cardiac specific transcription factor GATA4 [42]. Similarly, Hübner et al. demonstrated that the over-expression of lamin A mutant led to the sequestration of the lamin A/C interaction partners pRb (retinoblastoma protein) and SREBP1a (sterol responsive element binding protein 1a) into lamin A nuclear aggregates [34]. Such aberrant interactions with lamin A/C partners may also be considered as a potential pathophysiological mechanism for laminopathies.

LMNA gene mutations and the variety of human phenotypes

Defects in gene regulation and/or abnormalities in nuclear architecture causing cellular fragility are the main two hypotheses that have been proposed to explain the variability of phenotypes due to LMNA mutations [1]. Our previous study was in favor of nuclear fragility since we observed dramatic nuclear envelope discontinuity in cardiomyocytes from LMNA mutated patients [11]. Here, we better dissect the properties of each of lamins A and C specifically and show that they can be differentially affected by a given mutation. These results with others [12,13,17], clearly showed that the consequences of LMNA mutation on the cell physiology is different from one mutation to another. Therefore, we can conclude that if the type of mutation and of its consequence on the unique properties of each lamin specifically, are two key factors that has to be considered in predicting the potential consequences on nuclear function. The combination of these two factors can result in multiple consequences on the cell physiology which likely contributes to explain the variability and complexity of phenotypes in human disease and may be regarded as an additional working hypothesis to explain how mutations in *LMNA* gene lead to so many phenotypes in humans.

Lamins A and C support conjoint and also separate functions

Lastly, we showed that connections between the nuclear envelope and some mutated lamin C-FP (D192G, R386K) are absent which is not the case with the equivalent mutated lamin A. Conversely, other mutants, such as L85R led to aberrant lamin C aggregation but did not alter lamin A organization within the nuclear envelope. The fact that a mutation has different effects on lamin A and lamin C, shows that lamins A and C have to be investigated not only together but also separately in order to better dissect their function and specific role in the occurrence of disease. Also, this likely suggests that each protein may support distinct functions. This is in agreement with a previous study showing that lamins A and C do not play the same role in the nuclear lamina assembly characteristics [12]. In particular, the emerin-lamin A and emerin-lamin C interactions appear to be functionally different and are differently affected by some Emery–Dreifuss LMNA mutations [12]. As a conclusion, a closer look at the functions of lamins A and C specifically may allow resolution of conflicting results and may also help define

genotype–phenotype correlation in laminopathies which has been difficult thus far.

Acknowledgments

The Laboratory of Genetics of Cardiac diseases is part of the John and Jennifer Ruddy Canadian Cardiovascular Genetics Centre. This research was supported by Canadian Institutes for Health Research operating grants 38054 and 65152, and by Heart and Stroke Foundation grant NA 5101 awarded to F. Tesson. N. Sylvius was the recipient of the fellowship awarded by the Heart and Stroke Foundation of Ontario Program grant 5275 and by the Astra Zeneca/Canadian Society of Hypertension/CIHR fellowship.

REFERENCES

[1] N. Sylvius, F. Tesson, Lamin A/C and cardiac diseases, Curr. Opin. Cardiol. 21 (2006) 159–165.
[2] D.K. Shumaker, E.R. Kuczmarski, R.D. Goldman, The nucleoskeleton: lamins and actin are major players in essential nuclear functions, Curr. Opin. Cell Biol. 15 (2003) 358–366.
[3] C.J. Hutchison, Lamins: building blocks or regulators of gene expression? Nat. Rev. Mol. Cell Biol. 3 (2002) 848–858.
[4] R.L. Boguslavsky, C.L. Stewart, H.J. Worman, Nuclear lamin A inhibits adipocyte differentiation: implications for Dunnigan-type familial partial lipodystrophy, Hum. Mol. Genet. 15 (2006) 653–663.
[5] D. Constantinescu, H.L. Gray, P.J. Sammak, G.P. Schatten, A.B. Csoka, Lamin A/C expression is a marker of mouse and human embryonic stem cell differentiation, Stem Cells 24 (2006) 177–185.
[6] Y. Gruenbaum, A. Margalit, R.D. Goldman, D.K. Shumaker, K.L. Wilson, The nuclear lamina comes of age, Nat. Rev. Mol. Cell Biol. 6 (2005) 21–31.
[7] M.S. Zastrow, D.B. Flaherty, G.M. Benian, K.L. Wilson, Nuclear titin interacts with A- and B-type lamins in vitro and in vivo, J. Cell Sci. 119 (2006) 239–249.
[8] M.S. Zastrow, S. Vlcek, K.L. Wilson, Proteins that bind A-type lamins: integrating isolated clues, J. Cell Sci. 117 (2004) 979–987.
[9] N. Zhong, G. Radu, W. Ju, W.T. Brown, Novel progerin-interactive partner proteins hnRNP E1, EGF, Mel 18, and UBC9 interact with lamin A/C, Biochem. Biophys. Res. Commun. 338 (2005) 855–861.
[10] F. Haque, D.J. Lloyd, D.T. Smallwood, C.L. Dent, C.M. Shanahan, A.M. Fry, R.C. Trembath, S. Shackleton, SUN1 interacts with nuclear lamin A and cytoplasmic nesprins to provide a physical connection between the nuclear lamina and the cytoskeleton, Mol. Cell. Biol. 26 (2006) 3738–3751.
[11] N. Sylvius, Z.T. Bilinska, J.P. Veinot, A. Fidzianska, P.M. Bolongo, S. Poon, P. McKeown, R.A. Davies, K.L. Chan, A.S. Tang, S. Dyack, J. Grzybowski, W. Ruzyllo, H. McBride, F. Tesson, In vivo and in vitro examination of the functional significances of novel lamin gene mutations in heart failure patients, J. Med. Genet. 42 (2005) 639–647.
[12] J. Lammerding, P.C. Schulze, T. Takahashi, S. Kozlov, T. Sullivan, R.D. Kamm, C.L. Stewart, R.T. Lee, Lamin A/C deficiency causes defective nuclear mechanics and mechanotransduction, J. Clin. Invest. 113 (2004) 370–378.
[13] S. Tulac, C. Dosiou, E. Suchanek, L.C. Giudice, Silencing lamin A/C in human endometrial stromal cells: a model to investigate endometrial gene function and regulation, Mol. Hum. Reprod. 10 (2004) 705–711.
[14] L.G. Fong, J.K. Ng, J. Lammerding, T.A. Vickers, M. Meta, N. Cote, B. Gavino, X. Qiao, S.Y. Chang, S.R. Young, S.H. Yang, C.L. Stewart, R.T. Lee, C.F. Bennett, M.O. Bergo, S.G. Young, Prelamin A and lamin A appear to be dispensable in the nuclear lamina, J. Clin. Invest. 116 (2006) 743–752.
[15] T. Libotte, H. Zaim, S. Abraham, V.C. Padmakumar, M. Schneider, W. Lu, M. Munck, C. Hutchison, M. Wehnert, B. Fahrenkrog, U. Sauder, U. Aebi, A.A. Noegel, I. Karakesisoglou, Lamin A/C-dependent localization of Nesprin-2, a giant scaffolder at the nuclear envelope, Mol. Biol. Cell 16 (2005) 3411–3424.
[16] I. Motsch, M. Kaluarachchi, L.J. Emerson, C.A. Brown, S.C. Brown, M.C. Dabauvalle, J.A. Ellis, Lamins A and C are differentially dysfunctional in autosomal dominant Emery-Dreifuss muscular dystrophy, Eur. J. Cell Biol. 84 (2005) 765–781.
[17] G.E. Pugh, P.J. Coates, E.B. Lane, Y. Raymond, R.A. Quinlan, Distinct nuclear assembly pathways for lamins A and C lead to their increase during quiescence in Swiss 3T3 cells, J. Cell Sci. 110 (Pt 19) (1997) 2483–2493.
[18] W.H. Raharjo, P. Enarson, T. Sullivan, C.L. Stewart, B. Burke, Nuclear envelope defects associated with LMNA mutations cause dilated cardiomyopathy and Emery-Dreifuss muscular dystrophy, J. Cell Sci. 114 (2001) 4447–4457.
[19] A. Vaughan, M. Alvarez-Reyes, J.M. Bridger, J.L. Broers, F.C. Ramaekers, M. Wehnert, G.E. Morris, W.G.F. Whitfield, C.J. Hutchison, Both emerin and lamin C depend on lamin A for localization at the nuclear envelope, J. Cell Sci. 114 (2001) 2577–2590.
[20] E. Arbustini, A. Pilotto, A. Repetto, M. Grasso, A. Negri, M. Diegoli, C. Campana, L. Scelsi, E. Baldini, A. Gavazzi, L. Tavazzi, Autosomal dominant dilated cardiomyopathy with atrioventricular block: a lamin A/C defect-related disease, J. Am. Coll. Cardiol. 39 (2002) 981–990.
[21] A. Muchir, B.G. van Engelen, M. Lammens, J.M. Mislow, E. McNally, K. Schwartz, G. Bonne, Nuclear envelope alterations in fibroblasts from LGMD1B patients carrying nonsense Y259X heterozygous or homozygous mutation in lamin A/C gene, Exp. Cell Res. 291 (2003) 352–362.
[22] L. Verga, M. Concardi, A. Pilotto, O. Bellini, M. Pasotti, A. Repetto, L. Tavazzi, E. Arbustini, Loss of lamin A/C expression revealed by immuno-electron microscopy in dilated cardiomyopathy with atrioventricular block caused by LMNA gene defects, Virchows Arch. 443 (2003) 664–671.
[23] C. Vigouroux, M. Auclair, E. Dubosclard, M. Pouchelet, J. Capeau, J.C. Courvalin, B. Buendia, Nuclear envelope disorganization in fibroblasts from lipodystrophic patients with heterozygous R482Q/W mutations in the lamin A/C gene, J. Cell Sci. 114 (2001) 4459–4468.
[24] Y. Wang, A.J. Herron, H.J. Worman, Pathology and nuclear abnormalities in hearts of transgenic mice expressing M371K lamin A encoded by an LMNA mutation causing Emery-Dreifuss muscular dystrophy, Hum. Mol. Genet. 15 (2006) 2479–2489.
[25] J.L. Broers, H.J. Kuijpers, C. Ostlund, H.J. Worman, J. Endert, F.C. Ramaekers, Both lamin A and lamin C mutations cause lamina instability as well as loss of internal nuclear lamin organization, Exp. Cell Res. 304 (2005) 582–592.
[26] S. Hübner, J.E. Eam, K.M. Wagstaff, D.A. Jans, Quantitative analysis of localization and nuclear aggregate formation induced by GFP-lamin A mutant proteins in living HeLa cells, J. Cell Biochem. 98 (2006) 810–826.
[27] C. Ostlund, G. Bonne, K. Schwartz, H.J. Worman, Properties of lamin A mutants found in Emery-Dreifuss muscular dystrophy, cardiomyopathy and Dunnigan-type partial lipodystrophy, J. Cell Sci. 114 (2001) 4435–4445.
[28] J. Rankin, S. Ellard, The laminopathies: a clinical review, Clin. Genet. 70 (2006) 261–274.
[29] D. Fatkin, C. MacRae, T. Sasaki, M.R. Wolff, M. Porcu, M. Frenneaux, J. Atherton, H.J. Vidaillet Jr., S. Spudich, U. De

Girolami, J.G. Seidman, C. Seidman, F. Muntoni, G. Muehle, W. Johnson, B. McDonough, Missense mutations in the rod domain of the lamin A/C gene as causes of dilated cardiomyopathy and conduction-system disease, N. Engl. J. Med. 341 (1999) 1715-1724.
[30] G. Bonne, M.R. Di Barletta, S. Varnous, H.M. Becane, E.H. Hammouda, L. Merlini, F. Muntoni, C.R. Greenberg, F. Gary, J.A. Urtizberea, D. Duboc, M. Fardeau, D. Toniolo, K. Schwartz, Mutations in the gene encoding lamin A/C cause autosomal dominant Emery-Dreifuss muscular dystrophy, Nat. Genet. 21 (1999) 285-288.
[31] H. Cao, R.A. Hegele, Nuclear lamin A/C R482Q mutation in canadian kindreds with Dunnigan-type familial partial lipodystrophy, Hum. Mol. Genet. 9 (2000) 109-112.
[32] R.D. Phair, T. Misteli, High mobility of proteins in the mammalian cell nucleus, Nature 404 (2000) 604-609.
[33] S. Gilchrist, N. Gilbert, P. Perry, C. Ostlund, H.J. Worman, W.A. Bickmore, Altered protein dynamics of disease-associated lamin A mutants, BMC Cell Biol. 5 (2004) 46.
[34] S. Hübner, J.E. Eam, A. Hübner, D.A. Jans, Laminopathy-inducing lamin A mutants can induce redistribution of lamin binding proteins into nuclear aggregates, Exp. Cell Res. 312 (2006) 171-183.
[35] T. Dechat, T. Shimi, S.A. Adam, A.E. Rusinol, D.A. Andres, H.P. Spielmann, M.S. Sinensky, R.D. Goldman, Alterations in mitosis and cell cycle progression caused by a mutant lamin A known to accelerate human aging, Proc. Natl. Acad. Sci. U. S. A. 104 (2007) 4955-4960.
[36] T. Arimura, A. Helbling-Leclerc, C. Massart, S. Varnous, F. Niel, E. Lacene, Y. Fromes, M. Toussaint, A.M. Mura, D.I. Keller, H. Amthor, R. Isnard, M. Malissen, K. Schwartz, G. Bonne, Mouse model carrying H222P-Lmna mutation develops muscular dystrophy and dilated cardiomyopathy similar to human striated muscle laminopathies, Hum. Mol. Genet. 14 (2005) 155-169.
[37] L.C. Mounkes, S.V. Kozlov, J.N. Rottman, C.L. Stewart, Expression of an LMNA-N195K variant of A-type lamins results in cardiac conduction defects and death in mice, Hum. Mol. Genet. 14 (2005) 2167-2180.
[38] L.C. Mounkes, S. Kozlov, L. Hernandez, T. Sullivan, C.L. Stewart, A progeroid syndrome in mice is caused by defects in A-type lamins, Nature 423 (2003) 298-301.
[39] J.M. Holaska, K.L. Wilson, M. Mansharamani, The nuclear envelope, lamins and nuclear assembly, Curr. Opin. Cell Biol. 14 (2002) 357-364.
[40] T. Sullivan, D. Escalante-Alcalde, H. Bhatt, M. Anver, N. Bhat, K. Nagashima, C.L. Stewart, B. Burke, Loss of A-type lamin expression compromises nuclear envelope integrity leading to muscular dystrophy, J. Cell Biol. 147 (1999) 913-920.
[41] Y. Fan, A. Garg, A.K. Agarwal, Mislocalization of prelamin A Tyr646Phe mutant to the nuclear pore complex in human embryonic kidney 293 cells, Biochem. Biophys. Res. Commun. 355 (2007) 78-84.
[42] J. Wang, X.H. Feng, R.J. Schwartz, SUMO-1 modification activated GATA4-dependent cardiogenic gene activity, J. Biol. Chem. 279 (2004) 49091-49098.

APPENDIX III

SHORT COMMUNICATION – Accepted for print Journal of Human Genetics

A new p.R541G lamin A/C mutation causing dilated cardiomyopathy with regional LV wall motion abnormalities – genotype-phenotype correlation

Running title: New lamin A/C mutation and DCM

Łukasz A. Małek[1], Sarah Labib[2], Łukasz Mazurkiewicz[3], Michał Saj[4], Rafał Płoski[5], Frédérique Tesson[2], Zofia T. Bilińska[3]*

[1]Department of Invasive Cardiology and Angiology, Institute of Cardiology, Warsaw, Poland

[2]University of Ottawa, Faculty of Health Sciences, Ottawa, Canada

[3]Department of Coronary Artery Disease and Structural Heart Diseases, Institute of Cardiology, Warsaw, Poland

[4]Laboratory of Molecular Biology, Institute of Cardiology, Warsaw, Poland

[5]Department of Medical Genetics, Centre of Biostructure, Medical University of Warsaw, Poland

* Corresponding author:

Zofia T. Bilinska MD PhD

Department of Structural Heart Diseases

Institute of Cardiology, Alpejska 42, 04-628 Warsaw, Poland

tel. + 48 22 3434150

e-mail: z.bilinska@ikard.pl

Abstract

Mutations in the lamin A/C gene (*LMNA*) are established causes of familial dilated cardiomyopathy (DCM) with atrio-ventricular block although relatively little is known about genotype-phenotype correlations. We describe a 23-year-old patient who presented with infero-lateral wall thinning and hypokinesis with evidence of mid-myocardial fibrosis on cardiac magnetic resonance. Molecular analysis driven by clinical similarities with a previously described case harboring the p.R541C *LMNA* mutation revealed a novel p.R541G substitution whose pathogenenicity was confirmed by transfection of mouse myoblasts. Our results emphasize the role of *LMNA* mutations at position R541 in DCM cases with segmental LV wall motion abnormalities.

Keywords: mutation/lamin/dilated cardiomyopathy/cardiac magnetic resonance/delayed enhancement

Introduction

Mutations in the lamin A/C gene (*LMNA*, Genbank accession number: L123399, L12400, and L12401) are responsible for a significant proportion of cases with familial dilated cardiomyopathy (DCM)[1-3]. In these cases, DCM is usually preceded by arrhythmias and atrio-ventricular block, and often leads to severe heart failure[4,5] although reliable genotype-phenotype correlations are difficult to delineate. Cardiac magnetic resonance (CMR) can help elucidate discrete dysfunctional areas of the left ventricule (LV) and demonstrate a characteristic pattern of non-ischaemic delayed enhancement signifying fibrosis[6-8]. We describe a patient from a previously investigated family[9] with ventricular arrhythmias preceding DCM and evidence of

apical aneurysm in his aunt. The patient presented with regional wall motion abnormalities on CMR and was found to have a novel functional *LMNA* mutation. Interestingly, the molecular diagnosis was driven by phenotypic similarities with a previosuly described unrelated case of DCM harboring the p.R541C *LMNA* mutation[5].

Case Report

A 23-year old man with a family history of DCM was referred to us for the evaluation of asymptomatic LV dilation diagnosed 3 years earlier. The patient's father (proband) had an angiographically proven DCM [%left ventricular enlargement (%LVE) =162, LVEF=23%] and died while on the waiting list for heart transplantation at the age of 30 years (Figure 1). The father's sister was diagnosed with DCM at the age of 31 years and had global hypokinesis of the LV with mildly reduced LVEF and akinetic apex. She died suddenly at the age of 39 years.

Our patient was free from heart failure symptoms (NYHA class I), but underwent radiofrequency ablation (RFA) for paroxysmal atrio-ventricular nodal re-entrant tachycardia (AVNRT) 6 years before the current presentation. ECG demonstrated sinus rhythm with nonspecific intraventricular block and QRS of 124 ms (Figure 2A). Transthoracic echocardiography revealed dilation of the left ventricle (%LVE=121) and the presence of mild global hypokinesis (LVEF=50%). The presence of Q waves in lateral wall leads in the patient and regional LV dysfunction in the father's sister led to suspicion of *LMNA* mutation. To further characterize the LV morphology and function, the patient was referred for CMR. The study confirmed markedly increased LV end-diastolic volume with decreased LVEF=44% and demonstrated discrete regional areas of hypokinesis with muscle thinning (5mm) located in the mid-ventricular and periapical infero-lateral segments of the LV (Figure 2BC). A marked

hypertrabeculation in dysfunctional regions was also seen. Scans performed 10-15 minutes after gadolinium contrast injection revealed mid-myocardial almost transmural areas of delayed enhancement in the dysfunctional segment (Figure 2DE). To exclude the ischaemic origin of the LV dysfunction, the patient was subjected to coronary CT angiography which did not disclose any changes in coronary arteries (not shown).

Because of the family history, ECG pattern and CMR evidence of regional wall motion abnormalites very similar to observations in patients with p.R541C *LMNA* mutation initially described by Forrisier et al. [4] and later by Hookana et al. [7] and by our group[5], we decided to screen the patient for *LMNA* mutations as described previously[5]. Analysis excluded presence of p.R541C but, interestingly revealed a previously undescribed mutation at the same position, with Arginine to Glycine substitution (p.R541G) (Figure 3A). Introduction of the p.R541G mutant lamin A/C into C2C12 mouse myoblast cells led to the development of aggregates in about 80% of the cells (Figure 3B). In 60% of these aggregated cells, the aggregates formed sickle-shaped aggregates (Figure 3C) as opposed to the common circular aggregates[10].

Laboratory findings included mildly increased troponin levels, with NT-proBNP concentrations within reference range. Cardiopulmonary treadmill test showed generally preserved physical capacity ($V0_2max$=29.6 ml/kg/min, 62% predicted at RER 1.08, 8.5 METs) without complex ventricular extrasystole at peak exercise. Ambulatory ECG monitoring demonstrated 196 premature ventricular beats without complex forms of arrhythmia. Patient was scheduled to undergo ambulatory ECG monitoring every 3 months with subsequent restratification for ICD implantation at 6-12 months time.

The same mutation was found in the sister of the patient, age 28, who had a sinus bradycardia on ECG with the presence of Q waves in leads II and V_4-V_6. Holter monitoring

revelad supraventricular and ventricular arrhythmias (pairs, periods of bigeminia). She had a mildly elevated troponin levels, but normal echocardiographic (%LVE=100) and CMR picture.

Discussion

We present a patient belonging to a second generation of the family with confirmed DCM who was found to have a novel functional p.R541G *LMNA* mutation.

The R541 site is located in the C-terminal tail region of the lamin A/C protein. The tail is essential in the secondary structural organization of lamin dimers forming longitudinal polar head-to-tail polymers[10]. The novel point mutation results in the change of the Arginine into a Glycine, which contrary to Arginine has a non-polar neutral side chain. Experiments in cellular models demonstrated that p.R541G mutation presents a phenotype with multiple small aggregates of the mutant proteins, and frequent formation of sickles connecting the mutant aggregates. This indicates aberrant formation of the inner nuclear lamina, most likely due to misassembled lamin dimers caused by polarity change.

The phenotype of the novel mutation includes electrocardiographic abnormalities (left anterior hemiblock, pathological Q waves), local LV dysfunction (found in patient and his aunt) and ventricular arrhythmias (found in patient's father, aunt and sister). These manifestations are very similar to those observed in patients harboring another substitution at the same position which replaces Arginine with Cysteine[4,5,7]. However, in addition to the exact location of the mutation, expression of this phenotype clearly depends on the specific amino acid change as evidenced by reports of p.R541S mutation[10] and p.R541H mutation[11], both of which had no evidence of regional wall motion anomalies. In this context, it is relevant to note that Glycine

and Cysteine (but not Serine and Histidine) both have non-polar side chains and thus may have a similar functional effect.

CMR is a sensitive tool in the diagnosis of discrete segmental LV dysfunction, which may be easily overlooked in routine transthoracic echocardiography. CMR examination can demonstrate the characteristic mid-wall pattern of delayed enhancement (fibrosis) in the dysfunctional regions[6,7] and the presence of hypertrabeculation[1] which is also associated with *LMNA* mutations. Nevertheless it should be mentioned that CMR may not be able to demonstrate early signs of DCM even in patients with abnormal ECG pattern, ventricular arrhythmia and elevated troponin levels as demonstrated in patient's sister. The lack of visible abnormalities on CMR examination in this case may be at least partially related to later onset of the disease in women in comparison to men[9,12], as observed in patient's aunt.

References

1. Elliott, P., Andersson, B., Arbustini, E., Bilinska, Z., Cecchi, F., Charron, P. et al. Classification of the cardiomyopathies: a position statement from the european society of cardiology working group on myocardial and pericardial diseases. Eur. Heart. J. **29**, 270-276 (2008).

2. Møller, D.V., Pham, T.T., Gustafsson, F., Hedley, P., Ersbøll, M.K., Bundgaard, H. et al. The role of lamin A/C mutations in Danish patients with idiopathic dilated cardiomyopathy. Eur. J. Heart. Fail. **11**, 1031-1035 (2009).

3. Sylvius, N., Tesson, F. Lamin A/C and cardiac diseases. Curr. Opin. Cardiol. **21**, 159-65 (2006).

4. Forissier, J.F., Bonne, G., Bouchier, C., Duboscq-Bidot, L., Richard, P., Wisnewski, C. et al. Apical left ventricular aneurysm without atrio-ventricular block due to a lamin A/C gene mutation. Eur. J. Heart. Fail. **5**, 821-825 (2003).

5. Saj, M., Jankowska, A., Lewandowski, M., Szwed, H., Szperl, M., Ploski, R. et al. Dilated cardiomyopathy with profound segmental wall motion abnormalities and ventricular arrhythmia caused by the R541C mutation in the *LMNA* gene. Int. J. Cardiol. 2009; doi:10.1016/j.ijcard.2008.12.083. Published online ahead of print 22 January 2009

6. Raman, S.V., Sparks, E.A., Baker, P.M., McCarthy, B., Wooley, C.F. Mid-myocardial fibrosis by cardiac magnetic resonance in patients with lamin A/C cardiomyopathy: possible substrate for diastolic dysfunction. J. Cardiovasc. Magn. Reson. **9**, 907-913 (2007).

7. Hookana, E., Juntilla, M.J., Särkioja, T., Sormunen, R., Niemelä, M., Raatikainen, M.J. et al. Cardiac arrest and left ventricular fibrosis in a Finish family with the lamin A/C mutation. J. Cardiovasc. Electrophysiol. **19**, 743-747 (2008).

8. Koikkalainen, J.R., Antila, M., Lötjönen, J.M., Heliö, T., Lauerma, K., Kivistö, S.M. et al. Early familial dilated cardiomyopathy: identification with determination of disease state parameter from cine MR image data. *Radiology.* **249**, 88-96 (2009).

9. Bilinska, Z.T., Michalak, E., Piatosa, B., Grzybowski, J., Skwarek, M., Deptuch, T.W. et al. Familial dilated cardiomyopathy: evidence for clinical and immunogenetic heterogeneity. *Med. Sci. Monit.* **9**, CR219-226 (2003).

10. Sylvius, N., Bilinska, Z.T., Veinot, J.P., Fidzianska, A., Bolongo, P.M., Poon, S. et al. In vivo and in vitro examination of the functional significances of novel lamin gene mutations in heart failure patients. J. Med. Genet. **42**, 639-47 (2005).

11. Vytopil, M., Benedetti, S., Ricci, E., Galluzzi, G., Dello Russo, A., Merlini, L. et al. Mutation analysis of the lamin A/C gene (LMNA) among patients with different cardiomuscular phenotypes. *J. Med. Genet.* **40**, e132 (2003).

12. Mangin, L., Charron, P., Tesson, F., Mallet, A., Dubourg, O., Desnos, M. et al. Familial dilated cardiomyopathy: clinical features in French families. Eur. J. Heart. Fail. **1**, 353-361 (1999).

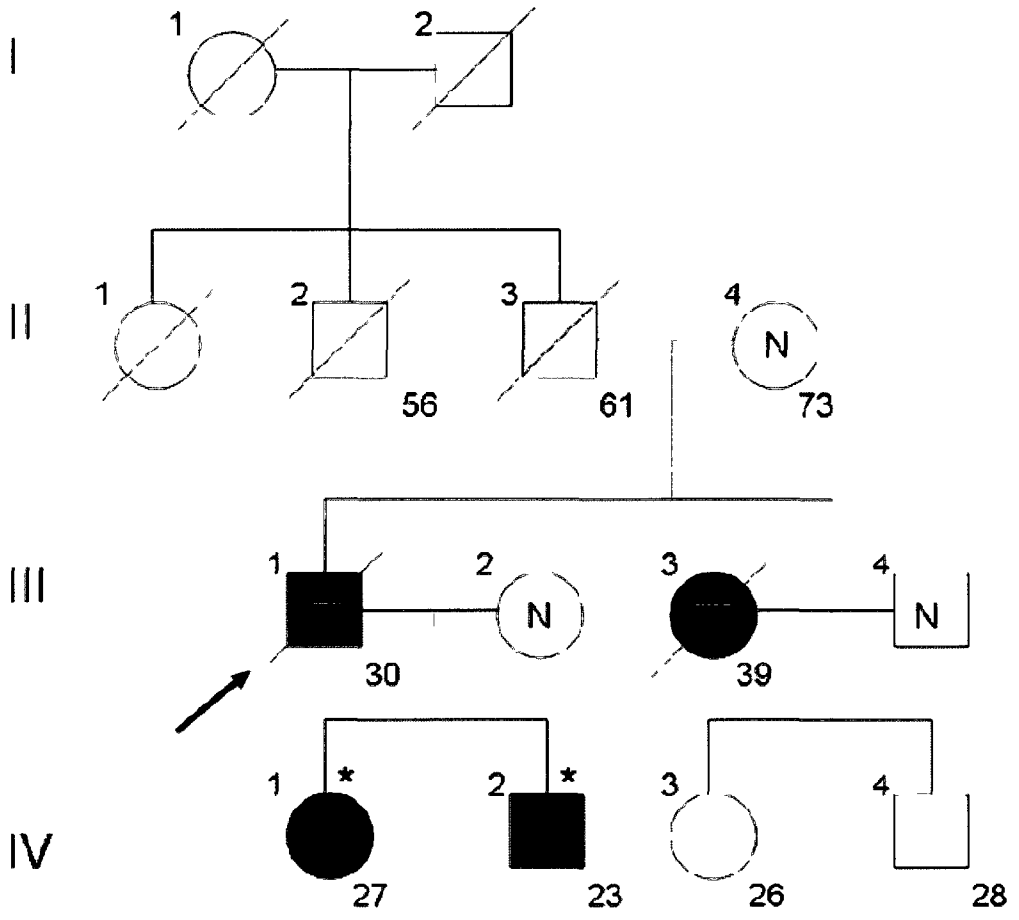

Figure 1. Family pedigrees. The arrow shows the proband (father of the presented patients). Blackened squares (male) and circles (female) indicate confirmed cases of DCM. Open symbols represent subjects not examined. N indicates phenotypically normal subjects. Shaded symbol indicates a likely obligate carrier. Stars indicate genotyped patients. Roman numerals indicate generations. Numbers above symbols indicate consecutive examined carriers. Numbers below symbols indicate age at diagnosis or last screening and in case of crossed subjects - at death.

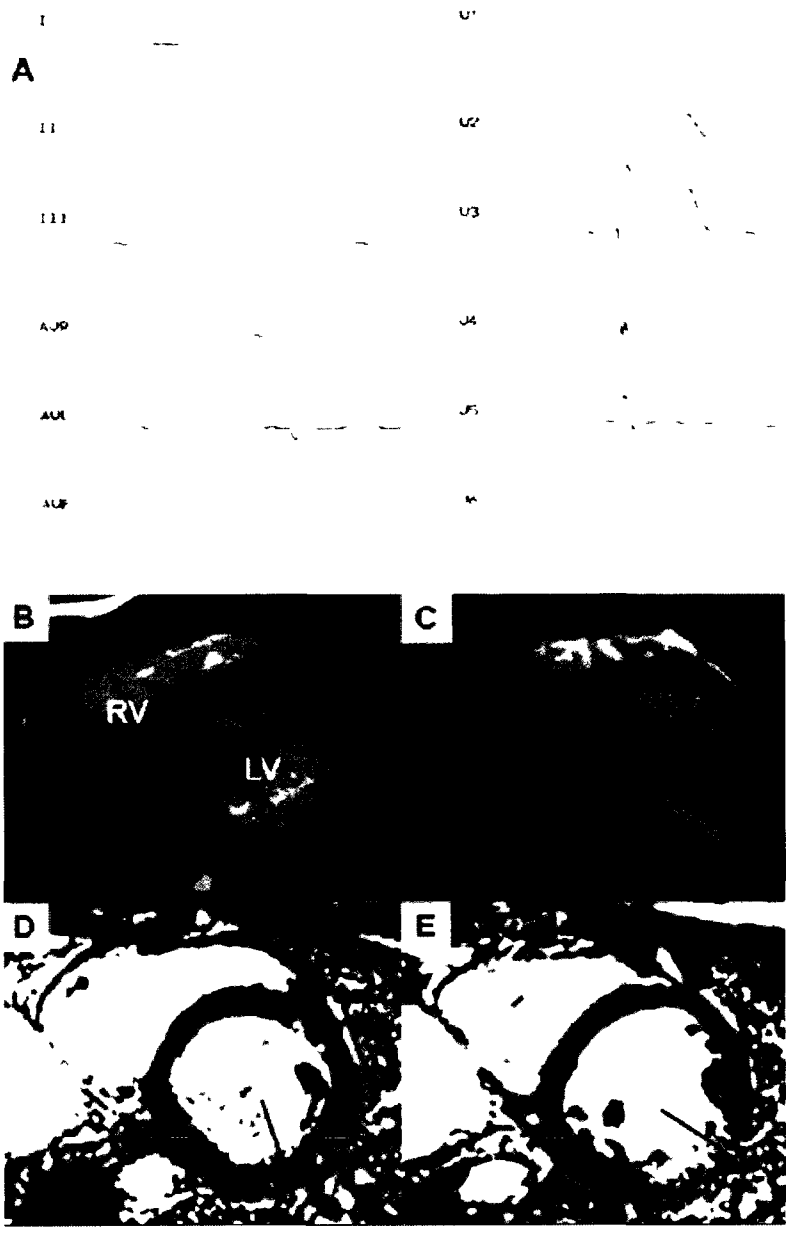

Figure 2. Clinical findings in the studied patient: A) 12-lead electrocardiogram; B-E) Cardiac magnetic resonance: B, C - marked thinning of the mid-ventricular infero-lateral segment in cine SSFP images in end-diastole (arrow); D,E - the presence of mid-myocardial almost transmural fibrosis in the same segments in PSIR images with visible deleyed enhancement (arrows). RV – right ventricle, LV – left ventricle.

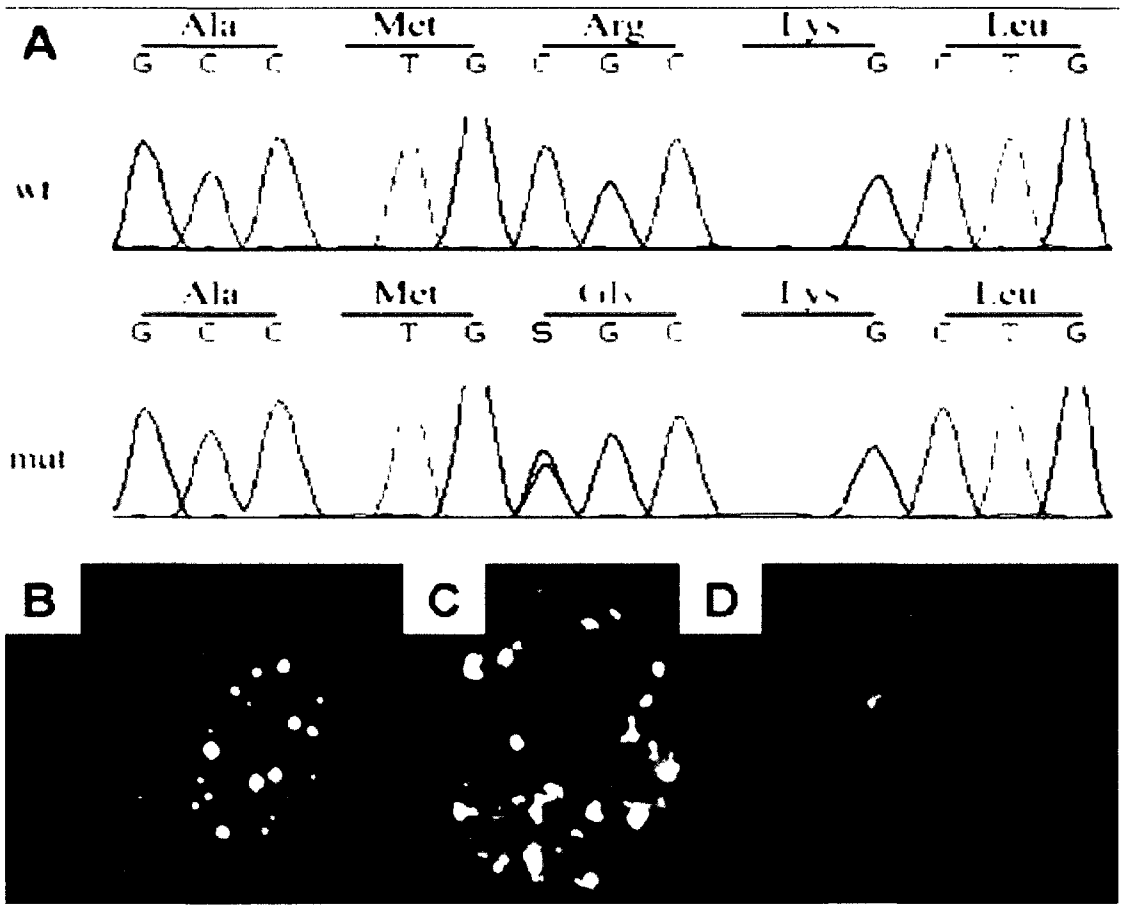

Figure 3. A) Result of direct sequencing demonstrating Arginine to Glycine (p.R541G) substitution in exon 10 of *LMNA.* (wt – normal variant, mut – variant with mutation). B-D) C2C12 mouse myoblasts transiently transfected with p.R541G mutant lamin A and lamin C in fluorescent expression vectors as described previously[10]: A - example of a cell with aggregates, B - example of a cell with sicle-shaped aggregates – see text for details. For comparison C - the wild type of lamins A and C transfected together with homogeneous distribution of the protein throughout the nucleus.

APPENDIX IV

Submitted to Cardiovascular Research

Rare and Common Variants of *LMNA* Gene in Atrial Fibrillation Patients:

A Possible Pathogenic Role of Thr528Met Mutation

M. Saj[1], R. Dabrowski[2], S. Labib[3], M. Szperl[1], M. Kiliszek[4], E. Kozluk[4], G. Broda[5], H. Szwed[2], F. Tesson[3], Z.T. Bilinska[6], R. Ploski[7,4]

[1] Laboratory of Molecular Biology, Institute of Cardiology, Warsaw, Alpejska 42, 04-628, Poland

[2] 2nd Ischemic Heart Disease and Clinical Department, Institute of Cardiology, Warsaw, Alpejska 42, 04-628, Poland

[3] University of Ottawa, Faculty of Health Sciences, 451 Smyth, Ottawa ON K1H 8M5, Canada

[4] 1st Department of Cardiology, Medical University of Warsaw, Warsaw, Banacha 1a, 02-097, Poland

[5] Department of Cardiovascular Epidemiology and Prevention, and Health Promotion, Institute of Cardiology, Warsaw, Alpejska 42, 04-628, Poland

[6] Department of Coronary Artery and Structural Heart Diseases, Institute of Cardiology, Warsaw, Alpejska 42, 04-628, Poland

[7] Department of Medical Genetics, Centre of Biostructure, Medical University of Warsaw, Pawińskiego 3C, 02-106, Poland

Michal Saj - sajmichal@yahoo.com, Rafal Dabrowski - r.dabrowski@ikard.pl, Sarah Labib - sarahlabib@gmail.com, Malgorzata Szperl - mszperl@yahoo.com, Marek Kiliszek - kiliszek@amwaw.edu.pl, Edward Kozluk - ekozluk@amwaw.edu.pl, Grazyna Broda - gbroda@ikard.pl, Hanna Szwed - hszwed@ikard.pl, Frederique Tesson - ftesson@uottawa.ca, Zofia T. Bilinska - zbilinska@ikard.pl, Rafal Ploski *

* Corresponding author:

Rafal Ploski, MD, PhD

Department of Medical Genetics, Centre of Biostructure, Medical University of Warsaw

Pawinskiego 3C, 02-106 Warsaw, Poland

tel.: + 48 22 572 0606

e-mail: rploski@wp.pl

keywords: atrial fibrillation, dilated cardiomyopathy, LMNA, Thr528Met

Abstract

Background *LMNA* gene mutations can in rare cases cause lone atrial fibrillation whereas the role of *LMNA* polymorphisms in predisposing to this disease has not been addressed. Our goal was to study the incidence of *LMNA* mutations/polymorphisms in the population of patients with non-valvular atrial fibrillation in a Polish population.

Methods We screened by sequencing the exons and intron/exon boundaries of *LMNA* in 103 patients with non-valvular atrial fibrillation.

Results In one subject a single missense Thr528Met mutation was found. Since Thr528Met was previously reported only in lipodystrophy or progeria and always together with other *LMNA* defects, we showed its pathogenicity by *in vitro* expression studies. Another interesting novel variant was Ile26Ile found in a patient with family history of heart disease, but absent in 246 healthy individuals. We also performed a preliminary study on the distribution of common variants of *LMNA* in atrial fibrillation. Based on the studied patients' findings and HapMap data, we noted the existence of a block of linkage disequilibrium comprising SNPs from exon 5 to exon 8. Analysis of a tagging SNP (rs505058) showed a statistically significant increase among patients vs. controls, which could not be reproduced in a second group of patients (n = 377) and controls (n = 467).

Conclusions In conclusion, in rare cases missense mutations such as Thr528Met and possibly mutations occurring in exonic splicing enhancer such as Ile26Ile may play a pathogenic role in atrial fibrillation.

Introduction

Lamin A/C are type V intermediate filament proteins bound to the inner nuclear membrane and encoded by the *LMNA* gene located in chromosome 1q21. Lamins are mainly responsible for the mechanical integrity of the nucleus, but also play important roles in chromatin organization, cell cycle regulation, DNA replication, RNA transcription and apoptosis [1].

More than 300 mutations have been identified in *LMNA* gene leading to many pathogenic phenotypes such as dilated cardiomyopathy (DCM), autosomal dominant Emery-Dreifuss muscular dystrophy, Dunnigan-type familial partial lipodystrophy, Charcot-Marie-Tooth disease and Hutchinson-Gilford progeria syndrome. Heterogeneity of *LMNA* mutations is further complicated by the lack of clear genotype-phenotype correlation, when different mutations in the same codon, or even the same mutation, produce a variety of clinical symptoms [2-4].

Mutations in the *LMNA* gene are one of the most frequently detected mutation genes in DCM with conduction system disease [5] and atrial fibrillation (AF) is often present in these populations [6, 7]. Recently Brauch et al. performed a screening for *LMNA* mutations in 268 patients with lone AF [8]. In 2008 we planned and since then have performed a similar study in patients with non-valvular AF looking for incidence of *LMNA* mutations in the AF patient population.

Methods

The subjects were recruited at the 2nd Ischemic Heart Disease Department of the Institute of Cardiology, Warsaw. During each subject's first visit, after the research protocol was accepted, an informed written consent was obtained and a detailed questionnaire of their medical history and ECG taken. Conventional M-mode, two-dimensional and Doppler

echocardiography examinations were performed using Sonos 5000 (Philips Medical Systems, Andover, USA). Left ventricular ejection fraction was estimated using Simpson biplane method. The inclusion criteria were: patient's age between 18 and 70 years, history of paroxysmal, persistent (episodes exceeding 7 days, reverting to sinus rhythm) and chronic forms of AF (ECG-confirmed AF episodes). The exclusion criteria were: significant valvular dysfunctions, prosthetic valves, inflammatory and systemic diseases. Blood samples were taken for DNA studies.

The study group comprised 103 Caucasian subjects, aged 59.7±11.4 years including 83 men (aged 58.7±11.7) and 20 women (aged 63.7±9.6). Mean duration of arrhythmia was 5 (2.0 - 7.0) years. The demographic and clinical characteristics of the patients are presented in Table 1. The second group of subjects with AF comprised of 377 consecutive patients that underwent catheter ablation within pulmonary veins in the years 2007-2009 at the 1st Department of Cardiology, Medical University of Warsaw, Poland. There were 253 men (67,1%) and 124 women (32,9%). Mean age of the patients was 53,1 years (21 - 69 years range), while mean arrhythmia duration time was 6,4 years. This group was used only to verify the distribution of polymorphisms in the identified linkage disequilibrium.

To obtain the incidence of this conserved block among healthy subjects two control groups with no history of AF were introduced. Firstly, a group comprising of 95 subjects was studied. Comparison between this and the primary study group of 103 non-vulvular AF patients led to extending the research to include another healthy population sample (n = 372). Subjects of both control groups were matched for age, sex and the presence of hypertension with the primary study group and derived from WOBASZ cohort [9].

DNA was obtained from the peripheral blood by the method of phenol isolation. Twelve exons of the *LMNA* gene were then amplified by the polymerase chain reaction using primer pairs described in earlier studies (list available at

http://www.dmd.nl/lmna_primers.html) or designed with the Primer3 program (v. 0.4.0) (sequences readily available upon request). The amplified regions were screened by direct sequencing with an ABI BigDye Terminator sequencing kit using ABI 3130 Genetic Analyzer (Applied Biosystems, Foster City, USA). The results were analyzed with Variant Reporter 1.0 Software (Applied Biosystems).

Mutation identified in the study was confirmed with RsaI enzyme (Fermentas, Vilnus, Lithuania), which was selected by PIRA-PCR software (available at http://cedar.genetics.soton.ac.uk/public_html/primer2.html). In mutation carrier samples, digestion of the PCR product yielded two bands of 248bp and 128bp in length, which were visualized by 2% agarose gel electrophoresis and ethidium bromide staining.

To characterize the consequence of the *LMNA* mutation at the cellular level, transient cell transfections were performed on C2C12 mouse myoblast cells with wild type or mutated lamin A and lamin C mRNA expressed as fusions to the C-terminus of cyan fluorescent protein (pECFP-C1) and yellow fluorescent protein (pEYFP-N1), respectively (Clonetech Laboratories). Mutations were introduced via site-directed mutagenesis (Stratagene) with forward primer 5'- GGG AAC AGC CTG CGT ATG GCT CTC ATC AAC TCC -3' and reverse primer 5'- GGA GTT GAT GAG AGC CAT ACG CAG GCT GTT CCC -3'. All the inserts were systematically verified by sequencing. C2C12 cells were cultured in Dulbecco's Modified Eagle Medium (Invitrogen) supplemented with 15% FBS and 1:100 L-glutamine, and incubated at 37°C with 5% CO2. Cells were transiently transfected using lipofectamine-2000 according to manufacturer's protocol (Invitrogen). After transfection, cells were fixed and visualized by fluorescent confocal microscopy (Olympus Fluoview FV1000 confocal microscope using the Olympus FV-10 acquisition software). Vector cloning, cellular transfection and cell fixation were described by Sylvius et al. [10].

One of the variants identified during the study was analyzed further to rule out its polymorphic character in a control group of 246 subjects with no history of AF. They derived from WOBASZ cohort [9] and were matched with the primary group of 103 non-vulvular AF patients for age, sex and presence of hypertension. The analysis was performed with Wave DHPLC instrument (Transgenomic, Omaha, USA).

In silico analysis was performed with Human Splicing Finder web tool (available at http://www.umd.be/HSF/HSF.html). The genotyping of polymorphism of linkage disequilibrium was examined using Custom TaqMan® Assay (Applied Biosystems, Foster City, USA) and by 7500 Real-Time PCR System (Applied Biosystems).

Linkage disequilibrium study was performed with Haploview software version 4.2 (Broad Institute, Cambridge, USA)

The approval for this work was granted by local bioethics committee (registration number: 1067, date: March 13th, 2008).

The investigation conforms with the principles outlined in the Declaration of Helsinki.

Results

Screening of the *LMNA* gene in AF patients revealed only one variant leading to amino acid change – Thr528Met mutation. The proband was a seventy-two-year-old Caucasian male with seven-year history of AF and a family history of sudden cardiac death. His father died of arrhythmia at the age of 66. His brother died suddenly, probably due to ventricular fibrillation at the age of 70, fifteen years earlier he had a cardiac arrest episode followed by prolonged hospitalization. The proband's AF recently converted into a chronic form. Since 2003 he had more than 30 episodes of arrhythmia, 14 hospitalizations due to AF and 3 electrical cardioversions.

In 2009, the patient had VVI pacemaker implanted due to an advanced atrioventricular block. MR and echocardiography examinations revealed enlargement of the left and right atria and small to moderate mitral and tricuspid regurgitations. The left ventricle ejection fraction and pulmonary artery systolic pressure were within normal limits (61% and 15 mmHg, respectively).

The same mutation was also found in two daughters of the proband (39 and 45 years old) (Fig. 1A). They had no significant abnormalities in ECG, echocardiography and ECG-exercise test.

In order to evaluate the pathogenicity of Thr528Met mutation further, *in vitro* expression studies were conducted. C2C12 cells were used due to their widespread use in laminopathy research and their transfection efficiency. Wild type lamin A and C were distributed homogeneously at the inner nuclear lamina. After Thr528Met mutant lamin A/C was introduced into C2C12 cells, characteristic aggregates were formed indicating an uneven distribution of lamin protein. Additionally, in 35% of cells with mutant lamin A/C, the aggregates were not circular, but sickle-shaped (Fig. 2).

Apart from Thr528Met mutation, six synonymous variants were identified, of which four were already present in NCBI database. One interesting non-described variant was Ile26Ile (Exon 1 - 279, c.78, C>T). This variant occurred in a NYHA class III heart failure patient with depressed LVEF (30%), normal coronary angiography and positive family history of heart disease (Fig. 1B). *In silico* analysis indicated that this nucleotide substitution disrupts an exonic splicing enhancer (ESE), which constitutes a binding site of SR protein SF2/ASF. The variant was not present in the control group of 246 healthy individuals.

In addition, five intronic variants were detected. Three of them were not described previously: IVS 4 - 13, NT:6595320 (T>A), IVS 5 + 12, NT:6595470 (C>T) and IVS 6 - 44, NT:6596316 (C>T). *In silico* analysis showed that these variants did not disrupt known ESE.

The distribution of these and other variants is presented in Table 2. We noted that in the patients studied four SNPs [rs538089 (Ala287Ala; Exon 5 + 51, c.861 GCT>GCC) rs534805 (IVS 6 + 16, NT 6596283 G>A), rs505058 (Asp446Asp; Exon 7 + 43, c.1338 GAT>GAC) and rs553016 (IVS 8 + 44, NT 6597218 C>T)] in the *LMNA* gene were in strong linkage disequilibrium (LD score = 1000) and that the rare alleles of the SNPs appeared together in all patients but one. An analysis of HapMap data confirmed that the identified cluster of variants was a part of a major block of strong linkage disequilibrium comprising SNPs from exon 5 to exon 8 and thus spanning a significant part of the *LMNA* gene.

To compare the frequency of this conserved block among patients and controls, we typed rs505058 in a control group of 95 subjects with no history of AF. Interestingly, we observed that the subjects carrying the rare allele of rs505058 were significantly more numerous among the patients than controls (23/103 or 22.3% vs. 8/95 or 8.4% for patients and controls, respectively, odds ratio = 2.6, $\chi^2 = 4.92$, p = 0.027). To verify the observed association, we studied an independently collected cohort of 377 AF patients and additional 372 healthy subjects but we were unable to replicate the original observation (presence of rare allele in 90/480 or 18.8% vs. 75/467 or 16.1%, for patients and controls, respectively; odds ratio = 1.206, $\chi^2 = 1.19$, p = 0.275).

Discussion

Our results confirm the findings of a recent report showing that *LMNA* mutations are not a frequent cause of AF [8]. A potentially interesting novel finding concerns the Thr528Met mutation. It had been previously described twice, but always in a heterozygous compound state with other mutations, and never in the context of AF with pacemaker requirement. First, Savage et al. [11] reported a Thr528Met together with Ser583Leu mutation which presented phenotypically as familial partial lipodystrophy. Then, Verstraeten

et al. [12] reported a heterozygous combination of Thr528Met and Met540Thr mutations in a proband with a Hutchinson-Gilford progeria syndrome. Since in both cases the heterozygous carrier parents were healthy, our report is the first to suggest a pathogenic effect of a single Thr528Met mutation.

The pathogenicity of Thr528Met mutation was further supported by *in vitro* studies. In mutant transfected cells, lamin A/C appeared in the form of aggregates clearly distinct from control cells. We also observed characteristic sickle-shape patterns, which might have resulted from mutant lamin forming extensions to other aggregates nearby. To our knowledge, this is the first case of such sickle-like aggregates in disease-associated lamin A/C mutant expression studies. Currently, we are studying the functional effects of the Thr528Met mutation further.

We and others have shown increased mobility of mutant lamins as well as a reduced ability to form contacts with the inner nuclear membrane [10, 13]. From these studies, we can infer that the aggregates and sickles are reducing the lamina stability, thus increasing the mutation-carrier's susceptibility to cellular disfunction.

Another interesting observation concerned the Ile26Ile variant which may, as suggested by *in silico* analysis, affect an exonic splicing enhancer site of SR protein SF2/ASF. Such inactivation of ESE could, in turn, cause the splicing mechanism to mistakenly skip an exon carrying the variant and produce abnormal protein [14]. The variant occurred in an NYHA III individual with a positive family history of heart disease, depressed LVEF (30%) and normal coronary angiography, thus meeting the criteria for DCM diagnosis. Unfortunately, no material suitable for expression studies was available from the patient or his family.

Regarding frequent variants of the *LMNA* gene, we noted, both in the patient cohort studied and in HapMap data, the existence of a major LD block comprising SNPs from exon 5 to exon 8. Some variant(s) included in this block could influence the expression of the *LMNA*

gene and/or the stability of its mRNA. As evidenced by the pathogenicity of single copy deletions, *LMNA* is a dose sensitive gene [15]. Thus, it could be speculated that variants which even slightly decrease its expression, as can be expected from SNP, may predispose to conduction system disorders and arrhythmia including AF. In order to investigate this possibility, we performed an association study and found that a rare allele of an SNP marking the LD block was significantly more common in patients than in controls. However, this observation was not reproduced when larger groups of AF patients and controls were studied, suggesting that the original finding was caused by chance. These results emphasize the role of replication for validity of association studies.

In conclusion, we confirm that mutations in *LMNA* are not frequent causes of AF. Tagged SNP within the LD block in *LMNA* gene is not associated with AF. However, our results suggest that in rare cases missense mutations such as Thr528Met and perhaps mutations occurring in exonic splicing enhancer such as Ile261Ile may play a role in disease development.

Competing interests

The author(s) declare that they have no competing interests.

Authors' contributions

Concept and design of the study: ZTB, RD, RP; drafting of the manuscript: MS, RP, ZTB; genetic study: MS, MSz, RP, ZTB; clinical study: RD, HS, ZTB; critical revision of the manuscript for important intellectual content: MS, RD, HS, FT, ZTB, RP; patient population recruitment: RD, HS, MK, EK, GB; gene expression study: SL, FT.

Acknowledgements

This work was supported by: Polish State Committee for Scientific Research and the Institute of Cardiology grant, registered: Institute of Cardiology, 2.20/II/08 - source of funding for M. Saj, R. Dabrowski, M. Szperl, M. Kiliszek, E. Kozluk, G. Broda, H. Szwed, Z T. Bilinska, R. Ploski; Heart and Stroke Foundation Grant NA 6628 awarded to F. Tesson - source of funding for S. Labib, F. Tesson; and Medical University of Warsaw grant 1WY/N/10 - source of funding for R. Ploski.

Funding bodies played no role in study design; in the collection, analysis, and interpretation of data; in the writing of the manuscript; and in the decision to submit the manuscript for publication.

Reference List

1 Worman HJ, Fong LG, Muchir A, Young SG. **Laminopathies and the long strange trip from basic cell biology to therapy.** *J Clin Invest* 2009; **119:**1825-1836.

2 Sylvius N, Bilinska ZT, Veinot JP, Fidzianska A, Bolongo PM, Poon S, McKeown P, Davies RA, Chan KL, Tang AS, et al. **In vivo and in vitro examination of the functional significances of novel lamin gene mutations in heart failure patients.** *J Med Genet* 2005; **42:**639-647.

3 Hermida-Prieto M, Monserrat L, Castro-Beiras A, Laredo R, Soler R, Peteiro J, Rodriguez E, Bouzas B, Alvarez N, Muniz J, et al. **Familial dilated cardiomyopathy and isolated left ventricular noncompaction associated with lamin A/C gene mutations.** *Am J Cardiol* 2004; **94:**50-54.

4 Wiesbauer M, Benedetti S, Ricci E, Galluzzi G, Dello RA, Merlini L, Boriani G, Galtina M, Morandi L, Politano L, et al. **Mutation analysis of the lamin A/C gene (LMNA) among patients with different cardiomuscular phenotypes.** *J Med Genet* 2003; **40:**e132.

5 Sylvius N, Tesson F. **Lamin A/C and cardiac diseases.** *Curr Opin Cardiol* 2006; **21:**159-165.

6 Charniot JC, Pascal C, Bouchier C, Sebillon P, Salama J, Duboscq-Bidot L, Peuchmaurd M, Desnos M, Artigou JY, Komajda M. **Functional consequences of an LMNA mutation associated with a new cardiac and non-cardiac phenotype.** *Hum Mutat* 2003; **21:**473-481.

7 Taylor MR, Fain PR, Sinagra G, Robinson ML, Robertson AD, Carniel E, Di Lenarda A, Bohlmeyer TJ, Ferguson DA, Brodsky GL, et al. **Natural history of dilated cardiomyopathy due to lamin A/C gene mutations.** *J Am Coll Cardiol* 2003; **41:**771-780.

8 Brauch KM, Chen LY, Olson TM. **Comprehensive mutation scanning of LMNA in 268 patients with lone atrial fibrillation.** *Am J Cardiol* 2009; **103:**1426-1428.

9 Broda G, Rywik S. **National Multicentre Health Survey - WOBASZ project.** *Kardiol Pol* 2005; **63:**601-686 (Polish).

10 Sylvius N, Hathaway A, Boudreau E, Gupta P, Labib S, Bolongo PM, Rippstein P, McBride H, Bilinska ZT, Tesson F. **Specific contribution of lamin A and lamin C in the development of laminopathies.** *Exp Cell Res* 2008; **314:**2362-2375.

11 Savage DB, Soos MA, Powlson A, O'Rahilly S, McFarlane I, Halsall DJ, Barroso I, Thomas EL, Bell JD, Scobie I, et al. **Familial partial lipodystrophy associated with compound heterozygosity for novel mutations in the LMNA gene.** *Diabetologia* 2004; **47:**753-756.

12 Verstraeten VL, Broers JL, van Steensel MA, Zinn-Justin S, Ramaekers FC, Steijlen PM, Kamps M, Kuijpers HJ, Merckx D, Smeets HJ, et al. **Compound heterozygosity**

for mutations in LMNA causes a progeria syndrome without prelamin A accumulation. *Hum Mol Genet* 2006, **15:**2509-2522.

13 Broers JL, Kuijpers HJ, Ostlund C, Worman HJ, Endert J, Ramaekers FC: **Both lamin A and lamin C mutations cause lamina instability as well as loss of internal nuclear lamin organization.** *Exp Cell Res* 2005, **304:**582-592

14 Desmet FO, Hamroun D, Lalande M, Collod-Beroud G, Claustres M, Beroud C. **Human Splicing Finder: an online bioinformatics tool to predict splicing signals.** *Nucleic Acids Res* 2009, **37:**e67.

15. Gupta P, Bilinska ZT, Sylvius N, Boudreau E, Veinot JP, Labib S, Bolongo PM, Hamza A, Jackson T, Ploski R et al: **Genetic and ultrastructural studies in dilated cardiomyopathy patients: a large deletion in the lamin A/C gene is associated with cardiomyocyte nuclear envelope disruption.** *Basic Res Cardiol* 2010, **105:**365-377

Tables

Table 1. Baseline general characteristics of study patients. n=103. AF: atrial fibrillation; RF ablation: radio-frequency ablation; CRT-D: cardiac resynchronization therapy; TIA: transient ischemic attack; OSAS: obstructive sleep apnea syndrome; LVEF: left ventricle ejection fraction; PASP: pulmonary artery systolic pressure; LAH: left anterior hemiblock; RBBB: right bundle branch block; LBBB: left bundle branch block;

	All	Men	Women
Gender: n (%)		82 (80.5)	20 (19.5)
Age (years)	59.7±11.4 (21-79)	58.7±11.7 (21-79)	63.7±9.6 (38-76)
Paroxysmal AF: n (%)	36 (34.9)	28 (33.7)	8 (40.0)
Persistent AF: n (%)	32 (31.)	24 (28.9)	8 (40.0)
Chronic AF: n (%)	35 (33.9)	31 (37.3)	4 (20.0)
AF duration in years, mean (range)	5 (2.0-7.0)	5.0 (1-8)	4.0 (2-6)
Pacemakers: n (%)	21 (20.3)	16 (19.2)	5 (25.0)
RF ablation: n (%)	12 (11.6)	8 (9.6)	4 (20.0)
CRT-D: n (%)	2 (1.9)	2 (2.4)	0
Strokes: n (%)	10 (9.7)	6 (5.8)	4 (20.0)
TIA: n (%)	3 (2.9)	3 (3.6)	0
Hypertension: n (%)	69 (66.9)	57 (68.7)	12 (60.0)
Diabetes type II: n (%)	8 (7.7)	7 (8.4)	1 (5.0)
Metabolic syndrome: n (%)	24 (23.3)	19 (18.4)	5 (25.0)
OSAS: n (%)	6 (5.8)	6 (5.8)	0
Coronary disease: n (%)	16 (15.5)	14 (16.9)	2 (10.0)
Heart infarction: n (%)	13 (12.6)	13 (15.7)	0
LVEF < 40%: n (%)	7 (6.8)	6 (5.8)	1 (5.0)
Heart failure (NYHA II-III): n (%)	13 (12.6)	12 (14.5)	1 (5.0)
PASP > 30 mmHg: n (%)	11 (10.7)	9 (10.8)	2 (10.0)
Thyroid disease: n (%)	13 (12.6)	5 (6.0)	8 (40.0)
Family history of AF: n (%)	17 (16.5)	14 (16.9)	3 (15.0)
ECG: PQ > 200 ms: n (%)	22 (21.3)	20 (24.0)	2 (10.0)

ECG: QRS > 120 ms: n (%)	6 (5.8)	5 (16.0)	1 (5.0)
ECG: LAH: n (%)	6 (5.8)	4 (3.9)	2 (10.0)
ECG: RBBB: n (%)	3 (2.9)	2 (1.9)	1 (5.0)
ECG: LBBB: n (%)	6 (5.8)	5 (16.0)	1 (5.0)

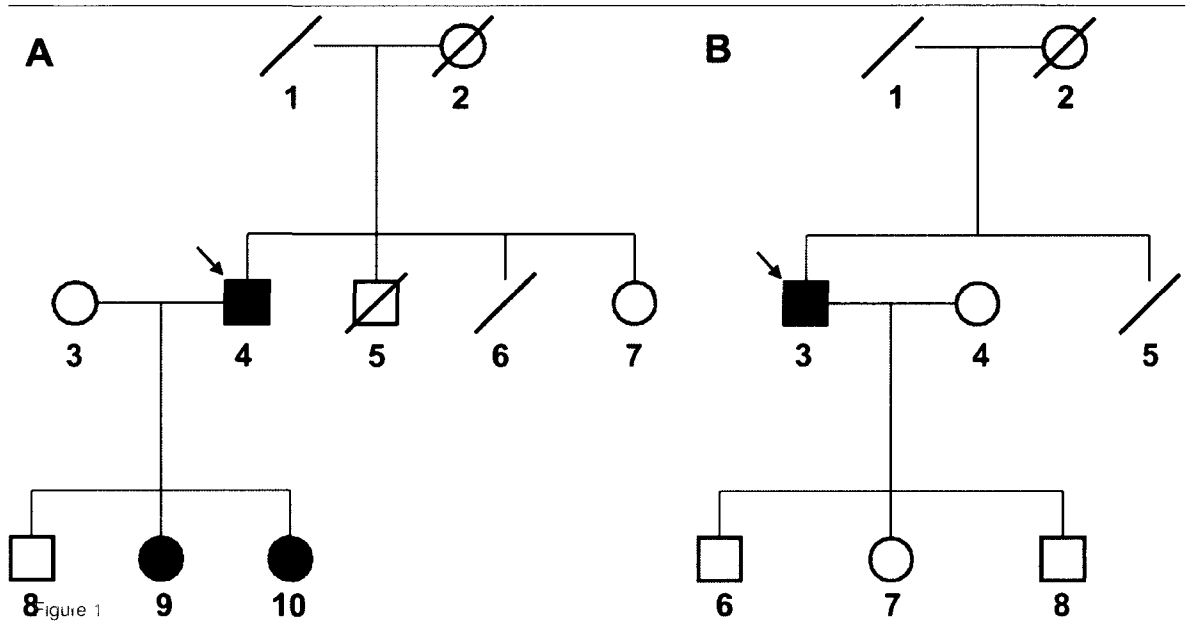

Figure 1

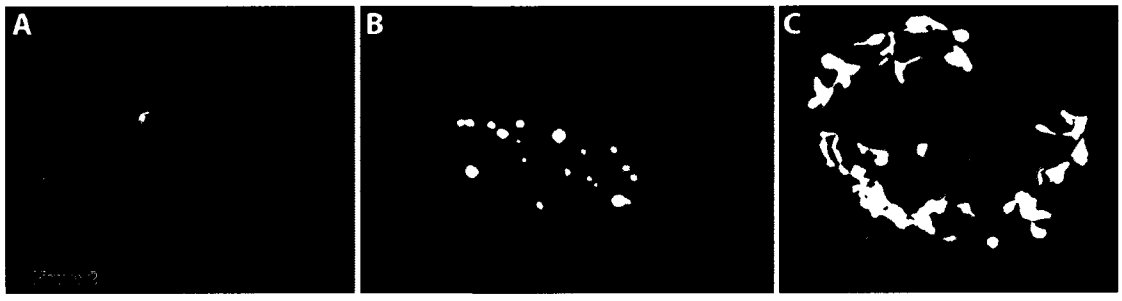
A
B
C

APPENDIX V

Submitted to Journal of Molecular Medicine

Lamin A/C mutants disturb sumo1 localization and sumoylation *in vitro* and *in vivo*

Emilie Boudreau[1], Sarah Labib[1], Anne Bertrand[2,3], Valerie Décostre[2,3], Pierrette Bolongo[1], Nicolas Sylvius[1], Pallavi Gupta[1], Gisèle Bonne[2,3,4], and Frédérique Tesson[1]

1 Laboratory of Genetics, University of Ottawa, Ottawa, Canada

2 Inserm, U974, Paris, F-75013, France;

3 Université Pierre et Marie Curie-Paris6, UMR-S974, CNRS, UMR7215, Institut de Myologie, IFR14, Paris, F-75013, France;

4 AP-HP, Groupe Hospitalier Pitié-Salpêtrière, U.F. Cardiogénétique et Myogénétique, Service de Biochimie Métabolique, Paris, F-75013, France

Corresponding Author

Frédérique Tesson: FTesson@uottawa.ca

Abstract

A-type lamins A and C are nuclear intermediate filament proteins in which mutations have been implicated in multiple disease phenotypes commonly known as laminopathies. In COS7 cells, we previously showed that the over-expression of a lamin C mutant associated with dilated cardiomyopathy (p.Asp192Gly) resulted in nuclear aggregation of lamin C and the sequestration of a protein modifier, sumo1, within the aggregates. Sumoylation is a post-translational protein modification that regulates a wide range of cell processes through the attachment of sumo1 to various substrates. In C2C12 myoblast cells we overexpressed sumo1 with wild-type and myopathic p.Leu85Arg, p.Asp192Gly, p.Glu353Lys, and p.Arg386Lys mutant lamin A and lamin C. We observed a trapping of sumo1 in p.Asp192Gly, p.Glu353Lys, and p.Arg386Lys aggregates of lamin A/C. This correlated with an increased steady-state level of sumoylation. However we could not detect the sumoylation of lamin A or C by sumo1. In myoblasts and myopathic muscle tissue from the *Lmna*$^{H222P/H222P}$ laminopathy knock-in mouse model, we also observed a mislocalization of sumo1. Our results suggest that mutant lamin A/C alters the dynamics of sumo1 and thus misregulation of sumoylation may be contributing to disease progression in laminopathies.

Introduction

Laminopathies, diseases associated with mutations in the lamin A/C gene (*LMNA*), are a collection of over ten distinct disease phenotypes including but not restricted to dilated cardiomyopathy (DCM), Emery-Dreifuss muscular dystrophy (EDMD), restrictive dermopathy, familial partial lipodystrophy (FPLD) and premature ageing (OMIM # 150330). However, there is no definitive genotype-phenotype relationship for over 300 mutations reported in this gene (for the full list of mutations, see UMD-*LMNA* database at www.umb.be:2000). *LMNA* is one of the most frequently reported mutated genes in familial DCM and is associated with a worse prognosis than other forms of DCM [1]. Also, mutations in *LMNA* are often responsible for an earlier onset and more severe form of EDMD than X-linked EDMD [2].

LMNA encodes the A-type lamin proteins, lamins A and C, which are expressed in all terminally differentiated and nucleated cells. Lamins A and C are type V intermediate filament proteins which constitute major components of the inner nuclear lamina with structural roles such as nuclear membrane strength and shape, positioning of the nuclear pore complexes, anchoring chromatin, and lamina assembly [3-5]. They also support regulatory roles as they are required for proper DNA transcription and gene expression [6,7].

Investigations into the molecular consequences of *LMNA* mutations have shown that point mutations can affect lamina, filament, and protein complex assembly in a mutation-dependent manner [8-10]. Expression of certain lamin A/C mutants result in intranuclear aggregations of the lamins while others do not appear to affect assembly or localization of the protein [11,12]. Furthermore, mutations in *LMNA* can differentially affect the lamin A or C isoforms [10]. The absence of the lamin A/C protein has been shown to cause mislocalization of other nuclear proteins such as emerin [13]. Previously, we demonstrated that *in vitro* over-expression of lamin C containing the p.Asp192Gly DCM-linked mutation resulted in the mislocalization and trapping of a post-translational protein modifier known as Small Ubiquitin-related MOdifier-1 (sumo1) inside lamin C aggregates [11]. The sequestration of sumo1 was abolished by the disruption of the sumo1 di-glycine motif required for sumoylation [11]. Sumoylation, which involves the covalent but reversible attachment of the ~10 kD sumo1 protein to a lysine residue on the target protein, has been shown to regulate an assortment of cell processes that include gene expression and nucleocytoplasmic transport [14, reviewed in 15]. It

was demonstrated that the ubiquitin-conjugating enzyme E2I (Ubc9), which conjugates sumo1 to target proteins, interacts with lamin A/C [16]. Furthermore, both lamins A and C contain three proposed common sumoylation consensus sequences [17]. Taken together, these findings suggest that lamin A/C may be modified by sumo1 and that mutations in *LMNA* may disturb the sumoylation process by disrupting sumo1 localization. Interestingly, it was observed in HeLa cells and mouse cardiomyocytes that lamin A/C is modified by sumo2/3 and that a DCM-associated mutation within the consensus sequence decreased the sumoylation [18]. However, it was shown that lamin A/C is sumoylated preferentially by sumo2/3 and not sumo1 [18]. Sumo2 and sumo3 are nearly identical paralogs of sumo1, with approximately 50% sequence identity with sumo1 and both common and unique protein substrates [19].

In the present study we tested the sumoylation of lamin A/C by sumo1 in the C2C12 mammalian myoblast cell model. We investigated whether the expression of DCM- and EDMD-associated mutant lamin A and C alter the localization of sumo1 and disturb the sumo1 sumoylation process in C2C12 cells. We confirmed our results using myoblasts isolated from the $Lmna^{H222P/H222P}$ knock-in mouse, which develops adult-onset muscle dystrophy and DCM comparable to the human phenotype [20]. We also validated sumo1 mislocalization results *in vivo* in soleus muscle tissue biopsies from the $Lmna^{H222P/H222P}$ mouse. Although there is still much to be elucidated, our results highlight the involvement of the sumo1 sumoylation pathway in the pathophysiology of laminopathies especially those involving myopathic tissue.

Materials and Methods

Expression vector preparation

Full length lamin A, lamin C, and sumo1 cDNA was previously cloned into fluorescent expression vectors (pECFP-C1, pDsRed2-C1, and pEYFP-N1 from Clonetech laboratories) as described in [11]. The p.Leu85Arg, p.Asp192Gly, and p.Arg386Lys point mutations were previously introduced into the lamin A and C cDNA by site-directed mutagenesis as described in [11]. The ubc9-HA vector was a kind gift from Peter Howley as seen in Yasugi and Howley (1996) [21]. The p.His222Pro point mutation was introduced into the lamin A and C cDNA by site-directed mutagenesis (Stratagene) with forward primer 5'-TCTCCACCAGTCGGGTCTC AGGA CGGCGCTTGGTCTCACGC-3' and reverse primer 5'-GCGTGAGACCAAGCGC CGTCCTGAGACCCGACTGGTGGAGA-3'. The p.Gln353Lys point mutation was introduced

using the forward primer 5'-CCGAGATGCGGGCAAGGATGAAGCAGCAGCTG GACGAGTAC-3' and reverse primer 5'-GTACTCGTCCAGCTGCTGCTTCATCCTTGCC CGCATCTCGG-3'. All the inserts were systematically verified by sequencing.

Cell culture and transfection

C2C12 mouse myoblasts and COS7 monkey kidney cells were cultured in Dulbecco's Modified Eagle Medium (DMEM) and transiently transfected using Metafectene Pro (Biontex). Primary mouse myoblasts were harvested from wild-type and *Lmna*$^{H222P/H222P}$ mutant mice as described in [22], cultured in Myo-1 medium, and transfected using electroporation (Amaxa).

Co-immunoprecipitation

Nuclear protein was incubated with M280 sheep anti-mouse magnetic beads (Dynal – Invitrogen) for 1 hour at 4^0C. Each sample was incubated with 2μg primary antibody (anti-GFP sc-9996, anti-lamin A/C sc-6215) then M280 sheep anti-mouse magnetic beads. Samples were washed in TEG buffer supplemented with 50mM NaCl and 0.1% TitonX-100. Washed beads were boiled with SDS sample buffer with DTT at 95^0C for 5 minutes then cooled.

Immunoblotting

Cells were harvested 24 hours post-transfection and either nuclear protein (Active Motif) or total protein was extracted. N-ethylmaleimide (NEM) was added to certain extractions to preserve sumoylation [23]. Primary antibodies used included goat anti-lamin A/C, rabbit anti-SP3, mouse anti-sumo1, mouse anti-β-Actin, mouse anti-GFP (Santa Cruz Biotechnology 6215, 644, 5308, 47778, and 69779), mouse anti-GAPDH (ABM G041), mouse anti-vinculin (Sigma-Aldrich 4505), and mouse anti-emerin (Novocastra NCL-EMERIN). Secondary HRP-conjugated antibodies used included goat anti-mouse, rabbit anti-goat, or goat anti rabbit (Santa Cruz 2005, 2768, 2004). Visualization was performed using ECL detection reagent (Amersham) in the Fluorochem chemiluminescent imager (Alpha Innotech). Blots were analyzed for densitometry using the AlphaEase program. GAPDH, β-actin, or vinculin were used as protein loading controls.

Densitometry and statistical analysis

Samples were normalized to GAPDH or β-actin housekeeping protein to account for protein loading differences. As densitometry values vary greatly between blots, wild-type values were set at 100% and mutant values were compared against the wild-type as a ratio. As these calculations have not been previously shown to follow a normal distribution, a non-parametric Wilcoxon rank test was used with statistical significance set at $p<0.01$.

Immunostaining and fluorescent microscopy

C2C12 images were captured on an Olympus Fluoview FV1000 confocal microscope using the Olympus FV-10 acquisition software. Cryostat soleus muscle cross sections 6μm thick were obtained from C57 Black 6 mice *Lmna*$^{+/+}$ and *Lmna*$^{H222P/H222P}$. Prior to staining, slides were treated with 0.01M citric acid (pH 6.0) and incubated with 0.05 mg/ml mouse Fab. Tissue sections and primary mouse myoblasts were incubated with 1:50 primary antibody overnight at 4°C and then 1:200 secondary antibody for 30-60min in the dark. Images were captured on a CarlZeiss Axiophot2 or Z1 Imager fluorescent microscopes.

Results

To investigate the impact of *LMNA* mutations on the sumo1 sumoylation pathway, we examined sumoylation of lamin A/C and sumo1 localization in the presence of wild-type lamin A and C as well as p.Leu85Arg, p.Asp192Gly, and p.Gln353Lys lamin A and C mutants associated with dilated cardiomyopathy and p.Arg386Lys and p.His222Pro lamin A and C mutants associated with Emery-Dreifuss muscular dystrophy.

Lamin A and C are not sumoylated by sumo1

We previously reported the disruption of sumo1 localization in COS7 cells over-expressing p.Asp192Gly mutant lamin C and demonstrated that this mislocalization was sumoylation-dependent [11]. Examination of the lamin A and C protein sequence unveiled three potential sumoylation consensus sites [17] at lysine amino acid positions 171, 201, and 270. Although not essential for sumoylation, these sites are found more frequently modified by sumo1 and consist of a four residue motif, Ψ-K-X-E/D, where Ψ is any large hydrophobic amino acid, K is the target lysine to which sumo1 is attached, X is any amino acid, and E/D is aspartic or

glutamic acid. To assess whether lamin A and C were sumoylated, we over-expressed tagged lamin A and lamin C in C2C12 cells. Due to the transient nature of sumoylation and the low steady-state levels of sumoylated proteins [23], cells were also transfected with tagged sumo1. However, no slower migrating bands corresponding to sumoylated lamin A nor lamin C by either endogenous or exogenous sumo1 were observed (Figure 1A). To ensure the result was not cell-type specific, we confirmed the results using COS7 cells (data not shown). As a positive control of our protocol and of the sumoylation process in the C2C12 cell line, the blot was stripped and re-probed for the reversibly sumoylated protein, SP3. We observed bands for SP3 sumoylated by both endogenously and exogenously expressed sumo1 (Figure 1B). Given that we previously demonstrated how p.Asp192Gly mutant lamin C sequesters sumo1 inside aggregates, we investigated whether the expression of this mutant and other disease associated mutant lamin C result in its sumoylation. We transfected tagged proteins: lamin C, sumo1, and Ubc9. Ubc9, the sumoylation conjugating enzyme, was co-transfected to further promote protein sumoylation. No bands corresponding to sumoylated lamin C were observed with any of the lamin C wild-type or mutants (Figure 1C) suggesting that wild-type as well the other lamin A and C mutants are not sumoylated. To confirm this result, co-immunopreciptations were performed. In C2C12 cells transfected with tagged sumo1, immunoprecipitation of endogenous lamin A/C did not reveal lamin-sumo1-conjugates (Figure 1D). These results were confirmed in COS7 cells transfected with tagged wild-type lamin A, lamin C and with sumo1 (Figure 1E). Furthermore, over-expression of ubc9 did not produce different results (data not shown).

Mutant lamin A/C expression in C2C12 cells alters localization of sumo1 and ubc9

We next investigated the effect of disease associated *LMNA* point mutations on the localization of sumo1 and ubc9 in C2C12 cells. Wild-type lamin A, lamin C, and sumo1 show a relatively even distribution in the nucleus (Figure 2). In agreement with previously published results in other cell lines, the p.Leu85Arg mutant lamin A/C shows a comparable phenotype to the wild-type samples, and the p.Asp192Gly mutant lamin A/C results in nuclear aggregation of co-localized lamin A and C. As shown previously with only p.Asp192Gly lamin C [11], expression of p.Asp192Gly lamin A and C aggregates disturb the localization of sumo1 by sequestering it within the aggregates. The p.Gln353Lys substitution results in variable sizes and distributions of aggregated lamins A and C within the nucleus as well as at the nuclear periphery.

This mutant also sequesters sumo1 within some of the aggregates. As previously reported, the p.Arg386Lys mutation also results in the formation of lamin A/C aggregates and we demonstrate here the trapping of the sumo1 protein. The p.His222Pro mutant lamin A/C retains the ability to localize to the nuclear lamina but also develops aggregates with partial sumo1 sequestration. To assess ubc9 localization, the cells were transiently co-transfected with ubc9-GFP, and wild-type or mutant tagged lamin A and lamin C. Ubc9 was observed to always co-localize with both wild-type and any mutant lamin A/C (Figure 3).

Mutant lamin A/C expression alters cellular sumoylation in C2C12 cells

Given that mutant lamin A/C affected sumo1 localization, we next investigated the effect of p.Leu85Arg, p.Asp192Gly, p.Arg353Lys, and p.Arg386Lys lamin A/C mutations on the steady-state level of sumoylation. Western blot was performed on nuclear extracts from C2C12 cells transfected with tagged lamin A, lamin C and sumo1 or lamin C, ubc9 and sumo1. It was observed that cells expressing mutant lamin A/C that trapped sumo1 in aggregates also showed an increase in steady-state sumoylation levels and non-conjugated sumo1-YFP (Figure 4). Densitometry analysis was then performed on the bands corresponding to proteins conjugated to sumo1 (>85kDa) and also on the band of non-conjugated sumo1 tagged with YFP (at ~41kDa). There was a statistically significant increase in the steady-state levels of conjugated sumo1-YFP in the cells expressing p.Asp192Gly, p.Arg353Lys, and p.Arg386Lys mutant lamin A/C however the values varied from 1.3-fold to 4-fold increases thus estimating a true mean of increased sumoylation is difficult. Also, as transfection efficiency was approximately 30-40% in the C2C12 cells, the effect of mutant lamins may be diluted by non-transfected cells. There was also an increase in the levels of non-conjugated sumo1-YFP in the cells expressing the p.Asp192Gly, p.Arg353Lys, and p.Arg386Lys mutant lamin A/C though trend was less pronounced and fell slightly below statistical significance.

Sumo1 localization and sumoylation are perturbed in *Lmna*$^{H222P/H222P}$ mouse myoblasts

In order to confirm our results in a more physiologically relevant model, we cultured primary skeletal muscle myoblasts harvested from *Lmna*$^{+/+}$ and *Lmna*$^{H222P/H222P}$ mice and stained for sumo1 (Figure 5 left panel). In *Lmna*$^{+/+}$ myoblasts, sumo1 shows homogenous nuclear and cytoplasmic distribution (Figure 5A). Approximately 75% of myoblasts of *Lmna*$^{H222P/H222P}$ mice

show sumo1 localizing into nuclear foci while approximately 25% of myoblasts show a pronounced appearance at the NE without foci (Figure 5A). As reported previously in striated muscles [20], lamin A/C is normally localized in myoblasts (data not shown). Mutated myoblasts transfected with tagged sumo1 demonstrated an exacerbation of the foci phenotype to approximately 87% (Figure 5B).

To determine if the sumoylation profile is disturbed in *Lmna*$^{H222P/H222P}$ myoblasts, we performed western blotting for sumo1 in total protein from sumo1-YFP transfected *Lmna*$^{+/+}$ and *Lmna*$^{H222P/H222P}$ primary myoblasts (Figure 5C). We did not detect a significant change in the levels of sumo1 conjugated proteins yet we observed an increase in the amount of non-conjugated sumo1-YFP. There was also an increased sumoylation of one unknown protein that migrates to approximately 60kDa which would correspond to a protein with an estimated molecular weight of 10-20kDa.

Altered localization of endogenous sumo1 in *Lmna*$^{H222P/H222P}$ mouse muscle tissue

As endogenous sumo1 was found mislocalized in myoblasts cultured from *Lmna*$^{H222P/H222P}$ mice, we wanted to determine if this occurred *in vivo* in dystrophic *Lmna*$^{H222P/H222P}$ muscle tissue [20]. Therefore we examined its localization directly by immunostaining for sumo1 in cross-sections of soleus muscle from *Lmna*$^{+/+}$ and *Lmna*$^{H222P/H222P}$ mice (Figure 6). Wild-type muscle tissue sumo1 shows consistent punctate myocyte staining and homogenous punctate nuclear localization (Figure 6 left panel) that is comparable to endogenous myoblast sumo1 staining (Figure 6 left panel). In the p.His222Pro mutant myoblasts, we observed a striking nuclear envelope localization of sumo1 in approximately 25% of nuclei (Figure 6 right panel). The cytoplasmic localization appears conserved in this tissue. A small proportion of nuclei (~6%) showed an intranuclear aggregation of sumo1.

Discussion

In this study, we showed that the expression of mutant lamin A/C results in the mislocalization and misregulation of sumoylation and/or sumo1 turnover. The lamin A/C protein sequence contains three sumoylation consensus sequences as well as interacts with the conjugating enzyme, ubc9 [16], yet we could not detect its sumoylation by sumo1. This is in

agreement with the study that found lamin A/C to be preferentially modified by sumo2/3 [18]. The mutations included in this study were located in the α-helical coiled coil rod domains of lamin A/C that are essential for both filament assembly and protein-protein interactions [24]. As we previously demonstrated the aggregation of lamin C and the sequestration of sumo1 [11], we investigated whether mutations in lamin C would produce a misfolding of the protein that might reveal an otherwise masked sumoylation site. However, we did not observe any sumoylation of mutant lamin C indicating that lamin A/C is not sumoylated by sumo1.

Over-expression of sumo1 with wild-type mutant lamin A and C showed normal localization of lamin A/C with no trapping of sumo1, as did expression of the p.Leu85Arg mutant. We observed that p.Asp192Gly and p.Arg386Lys mutant lamin A/C formed intranuclear aggregates of lamin A/C as expected [10] however we further demonstrated sequestration of sumo1 within the aggregates. We report here for the first time, the *in vitro* over-expression of p.Gln353Lys (DCM) and p.His222Pro (EDMD) mutant lamin A/C. The p.Gln353Lys mutant lamin A/C shows intranuclear aggregations that sequester sumo1. We observed that p.His222Pro mutant lamin A/C localizes to the nuclear envelope yet forms intranuclear aggregates that partially sequester sumo1. This is in contrast to the reported normal localization in both cardiac and skeletal muscle from the $Lmna^{H222P/H222P}$ mouse [20]. This discrepancy may be due to the lack of a compensatory mechanism in C2C12 cells that may exist in mice or conversely to the over-expression of lamins and the exaggeration of normally undetectable changes in lamin filament formation. In myoblasts solely expressing p.His222Pro mutated lamin A/C, we observed an abnormal nuclear rim and/or intranuclear aggregation of both endogenous and exogenously expressed sumo1 as was seen in C2C12 cells. In skeletal muscle cross-sections, we observed a prominent staining of sumo1 at the nuclear envelope in a subset of myocyte nuclei. Certain sumoylation-desumoylation enzymes localize to the nuclear pore complexes (NPCs) [36] and the proper assembly and positioning of NPCs is dependent on lamin A/C [37]. In fact, ubc9, which is critical for conjugation of sumo1 to targets, is found both in the nucleus and at NPCs [36]. Furthermore, we have shown in C2C12 cells that ubc9 co-localizes with wild-type and mutant lamin A/C. SENP1 and SENP2 are sumo-specific proteases that de-sumoylate modified proteins and are found in the nucleus and at the nucleoplasmic face of the NPCs, respectively [38-39]. Also, RanBP2, a protein with sumoylation E3 ligase function also localizes to the

cytosolic filaments of the NPCs [40]. Therefore, mutant lamin A/C may be altering the assembly or function of the lamina, ubc9, and NPCs and thus disrupting the location or protein-protein interactions of the enzymes involved in the sumoylation cascade.

In C2C12 cell model, the sequestration of sumo1 within mutant lamin aggregates paralleled with an increase in the steady-state levels of sumoylated proteins in nuclear extracts. There was also a modest increase in the amount of non-conjugated sumo1. Our results suggest that the trapping of sumo1 in the lamin A/C aggregates may conceal sumoylated proteins from normal regulation of de-conjugation and/or sumo1 degradation. Furthermore, although not sequestered within the aggregates, we found ubc9 to co-localize with both wild-type and mutant lamin A/C regardless of aggregation phenotype. This co-localization of ubc9 at lamin aggregates may be maintaining or promoting the higher levels of sumoylation. As there are hundreds of proteins known to undergo sumoylation, the consequences of sumo1 mislocalization could have disastrous consequences on the regulation of many cell processes. Previous research in cardiac and skeletal muscles of the *Lmna*$^{H222P/H222P}$ mouse demonstrated an increase in the nuclear accumulation of Smad proteins, which are potent effectors of the TGFβ$_1$ signalling cascade correlating with increased fibrosis in the mice [20, 28]. Both the TGFβ receptor type I (TβRI) which activates the Smad proteins as well as Smad4 are sumoylated [29-30]. TβRI is sumoylated in response to TGFβ and amplifies the signal by modulating gene expression [30]. However, there are conflicting reports whether sumoylation stimulates or represses Smad4 [29, 31-35]. The nuclear accumulation of Smad proteins might result from the alteration of sumoylation of Smad4 and/or TβRI in the presence of lamin A/C mutants. Interestingly, we also observed an increase in the sumoylation of one unknown substrate protein only in homozygous p.H222P myoblasts transfected with sumo1 and not in wild-type nor heterozygous myoblasts. This band would correspond to a small (10-20kDa) sumoylated protein which we are currently investigating. Determining a protein whose sumoylation is misregulated prior to muscle differentiation could give insight into early disease pathogenesis.

Overall, our results suggest that disease-associated mutations in the *LMNA* gene that result in the expression of mutated lamin A/C mediate a mislocalization of sumo1, ubc9, and likely sumoylated proteins in a mutation-dependent manner. There is consequently deficient

deconjugation and/or degradation of sumo1 indicating a misregulation of the sumoylation process. In affected mouse tissue, sumo1 is found concentrated at the nuclear envelope where mutant lamin A/C and many of the sumoylation enzymes are targeted. As sumoylation is a highly conserved and tightly regulated cellular process with numerous targets, we propose that altered sumo1 dynamics may play a role in the pathophysiology of laminopathies.

Acknowledgements

The authors would like to thank Dr. Peter Howley (Harvard Medical School) for the kind gifts of the ubc9 vector as well as Dr. Heidi McBride (University of Ottawa Heart Institute) for her assistance with the Olympus Confocal microscope. This research was supported by an operating grant from the Heart and Stroke Foundation (NA 6628) awarded to F. Tesson, an operating grant from the Canadian Institutes of Health Research (77685) awarded to F. Tesson, a Government of France scholarship awarded to E. Boudreau, and INSERM (Institut national de la santé et de la recherche médicale) and Université Paris 6.

References

1. Sylvius N, Tesson F. Lamin A/C and cardiac diseases. Curr Opin Cardiol 2006;21:159-165. [PubMed: 16601451]
2. Brown SC, Piercy RJ, Muntoni F, Sewry CA. Investigating the pathology of Emery-Dreifuss muscular dystrophy. Biochem Soc Trans 2008;36:1335-1338. [PubMed: 19021551]
3. Glass CA, Glass JR, Taniura H, Hasel KW, Blevitt JM, Gerace L. The alpha-helical rod domain of human lamins A and C contains a chromatin binding site. EMBO J 1993;12:4413-4424. [PubMed: 8223451]
4. Sullivan T, Escalante-Alcalde D, Bhatt H, Anver M, Bhat N, Nagashima K, Stewart CL, Burke B. Loss of A-type lamin expression compromises nuclear envelope integrity leading to muscular dystrophy. J Cell Biol 1999;147:913-920. [PubMed: 10579712]
5. Liu J, Rolef Ben-Shahar T, Riemer D, Treinin M, Spann P, Weber K, Fire A, Gruenbaum Y. Essential roles for Ceanorhabditis elegans lamin gene in nuclear organization, cell

cycle progression, and spatial organization of nuclear pore complexes. Mol Biol Cell 2000;11:3089-3099. [PubMed 11071918]

6. Kumaran RI, Muralikrishna B, Parnavik VK. Lamin A/C speckles mediate spatial organization of splicing factor compartments and RNA polymerase II transcription. J Cell Biol 2002;159:783-793. [PubMed: 12473687]
7. Verstraeten VL, Broers JL, Ramaekers FC, van Steensel MA. The nuclear envelope, a key structure in cellular integrity and gene expression. Curr Med Chem 2007;14:1231-1248. [PubMed: 17504143]
8. Muchir A, Medioni J, Laluc M, Massaart C, Arimura T, van der Kooi AJ, Desguerre I, Mayer M, Ferrer X, Briault S, Hirano M, Worman HJ, Mallet A, Wehnert M, Schwartz K, Bonne G. Nuclear envelope alterations in fibroblasts from patients with muscular dystrophy, cardiomyopathy, and partial lipodystrophy carrying lamin A/C gene mutations. Muscle Nerve 2004;30:444-450. [PubMed: 15372542]
9. Weisel N, Mattout A, Melamed-Book N, Herrmann H, Medalia O, Aebi U, Gruenbaum Y. Laminopathic mutations interfere with the assembly, localization, and dynamics of nuclear lamins. Proc Natl Acad Sci USA 2008;105:180-185. [PubMed: 18162544]
10. Sylvius N, Hathaway A, Boudreau E, Gupta P, Labib S, Bolongo PM, Rippstein P, McBride H, Bilinkska ZT, Tesson F. Specific contribution of lamin A and lamin C in the development of laminopathies. Exp Cell Res 2008;314:2362-2375.
11. Sylvius N, Bilinska ZT, Veinot JP, Fidzianska A, Bolongo PM, Poon S, McKeown P, Davies RA, Chan KL, Tang AS, Dyack S, Grzybowski J, Ruzyllo W, McBride H, Tesson F. In vivo and in vitro examination of the functional significances of novel lamin gene mutations in heart failure patients. J Med Genet 2005;42:639-647. [PubMed: 16061563]
12. Hubner S, Eam JE, Wagstaff KM, Jans DA. Laminopathy-inducing lamin A mutants can induce redistribution of lamin binding proteins into nuclear aggregates. Exp Cell Res 2006;312:171-183. [PubMed 16289535]
13. Muchir A, van Engelen BG, Lammens M, Mislow JM, McNally E, Schwartz K, Bonne G. Nuclear envelope alterations in fibroblasts from LGMD1B patients carrying nonsense Y259X heterozygous or homozygous mutation in lamin A/C gene. Exp Cell Res 2003;10:352-362. [PubMed: 14644157]

14. Panse VG, Kressler D, Pauli A, Petfalski E, Gnadig M, Tollervey D, Hurt E. Formation and nuclear export of preribosomes are functionally linked to the small-ubiquitin-related modifier pathway. Traffic 2006;7:1311-1321. [PubMed: 16978391]
15. Geiss-Friedlander R, Melchior F. Concepts in sumolyation: a decade on. Nat Rev Mol Cell Biol 2007;8:947-956. [PubMed: 18000527]
16. Zhong N, Radu G, Ju W, Brown WT. Novel progerin-interactive partner proteins hnRNP E1, EGF, Mel 18, and UBC9 interact with lamin A/C. Biochem Biophys Res Commun 2005;338:855-861. [PubMed: 16248985]
17. Rodriguez MS, Dargemont C, Hay RT. SUMO-1 conjugation in vivo requires both a consensus modification motif and nuclear targeting. J Biol Chem 2001;276:12654-12659. [PubMed: 11124955]
18. Zhang YQ, Sarge KD. Sumoylation regulates lamin A function and is lost in lamin A mutants associated with familial cardiomyopathies. J Cell Biol 2008;182:35-39. [PubMed: 18606848]
19. Makhnevych T, Sydorskyy Y, Xin X, Srikumar T, Vizeacoumar FJ, Jeram SM, Li Z, Bahr S, Andrews BJ, Boone C, Raught B. Global map of SUMO function revealed by protein-protein interaction and genetic networks. Mol Cell 2009;33:124-135. [PubMed: 19150434]
20. Arimura T, Helbling-Leclerc A, Massart C, Varnous S, Niel F, Lacene E, Fromes Y, Toussaint M, Mura AM, Keller DI, Amthor H, Isnard R, Malissen M, Schwartz K, Bonne G. Mouse model carrying H222P-Lmna mutation develops muscular dystrophy and dilated cardiomyopathy similar to human striated muscle laminopathies. Hum Mol Genet 2005;14:155-169. [PubMed: 15548545]
21. Yasugi T and Howley PM. Identification of the structural and functional human homolog of the yeast ubiquitin conjugating enzyme UBC9. Nucleic Acids Res 1996;24:2005-2010. [PubMed: 8668529]
22. Rosenblatt JD, Lunt AI, Parry DJ, Partridge TA. Culturing satellite cells from living single muscle fiber explants. In Vitro Cell Dev Biol anim 1995;31:773-779. [PubMed: 8564066]
23. Pichler A. Analysis of sumoylation. Methods Mol Biol 2008;446:131-138. [PubMed: 18373254]

24. Dechat T, Pfleghaar K, Sengupta K, Shimi T, Shumaker DK, Solimando K, Goldman RD. Nuclear lamins: major factors in the structural organization and function of the nucleus and chromatin. Genes Dev 2008;22:832-853. [PubMed: 18381888]
25. Lee YJ, Miyake S, Wakita H, McMullen DC, Azuma Y, Auh S, Hallenbeck JM. Protein SUMOylation is massively increased in hibernation torpor and is critical for the cytoprotection provided by ischemic preconditioning and hypothermia in SHSY5Y cells. J Cereb Blood Flow Metab 2007;27:950-962. [PubMed: 16955077
26. Ja Lee Y, Castri P, Bembry J, Maric D, Auh S, Hallenbeck JM. SUMOylation participates in induction of ischemic tolerance. J Neurochem 2009;109:257-267. [PubMed: 19200349]
27. Girdwood DW, Tatham MH, Hay RT. SUMO and transcriptional regulation. Semin Cell Dev Biol 2004;15:201-210. [PubMed: 15209380]
28. Rosenkranz S. TGF-beta1 and angiotensin networking in cardiac remodelling. 2004;63:423-432. [PubMed: 15276467]
29. Lin X, Liang M, Liang YY, Brunicardi FC, Melchior F, Feng XH. Activation of transforming growth factor-beta signalling by SUMO-1 modification of tumor suppressor Smad4/DPC4. J Biol Chem 2003;278:18714-18719. [PubMed: 12621041]
30. Kang JS, Saunier EF, Akhurst RJ, Derynck R. The type I TGF-beta receptor is covalently modified and regulated by sumoylation. Nat Cell Biol 2008;10:654-664. [PubMed: 18469808]
31. Lin X, Liang M, Liang YY, Brunicardi FC, Feng XH. SUMO-1/Ubc9 promotes nuclear accumulation and metabolic stability of tumour suppressor Smad4. J Biol Chem 2003;278:31043-31048. [PubMed: 12813045]
32. Ohshima T, Shimotohno K. Transforming growth factor-beta-mediated signaling via the p38 MAP kinase pathway activates Smad-dependent transcription through SUMO-1 modification of Smad4. J Biol Chem 2003;278:50833-50842. [PubMed: 14514699]
33. Liang M, Melchior F, Feng XH, Lin X. Regulation of Smad4 sumoylation and transforming growth factor-beta signalling by protein inhibitor of activated STAT1. J Biol Chem 2004;279:22857-22865. [PubMed: 15028714]

34. Shimada K, Suzuki N, Ono Y, Tanaka K, Maeno M, Ito K. Ubc9 promotes the stability of Smad4 and the nuclear accumulation of Smad1 in osteoblast-like Saos-2 cells. Bone 2008;42:886-893.
35. Long J, Wang, He D, Liu F. Repression of Smad4 transcriptional activity by SUMO modification. Biochem J 2004;379:23-29. [PubMed: 14750902]
36. Palancade B, Doye V. Sumoylating and desumoylating enzymes at nuclear pores: underpinning their unexpected duties? Trends Cell Biol 2008;18:174-183. [PubMed: 18313922]
37. Hutchison CJ. Lamins: building blocks or regulators of gene expression? Nat Rev Mol Cell Biol 2002;3:848-858. [PubMed: 12415302]
38. Zhang H, Saitoh H, Matunis MJ. Enzymes of the SUMO modification pathway localize to filaments of the nuclear pore complex. Mol Cell Biol 2002;22:6498-6508. [PubMed: 12192048]
39. Hang J, Dasso M. Association of the human SUMO-1 protease SENP2 with the nuclear pore. J Biol Chem 2002;277:19961-19966. [PubMed: 11896061]
40. Mahajan R, Delphin C, Guan T, Gerace L, Melchior F. A small ubiquitin-related polypeptide involved in targeting RanGAP1 to nuclear pore complex protein RanBP2. Cell 1997;88:97-107. [PubMed: 9019411]

Figure Legends

Figure 1: Lamin A and C are not sumoylated by sumo1. (A-C) Western blots of C2C12 nuclear proteins: (A) Untransfected (UNT) or sumo1-YFP transfected, or triple transfected wild-type lamin A-CFP, lamin C-Red and sumo1-YFP probed for lamin A/C. N-ethylmaleimide (NEM) was included with harvesting of selected samples to stabilize sumo conjugation. (B) Western blot A stripped and reprobed for SP3. (C) UNT or triple transfected wild-type and mutant lamin C-Red, wild-type sumo1-YFP and wild-type Ubc9-HA probed for lamin A/C. (D-E) Immunoprecipitation of endogenous and exogenous lamin A and C. (D) Nuclear extracts of sumo1-HA transfected C2C12 cells were immunoprecipitated using anti-lamin A/C antibody and western blotting was performed for lamin A/C. (E) Nuclear extracts of lamin A-CFP, lamin C-CFP, or empty CFP vector transfected COS7 cells were immunoprecipitated using anti-GFP tag antibody and western blotting was performed for the GFP tags. All protein was harvested in the

presence of NEM. Emerin, a known lamin A/C binding partner, was included as a positive control for immunoprecipitation.

Figure 2: Sumo1 localization is disturbed by mutant lamin A/C in a mutation-dependent manner. Confocal microscopy images of nuclei of C2C12 cells expressing wild-type and mutant lamin A-CFP, lamin C-Red and wild-type sumo1-YFP. Lamin A and lamin C images are represented in one panel as they co-localize in all cells. Each picture presented is representative of the most commonly observed phenotype.

Figure 3: Ubc9 co-localizes with wild-type and mutant lamin A/C. Confocal microscopy images of nuclei of C2C12 cells expressing wild-type and mutant lamin A-CFP, lamin C-Red and wild-type sumo1-YFP. Lamin A and lamin C images are represented in one panel as they co-localize in all cells. Each picture presented is representative of the most commonly observed phenotype.

Figure 4: Mutant lamin A/C expression correlates with an increase in levels of sumoylated proteins. Western blot analysis of sumo1 in nuclear protein harvested from C2C12 cells transfected with wild-type and mutant lamin C-CFP and sumo1-YFP harvested with NEM. Blot was re-probed for β-actin as a loading control. Blot is representative of increased sumoylation observed in both lamin C, ubc9 and sumo1 transfections (n=2) as well as lamin A, lamin C, and sumo1 transfections (n=6).

Figure 5: Sumo1 localization and sumoylation of an unknown protein is disturbed by endogenous p.*His222Pro* mutant lamin A/C in primary mouse myoblasts. (A-B) Fluorescent microscopy images of non-transfected and sumo1-YFP transfected $Lmna^{+/+}$ (WT) and $Lmna^{H222P/H222P}$ primary myoblast nuclei. (A) Untransfected myoblasts immunostained for endogenous sumo-1 (green). (B) Sumo1-YFP transfected myoblasts expressing YFP-tagged sumo1 (green). All myoblasts were counterstained for DAPI (blue). Each picture presented is representative of the most commonly observed phenotype. (C) Western blot analysis of sumo1 in whole cell extracts from $Lmna^{+/+}$ and $Lmna^{H222P/H222P}$ myoblasts transfected with wild-type sumo1-YFP harvested with NEM. Bottom Blot was reprobed for vinculin as a loading control.

The asterisk (*) marks an unknown sumoylated protein whose sumoylation is increased in the *Lmna*$^{H222P/H222P}$ myoblasts. The blot is representative of two independent experiments.

Figure 6: Sumo1 localization disrupted in soleus muscle sections from *Lmna*^{H222P} mice. Fluorescent microscopy images taken at 63X magnification of cross sections of soleus muscle from *Lmna*$^{+/+}$ and *Lmna*$^{H222P/H222P}$ mice. Top row sections were stained for sumo1 (green). Bottom row sections were stained with only secondary antibody to show background signal of anti-mouse-568nm antibody (green). All sections were counterstained for DAPI (blue). Each picture presented is representative of the most commonly observed phenotype.

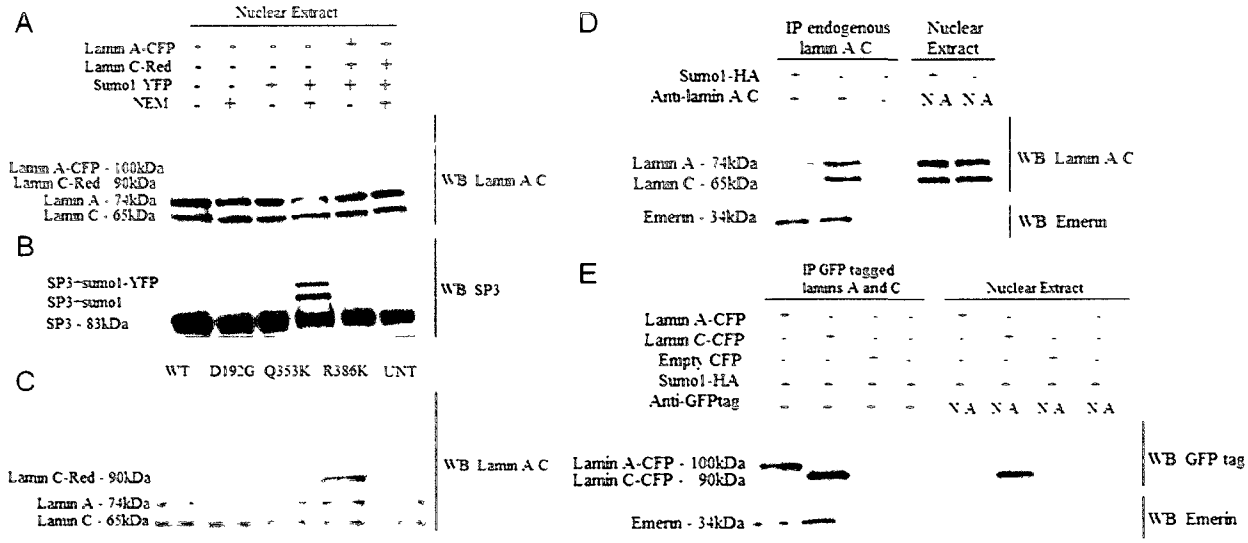

Figure 1

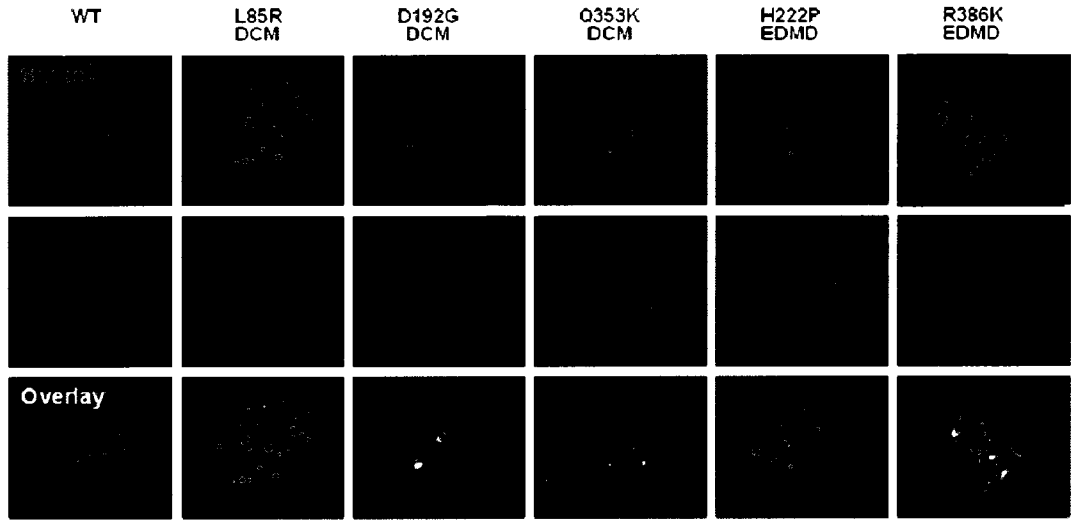

Figure 2

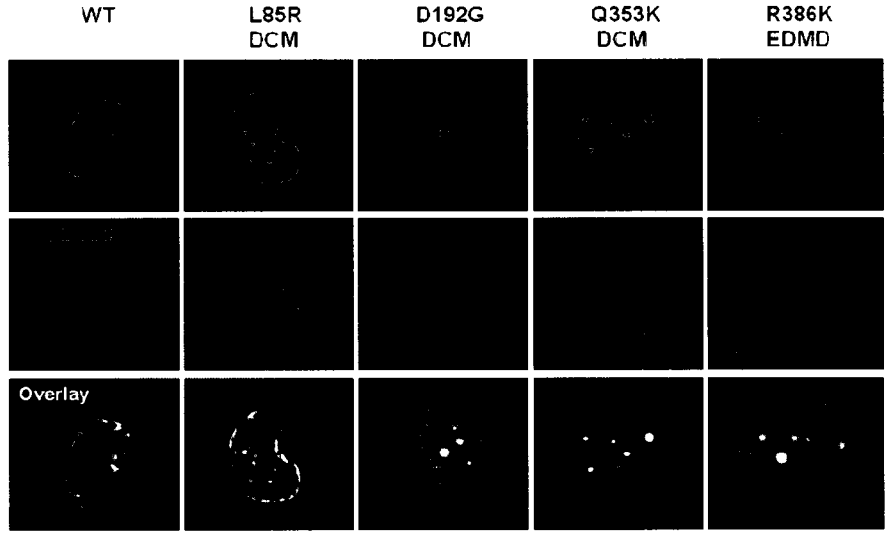

Figure 3

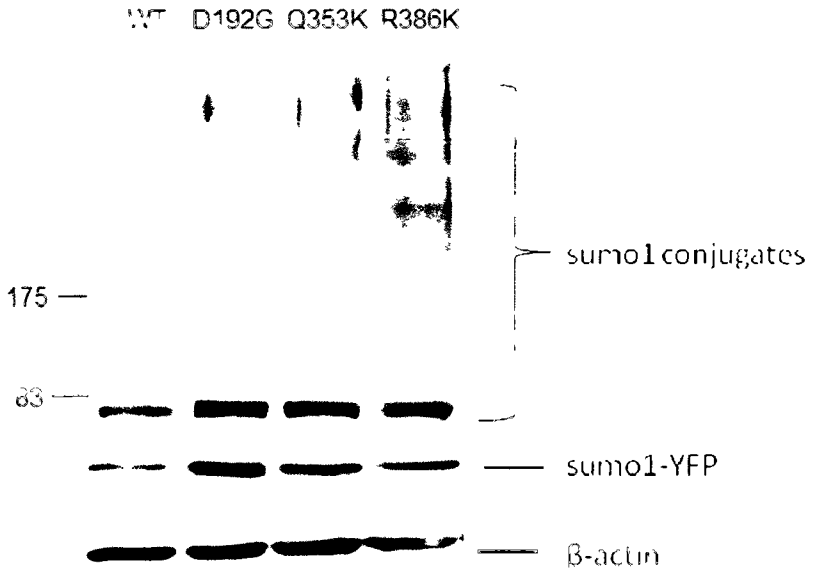

Figure 4

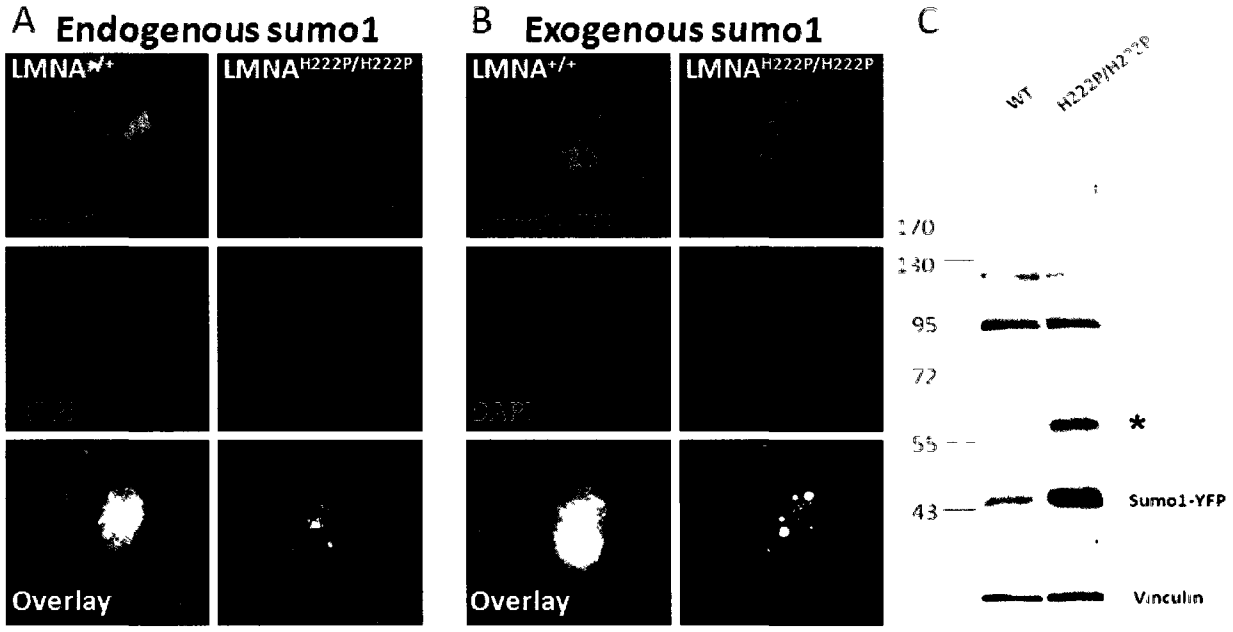

Figure 5

Figure 6

Curriculum Vitae

Sarah Labib

EDUCATION

Doctoral Candidate. Start Date January 2011.
Department of Biology, Specialization in Chemical and Environmental Toxicology, University of Ottawa

Masters of Science, Biochemistry, Defended September 2010.
Department of Biochemistry, Microbiology and Immunology, University of Ottawa
Thesis: (a) The effect of dilated cardiomyopathy associated LMNA gene mutations on the Sumo1 process. (b) Understanding the differential pathophysiology of LMNA mutations associated with atrial fibrillation and dilated cardiomyopathy.
Advisor: Frédérique Tesson, PhD.

Bachelor of Science, Honours Biology, December 2006.
Department of Biology, University of Ottawa
Thesis: Determining the effect of opening and closing $BKCa^{2+}$ channels on skeletal muscle fatigue resistance.
Advisor: Jean-Marc Renaud, PhD.

PUBLICATIONS

Labib S, Tesson F. Mission Impossible: The quest to predict cardiac-specific diseases associated with mutations in the LMNA gene. Cardiology Journal. Manuscript in Preparation.

Boudreau E, Labib S, Bertrand A, Gupta P, Decostre V, Bolongo P, Sylvius N, Bonne G, Tesson F. Mutant lamin A/C expression mediates an alteration of sumo1 localization and sumoylation in vitro and in vivo. Submitted to Journal of Molecular Medicine.

Saj M, Dabrowski R, Labib S, Szperl M, Kiliszek M, Kozluk E, Broda G, Szwed H, Tesson F, Bilinska ZT, Ploski R. Rare and common variants of LMNA gene in atrial fibrillation patients: a possible pathogenic role of Thr528Met mutation. Submitted to Cardiovascular Research.

Malek LA, Labib S, Mazurkiewicz L, Saj M, Ploski R, Tesson F, Bilinska ZT. From phenotype to genotype and back – a novel R541G LMNA mutation in a patient with familial dilated cardiomyopathy with segmental LV wall motion abnormalities. Submitted Journal of Human Genetics. Accepted pending revisions.

Gupta P, Bilinska ZT, Sylvius N, Boudreau E, Veinot JP, Labib S, Bolongo PM, Hamza A, Jackson T, Ploski R, Walski M, Grzybowski J, Walczak E, Religa G, Fidzianska A,

Tesson F. Genetic and ultrastructural studies in dilated cardiomyopathy patients: a large deletion in the lamin A/C gene is associated with cardiomyocyte nuclear envelope disruption. Basic Research in Cardiology. 105: 365-377. 2010.

Sylvius N, Hathaway A, Boudreau E, Gupta P, Labib S, Bolongo PM, Rippstein P, McBride H, Bilinska ZT, Tesson F. Specific contribution of lamin A and C in the development of laminopathies. Experimental Cell Research. 314: 2362-2375. 2008.

CONFERENCE AND SYMPOSIA PRESENTATIONS

Labib S, Tesson F. Lone atrial fibrillation and LMNA mutations: the potential for PKCalpha to play a therapeutic role in disease management. Poster. Canadian Cardiovascular Congress. October 2010.

Labib S, Burgon PG, Tesson F. Dilated cardiomyopathy and the LMNA gene: effect of mutations on sumoylated binding partners. Poster. Canadian Cardiovascular Congress. 2009.

Labib S, Burgon PG, Tesson F. The LMNA gene: effect of mutations on sumoylated binding partners. Poster. Canadian Human Genetics Conference. 2009.

Labib S, Burgon PG, Tesson F. Laminopathies: the tissue-specific impairment of the Sumo1 process via disruption of lamin A/C interaction with Ubc9. Poster. Young Investigator's Forum. 2009.

Labib S, Bolongo P, Burgon PG, Tesson F. Dilated cardiomyopathy and lamin A/C mutations: effect on interaction with Sumo E2 conjugating enzyme Ubc9. Poster. Canadian Cardiovascular Congress. 2008.

Labib S, Boudreau E, Gupta P, Hamza A, Bolongo P, Bilinska ZT, Davies RA, Stewart AFR, Burgon PG, Tesson F. Effect of DCM-causing lamin A/C mutations on the interaction with Sumo E2 conjugating enzyme Ubc9. Poster. Canadian Human Genetics Conference. 2008.

RELATED EXPERIENCE

Research

MSc Research, Department of Biochemistry, University of Ottawa
September 2007 – present

- Confirmed that lamin A/C is not sumoylated by Sumo1
- Identified one novel lamin A/C binding partner that are sumoylated by Sumo1 using co-immunoprecipitation and mass spectrometry and detected three novel unidentified lamin A/C binding partners that are sumoylated by Sumo1.
- Demonstrated that the cellular distribution of the Sumo E2 conjugating enzyme Ubc9 is disrupted by certain disease associated LMNA mutations.
- Designed and conducted experiments for the co-immunoprecipitation of wild type lamin A/C and the Sumo E2 conjugating enzyme

MSc Research, Department of Biochemistry, University of Ottawa
September 2007 – present

- Characterized the altered nuclear localization of four novel disease associated LMNA mutations.
- Established that lamin A/C binding partner PKCalpha localization is affected by lone atrial fibrillation associated LMNA mutations and dilated cardiomyopathy associated LMNA mutations.

BSc Research, Department of Biology, University of Ottawa
September 2005 – April 2006

- Determined there was no effect on fatigue resistance and force recovery upon opening or closing large conductance calcium activated potassium channel ($BKCa^{2+}$ channel).
- Isolated soleus and flexor digitorum brevis (FDB) whole muscle.
- Elicited fatigue to muscles via tetanic contractions and measured force generated during stimulation.

Teaching

Class Lecturer, Department of Health Sciences, University of Ottawa
November 2009

- Taught one lecture on current research in the field of Cardiovascular Genetics for undergraduate course - HSS3301 Biological Basis of Disease

Teaching Assistant, Department of Health Sciences, University of Ottawa
January – April 2010.

- Advised undergraduate students during office hours for course – HSS2501 Problèmes de sante.
- Prepared midterm and final examination.

Teaching Assistant, Department of Health Sciences, University of Ottawa
May - August 2009

- Presented lecture on the use of Immunology in the wet lab for undergraduate course – BAC2100 Microbiology and Immunology.
- Advised undergraduate students during office hours.
- Prepared midterm and final examination

RESEARCH SKILLS

Cell culture, Cloning, Site-Directed Mutagenesis, Transfection, Cellular Staining, Nuclear Protein Extraction, Co-Immunoprecipitation, Western Blotting.

EMPLOYMENT HISTORY

Science and Technology Researcher, Natural Resources Canada, Ottawa
March 2007 – July 2007

Customer Experience Representative, Chapters Books, Ottawa
May 2003 – May 2006

Concession and Usher, Cineplex Odeon Cinemas, Ottawa
April 2003 – April 2004

Sales Associate, West End Kids Clothing, Ottawa
June 2002 – April 2003

EXTRACURRICULAR ACTIVITIES

Interests

Yoga (Astanga, Bikram, Hatha), Reading, Salsa Dancing, Soccer (OCSSC), Softball (OCSSC), SpinFit

LANGUAGE COMPETENCIES

English, French, Farsi, Hebrew

REFERENCES

Available Upon Request